Evaluating antimicrobial resistance in dairy farming: understanding real world interactions within the wastewater slurry environment.

Christopher Lanyon

supervised by:
Professor John R. King (Mathematics)
Professor Rachel L. Gomes (Engineering)
Professor Dov J. Stekel (Biosciences)
Professor Theodore Kypraios (Mathematics)

June 1, 2021

Abstract

Agriculture is a known source of environmental antimicrobial resistance (AMR). However, the ecological and human-health impact of antibiotic use and the related AMR in animal husbandry is poorly understood. One possible vector of AMR from agriculture to the environment is dairy slurry. Slurry stores are repositories of bovine faeces and urine, as well as waste milk, used footbath contents, parlour washings and other farm wastewater. As antibiotics, bacteria and antimicrobial resistance genes are present in bovine excreta and waste milk, and footbaths and farm wastewater may contain copper, zinc, formalin and other biocides, this creates an environment in which selective pressure may cause the proliferation and spread of AMR. Dairy slurry is often spread on arable and crop lands, potentially acting as a source of AMR into the environment, but also into the human and bovine food chains.

Mathematical modelling is a useful predictive tool, but can also be used to understand complex phenomena and identify key processes, especially in circumstances where experimental analysis is costly or time consuming. In this thesis, the prevalence of AMR and antibiotics in dairy slurry is investigated through mathematical modelling.

The prevalence of antibiotic resistant *Escherichia coli* in dairy slurry stores throughout Great Britain was investigated by the Should We Worry About Slurry (SWWAS) project. SWWAS was devised in 2016 by Christopher Lanyon and Emma Gregson, and was awarded funding by the EPSRC Bridging the Gaps initiative in order to survey farms across Great Britain. The project was an investigation into the presence of extended-spectrum β-lactamase (ESBL) producing *E. coli* in slurry stores, alongside antibiotic residue concentrations, heavy metal and mineral concentrations and farm practice data. The goal of the project was to study AMR and farm practices across GB, but also to generate an understanding of data collection practices in agriculture and to inform on how data is synthesised and utilised in mathematical modelling. ESBL *E. coli* were found on nine of the 15 farms and antimicrobial resistance genes not previously reported in agriculture were also found. Of nineteen antibiotics screened for, seven were detected. Eight metals known to be AMR co-selective agents were found in the farm slurry. Zinc and Copper were found above recorded minimum co-selective concentrations in similar media. Correlations were found between the detection of ESBL *E. coli* and herd size, arsenic concentration and reported use of neomycin and kanamycin.

Informed by the literature and data from the SWWAS project, three models of antimicrobial resistance in a slurry tank environment were developed. The first

model uses ordinary differential equations to describe the persistence and spread of AMR *E. coli* interacting with bacteriolytic and bacteriostatic antibiotics in a slurry store. The model incorporates bacterial growth and death, horizontal gene transfer, antibiotic degradation, and tank filling and emptying effects. The model simulated various conditions: a sensitivity analysis was performed and inference was performed to predict parameter values for a working dairy farm. Through this analysis it is shown that the tank emptying regime and type of antibiotics used affect the development of multidrug-resistant bacteria.

The second model builds on the first, but additionally incorporates a spatial dimension and settling dynamics. A model of solids settling in a slurry tank was established, then sorption dynamics were used to determine the available concentration of antibiotics throughout the tank. Lastly, the population dynamics of bacteria were simulated to determine the effect of settling on the makeup of the bacterial population. This model illustrates the antibiotic removal effects of sorption and degradation and the resulting effects on the development of AMR. Once again sensitivity analysis was performed to determine how the settling parameters affect the model outputs.

The final model is a partial differential equation (PDE) model of a slurry tank, which incorporates fluid flow dynamics. This model was based on an advection-diffusion-reaction system and simulated in one and two dimensions. Finite difference and finite element frameworks for modelling were established for the one and two dimensional problems, respectively. Similar to the settling model, the PDE model indicates that antibiotic is removed as it moves through the tank and that multidrug resistant bacteria become the dominant phenotype. However, instabilities in the simulations make it difficult to draw conclusions from this model.

The three models developed in this thesis, alongside data from the SWWAS project, highlight particular avenues for future research: the use of bacteriolytic antibiotics, tank filling and emptying regimes, and the effects of sorption on antibiotic removal in dairy slurry. It is key that more data is collected to truly assess the risks that the prevalence and spread of AMR in dairy slurry storage pose to the human and environmental resistomes.

Acknowledgements

I'd like to begin by thanking my supervisors, Professor John R. King, Professor Rachel L. Gomes, Professor Dov J. Stekel and Professor Theodore Kypraios, for their advice, encouragement and support throughout the process of researching and writing this thesis.

I'm very grateful to Dr Emma Gregson for collaborating with me and leading the Should We Worry About Slurry project. Without her help, time, expertise, good humour and ability to spot the perfect cow-pat, the project would not have been possible. I'd also like to thank all those who contributed to the data collection and analysis: Dr Jennifer Hankin, Professor Rachel L. Gomes, Professor Jon L. Hobman and Dr Vikki Archibald. Finally I thank the EPSRC Bridging the Gaps initiative for funding the project.

I'd like thank the EVAL-FARMS team and Dr Rosa Baena-Nogueras for allowing me to use their data in Chapter 6 of this thesis.

I'd like to thank all four MASS cohorts for their friendship, support, tolerance and rubber-ducking throughout the last four years. My gratitude also to the Food Water Waste group for their warmth and encouragement and for the top tier Christmas meals.

I am grateful to the Leverhulme Trust for sponsoring my PhD.

Thank you to my family, Carol, Bill and Holly, for their love and support and for listening to me talk about cow poo more than I expect they ever thought they'd have to. Thank you to the 46 Jacobs Wells crew, Mat, Claire, Richard and Marie, for teaching me so much about myself and how to be better, for always staying in touch, for forgiving my inability to read book club books, for over a decade of friendship. Thank you to my friends, those from Cornwall, Bristol, London, Nottingham, for being a part of my life. In particular, thank you to Sarah, Jake, Josh, Laurence, Luke, Steven, Amy, Sam, Nat, Mikey, Viccy, Emma and Bex. Finally, thank you to Leanne for three years of happiness: for living with me, for loving me, for the opportunity to co-parent an incredibly fussy cat.

Contents

1 Introduction **1**

1.1 Aims and Objectives 3

1.2 Structure of Thesis 4

2 Literature Review **7**

2.1 What is Antimicrobial resistance? 7

2.1.1 The Biology of AMR Development and Spread 7

2.2 Antimicrobials 10

2.2.1 Modes of Action and Resistance 11

2.2.2 Chemical Fate and Properties of Antibiotics 13

2.3 Agriculture and the Challenge of AMR 18

2.3.1 Farm Slurry and its additional Challenges 19

2.3.2 What policies are in place to stop AMR in agriculture? . . 20

2.4 Factors affecting AMR within the slurry tank environment 21

2.5 Mathematical modelling of AMR 23

2.5.1 Existing Mathematical Models 24

2.5.2 Modelling Considerations 37

2.6 Summary 37

3 Should We Worry About Slurry? **39**

3.1 Project inspiration and vision 40

3.2 Materials and Methods 42

3.2.1 Statistical methods 42

3.3 Results and discussion 43

3.3.1 AMR Presence in slurry 43

3.3.2 Survey Results 45

3.3.3 Elemental analysis 51

3.3.4 Antibiotic Residue 51

3.4 Summary 59

4 Conceptual Model **66**
4.1 A conceptual model of the prevalence and spread of antimicrobial resistance in the dairy slurry storage environment 66
4.1.1 Features 66
4.1.2 Events 67
4.1.3 Processes 68

5 A model of multidrug-resistance in the dairy slurry tank **71**
5.1 Model Development 72
5.1.1 Model Design and Parameterisation 75
5.1.2 Mathematical model 82
5.2 Results and Discussion 85
5.2.1 Effects of altering the tank emptying regime 89
5.2.2 Sensitivity Analysis 93
5.2.3 Bacteriolytic and Bacteriostatic Antibiotics 100
5.3 Stability Analysis 102
5.3.1 Indefinite filling 103
5.3.2 Constant tank volume 108
5.3.3 Discussion and recommendations for future work 110
5.4 Summary 114

6 Parameter estimation for the ODE model **115**
6.1 The Data 116
6.1.1 Antibiotic Concentration 117
6.1.2 Microbial Counts 118
6.1.3 Bacterial phenotype data 119
6.2 Methods 121
6.2.1 The mathematical model 121
6.2.2 Methods of inference 124
6.3 Results and Discussion 129
6.3.1 Estimating the carrying carrying capacity of liquid slurry . 132
6.3.2 Estimation of the antibiotic parameters using the bacterial phenotype data 135
6.3.3 Estimating the horizontal gene transfer parameters 140
6.4 Summary 152

7 Modelling the effects of sorption on antimicrobial resistance **155**
7.1 Methods 157
7.1.1 Modified Takács Settling Model 157
7.1.2 Antibiotic Modelling 164

7.1.3 Bacterial equations . . . 166
7.2 Results . . . 167
7.2.1 Using antibiotic parameters inferred from data . . . 178
7.2.2 Sensitivity Analysis . . . 181
7.3 Summary . . . 192

8 An advection-diffusion-reaction model of AMR in the slurry tank 194
8.1 Methods . . . 196
8.1.1 1 Dimensional Governing Equations . . . 196
8.1.2 2 Dimensional Governing Equations . . . 199
8.1.3 Finite Element Formulation of the ADR Problem . . . 201
8.1.4 Single-antibiotic model . . . 205
8.1.5 Two-antibiotic model . . . 205
8.2 Results and Discussion . . . 207
8.2.1 One dimensional modelling . . . 207
8.2.2 Two dimensional modelling . . . 214
8.2.3 Discussion . . . 223
8.3 Summary . . . 226

9 Conclusion 228

Appendix A Should We Worry About Slurry Supporting Documents 233
A.1 Slurry Questionnaire . . . 233
A.2 SWWAS Pharmacy report . . . 236
A.3 SWWAS APHA report . . . 244

Appendix B Acronym Glossary 249

List of Figures

1.1 A simple schematic of the interactions between the slurry tank, dairy herd and the environment. 2

2.1 A simplified schematic of environmental pressure leading to AMR via horizontal gene transfer in microbial populations. A. A population of susceptible bacteria accompanied by a few microbes with resistance phenotypes on mobile genetic elements. B. On the addition of an antimicrobial most susceptible microbes die out, leaving the resistant portion of the population. C. Unhindered by the antibiotic the resistant microbes reproduce. D. Any remaining susceptible bacteria within the community can become resistant through horizontal gene transfer. 8

2.2 AMR Prevalence under the Smith et al. model as animal antibiotic use (λ) and medical antibiotic use (ρ) vary. Here prevalence is given by $X + Y + Z$, the proportion of the population with some level of AMR exposure. Though animal antibiotic use has some effect on the prevalence of AMR, the effect of medical antibiotic use is much clearer. 30

2.3 Emergence of AMR Prevalence under the Smith et al. Model. Three realisations of the Smith et al. model [17]. Red: Parameter values as in Table 2.3. Blue: No animal antibiotic usage (AAU), $\lambda = 0$, all other parameters as in Table 2.3. Yellow: Increased medical antibiotic usage (MAU), $\rho = 0.0045$, all other parameter values as in Table 2.3. Reduced AAU increases the time taken to reach AMR equilibrium prevalence but only has a small impact on the equilibrium value. Increased MAU, on the other hand, both reduces the time to equilibrium and increases equilibrium prevalence. 31

2.4 $x = 4$, $y = 1$, $w = 3$, $z = 4$ 36

2.5 $x = 3$, $y = 2$, $w = 4$, $z = 1$ 36

2.6 $x = 4$, $y = 2$, $w = 3$, $z = 1$ 36

2.7 $x = 1$, $y = 2$, $w = 2$, $z = 3$ 36

3.1 The 26 antibiotics farmers reported using within 12 months of the survey, collated by the number of farms that used them. Many of these antibiotics were used as part of combination medicines, see Table 3.4. 48
3.2 The total number of antibiotics each farm reported using within 12 months of the survey. 50
3.3 The six cleaning and herd hygiene chemicals that farmers reported using within 12 months of the survey, collated by the number of farms that used them. 50
3.4 The total number of cleaning and herd hygiene chemicals used by each farm within 12 months of the survey. 52
3.5 Correlations between recorded ESBL *E. coli* and farm practice factors. Here, the top row shows the Pearson coefficients for correlations between detected ESBL *E. coli* and farm practice factors. The remaining rows show the Pearson coefficients for correlations between the various farm practice factors. The colour bar and dot size indicate correlation strength. 52
3.6 Heavy metal concentrations across the farms shown using box and whisker plots. Here, the boxes contain from the 25th to 75th percentile, the line within the box is the median. Whiskers are 1.5 times the interquartile range, and outliers are those points which lie outside that range. 53
3.7 Correlations between recorded ESBL *E. coli* and elemental concentrations found in the slurry. Here the top row shows the Pearson coefficients for correlations between detected ESBL *E. coli* and the elemental concentrations found in slurry samples. The remaining rows show the Pearson coefficients for correlations between the detection of the various different elements. The colour bar and dot size indicate correlation strength. 54
3.8 Correlations between recorded ESBL *E. coli* and reported use of antibiotics. Here the top row shows the Pearson coefficients for correlations between detected ESBL *E. coli* and reported use of antibiotics. The remaining rows show the Pearson coefficients for correlations between the reported use of the various reported antibiotics. The colour bar and dot size indicate correlation strength. 60

3.9 Correlations between recorded ESBL *E. coli* and antibiotic residues found in the slurry. Here the top row shows the Pearson coefficients for correlations between detected ESBL *E. coli* and antibiotic residue found in slurry samples. The remaining rows show the Pearson coefficients for correlations between the various antibiotic residues that were found in the slurry. The colour bar and dot size indicate correlation strength. 61

5.1 Comparison plots of the four microbial strains using the the mass action model (see equation 5.15) and the force of transfer model (see equation 5.11). The two models behave very similarly, so much so that it is hard to distinguish between them. 79

5.2 The difference in bacterial concentrations between the mass action model (see equation 5.15) and the force of transfer model (see equation 5.11). Here the force of transfer model is subtracted from the mass action model. The varying line thickness arises due to fluctuations in the difference between the models. 80

5.3 A simulation of the model described by equations 5.17 to 5.22, using the parameter values given in Table 5.3. 86

5.4 The model described by equations 5.17 to 5.22, simulated for 400 years, using parameter values given in Table 5.3. 87

5.5 The Resistance transfer terms for the model simulation shown in 5.3, plotted on a log scale. 88

5.6 A simulation of the model described by equations 5.17 to 5.22, using the parameter values given in Table 5.3 and setting the rate of MDR transfer, β_u, to zero. 89

5.7 A simulation of the model described by equations 5.17 to 5.22, using the parameter values given in Table 5.3 and setting the relative cost of MDR, α_u, to 0.2. 90

5.8 A simulation of the model described by equations 5.17 to 5.22, using the parameter values given in Table 5.3. In this simulation, the volume of slurry is calculated using a seasonal emptying regime; the tank is emptied every week 1st May to 31st October and every 90 days in the other months. 92

5.9 Plots of the total antibiotic concentration in the slurry ($A_l + A_s$) and the total volume of slurry in the tank, using the parameter values given in Table 5.3, under no-emptying and seasonal emptying regimes. 93

5.10 Effects of varying the time between tank emptying, τ_e, and the initial tank volume, V_1, on the time to reach 95% multidrug-resistant bacteria, R_u, within the tank. The dot in 5.10a indicates the time to 95% MDR using the seasonal emptying frequency. A seasonal emptying regime is being used in 5.10b. 94
5.11 Plot of the time at which an intervention would need to occur, τ_e, to stop the multidrug proportion exceeding a given limit. This was simulated using the parameter values given in Table 5.3. The volume of slurry is calculated using a seasonal emptying regime; the tank is emptied every week 1st May to 31st October and every 90 days in the other months. 95
5.12 Sensitivity analysis of the model parameters where proportion of multidrug-resistant bacteria after 20 years is the output of interest under the no emptying regime. Here the boxplots show the results of calculating equation 5.31 for various parameter values. See Table 5.4 for parameter definitions and ranges. The system is particularly sensitive to α_u, the relative cost of multidrug-resistance and θ_l the inflow rate of bacteriolytic antibiotic. It is also sensitive to other parameters relating to bacteriolytic antibiotics. Here, the boxes contain from the 25th to 75th percentile, the line within the box is the median. Whiskers are 1.5 times the interquartile range, and outliers are those points which lie outside that range. 96
5.13 The proportion of multidrug-resistant bacteria, R_u, after 20 years as each of the parameters in Table 5.4 varies. This is based on simulations of the model described by equations 5.17 to 5.22. The remaining parameter values are as in Table 5.3. 98
5.14 Sensitivity analysis of the model parameters where proportion of multidrug-resistant bacteria after 20 years is the output of interest and a seasonal emptying regime is used. Here the boxplots show the results of calculating equation 5.31 for various parameter values. See Table 5.4 for parameter definitions and ranges. Compared to the infinite tank simulations the system is much less sensitive (see Figure 5.12), but α_u, the relative cost of multidrug-resistance remains the most parameter to which the model is most sensitive. Similarly, the system is also sensitive to θ_l, the inflow rate of bacteriolytic antibiotic, and α_l the cost of bacteriolytic-resistance. Here, the boxes contain from the 25th to 75th percentile, the line within the box is the median. Whiskers are 1.5 times the interquartile range, and outliers are those points which lie outside that range. . 99

5.15 Heatmaps showing the multidrug-resistant proportion, R_u, in the tank after 20 years when varying the relative cost of bacteriolytic-resistance, α_l, and the relative cost of MDR, α_u against the inflow rate of bacteriolytic antibiotic, θ_l under no-emptying and seasonal emptying regimes. This is based on simulations of the model described by equations 5.17 to 5.22. The remaining parameter values are as in Table 5.3. 101
5.16 Heatmaps showing the multidrug-resistant proportion in the tank after 20 years when varying the inflow rate of bacteriostatic antibiotic, θ_s, and the inflow rate of bacteriolytic antibiotic, θ_l under a no-emptying regime and a seasonal emptying regime. This is based on simulations of the model described by equations 5.17 to 5.22. The remaining parameter values are as in Table 5.3. 102
5.17 The number of steady states as A_s and A_l vary. These were calculated by solving equations 5.39 to 5.42, using the parameter values given in 5.3. 105
5.18 The number of stable steady states as A_s and A_l vary. These were calculated by solving equations 5.39 to 5.42, using the parameter values given in 5.3. 106
5.19 Stable steady states of S and R_u as A_s and A_l vary. These were calculated by solving equations 5.39 to 5.42, using the parameter values given in 5.3. 106
5.20 The steady states as the antibiotic concentration varies, here $Ab = A_s = A_l$. These were calculated by solving equations 5.39 to 5.42, using the parameter values given in 5.3. 107
5.21 The steady state as V_1 varies in the constant filling and emptying scenario using typical parameter values. These were calculated by solving equations 5.47 to 5.50, using the parameter values given in 5.3. 110
5.22 The steady state as V_1 varies in the constant filling and emptying scenario with $\alpha_u = 0.2$. These were calculated by solving equations 5.47 to 5.50, using the parameter values given in 5.3. 111

6.1 Presumptive *E. coli* Counts on MacConkey agar (Mac) TBX plates, TBX plates with added ampicillin (TBX+AMP16), TBX plates with added cefotaxime (TBX/CTX). The limit of detection (300 CFU ml^{-}1) was determined by the methods used by EVAL-FARMS researchers [36]. 119

6.2 Graph of A_s and A_l usin bacteriostatic and bacteriolytic rate of degradation (γ_s and γ_l, respectively) and rate of inflow (θ_s and θ_l, respectively) which maximise the log likelihood (equation 6.30), plotted alongside the data collected by Baena Nogueras et al. [37]. Model values are generated using equations 6.11 and 6.12. 131
6.3 MCMC trace plots for the antibiotic parameters using the antibiotic concentration data. These plots were generated using the Metropolis Hastings algorithm to infer bacteriostatic and bacteriolytic rate of degradation (γ_s and γ_l, respectively) and rate of inflow (θ_s and θ_l, respectively) using the data from [37]. The MLE values were also calculated the data from [37], by maximising equation 6.30. 132
6.4 MCMC Histograms for the antibiotic parameters using antibiotic concentration data from [37]. These plots were generated using the Metropolis Hastings algorithm to infer bacteriostatic and bacteriolytic rate of degradation (γ_s and γ_l, respectively) and rate of inflow (θ_s and θ_l, respectively) using the data from [37]. The MLE values were also calculated the data from [37], by maximising equation 6.30. 133
6.5 The concentration of bacteria predicted by the model using likelihood maximising μ_{TBX}, plotted against the presumptive counts of *E. coli* found on the TBX plates from [36]. The MLE value was calculated by maximising equation 6.23 using data from [36]. . . . 134
6.6 The concentration of bacteria predicted by the model using likelihood maximising μ_{Mac}, plotted against the presumptive counts of *E. coli* found on the MacConkey agar plates from [36]. The MLE value was calculated by maximising equation 6.24 using data from [36]. 134
6.7 The likelihood maximising value of μ_{TBX}, plotted against the MCMC trace plot from the Metropolis Hastings algorithm. The MLE value was calculated by maximising equation 6.23 using data from [36]. The graph shows that the MLE value is relatively close to the MCMC value. 135
6.8 The likelihood maximising value of μ_{Mac}, plotted against the MCMC trace plot from the Metropolis Hastings algorithm. The MLE value was calculated by maximising equation 6.23 using data from [36]. The graph shows that the MLE value is relatively close to the MCMC value. 136

6.9 S, R_s, R_l and R_u proportion (lines) using θ_s, θ_l, γ_s and γ_l inferred from the bacterial phenotype data from [36] using MLE (equation 6.30), plotted against the bacterial phenotype data. 138
6.10 Graph of A_s and A_l using θ_s, θ_l, γ_s and γ_l inferred from the bacterial phenotype data from [36] using MLE (equation 6.30), plotted alongside the data collected by Baena Nogueras et al. 139
6.11 Predicted S, R_s, R_l and R_u proportion (lines) plotted alongside the bacterial phenotype data (points) from [36]. Here the horizontal gene transfer parameters are the likelihood maximising values (equation 6.34) of the horizontal gene transfer rates of bacteriostatic, bacteriolytic and multidrug resistance (β_s, β_l and β_u, respectively), using parameter values from Table 6.10. 143
6.12 Trace plots of the β parameters generated using the original parameters, as in Table 6.10. These plots were generated using the Metropolis Hastings algorithm to infer the horizontal gene transfer rates of bacteriostatic, bacteriolytic and multidrug resistance (β_s, β_l and β_u, respectively) using the data from [36]. The MLE values were also calculated using the data from [36], by maximising equation 6.34. 144
6.13 Histograms of the β parameters posterior distributions, generated using the original parameters as in Table 6.10. These plots were generated using the Metropolis Hastings algorithm to infer the horizontal gene transfer rates of bacteriostatic, bacteriolytic and multidrug resistance (β_s, β_l and β_u, respectively) using the data from [36]. The MLE values were also calculated using the data from [36], by maximising equation 6.34. 145
6.14 Predicted S, R_s, R_l and R_u proportion (lines) plotted alongside the bacterial phenotype data (points) from [36]. Here the horizontal gene transfer parameters are the likelihood maximising values (equation 6.34) of the horizontal gene transfer rates of bacteriostatic, bacteriolytic and multidrug resistance (β_s, β_l and β_u, respectively), using parameter values from Table 6.12. 148
6.15 Trace plots of the β parameters generated using the original parameters, as in Table 6.12. These plots were generated using the Metropolis Hastings algorithm to infer the horizontal gene transfer rates of bacteriostatic, bacteriolytic and multidrug resistance (β_s, β_l and β_u, respectively) using the data from [36]. The MLE values were also calculated using the data from [36], by maximising equation 6.34. 149

6.16 Histograms of of the β parameters generated using the original parameters, as in Table 6.12. These plots were generated using the Metropolis Hastings algorithm to infer the horizontal gene transfer rates of bacteriostatic, bacteriolytic and multidrug resistance (β_s, β_l and β_u, respectively) using the data from [36]. The MLE values were also calculated using the data from [36], by maximising equation 6.34. 150
6.17 Predicted S, R_s, R_l and R_u proportion (lines) plotted alongside the bacterial phenotype data (points) from [36]. Here the horizontal gene transfer parameters are the means of the posterior distributions of the horizontal gene transfer rates of bacteriostatic, bacteriolytic and multidrug resistance (β_s, β_l and β_u, respectively), generated by the Metropolis Hasting algorithm, using parameter values from Table 6.12. 151

7.1 A simple schematic of a cylindrical slurry tank with a capacity of three-million litres (not to scale). These dimensions replicate the slurry tank at Sutton Bonington but could be adjust to model other commercially available cylindrical slurry tanks [253]. 156
7.2 Tank interactions schematic at layer i. Here X is suspended solids, A_s and A_l are bacteriostatic and bacteriolytic antibiotics, respectively; S, R_s, R_l and R_u are susceptible, bacteriostatic-resistant, bacteriolytic-resistant and multidrug-resistant *E. coli*, respectively; and β_s, β_l and β_u are the horizontal gene transfer rates for bacteriostatic-resistance, bacteriolytic-resistance and multidrug-resistance, respectively. Here a dot indicates sorption of a substance to the settling solids. For example $As.X$ indicates bacteriostatic antibiotic sorbed to solids. 158
7.3 Tank settling schematic. Here Q is the influent flow rate of slurry, X_{in} is the concentration of solids in the influent, A is the cross-sectional area of each layer and $J_{s,i}$ is the settling flux of solids from layer i to layer $i+1$. 163
7.4 Concentration of total suspended solids (TSS) after 50000 hours with initial conditions $X_i(0) = 0$ for all i (equations 7.6 to 7.8). . 169
7.5 Concentration of total suspended solids (TSS) in each layer of the tank over time (equations 7.6 to 7.8). Here, colour indicates concentration. 170
7.6 Available fractions of A_s (f_{as}) and A_l (f_{al}) in each layer of the tank after 50000 hours (equations 7.21 to 7.23). 170

7.7 Available concentration of antibiotics in each layer of the tank over time (equations 7.21 to 7.23. Here, colour indicates concentration. Available fraction is calculated using equations 7.26 and 7.27. . . 171
7.8 Total and available antibiotic concentrations in each layer of the tank after 50000 hours. 173
7.9 The difference in antibiotic concentration when sorption is omitted and included (see Figures 7.8a and 7.8b). The left panel shows the difference in bacteriostatic antibiotic concentration, A_s, and the right panel shows the difference in bacteriolytic antibiotic concentration, A_s. 174
7.10 Concentration of bacteria in each layer of the tank over time (equations 7.28 to 7.30), simulated with parameter values as in 7.3. Here, colour indicates concentration. 175
7.11 A comparison of bacterial concentrations when sorption is omitted and included. 176
7.12 The difference in bacterial phenotype proportion when sorption is omitted and included (see Figures 7.11b and 7.11a). Here the differences in susceptible (S), bacteriostatic resistant (R_s), bacteriolytic resistant (R_l) and multidrug resistant (R_u) proportions are shown. 177
7.13 A comparison of the total and available antibiotic concentrations when using parameters inferred in Chapter 6. Available fraction is calculated using equations 7.26 and 7.27. 179
7.14 A comparison of bacterial concentrations when sorption is omitted and included (using parameters inferred in Chapter 6). 180
7.15 Sensitivity analysis of the mean suspended solids concentration model described by equations 7.6 to 7.8, in relation to the settling parameters listed in Table 7.4. 183
7.16 Mean suspended solids concentration in the model described by equations 7.6 to 7.8, after 20 years as the parameters in Table 7.4 vary. 184
7.17 The distribution of total suspended solids (TSS) after 20 years when $r_h = 5 \times 10^{-4}$, in the model described by equations 7.6 to 7.8 185
7.18 Sensitivity of average total antibiotic concentration in the model described by equations 7.21 to 7.23, in relation to the settling parameters listed in Table 7.4 187
7.19 Average total concentration of available antibiotics in the model described by equations 7.21 to 7.23 after 20 years as the parameters in Table 7.4 vary. 188

7.20 Concentrations of A_s and A_l in the model described by equations 7.21 to 7.23 at 20 years across the tank when $r_h = 0.5 \times 10^{-3}$ . . . 189
7.21 Sensitivity of multidrug-resistant proportion in the model described by equations 7.28 to 7.30, in relation to the settling parameters listed in Table 7.4 . . . 190
7.22 Multidrug-resistant proportion in the model described by equations 7.28 to 7.30, after 20 years as the parameters in Table 7.4 vary. . . . 191

8.1 An volume element with changing cross-sectional area, used as an example to derive equation 8.1. . . . 197
8.2 A 2D approximation of the SB farm slurry tank (not to scale). Γ_1 and Γ_2 are the walls of the tank and Γ_{in} and Γ_{out} are the inflow and outflow, respectively. . . . 200
8.3 The velocity field, $\mathbf{u}$ in the tank at $t = 1$, $t = 15$, $t = 35$ and $t = 50$, generated by solving equations 8.32 to 8.34 with boundary conditions shown in equations 8.35 to 8.37. . . . 204
8.4 The velocity profile in the tank with a circular inflow pipe with a 0.5m diameter, calculated using equation 8.11. . . . 209
8.5 The velocity profile in the tank with a circular inflow pipe with a 3m diameter, calculated using equation 8.11. . . . 210
8.6 The concentrations of susceptible and resistant bacteria (S in blue and R in red) over time in the one dimensional, single-antibiotic model, where the diffusion coefficients, D_A and D_B, have been artificially increased to $D_A = 3.6 \times 10^{-2}$ and $D_B = 7.2 \times 10^{-3}$, to increase the stability of the simulation. . . . 211
8.7 The concentration of antibiotic (A) over time in the one dimensional, single-antibiotic model, where the diffusion coefficients, D_A and D_B, have been artificially increased to $D_A = 3.6 \times 10^{-2}$ and $D_B = 7.2 \times 10^{-3}$, to increase the stability of the simulation. . . . 212
8.8 The concentrations of susceptible and resistant bacteria (S and R) over time in the one dimensional, single-antibiotic model, where the area of the inflow pipe has been artificially increased to 6m^2, to increase the stability of the simulation. . . . 213
8.9 The concentration of antibiotic (A) over time in the one dimensional, single-antibiotic model, where the area of the inflow pipe has been artificially increased to 6m^2, to increase the stability of the simulation. . . . 214

8.10 The concentrations of susceptible, bacteriostatic-resistant, bacteriolytic-resistant and multidrug-resistant bacteria (S, R_s, R_l and R_u, respectively) over time in the one dimensional, two-antibiotic model, where the diffusion coefficients, D_A and D_B, have been artificially increased to $D_A = 3.6 \times 10^{-2}$ and $D_B = 7.2 \times 10^{-3}$, to increase the stability of the simulation. 215
8.11 The concentrations of susceptible, bacteriostatic-resistant, bacteriolytic-resistant and multidrug-resistant bacteria (S, R_s, R_l and R_u, respectively) over time in the one dimensional, two-antibiotic model, where the area of the inflow pipe has been artificially increased to 6m^2, to increase the stability of the simulation. 216
8.12 The concentrations of antibiotic and of susceptible and resistant bacteria (A, S and R) over time in the two dimensional, single-antibiotic model. The model failed to converge at $t = 24$h. 218
8.13 A close up of the concentration of resistant bacteria at the inflow of the tank in the two dimensional, single-antibiotic model, showing large numerical oscillations. 218
8.14 The concentrations of antibiotic and of susceptible and resistant bacteria (A, S and R) over time in the two dimensional, single-antibiotic model, stabilised using a Streamlined Upwind Galerkin Method. The model failed to converge at $t = 29$h. 220
8.15 A close up of the concentration of susceptible bacteria at the inflow of the tank, in the two dimensional, single-antibiotic model, stabilised using a Streamlined Upwind Galerkin Method, showing large numerical oscillations. 220
8.16 The concentrations of antibiotic and of susceptible and resistant bacteria (A, S and R) over time in the two dimensional, single-antibiotic model, where the diffusion coefficients, D_A and D_B, have been artificially increased to $D_A = 3.6 \times 10^{-1}$ and $D_B = 3.6 \times 10^{-2}$, to increase the stability of the simulation. 221
8.17 The concentrations of antibiotic and of susceptible and resistant bacteria (A, S and R) over time in the one dimensional, single-antibiotic model, where the diffusion coefficients, D_A and D_B, have been artificially increased to $D_A = 3.6 \times 10^{-1}$ and $D_B = 3.6 \times 10^{-2}$, to increase the stability of the simulation. 222

8.18 The concentrations of the bacteriostatic and bacteriolytic antibiotic and susceptible, bacteriostatic-resistant, bacteriolytic-resistant and multidrug-resistant bacteria (A_s, A_l, S, R_s, R_l and R_u, respectively) over time in the two dimensional, single-antibiotic model, where the diffusion coefficients, D_A and D_B, have been artificially increased to $D_A = 3.6 \times 10^{-1}$ and $D_B = 3.6 \times 10^{-2}$, to increase the stability of the simulation. 224
8.19 The concentrations of the bacteriostatic and bacteriolytic antibiotic and susceptible, bacteriostatic-resistant, bacteriolytic-resistant and multidrug-resistant bacteria (A_s, A_l, S, R_s, R_l and R_u, respectively) over time in the two dimensional, single-antibiotic model, where the diffusion coefficients, D_A and D_B, have been artificially increased to $D_A = 3.6 \times 10^{-1}$ and $D_B = 3.6 \times 10^{-2}$, to increase the stability of the simulation. 225

List of Tables

2.1 Typical Parameter Values from Baker et al. [38] 27
2.2 Typical Parameter Values from Volkova et al. [39] 28
2.3 Parameter Values from Smith et al. [17] 29
2.4 Parameter Values from Spicknall et al. [128] 33
2.5 Payoff Matrix for the Conlin et al. game [54]. P indicates a β-lactamase producing bacterium and N a non-producer. 35

3.1 Results from the Two samples from each farm were analysed for the presence of ESBL *E. coli*, except in the case of farms 7 and 8, where only one sample was analysed. This was due to the choice to analyse samples from the pre-storage and biodigester on farm 10 45
3.2 The requirements for each of the Farming Systems used in the study. 46
3.3 Details of slurry storage facilities on each of the 15 farms in the SWWAS project. 46
3.4 Medicines used on the farms, as reported by farm managers, and their constituent antibiotics. 49
3.5 The elements quantified in the slurry samples from the SWWAS project. Co-selective characterisation data from [64] and [145]. Agricultural limits from [160]. 55
3.6 The nineteen antibiotics screened for in the SWWAS project. . . 56
3.7 Antibiotics quantified in slurry. Concentrations in μg l^{-1} 57
3.8 Table showing antibiotics "used but not found" and "found but not used". 0 indicates "not used not found", 1 indicates "not used but found", 2 indicates "used and not found", 3 indicates "used and found". The "not used by found" case is the most concerning, as it either indicates a problem with the survey results, the sample analysis or that antibiotic residues are entering the tank from some other source or has been misidentified. 58
3.9 A summary table of findings from the SWWAS study. 64

4.1 A summary of the features, processes and events which may contribute to the development and spread of AMR in the slurry tank. 70

5.1 A summary of the features, processes and events from the conceptual model in chapter 4 that are included or omitted in the model presented in this chapter. 73
5.2 Mean average percentage error (MAPE) values comparing the similarity of the two models. 78
5.3 Typical parameter values used for initial simulations of the model. 83
5.4 The parameters considered for sensitivity testing and the ranges used. 97

6.1 Antimicrobials tested by Baena Nogueras et al. [37] in the SB slurry tank. 117
6.2 The concentration of antibiotics found at above detection limits in the slurry (μg l^{-1}). Here a zero value implies that the quantity of antibiotic in the slurry at that sampling point was below the limits of detection. 118
6.3 Bacteriostatic and Bacteriolytic concentrations from [37]. 118
6.4 Presumptive counts of *E. coli* in the SB slurry tank, cultured on MacConkey Agar (MAC) and TBX plates [36]. 120
6.5 Antimicrobials quantified by EVAL-FARMS in the SB slurry tank. Percentage resistance refers to the percentage of bacterial strains cultured that were resistant to each antibiotic, from a total of 287 strains. 120
6.6 Bacterial phenotype data showing the number of strains of each phenotype on the collection dates, from EVAL-FARMS [36]. . . . 121
6.7 Typical parameter values used for initial simulations of the model given by equations 6.1 to 6.12. 123
6.8 Parameter estimation of bacteriostatic and bacteriolytic rate of degradation (γ_s and γ_l, respectively) and rate of inflow (θ_s and θ_l, respectively) with varying number of simulated data points, n, and varying noise variance, σ^2. Here "SD" indications the standard deviation of the inferred parameter value. 130
6.9 The parameter values used to estimate the antibiotic parameters using the bacterial phenotype data. 137
6.10 Parameter values used when inferring the β parameters from the bacterial phenotype data from [36]. 141

6.11 Parameter estimation for the horizontal gene transfer rates of bacteriostatic, bacteriolytic and multidrug resistance (β_s, β_l and β_u, respectively) using simulated data generated with the parameters in Table 6.10, with varying numbers of *E. coli* strains per sample, n, and varying total data points. 142
6.12 Parameter values used based on inference from the previous sections, used to infer the horizontal gene transfer parameters β_s, β_l and β_u. 146
6.13 Parameter estimation for the horizontal gene transfer rates of bacteriostatic, bacteriolytic and multidrug resistance (β_s, β_l and β_u, respectively) using simulated data generated with the parameters in Table 6.12, with varying numbers of *E. coli* strains per sample, n, and varying total data points. 147
6.14 Summary table of parameter estimation results. 152

7.1 A summary of the features, processes and events which are included and omitted in the settling model presented in this chapter, based on the conceptual model described in Chapter 4. 159
7.2 Typical parameter values used for the modified Takács settling model, given by equations 7.6 to 7.8. 164
7.3 Typical parameter values used for the antibiotics and bacterial equations in the settling model (equations 7.21 to 7.23 and equations 7.28 to 7.30). 168
7.4 The parameters considered for sensitivity testing the solids concentration model described by equations 7.6 to 7.8, and the ranges used. 181

8.1 A summary of the features, processes and events which are included and omitted in the model presented in this chapter. 195
8.2 Parameter values used to simulate the single-antibiotic advection diffusion model in 1D. 206
8.3 Typical parameter values used for initial simulations of the two-antibiotic model. 208
8.4 The minimum inlet area, a_{in} that led to convergence for varying values of the temporal and spatial step sizes, δt and δx, respectively. 209

Chapter 1

Introduction

Antimicrobial resistance (AMR) is the mechanism by which microorganisms (both disease-causing and benign) become resistant to antimicrobial agents traditionally used to treat infections [1]. AMR has long been recognised as a threat to environmental, animal and human health. Recent analysis predicts that by 2050 our inability to treat previously curable diseases will lead to more deaths than cancer [2]. Beyond healthcare, human use of antibiotics means that AMR is now highly prevalent in agriculture and the environment. Though AMR persists at low levels in nature, it is particularly prevalent in circumstances where large quantities of antimicrobials or antibiotics are present, for example in antibiotic manufacturing effluent [3,4] municipal sewage [5,6], and in agricultural runoff [7], all of which are sources of AMR to the environment [8,9].

Between the 1980s and the early 2010s drug discovery and approval decreased significantly. By 2008 only five pharmaceutical companies had active drug discovery programmes. Between 2009 and 2012 only 5 new antibiotics were launched [10]. However, due to financial incentives there has been an increase during the latter half of the decade: the number of new antibiotics approved by the U.S. Food and Drug Administration (FDA) tripled between 2013 and 2019 [11] and the first entirely new class of antibiotic in 30 years was discovered in 2015 [12].

As the mechanisms for AMR can be passed both between microbial genus and species and across them, it is possible that that previously susceptible microbes become resistant just through contact with resistant strains, this is especially exacerbated by selective pressure in the presence of antimicrobials [2,13,14].

The human health impact of antimicrobial use in agriculture is poorly understood [9], despite agricultural usage accounting for around 44% of antibiotics by weight in the UK and an estimated 70% in the U.S. [2,15]. It has also been shown that the use of antimicrobial agents in agriculture affects the human resistome [16,17]. Furthermore, there is evidence that animal husbandry can impact

the nasal and gut microbiomes of farmers [18]. In the case of colistin, a so called "last-line" or "last-resort" antibiotic [19, 20], there is evidence that the resistance gene mcr-1 has been transferred to human populations as a result of agricultural use [21]. This prompts the need for more in-depth research into the effects of farm practice and antibiotic usage on the development of AMR in the farming and recipient environments.

On dairy farms, cows are treated by vets for illnesses such as mastitis, with antibiotics which are often not fully metabolised and are then passed in urine and faeces either unaltered or as active metabolites [22, 23]. For example the antibiotic oxytetracycline, used to treat mastitis [24–26], has been found in concentrations between 0.5 and 200 mg l^{-1} in cow manure [23]. Dairy manure has also been found to host ARGs related to tetracycline, β-lactam, kanamycin and chloramphenicol resistance [27]. Contaminated urine, faeces and any milk produced during the treatment period are added to dairy slurry tanks. Additionally, footbaths, once used, are added to the slurry tank [28] along with any run-off from parlour washings [29]. These footbaths may contain heavy metals such as copper and zinc and bactericides such as formalin [30]. In Nitrate Vulnerable Zones (NVZ) slurry (and other organic manures) can be used as a fertiliser and spread on soils used to grow both human and livestock food crops between 1st February and 31st October each year, potentially creating a transmission vector for AMR into the human population [31].

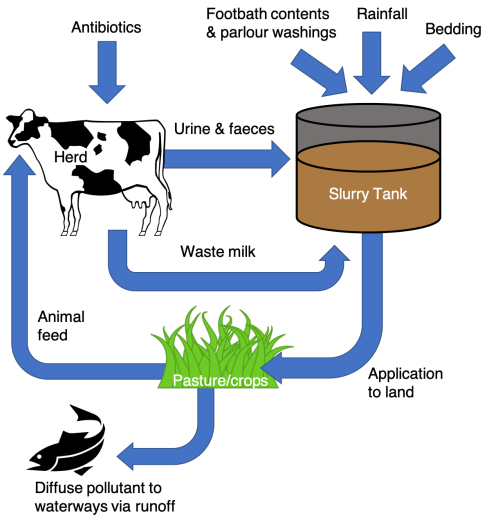


Figure 1.1: A simple schematic of the interactions between the slurry tank, dairy herd and the environment.

This thesis focuses on dairy farm slurry storage: repositories for dairy farm wastewater, including bovine faeces and urine, parlour washings, waste milk and waste footbath contents. Antimicrobial resistance genes (ARGs), antimicrobial resistant microbes and antibiotics are discharged by cows [32, 33], combining this with the natural presence of bacteria means that the slurry tank is potentially a site for the development and proliferation of AMR. Slurry from the tank is spread onto soils used to grow human and livestock crops,

Figure 1.1 shows a simple schematic of the real world interactions between the slurry tank and the environment. Farm slurry is spread on both animal feed croplands and those for human consump-

tion. As there is evidence that humans can be colonised by *E. coli* from eating plants [34] and that resistant *E. coli* on lettuce can be transferred to the gut microbiome [35], the extent to which the slurry tank environment drives the development and spread of AMR is of particular interest from both human health and farm sustainability perspectives. A greater understanding of these dynamics is also important for effecting policy change to better protect against the risks of AMR developing within the agricultural sector.

Collection of data to better understand the dynamics of AMR in dairy farming and its impact on the wider environment is ongoing [36, 37]. However, there is an imbalance between the availability of data and representation in the real world context. Particularly for topics with significant potential risks to organisms, ecosystem function and services, data collection can be difficult, time consuming or even dangerous. As an alternative, mathematical modelling can be used to quickly and efficiently identify important process factors using computer simulation. This is of particular relevance in agriculture, since altering farming practice on working farms is often untenable. Particularly in the case of slurry storage, where practical experiments may conflict with a farmer's needs, models can be used to simulate changes in farm practice over a number of years without having to enact those changes. Modelling can then be used, not only as a predictive tool, but to identify knowledge gaps, as well as the required quantity and granularity of data, and to understand how researchers can leverage what they already know to best determine areas of future research.

1.1 Aims and Objectives

The aim of this thesis is to develop and test mathematical models of the prevalence and spread of AMR in the dairy slurry environment, in order to identify possible risk factors for drug resistance. To achieve this, it is important to understand the interactions between the environmental, biological and chemical processes at play in the dairy farm wastewater system, alongside knowledge of existing mathematical models.

Objectives

1. Review the literature and existing mathematical models of agricultural AMR
2. Collect and analyse data from farms across Great Britain
3. Outline a conceptual model of the prevalence and spread of AMR in the slurry storage environment

4. Develop new mathematical models of AMR in the dairy slurry storage environment

5. Parameterise these models using existing data

6. Analyse model outputs to identify parameters which most affect the persistence and spread of AMR

7. Identify avenues of future research and data collection

1.2 Structure of Thesis

The thesis is composed of nine chapters, including this introduction. Chapter 2 presents a literature review, which covers the basic science of AMR; an overview of antimicrobials and their modes of action and physicochemical properties; the particular challenge of AMR in agriculture; factors which affect AMR in the slurry storage environment; and an overview of existing mathematical models of both AMR in agriculture and in clinical settings.

Chapter 3 discusses the Should We Worry About Slurry? (SWWAS) project, a field study of AMR in dairy slurry stores across the UK. Funding was acquired by the author and Dr Emma Gregson as part of the EPSRC bridging the gaps initiative. Slurry was sampled from fifteen farms across Great Britain and analysed for the presence of extended spectrum β-lactamase (ESBL) producing *Escherichia coli* (*E. coli*), antibiotic residues and heavy metal and mineral concentrations. Additionally, farmers were asked to fill out a survey detailing factors such as herd size, grazing schedule, slurry storage processes and the antibiotics used on the farm. The resulting data set provides an overview of farm practice and slurry contents which might drive AMR and ESBL presence in GB dairy farms. This is useful for the development and parameterisation of mechanistic models of AMR in the slurry storage environment. The data was also analysed to find correlations between ESBL *E. coli* detection and antibiotic residues, element concentrations and farm practice factors.

Using information from the literature and the SWWAS project, Chapter 4 establishes a conceptual model for AMR in dairy slurry storage facilities. The model summarises the known features of a slurry store (e.g. the store, the influent and the effluent), the events which occur in and around the store (e.g. the filling and emptying regime), and the processes at play which affect the persistence and spread of AMR in the slurry environment (e.g. horizontal gene transfer, antibiotic degradation, etc.). This then provides a framework for the development of mathematical models in the following chapters.

Chapter 5 details the development of an ordinary differential equation (ODE) model of the prevalence and spread of AMR in slurry storage. The model builds on the those developed by Baker et al. [38] and Volkova et al. [39], but incorporates the action of both bacteriostatic and bacteriolytic antibiotics and bacterial resistance to either or both types of antibiotic. The model also accounts for the filling and emptying regimes of the slurry store. The model was simulated under various conditions and sensitivity and steady state analyses were performed to determine which parameters most affect the development of AMR. It was found that over a twenty year timescale (the minimum expected lifespan of a slurry store), the cost of multidrug-resistance to bacteria, and parameters relating to bacteriolytic antibiotics had the greatest effect of the persistence and spread of AMR. It was also found that the tank emptying regime affected the speed at which AMR develops and that by taking steps to reduce the overall concentration of antibiotics in the tank, the development of multidrug-resistance could be delayed.

In Chapter 6, data from the University of Nottingham Sutton Bonington Dairy farm was used to infer key parameters of the model presented in Chapter 5. Three data sets were available, presumptive *E. coli* counts [36], *E. coli* resistance phenotype data [36] and antibiotic concentration data [37]. The *E. coli* count data was used to infer the carrying capacity of the slurry; interestingly, the predicted value is lower than the concentration of bacteria entering the slurry storage that is proposed in the literature, which, if accurate, would indicate that slurry storage is inhibiting the growth of *E. coli* communities. The antibiotic concentration data was used to estimate the bacterial parameters from the ODE model. The rates of horizontal gene transfer were also inferred using the estimated carrying capacity and antibiotic parameters. It was predicted that the genes for bacteriolytic and bacteriostatic-resistance were transferred an order of magnitude faster than the genes for multi-drug resistance. This inference process indicated that the model can be used to predict the real-world system if appropriate model-fitting practices are utilised.

In Chapter 7, a model of the slurry tank which incorporates settling dynamics is proposed. This model incorporates the bacteriolytic and bacteriostatic-resistance dynamics introduced in Chapter 5, in addition to solids settling and antibiotic sorption. A modified version of the Takács settling model [40] was used to simulate solids settling a slurry tank. Then partition coefficients were used to calculate the proportion of antibiotic which sorbed to the solids throughout the tank. When simulating the bacterial dynamics it was assumed that the sorbed portion of the antibiotics was not available to affect the bacterial population. Sensitivity analysis was performed to determine which of the settling parameters

most affected the model outputs. One of the main outcomes this chapter is an understanding of the effect of slurry storage on antibiotic removal, which is a key factor when considering the spreading of slurry onto crop lands and pasture.

In this chapter, two advection-diffusion-reaction models of AMR persistence and spread in the slurry tank is developed. These models incorporates fluid dynamics alongside tank-geometry as well as bacterial-antibiotic interactions. The first model describes a single antibiotic interacting with a single strain of bacteria (similar to [38]), while the second model is based on the dynamics of the model in Chapter 5. Finite difference and finite element formulations of both models were generated and both models were simulated. Due to the high Péclet number of the system, the initial simulations of both models were unstable. Parameter adjustments were made so that the models could be simulated without diverging. As in Chapter 7, one of the key outcomes was the potential removal of antibiotics from the slurry by the time it reached the effluent. Furthermore these models provide a framework which could be utilised to model AMR in other systems where fluid is flowing.

This final chapter summarises the main results presented throughout the thesis and describes possible future directions for data collection and modelling in the field of agricultural AMR.

Appendix A contains key documents from the SWWAS study and Appendix B is an acronym glossary.

Chapter 2

Literature Review

2.1 What is Antimicrobial resistance?

Antimicrobial resistance (AMR) is the mechanism by which microorganisms become resistant to the antimicrobial agents used to treat them. AMR arises in situations where evolutionary or selective pressure is exerted on microbes by antimicrobials and is conferred genetically, either by genetic mutations within susceptible organisms or by *horizontal evolution* [41], the microbial ability to exchange genetic material with other microbes and the environment [42–45]. Genes which confer AMR then persist and spread within the microbial community through reproduction and horizontal gene transfer (HGT). A simple illustration of how AMR spreads in microbial populations is shown in Figure 2.1.

AMR has been present in healthcare the inception of antibiotic treatment: just three years after the introduction of the first systemically used antimicrobials (the sulfonamides) in 1937, sulfonamide resistance was reported [13]. However, AMR has existed in the environment since before the widespread anthropogenic dispersal of antibiotics; before humans began using antimicrobials, they were produced by fungi (for example *Penicillium chrysogenum* produces the antibiotic, penicillin [46]) or, in the case of antibiotics like streptomycin and tetracycline, by microbes themselves [47]. Microbes developed genetic strategies to counter these naturally occurring antimicrobials, which, alongside the microbial ability to exchange genetic material, laid the groundwork for the widespread resistance to manmade antibiotics [48].

2.1.1 The Biology of AMR Development and Spread

AMR is conferred to microorganisms via antimicrobial resistance genes (ARGs), these genes persist and spread within a microbial community via reproduction and horizontal gene transfer (HGT) [48]. The acquisition of resistance phenotypes can

occur via mutations in the genetic material of microorganisms, if the mutation is beneficial in the presence of antimicrobials it will likely spread and proliferate. Given the average rate of mutation, a pool of 10^{10} bacteria in contact with some antimicrobial might be expected to have mutations on 1000 genetic loci, if one of these mutations confers mechanisms for resistance to said antimicrobial, it will likely proliferate via reproduction [49]. In the absence of antibiotic treatment, the persistence of a mutation becomes dependent on whether the mutation induces a fitness cost [50], mutations with little to no fitness cost for the bacteria are more likely to persist.

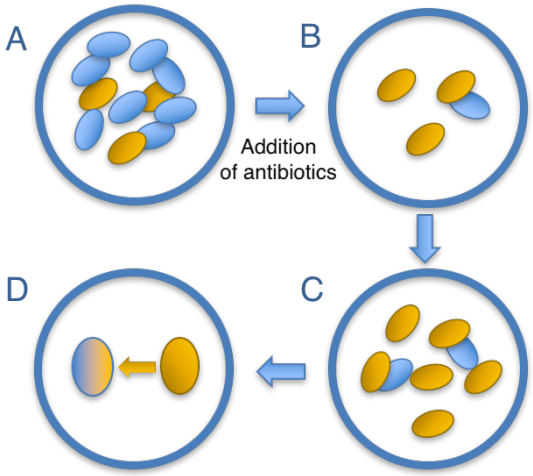


Figure 2.1: A simplified schematic of environmental pressure leading to AMR via horizontal gene transfer in microbial populations. A. A population of susceptible bacteria accompanied by a few microbes with resistance phenotypes on mobile genetic elements. B. On the addition of an antimicrobial most susceptible microbes die out, leaving the resistant portion of the population. C. Unhindered by the antibiotic the resistant microbes reproduce. D. Any remaining susceptible bacteria within the community can become resistant through horizontal gene transfer.

On the other hand, HGT is the mechanism by which bacteria acquire new genetic elements from outside sources [42–45] and it is recognised as one of the most important factors in bacterial evolution [44, 45]. As most genes acquired through HGT are likely to cause deleterious effects to the host microbe, strains which acquire these genes are likely to die out, meaning that such chains in the genetic code do not proliferate. In the cases where gene acquisitions are neutral or "do no harm" [44] their prevalence, or even survival, is down to chance [43]. Genetic elements which confer a selective advantage are likely to survive and quickly proliferate throughout bacterial populations [43]. As well as AMR, HGT can impart metabolic properties such as lactose fermentation, and pathogenic properties can also be transferred between organisms [42].

For HGT to occur three conditions must be met: firstly, there must be a transport mechanism for the donor DNA to the reach the recipient cell; secondly, the new DNA must be incorporated into the genome; thirdly the genetic expression of the new DNA must be beneficial to the recipient [42, 44].

When microbes are under selective pressure from antibiotics, heavy metals and biocides, new ARGs become beneficial to possible recipients, allowing them

to proliferate. It is generally agreed, however, that ARGs introduce a biological fitness cost (for example the cost of producing β-lactamase) [51,52]. These fitness costs have been calculated experimentally [53]. In some mathematical models there is an assumption that the fitness cost causes resistant bacteria to be at a disadvantage to susceptible bacteria, this is generally modelled by adjusting the growth rate of resistant bacteria [38, 54]. There is evidence that microbes can acquire compensatory mutations which mitigate against this fitness cost [50–52]. One way of modelling this might be using a model of horizontal gene transfer which includes both the transfer of ARGs but also the transfer of complimentary genes.

There are three main mechanisms by which HGT can occur: transformation, conjugation and transduction [42, 43]. During transformation, microbes uptake naked DNA from the environment. This DNA is released into the environment by dying and decomposing cells or by living donor organisms. The ability to uptake extracellular DNA is referred to as "competence" [43]. Certain bacterial strains (for example *Neisseria gonorrhoeae*) are perpetually competent, whereas others (i.e. *Bacillus subtilis*) are only competent at certain stages of their lifecycle [42]. Once excreted, DNA must then persist in the environment long enough to be accepted by a competent bacterium, the degradation rates of DNA in certain substances affect the so-called transformation frequency. In soils and in silage it has been shown that DNA can survive for weeks, allowing long timescales on which transformation may occur [55]. Though some species have selection mechanisms for which DNA strands are translocated across the membrane, most transformation occurs indiscriminately for both plasmids and chromosomal DNA[1], though plasmid transformation is often less efficient than for chromosomal DNA.

Conjugation is a process that requires microbes to be in direct contact, exchanging DNA via cell-cell junctions known as pilin bridges. If this DNA is stabilised the recipient organism can then act as a donor, continuing the cycle. This process tends to favour the exchange of plasmids, as the junctions may break down in the time it takes to transfer a longer DNA strand [43, 56]. Conjugation is recognised as an important process in the spread of genetic information and it has been posited that it explains the appearance of similar DNA sequences among distantly related microbial species [56]

Finally, the transfer of bacterial DNA by transduction occurs between a bacterium infected with a bacteriophage (a virus that infects bacteria and incorporates a genetic element or prophage into the bacterium's DNA [57]) and a bacteriophage-susceptible bacterium [42, 56]. DNA is packaged into the phage randomly during replication (generalised transduction) or from the genetic mate-

[1]Plasmids are short sections of non-chromosomal, self-replicating DNA. [43]

rial surrounding the prophage (specialised transduction). When the phage then infects a new bacterium, these genetic elements are conferred.

Once genetic material has crossed into the cell in it needs to be recombined into the host genome, the probability of a recombination event is dependent on both the length of the segment and on the similarity to the host genome. Most of these events maintain the size and function of the recombined segment, but additive integration may cause the area to increase in size, potentially through recombinations of chromosomal DNA and linear DNA [43]. A key factor in the recombination of ARGs are integrons [58], a class of genetic element which capture gene cassettes through site-specific recombination, locating new ARGs into similar locations within the genome. Gene casettes are nonreplicating DNA circles which are large enough to accommodate an ARG. Once the new genetic material has been recombined the genes are expressed by the bacteria and if the new phenotype is advantageous this genetic change may proliferate through a bacterial community.

2.2 Antimicrobials

For certain phenotypic changes to be advantageous to a microorganism, there must be some kind of evolutionary pressure. In the case of AMR, this pressure is exerted by the presence of antimicrobial agents in the environment: mainly antibiotics, biocides and certain heavy metals. Despite the fact that some antibiotics are bactericidal (they kill bacteria and microorganisms) they are generally not classed as biocides. Instead, the term biocides tends to refer to chemicals which are not used specifically to attack microbes, this includes disinfectants, antiseptics and preservatives [59].

Of particular interest when investigating the impact of antibiotics on man-made systems and the environment is the physicochemical behaviour of antimicrobial compounds; the persistence, location, susceptibility to transport mechanisms, tendency to sorb to solids and the bioavailability of chemicals will affect the level of evolutionary pressure exerted onto microorganisms. Hence, understanding the physical behaviour of antibiotics in slurry (e.g. volatilisation, degradation, etc.) is important from a modelling perspective, as the removal of antibiotics from a slurry storage facility (via sorption or degradation) and the spatial distribution of the chemicals are likely to play an important part in the development of AMR in the slurry storage facility. In this section antibiotic modes of action (and the corresponding modes of resistance) are discussed, followed by a brief outline of the physicochemical properties of veterinary antibiotics and how these might relate to mathematical modelling.

2.2.1 Modes of Action and Resistance

A consideration for modelling is the antimicrobial mode of action. For example, models which incorporate factors like antibiotic resistance co-selection with heavy metals will need to consider whether a resistance trait for a particular antibiotic will also cause resistance to a heavy metal.

Antimicrobial agents generally fall into three major pharmaceutical categories [60]:

- Cell-wall biosynthesis inhibitors (CWBI)
- Protein synthesis inhibitors (PSI)
- Nucleic acid synthesisers (NAS)

Cell-wall strength is conferred by the peptidoglycan, held together by the action of transpeptidases and transglycolases [49]. CWBIs, such as β-lactam antibiotics (e.g. cephalosporins), target enzymes containing both these transpeptidases and transglycolases, acting as pseudosubstrates which prolong the time that enzyme active sites are occupied, meaning that the normal cross linking of peptide chains cannot occur and the cell wall is left weak and susceptible to breaking under changes in pressure. Antibiotics which cause cell lysis are referred to as bacteriolytic.

Many important antibiotics, including tylosin, the tetracyclines and the erythromycins are PSIs. These inhibit key protein assembly processes within the ribosome that lead to bacteria being incapable of reproduction and hence unable to proliferate [49, 60]. These processes can include mRNA misreading and translocation step inhibition. An antibiotic which inhibits bacterial reproduction is referred to as bacteriostatic.

By inhibiting the DNA gyrase enzyme, NAS antibiotics such as the fluoroquinolones stop the process of DNA replication, this causes double-strand breaks in the DNA, leading to a reaction within the cell which ultimately kills it [49]. Fluoroquinolones therefore exhibit both bacteriostatic and bactericidal activity [61].

Bacteria have developed four main resistance mechanisms to neutralise the threat of antimicrobial agents [62]:

- enzymatic degradation of antibiotics
- binding protein mutations
- reduced membrane permeability to antibiotics
- Efflux pumps

Microorganisms that are resistant to the β-lactam antibiotics have often acquired genes which allow them to produce β-lactamase, an enzyme which destroys the antibiotic and renders it inert. For example, in the presence of penicillinase, penicillin becomes penicilloic acid which has no effect on cell-wall biosynthesis [49].

Binding protein mutations alter the target sites of antibiotics so that they cannot inhibit processes integral to cell growth. Resistance to quinolone antibiotics occurs via mutations in the quinolone resistance-determining region so that the antibiotics can no longer inhibit DNA replication [60]. Mutations can both completely alter target sites so that antibiotics can no longer bind to them, or simply reduce the affinity of the binding site with the antibiotic [49].

The permeability of the cell wall is a determining factor in the susceptibility of bacteria to antibiotics. In Gram-negative bacteria, hydrophilic drugs enter the cell interior through pore forming porin proteins, while hydrophobic drugs diffuse across the lipid bilayer (though there are antibiotics which can enter the cell through both pathways, such as tetracyclines [63]). Changes in the permeability greatly affect the ability of antimicrobials to enter a cell. Carbapenem antibiotics are β-lactams that are particularly resistant to β-lactamase. Through a mutation in the OprD porin gene, strains of *P. aeruginosa* have become resistant to carbapenems [63].

By pumping out antibiotics before they can reach their target sites, microorganisms can mitigate their presence. Tetracycline resistant organisms tend to overproduce proteins which flush out the drug, rendering the antibiotics useless [49].

Many microbial mechanisms for resisting antibiotics closely mirror those for resisting heavy metals [64]. For example, reducing membrane permeability provides resistance against both Cu and Zn and tetracycline and β-lactams antibiotics. Co-resistance to both heavy metals and antibiotics occurs when microbes acquire resistance or tolerance genes to both substances on the same genetic element [64,65], meaning that the development of resistance to one substance results in resistance to other toxic agents.

It is understood that AMR develops under selective environmental pressure, but comes at a fitness cost [52]. Hence, a reduction in antimicrobial use should result in a reduction in resistant phenotypes, and this is supported by various experiments and theoretical models [52,66,67]. However, co-selection for resistant traits complicates this process *in vivo*. If exposure to a certain toxicant is reduced but contact with another remains, resistance to the removed agent may still proliferate through the environment, this could be true both of heavy metals and of other contaminants added to the tank. This may well be an important factor

when modelling complicated environments like dairy slurry stores.

Gram-positive/Gram-negative effectiveness

Bacteria are often sorted into two sub-groups, gram-positive and gram-negative. One of the key differences between them is the structure of the cell wall. Gram-negative bacteria have a cell wall surrounded by periplasmic space and encircled by a cell membrane, on the other hand, Gram-positive bacteria have no outer membrane and are instead surrounded by a thick cell wall [68]. These differences mean that certain antimicrobials are effective against only one of the two types.

2.2.2 Chemical Fate and Properties of Antibiotics

This section details various pharmacokinetic, pharmacodynamic and physical properties of antibiotics which may affect their distribution and persistence as drivers for AMR and impact subsequently on AMR development and spread within the slurry tank.

Degradation, Volatilisation and Sorption

Chemical degradation is a collection of processes that act to remove chemicals from the slurry tank; at the highest level this can be broken down between biotic and abiotic degradation, each of which describe a number of further processes. Biotic degradation is the enzymatic breakdown of chemicals which is caused by micro-organisms. This can further be divided into aerobic and anaerobic biodegration, both of which generally favour different chemicals. Abiotic degradation processes occur without biological input, examples include photodegradation, hydrolysis and oxidisation. Photodegradation is the process by which chemicals are broken down by exposure to light, these effects would only occur at the top level of an uncovered slurry tank. Some antimicrobials undergo hydrolysis, and are broken down by water, these include veterinary antibiotics like florfenicol and tylosin [69–71].

Volatilisation is the evaporation or sublimation of chemicals into the air, as with photodegradation this process can only occur at the top of an uncovered slurry store.

Sorption is the process of chemical partitioning between the liquid and solid phases in the tank. It can be further broken down between adsorption, where chemicals stick to the outer surfaces of a solid, and absorption, where the chemical diffuses into the interior of the solid. In the cases where the adsorption process is reversible, these molecules can undergo desorption and be released from the solid phase [72]. Adsorption can be roughly split between chemical and physical

adsorption. Where chemical adsorption occurs as a reaction between the solid and the substance sorbing to the surface, and physical adsorption occurs as a result of bonding forces such as hydrogen bonding or van der vaals forces.

pKa

The ionisation state of an antibiotic (whether it is in an anionic, cationic or neutral state) is determined by the pH of the solution that the antibiotic exists in, and the acidic and basic acid dissociation constants (pKa_a and pKa_b) [73]. The pKa_a denotes the (usually acidic) pH value below which an antibiotic compound is cationic (positively charged), whereas pKa_b is the pH value above which the compound is anionic (negatively charged). The ionisation state of a compound is of interest in this study, as it has the potential to affect the physicochemical behaviour of an antibiotic in slurry, properties such as "water solubility, volatility, UV absorption, and reactivity with chemical oxidants" are all affected by the ionisation state of a compound.

Partition and Distribution Coefficients

The distribution coefficient K_d is used to describe the proportion of chemical that sorbs to the solid state and is the ratio between the concentration of the compound in the solid state and the concentration in the liquid state at equlibrium [69, 74] and are specific to the chemical and the medium (e.g. the K_d for penicillin and dairy slurry may well be different to the K_d for penicillin and a loamy soil). K_{ow} is the octanol-water partition coefficient and is used to measure the lipophilic properties of an antibiotic [69, 75], it is defined as the ratio of a chemical's concentration in octanol to its concentration in water. Hence the distribution and partition coefficients of a compound X are given by:

$$K_d = \frac{[X]_s}{[X]_w} \tag{2.1}$$

and

$$K_{ow} = \frac{[X]_o}{[X]_w}, \tag{2.2}$$

respectively. Where the subscripts s, w and o refer to the solid, water and octanol phases. Chemicals with lower K_{ow} values dissolve more easily in water and are less sorbent to solids.

If it is unknown, K_d can be estimated using a known K_{ow} value, using the relation

$$K_d = f_{oc} \times K_{oc} \tag{2.3}$$

where f_{oc} is the fraction of organic carbon in a porous medium and K_{oc} is the carbon-water partitioning coefficient, where there is a known relationship between K_{oc} and K_{ow}. For examples of this relationship see Hemond and Fechner, p.275 [69]. distri How a chemical partitions will affect its availability within a system. For example, an antibiotic which is more likely to exist in the solid state of a medium is likely to be less available to interact with microbes. When modelling the slurry tank, this type of information is important for prediction of antibiotic-microbe interactions.

The use of partition and distribution coefficients assumes a linear correlation between the concentration of chemical in solution and the concentration of sorbed chemical. Though this assumption may not hold true, the practical simplicity of the partition coefficient model means that it remains widely used [74, 76]. One of the potential problems with the K_d model is the so-called particle concentration effect [76], where measured K_d values decrease as particle concentration increases. This has implication for using K_d in models with varying solids concentrations. In chapter 7, a K_d model is used to describe the sorption of antibiotics to solids in the slurry tank, the concentrations of which vary throughout the tank, likely this means that the sorption in the areas of higher solids concentration will have been overestimated.

Adsorption isotherms

In cases where there is a non-linear relationship between free concentration and adsorbed concentration, this can be modelled using sorption isotherms, equations which express the adsorption of a sorbate in relation to the equilibrium adsorption. As sorption is complicated and dependent on many factors, including pH, temperature, solid particle shape and binding sites, many isotherms have been derived, determining which one fits requires experimentation [77]. The simplest isotherms are single-component, for cases when there is only a single substance sorbing to the solids. In the case where there are multiple sorbing substances multi-component isotherms are used. There are many different models and isotherms in use, over 25 different models are detailed in [78]. Some of the commonly used isotherms are presented below.

Single-component Isotherms

The Langmuir isotherm is based on three assumptions:

- the sorbate forms a single layer (monolayer chemical adsorption),
- the adsorption surfaces of the solids are homogeneous,

- the energy released when a particle sorbs to the solid does not vary dependent on the adsorption coverage,

and is characterised by the following equation:

$$q_e = \frac{q_m b C_e}{1 + bC_e}, \tag{2.4}$$

where q_e is the equilibrium concentration of the adsorbed sorbate, q_m is the maximum possible concentration of the adsorbed sorbate, C_e is the equilibrium concentration of the sorbate, and $b = k_{Ad}/k_{De}$ is the Langmuir constant [77,79,80].

The Freundlich isotherm is more adaptable than the Langmuir isotherm, as it can be also used in situations where the adsorption surfaces are heterogeneous and can be used to model both chemical and physical adsorption [77]. The Freundlich isotherm is expressed as

$$q_e = K C_e^{1/n}, \tag{2.5}$$

where, once again, q_e is the equilibrium concentration of the adsorbed sorbate, C_e is the equilibrium concentration of the sorbate and K and n are Freundlich parameters to be determined.

The Sips isotherm combines the Langmuir and Freundlich isotherms and is given by

$$q_e = \frac{q_m b C_e^{\beta_s}}{1 + a_s C_e^{\beta_s}}, \tag{2.6}$$

here β_s is the Sips isotherm exponent and a_s is the Sips isotherm model constant [78]. At low sorbate concentrations the Sips model behaves similarly to the Freundlich model and as the sorbate concentration increases it simulates monolayer adsorption as in the Langmuir model.

Multi-component Isotherms

In the case where there are multiple sorbates in the liquid phase, adsorption becomes competitive. This means that the single-componenet isotherm models no longer apply, so multi-component isotherms were developed instead. Two examples are provided below for a system with N competing sorbates.

The multi-component Langmuir isotherm is given by

$$q_{e,i} = \frac{q_m b_i C_{e,i}}{1 + \sum_{j=1}^{N} b_j C_{e,j}}, \tag{2.7}$$

where the i subscript refers to sorbate i. The multi-component Langmuir–Freundlich

is given by

$$q_{e,i} = \frac{q_m b_i C_{e,i}^{k_i}}{1 + \sum_{j=1}^{N} b_j C_{e,j}^{k_i}}, \tag{2.8}$$

where k_i is a kinetic parameter to be determined [77, 81].

Pharmacodynamic models

Pharmacodynamic (PD) models describe the relationship between antibiotic concentration and antibiotic effect [82, 83]. There are three primary types of PD model: direct effect models, biophase distribution models and indirect response models [82–84]. Direct effect models directly correlate a drug's concentration, C, with some measured effect, E (for example, in the case of applying antibiotics to bacterial populations, E might be inhibition of cell reproduction or cell death). There are various direct effect models, the simplest is the fixed effect model:

$$E = E_f \text{ if} C > C_t. \tag{2.9}$$

Here, E_f is the fixed effect, and C_t is a threshold concentration [82]. This model is appropriate for cases where the effect of interest is an either/or scenario, for example, E_f could be the total elimination of a population of bacteria by some antimicrobial. However, if the modeller had any interest in the population dynamics up until that point, a more complicated model would be required. One example of such a model is the sigmoid E_{max} model:

$$E = \frac{E_{max} C^n}{EC_{50}^n + C^n}, \tag{2.10}$$

where E_{max} is the maximum effect, EC_{50} is the concentration at which half of the maximum effect occurs and n is a Hill coefficient which determines the steepness of the slope. The $n = 1$ case is the standard E_{max} model [82–85]. The E_{max} model was introduced to replace earlier linear models of the concentration-effect relationship, as it was found that linear models were only valid in very limited cases [84]. The E_{max} model is widely used in dose-response modelling [86] and has been used in models of agricultural antimicrobial resistance [38, 39].

Biophase distribution models were designed to explain the delay between a drug concentration in a body fluid (such as plasma) and the effect of the drug. These are useful as in animals or humans, as it can be difficult to determine the drug concentration at the target site [85]. However, in the case of slurry modelling, the "target site" is bacteria in the slurry, so there is no equivalent plasma to target site delay.

Indirect response models describe a delayed drug effect due to some indirect mechanism of action [84,85]. For example, the drug may inhibit the production of some chemical, and the existing concentration of that chemical at the target site causes a delay between the drug administration and the measured effect. In indirect response models, drug effect is usually calculated using ordinary differential equations and will sometimes incorporate elements from direct effect models, such as the E_{max} model, to describe concentration-effect relationships over time [84].

PK/PD modelling

PK/PD modelling links the pharmacokinetic (PK) and pharmacodynamic (PD) approaches to describe the relationship between dose and drug effect (as opposed to the dose-concentration relationship or the concentration-effect relationship) [82]. To do this, PK/PD models combine elements of PK and PD models. This approach can also be extended to include population modelling [87]. In the models discussed in later chapters, elements of PK and PD models are used to model bacterial populations.

The next section discusses the particular problem of AMR in agriculture, alongside the existing legislation in place to reduce the spread of AMR.

2.3 Agriculture and the Challenge of AMR

The uses of antimicrobials in agriculture are various; they are administered both subtherapeutically (for growth promotion and production) and prophylactically (to preemptively avoid diseases) [88, 89]; they have been found to aid growth promotion in food animals (though this practice was banned by the EU in 2006 [90, 91], it is still approved by the Food and Drug Administration (FDA) in the USA [92]); antibiotics are used for disease treatment, for example mastitis in dairy cows [93]; and heavy metals are used in foot baths for cattle [94]. There are some restrictions placed on the prophylactic use of antibiotics (and growth promotion in America), for example the FDA limits the use of cephalosporins and other drugs important for human-health [91].

The mechanisms by which agricultural antimicrobial use might affect human health are not very well understood. This is often due to the indirect nature of potential acquisition of resistance. However, there is evidence that farmers can be affected by antimicrobial use and that there are correlations between resistance in animals and resistance in farmers [95–97]. There are also risks of colonisation or incubation for companion animals [98] and of nearby wildlife, which may spread AMR to waterways [2, 31].

Tang et al. [97] performed a meta-analysis to determine the effects of interventions which reduced antibiotic use in food-producing animals. They found that reducing antibiotic use in animals decreased the prevalence of antibiotic resistance in animals by around 15% and the prevalence of multidrug resistant bacteria by $24 - 32\%$. The analysis also revealed that reduced antibiotic use in animals led to a 24% reduction in antibiotic resistance prevalence in humans. However, this result is less robust, as there were only 13 studies available for analysis, and they were primarily (9 out 13) studies of farmworkers and not the general population. Booton et al. [99] modelled the impacts of antibiotic use on human health and found that reducing animal antibiotic usage and animal to human transmission could have a substantial effect on human colonisation (16.8% and 17.1% reduction in prevalence, respectively), but that for human health, the reduction of human antibiotic use was much more effective in reducing AMR prevalence.

2.3.1 Farm Slurry and its additional Challenges

There are approximately 13,000 Dairy farms in the UK (including bovine, sheep, goat and buffalo milk producing farms) [100]. The government advises that all dairy farms have a slurry storage capacity for at least four months of waste [101]. Dairy farm slurry tanks are filled with faeces and urine, waste milk, used footbaths, bedding and the runoff from parlour washings. This creates a potent environment for the growth of microorganisms, but also potentially for AMR. Though the Department of Health recognises the spreading of slurry onto crops as a factor influencing the development of AMR[2], current slurry storage and management regulations guidelines concentrate heavily on structural requirements and farmworker safety during mixing or other slurry disturbing actions rather than on AMR prevention or pollutant removal. Existing guidelines include regulations on store location, capacity and drainage pipe design [15, 101, 102].

There are various mechanisms that affect the distribution and removal of antimicrobials in the slurry tank [69]. Different processes are likely to dominate at different levels of the tank and this will also depend on which antibiotics are present. For example, photodegradation will only occur on the surface layer of slurry, aerobic degradation will occur near the top of the tank but deeper down where the environment becomes more anoxic only anaerobic degradation can take place. Understanding the dynamics of these processes could be essential for the development of physical models. Farm slurry contains various solids, from bovine

[2]Slurry is spread onto crops for both human and livestock consumption, this second action potentially creates a kind of AMR feedback loop, where crops covered with ARGs and antimicrobials are eaten by cows, excreted back into the slurry tank and then spread on crops again.

faeces, muck in the waste footbaths and from waste bedding.

2.3.2 What policies are in place to stop AMR in agriculture?

As farm slurry spread on agricultural land may be a route for pathogens into the human food chain [103] the extent to which the slurry tank environment drives the development and spread of AMR is of particular interest from a human health perspective. A greater understanding of on-farm dynamics is also important for effecting policy change to better protect against the risks of AMR developing within agriculture. Though there is government policy in place intended to combat the development of agricultural AMR, it is mostly concerned with the reduction of antibiotic use, which is a high priority [104]. For example, in the UK (and EU), antibiotics cannot be used as growth promoters [90–92]. Furthermore, in 2018 the EU approved legislation banning the use of antibiotics as prophylactics in farming, to come into force in 2022 [105]. The existing UK policy around slurry storage and spreading is generally intended to manage soil nutrient levels [106] and not AMR, despite the fact that there is evidence that run-off from farms and manure-fertilised fields may result in the contamination of the local environment [107]. The Food Standards Agency (FSA) provides guidance for slurry storage and management with the aim of reducing pathogen transfer to ready to eat foods, though there is no mention of AMR and farmers are not obligated to follow the guidance [108]. Though the FSA advises storing slurry for longer to reduce the number of pathogens in the tank, it is not known what the effects of long storage times are on the prevalence and spread of AMR. As policy influences farm practice, if there are slurry storage processes, such as tank filling and emptying, which are increasing the risk of agricultural AMR, it is important that they are understood so that policy can be put into place appropriately.

In the UK, the Responsible Use of Medicines in Agriculture Alliance (RUMA) set a series of targets for reducing the use of antibiotics in eight sectors of agriculture in 2017, including the dairy sector [109]. These targets aim to both reduce the total quantity of antibiotics used, and limit the use of antibiotics that are of a high priority for human health. By the end of 2018 the dairy sector reported a 35% reduction in total antibiotics used, bringing it under the proposed target of a 20% reduction by 2020. RUMA refer to this as "significant progress" [110] and also note that both the beef and dairy networks formed stewardship groups that are working together to efficiently manage antibiotic usage in cattle. Other sectors, such as pig farming, did not meet their overall targets, but did limit the use of high-priority antibiotics [110].

AMR has been recognised as a threat in agriculture and as such there are policies in place across the globe to limit the development and persistence of resistant bacteria. Maron et al. [91] broadly split agricultural antimicrobial policy into three groups across the globe:

- Restricted, where both:
  - Antimicrobials cannot be used as growth promoters.
  - Farmers require a veterinary prescription to use antimicrobials in feed.
- Semi-restricted, where either:
  - Ban or partial ban on the use of antimicrobials as growth promoters.
  - Farmers require a veterinary prescription to use antimicrobials in feed.
- No restrictions:
  - No legislation on the use of antimicrobial growth promoters (AGP).
  - No requirement for veterinary prescriptions for the use of antimicrobials.

The UK (and the rest of the EU) fall into the restricted category. Denmark was an early adopter of high level restrictions on AGPs and so in many ways are the best test case for the economic effects of the regulation of AGPs, and they have seen a large decrease in both agricultural antimicrobial use and resistance [111, 112].

2.4 Factors affecting AMR within the slurry tank environment

The presence of antibiotics from bovine excretions and waste milk, and the biocides present in footbaths means that there are potentially high levels of selective pressure within dairy farm slurry stores, the contents of which are spread over both human and animal food crops at certain times of year.

The composition of dairy slurry as well as various environmental and process factors may affect the persistence and spread of AMR. For example, the solubility of chemicals is affected by pH. In alkaline conditions metal ions in +2 ionisation states adsorb more readily onto solids which will affect their interactions with microbes in the tank. Similarly pH might affect the degradation rate of antibiotics; enrofloxacin removal from aqueous matrices can increase in acidic conditions [113]. Furthermore, drugs like enrofloxacin degrade more readily at

higher temperatures. The combined effects of pH and temperature also affect microbial growth, as modelled by Rosso et al. [114], indicating that both factors may play a role in how AMR develops in the slurry tank. Alongside this the solid to liquid ratio within the tank will also affect partitioning and distribution of antibiotics, whilst the availability of nutrients, metals and antibiotics in the solids and liquids will effect the growth of microbial communities.

Farm practices inform on the storage environment and also have the potential to affect AMR in the slurry tank. The rate with which it is filled and emptied, how long the slurry is stored for, how often (and how assiduously) the tank is cleaned, the extent of tank mixing, and decisions about what is deposited into the slurry tank all could affect the presence and persistence of AMR.

As mentioned in subsection 2.2.1, the mode of resistance for heavy metals and other biocides is often similar to those against antibiotics. Footbaths containing formalin, Cu and Zn are regularly used in dairy farming and are often disposed of into a manure store or slurry tank [94]. This is also true of the Sutton Bonington Dairy farm at the University of Nottingham. This adds another dynamic to the development of AMR in the slurry tank: co-selection of antibiotic, biocide and metal resistance.

There is also evidence that seasonality has some effect on the development of AMR in agricultural environments. Work by Chen et al. [115] suggests that there may be some seasonal variation in AMR spread in swine wastewater[3]. Furthermore, Awad et al. [116] found that, in general, concentrations of tetracycline and sulfonamide antibiotics sampled from a river used to feed swine were higher in September than in June. Seasonal changes in antibiotic concentration could potentially lead to selection pressure for AMR, leading to an increase in ARG prevalence in wastewater.

Sui et al. [117] measured the prevalence and removal efficacy of three tetracycline resistance genes, four macrolide resistance genes, a class 1 integron gene and bacterial 16s rRNA genes over two swine wastewater treatment systems in summer and winter. Sui et al. [117] found a significant difference in abundance of all ARGs between summer in winter at both farms and at all sampling points. In general, ARGs were more prevalent during the winter. This could be caused by the persistence of antibiotics in the environment as found by Awad et al. [116] or could be due to antibiotic prescription patterns as posited by Sui et al. [117]. Göbel et al. [118] found that sulfonamide and macrolide antimicrobial abundances in wastewater from municipal wastewater treatment plants correlated well with

[3]Chen et al. [115] analysed samples of wastewater to examine the occurence of erythromycin and tetracycline resistance genes and found that there was some evidence of seasonal variation, but that further comparative study was necessary.

yearly consumption data.

A further option is that the temperature affects the degradation of antibiotics within the wastewater[4]. Without knowing the extent of the seasonal temperature fluctuations in the tank it is hard to test this theory.

2.5 Mathematical modelling of AMR

Mathematical models of physical systems can provide insight into the underlying mechanisms which drive real world processes. The combination of modelling and real data allows scientists to simulate experiments that would be costly or impossible in regulated environments. This could prove particularly useful in agriculture, as altering farming practice on working farms is often untenable. For example, altering the mix of chemicals dumped into dairy slurry storage would not be possible on a working farm without finding potentially costly alternative disposal methods, whereas with an appropriately conceived mathematical model all that would be required is an alteration of the parameters.

As noted by Thanner et al. [9], the existing mathematical models of AMR in agriculture lack depth: they often model the emergence of a single resistant pathogen (or treat all pathogens as a homogenous mass), the single pathogen is often considered only in the context of a single antibiotic, not taking into account the use of other antimicrobials, and the wider environmental context is widely ignored, despite the fact that variables such as temperature and seasonality affect the development of AMR [117,119]. Existing agricultural models can be split into two categories: those that model the effect of antibiotic use in agriculture on humans and those that model the spread and prevalence of AMR in agricultural systems. Smith et al. [17] and Bunnik & Woolhouse [120] both take an epidemiological approach, modelling the spread of AMR bacteria between humans. Here the variable of interest is the number of humans infected with a resistant pathogen. Both reach a similar conclusion: that the quantity of antibiotics used in agriculture has little effect on the prevalence of AMR in humans. Smith et al. also posit that agricultural antibiotic usage may hasten the development of AMR in humans, despite having little effect on its prevalence, while Bunnik & Woolhouse identify the reduction of human-animal AMR transmission as a potential method for reducing AMR in humans. The work of by Volkova et al. [39] and Baker et al. [38] model the spread and prevalence of AMR in cow stomachs and dairy slurry tanks, respectively. In these models the variable of interest is the

[4]There is some evidence that this may not have an effect, as Dolliver et al. [119] found that temperature did not have a significant effect on antibiotic degradation rates during manure composting.

number or proportion of resistant bacteria within the system. Both show that, under their model structures, one of the biggest factors for AMR prevalence is the rate of transfer of resistance genes between microbes.

Parameter value selection is a particularly difficult task when building models in agricultural AMR. For example, horizontal gene transfer (HGT) is an integral process in the development and spread of AMR, a simple "rate of transfer" coefficient to describe HGT, as used by Baker et al. and Volkova et al. [38, 39], is difficult to calculate due to the factors which affect it, which include the composition of the medium, the presence of bacteriophages and the persistence of ARGs in the environment [121]. However, to properly model AMR at a microbial level, HGT is a necessary model component.

Smith et al. were criticised by Barber et al. [122] for the lack of clarity surrounding the choice of their parameter values. Furthermore Barber et al. [122] have shown through sensitivity analysis that potentially plausible changes to parameter values within Smith et al.'s model lead to drastic changes in the equilibrium prevalence of AMR. This seems to be a relatively common occurrence in models of AMR; Leclerc et al. [121] found that, in survey of 43 models that include HGT, nearly half of the models in their survey included assumed parameter values without giving any citation.

Despite these limitations, mathematical modelling of the problem has still been used to identify possible avenues of future research. Both Baker et al.'s and Volkova et al.'s models emphasise the importance of between-microbes gene transfer on the persistence of AMR [38,39]. On a population scale Smith et al. [17] claim that agricultural use has little effect on the total level of AMR in humans but do not address the problem of environmental health. Similarly, in van Bunnik et al.'s model analysis, they purport that the amount of antibiotic used has little effect on AMR in humans but slowing the transfer of resistance between humans and animals may be more effective at reducing AMR than reducing the quantities of antibiotics used [120]. These all open up interesting pathways and focus points for further research, as well as creating space to design improved models.

2.5.1 Existing Mathematical Models

This section details existing some of the existing agricultural models and a number of models developed outside of the agricultural setting which could be developed to aid modelling in a slurry tank environment.

Agricultural models

There are relatively few mathematical models which explicitly model AMR in agriculture or the effect of agricultural AMR on the wider population. In their survey of models that study HGT, Leclerc et al. [121] found, of 43 models, 7 relating to agriculture, specifically in cattle, beef feedlots and dairy slurry tank. Alongside models of specific agricultural environments, the models developed by Smith et al. and van Bunnik et al. use ODEs to model the effects of agricultural AMR on the human population [17, 120].

The only existing model of AMR in dairy slurry was developed by Baker et al. [38] and draws on the Volkova et al. model discussed below. Their coupled ODE model quantifies the development and spread of antimicrobial resistance in stored dairy-farm slurry, using parameter values from the University of Nottingham research farm at Sutton Bonington. The model assumes the distribution of chemicals and bacteria is spatially homogeneous and is modelled using ODEs. A pair of coupled ordinary different equations describe the proliferation of resistant and susceptible bacteria using parameters focussed on the Sutton Bonington slurry tank. Baker et al. assume the tank fills continuously at rate λ from an initial volume of V_1, hence the volume of slurry in the tank is given by $V(t) = V_1 + \lambda t$. The total number of possible bacteria N_{max} is given by the carrying capacity of liquid slurry multiplied by the total volume of slurry in the tank, hence $N_{max}(t) = \mu V(t)$. The dynamics of the antibiotic, $A(t)$ are modelled using an ODE describing exponential decay and constant inflow:

$$\frac{dA}{dt} = -\gamma A + \theta \tag{2.11}$$

where γ is the rate of antibiotic decay and θ is the rate of antibiotic inflow. Solving this equation with initial condition $A(0) = A_1$ gives

$$A(t) = \left(A_1 - \frac{\theta}{\gamma}\right) e^{-\gamma t} + \frac{\theta}{\gamma}. \tag{2.12}$$

In this model bacterial growth is modelled using a modified version of logistic growth. Under a standard logistic growth regime the the growth of a single bacteria strain, B, with no other bacterial strains present is given by

$$\frac{dB}{dt} = r\left(1 - \frac{B}{N_{max}}\right) B, \tag{2.13}$$

where r is the bacterial growth rate and N_{max} is the total possible number of bacteria in the system. Baker et al. incorporate an additional multiplier, (E_r or E_s, depending on whether or not the bacterial strain is resistant or susceptible,

respectively), to account for the effects of antibiotic on bacterial growth. Typical parameter values are shown in Table 2.1. By using one-at-a-time sensitivity analysis they find that their model is most sensitive to the rate of horizontal gene transfer and the time at which the tank is emptied (assuming that when the tank is emptied it is also cleaned). By choosing a Hill-function dependence on antibiotic concentration E_R and E_S are given by

$$E_R = 1 - \frac{E_{max}\left(\frac{A}{V}\right)^H}{MIC_R^H + \left(\frac{A}{V}\right)^H} \tag{2.14}$$

$$E_S = 1 - \frac{E_{max}\left(\frac{A}{V}\right)^H}{MIC_S^H + \left(\frac{A}{V}\right)^H}, \tag{2.15}$$

where E_{max} is the maximum effect of antibiotics on bacterial growth, H is the hill coefficient, MIC_R is the minimum inhibitory concentration of resistant bacteria and, similarly, MIC_S is the minimum inhibitory concentration of susceptible bacteria. To model horizontal gene transfer (HGT) a "force of transfer" function is used ($\beta R/N$, where β is the rate of HGT). Though not mentioned explicitly in the text, it appears that Baker et al. are only modelling conjugation and not transformation or transduction. Their parameterisation of β draws only on reported rates of conjugation [53, 123]. Furthermore, both transformation and transduction rates are dependent on processes not measured in Baker et al.'s model: cell death and phage presence, respectively [42]. Finally the rate of inflow of each bacterial strain to the tank is given by the total inflow multiplied by concentration of each bacterial strain into the tank. Hence, using $N = S + R$ the equations which describe the growth of susceptible and resistant strains of bacteria, respectively, are:

$$\frac{dS}{dt} = r\left(1 - \frac{N}{N_{max}}\right)E_s S - \frac{\beta SR}{N} + \lambda(1-\rho)\nu \tag{2.16}$$

$$\frac{dR}{dt} = r(1-\alpha)\left(1 - \frac{N}{N_{max}}\right)E_r R + \frac{\beta SR}{N} + \lambda\rho\nu. \tag{2.17}$$

This model omits several environmental factors and also concentrates exclusively on one type of microbe (*E. coli*) interacting with a single antibiotic. The modelling is specific to *E. coli* ostensibly only in its parameterisation. It could therefore be adapted to model other bacterial strains relatively easily by selecting or inferring different parameter values. In reality, slurry stores are likely host to various microbes and polluted by various antimicrobials, heavy metals and other chemicals and is subject to various environmental changes. Also, the model is primarily concerned with the microbe-antibiotic interactions and does not take

environmental and slurry-storage practices like stirring and tank emptying into account.

Parameter	Description	Typical Value
r	Specific growth rate of *E. coli*	0.5 h^{-1}
β	Gene transfer term	0.001 h^{-1}
λ	Rate of slurry inflow to tank	613 lh^{-1}
ν	Concentration of bacteria in slurry inflow	6×10^7 $CFUl^{-1}$
ρ	Proportion of resistant bacteria in inflow	0.4
α	Resistance fitness cost as a fraction of r	0.1
V_1	Initial volume of slurry in the tank	150,000 l
A_1	Initial quantity of antibiotics in the tank	0 μg
θ	Rate of antibiotic inflow	3422 μgh^{-1}
E_{max}	Maximum effect of antibiotics on bacterial growth	2
H	Hill coef cient in E_{max} model	2
MIC_S	MIC for sensitive bacteria	8 μg
MIC_R	MIC for resistant bacteria	2000 μg
μ	Carrying capacity of liquid slurry	10^{10} $CFUl^{-1}$
γ	Decay rate of antibiotics	0.0029 h^{-1}
t	time	$t \in \mathbb{R}$ h

Table 2.1: Typical Parameter Values from Baker et al. [38]

The Volkova et al. model [39] is a similarly spatially homogeneous model of the development and maintenance of ceftiofur cephalosporin resistant *E. coli* in cattle gut. Like the Baker et al. [38] model it consists of a set of coupled differential equations describing the development of growth dynamics of susceptible and resistant bacteria before and during treatment with antibiotics. The before-treatment dynamics are given by:

$$\frac{dN_S}{dt} = r\left(1 - \frac{N}{N_{max}}\right)N_s - \frac{\beta N_r N_S}{N} + (1-\eta)\gamma N - \gamma NS \quad (2.18)$$

$$\frac{dN_r}{dt} = r(1-\alpha)\left(1\frac{N}{N_{max}}\right)N_r + \frac{\beta N_r N_S}{N} + \eta\gamma N - \gamma N_r \quad (2.19)$$

and during treatment:

$$\frac{dN_S}{dt} = r\left(1 - \frac{N}{N_{max}}\right)E_s N_s - \frac{\beta N_r N_S}{N} + (1-\eta)\gamma N - \gamma N_S \quad (2.20)$$

$$\frac{dN_r}{dt} = r(1-\alpha)\left(1\frac{N}{N_{max}}\right)E_r N_r + \frac{\beta N_r N_S}{N} + \eta\gamma N - \gamma N_r \quad (2.21)$$

here N_r and N_s are the numbers of resistant and susceptible bacteria, respectively

and

$$E_i = 1 - \frac{E_{max} C^H}{MIC_i^H + C^H} \tag{2.22}$$

for $i = r, s$ where C is the ceftiofur concentration and all other parameters are as described in Table 2.2.

Parameter	Description	Typical Value
r	Specific growth rate of bacteria	0.17
γ	Fractional in-flow/outflow	0.01
N_{max}	Max *E. coli*	-
H	Hill coefficient	1.5
MIC_S	Minimum inhibitory concentration for susceptible bacteria	1
MIC_R	Minimum inhibitory concentration for resistant bacteria	8

Table 2.2: Typical Parameter Values from Volkova et al. [39]

The model suggests that resistant bacteria could persist between ceftiofur treatments, in the absence of selective pressure. Volkova et al. assume that there is some fitness cost to resistance, which results in a low fraction of resistant bacteria between treatments. However, Roux et al. [124] found that in certain cases, ARGs can, in fact, contribute to a greater bacterial fitness. If this is the case for ARGs found in cattle gut or slurry, it might drastically change the quantity of resistant bacteria entering the slurry tank.

A number of other models also focus on cattle gut bacteria [125–127]. All of these models are deterministic, except for [125], which examines the effects of stochasticity on the development of AMR in enteric *E. coli*, and found that stochasticity in the model parameters increased the distribution of resistant *E. coli*.

On a worldwide scale, an infection style model to analyse the effect of total animal antibiotic usage (AAU) and total medical antibiotic usage (MAU) on humans has been developed by Smith et al. [17]. This model includes the use of antimicrobials across all food producing animals, for growth promotion as well as disease treatment and control[5]. Their model follows a similar structure to an SIR model and is simulated using the following system of coupled differential equations:

$$\dot{X} = (\mu + \lambda + \nu Y + \beta Z)W - (\theta + \alpha + \rho)X \tag{2.23}$$

$$\dot{Y} = \theta X + \phi Z - (\rho + \sigma)Y \tag{2.24}$$

[5]N.B. the practice of using antibiotics as growth promoters was banned in the EU in 2006 [90, 91].

$$\dot{Z} = \rho(X+Y) - (\gamma+\phi)Z \tag{2.25}$$

$$\tag{2.26}$$

where X, Y and Z are the proportion of exposed, colonised and amplified humans, respectively. Amplified humans are those with elevated levels of resistant bacteria, amplified by antibiotic use. See Table 2.3 for parameter values.

Parameter	Description	Typical Value
X	Proportion Exposed Humans	Varies
Y	Proportion Colonised Humans	Varies
Z	Proportion Amplified Humans	Varies
W	Proportion Unexposed Humans	$W = 1 - X - Y - Z$
μ	Rate of background exposure	10^{-6}
λ	Rate of exposure from agriculture	10^{-3}
α	Transient loss rate	0.1 per day
θ	Colonisation rate	0.001 per day
σ	Colonised loss rate	0.003 per day
γ	Amplified loss rate	0.007 per day
ϕ	Recolonisation rate	0.003 per day
ρ	Prescription rate	0.003 per day
ν	Contact rate, colonised	10^{-5} per day
β	Contact rate, amplified	0.5 per day

Table 2.3: Parameter Values from Smith et al. [17]

Through the design of the model and the pressure exerted by the combination of background AMR bacteria and medical antimicrobial use, the presence of AAU does has little effect on the equilibrium prevalence of antimicrobial resistance, whereas increased MAU has a larger effect on the equilibrium prevalence. Figure 2.2 shows the prevalence ($X + Y + Z$) equilibrium value as AAU (λ) and MAU (ρ) vary. However, increased AAU does reduce the time to emergence of AMR strains, meaning that the equilibrium level is attained almost four years earlier, as shown in Figure 2.3. The impact of this is that if a drug is approved for agricultural use before or at the same time as for medical use, it can cause AMR to develop much more quickly than if the antibiotic were used solely for medical purposes. Hence, according to this model, restricting AAU is most effective when AR bacteria remain rare.

An ODE modelling approach was also adopted to explore the impact of agricultural AMR on the human population by van Bunnik and Woolhouse [120]. Their model consists of a pair of coupled ODEs to describe the exchange of resistant bacteria between a human population and a food animal population. In

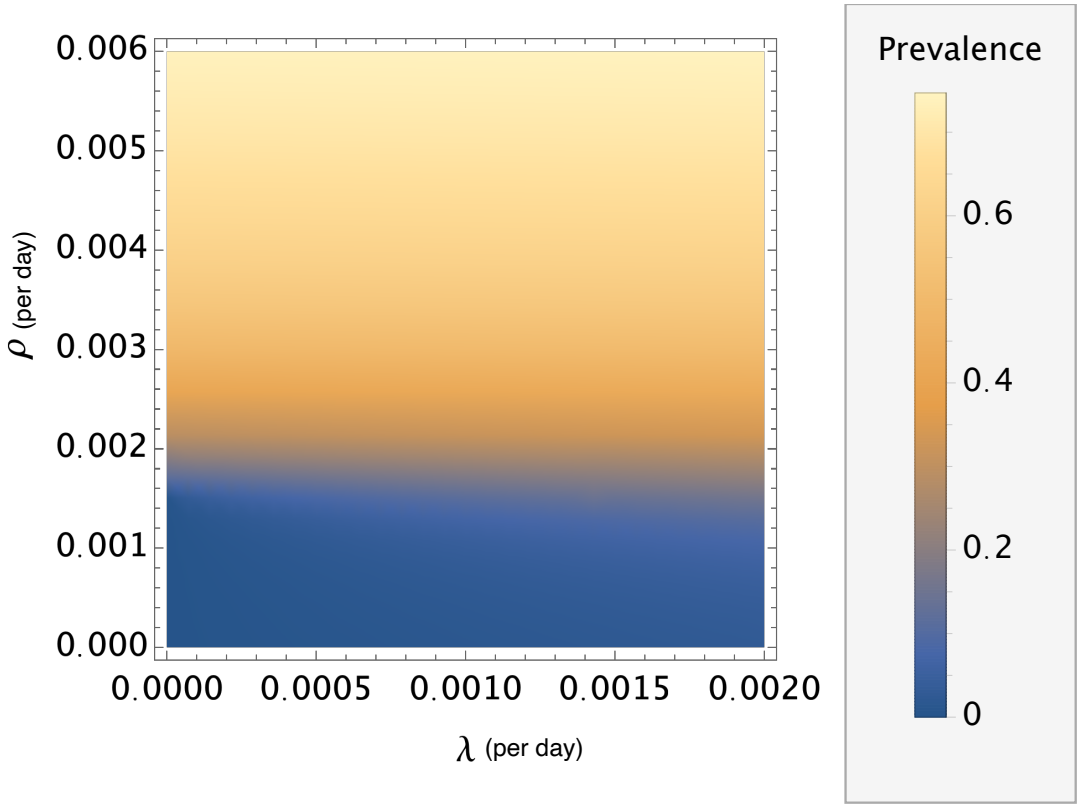


Figure 2.2: AMR Prevalence under the Smith et al. model as animal antibiotic use (λ) and medical antibiotic use (ρ) vary. Here prevalence is given by $X + Y + Z$, the proportion of the population with some level of AMR exposure. Though animal antibiotic use has some effect on the prevalence of AMR, the effect of medical antibiotic use is much clearer.

the model humans and animals gain AMR through use of antibiotics and contact with infected humans and animals. Both humans and animals can revert to only harbouring susceptible bacteria. The equations model the fraction of humans with resistance (R_H) and the fraction of resistant food animals (R_A):

$$\frac{dR_H}{dt} = \overbrace{\Lambda_H(1-R_H)}^{\text{Antibiotic use}} + \underbrace{\beta_{HH}R_H(1-R_H)}_{\text{Human exposure}} + \overbrace{\beta_{AH}R_A(1-R_H)}^{\text{Animal exposure}} - \underbrace{\mu_H R_H}_{\text{Revert to susceptible}} \tag{2.27}$$

$$\frac{dR_A}{dt} = \Lambda_A(1-R_A) + \beta_{AA}R_A(1-R_A) + \beta_{HA}R_H(1-R_A) - \mu_A R_A, \tag{2.28}$$

where Λ_H and Λ_A are the per capita rates at which humans and animals acquire resistant bacteria through antibiotic exposure, respectively; β_{HH} and β_{AA} are the per capita rate at which humans acquire resistant bacteria through contact with with other humans and the rate at which animals acquire resistant bacteria through contact with other animals, respectively; β_{HA} is the rate at which humans acquire resistant bacteria through contact with animals and β_{AH} is the reverse;

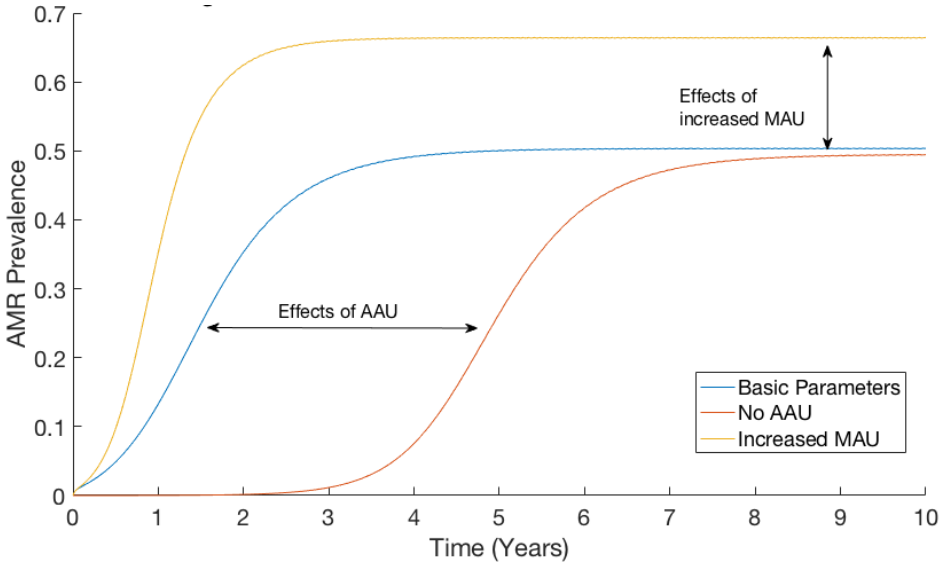


Figure 2.3: Emergence of AMR Prevalence under the Smith et al. Model. Three realisations of the Smith et al. model [17]. Red: Parameter values as in Table 2.3. Blue: No animal antibiotic usage (AAU), $\lambda = 0$, all other parameters as in Table 2.3. Yellow: Increased medical antibiotic usage (MAU), $\rho = 0.0045$, all other parameter values as in Table 2.3. Reduced AAU increases the time taken to reach AMR equilibrium prevalence but only has a small impact on the equilibrium value. Increased MAU, on the other hand, both reduces the time to equilibrium and increases equilibrium prevalence.

μ_H and μ_A are the human and animals rates of reversion to only harbouring susceptible bacteria, respectively.

Like Smith et al. [17], van Bunnik and Woolhouse [120] conclude from their model that AAU has little impact on the level of resistance in humans. However, their model indicates that it is in fact the rate of transmission from animals to humans that might play an important role in the fight against resistance. This has relevance to the slurry tank problem, as the spreading of slurry onto human crops may contribute to the rate of human to animal transmission.

Non-agricultural models

Compared to agricultural models of AMR, there are many more models of AMR in hospital or clinical settings (a number of which are detailed in depth by Spicknall et al. [128]). This is potentially due to the fact that AMR in hospitals presents a much more obvious and seemingly immediate threat to human health, as it has been recognised that calculating the threat of agricultural AMR to human health is difficult [97].

To give some sense of the disparity in the research outputs between clinical and agricultural AMR, at the time of writing, a Web Of Science search for the keywords "antimicrobial resistance" and "hospital" returns 13949 records, whereas a search for the keywords "antimicrobial resistance" and "agriculture" returns only

758. Here, a summary of various clinical and non-agricultural models of AMR is given, especially highlighting models which might inform further work with an agricultural focus.

Kim et al. [129] propose a model to calculate the production capacity of seven tetracycline resistant genes (TRG) and of tetracycline resistant bacteria (TRB) in activated sludge[67].

Using mass balance equations, they provide a mathematical framework for the production of these elements. The production capacities (PCs) for TRB and TRG are given by:

$$PC_{TRB} = \frac{X_{TRB}\tau}{\theta_C}(1 + b_{TRB}\theta_C) - X_{TRB,in} + X_{TRB,eff} \tag{2.29}$$

$$PC_{TRG} = \frac{X_{TRG}\tau}{\theta_C}(1 + b_{TRG}\theta_C) - X_{TRG,in} + X_{TRG,eff} \tag{2.30}$$

where X_i is the total concentration of gene i, $X_{i,in}$ is the concentration of gene i in the inflow to the system, $X_{i,eff}$ is the concentration of gene i in the effluent, τ is the hydraulic retention time, θ_C is the solids retention time and b_i is the decay coefficient of gene i. These equations were then used to calculate the TRB and TRG production capacities of three wastewater treatment plants.

Kim et al. discovered that though net TRB was not significantly different from zero in all three plants, the TRG production capacity of two out of the three plants was negative, suggesting some attenuation of this gene. Across these three plants activated sludge is not producing TRB. However, there is no attenuation, suggesting that treatment plants could still be a significant point source of resistant bacteria into the environmental resistome.

Analysis of the effects of treatment plants on the environmental resistome is conducted using three non-linear regression models by Amos et al. [131]. Their first model predicts that waste water treatment plants can account for approximately fifty percent of the variance of AMR between different sampling sites on the Thames, confirming the impact of treatment plants on the resistome. Their second model, which includes environmental factors like land coverage and rainfall, can explain around eighty-three percent of the variability in class 1 integron[8] prevalence at a single point in the river and can be used to simulate the impact of introducing a treatment plant to a clean site.

[6]Tetracyclines are used both in agriculture and to treat human disease [89].

[7]The activated sludge process is the inoculation of sewage or wastewater with bacteria to increase the efficiency of wastewater treatment. [130]

[8]Class 1 integrons are genetic elements strongly associated with AMR. Integrons allow bacteria to to acquire and express new genes, they are often inserted into transposons and plasmids, which makes them important for HGT. Class 1 integrons are so important in the study of AMR because nearly half of those found in the environment carry *qac* genes which code for membrane efflux proteins, an important mechanism for flushing out certain antimicrobial agents [132, 133].

Spicknall et al. [128], conducted a literature review of mathematical models of the evolution and spread of AMR between hosts within a hospital setting. They classify hosts into four categories; susceptible, infected with sensitive bacteria, infected with resistant bacteria and the "super infected", those infected with both susceptible and resistant bacteria. The models from over sixty different papers can then be summarised using six basic model structures detailing the transitions between three or more of the above states. As an example, the replacement infection model is governed by the following coupled differential equations:

$$\frac{dS}{dt} = -\beta_w I_w S - \beta_z I_z S + \gamma(1-\epsilon)I_w + \gamma'\epsilon I_w + \gamma I_z \quad (2.31)$$

$$\frac{dI_w}{dt} = I_w(\beta_w S - \gamma(1-\epsilon) - \gamma'\epsilon - (\beta_w - \beta_z)I_z) \quad (2.32)$$

$$\frac{dI_z}{dt} = I_z(\beta_z S - \gamma - (\beta_w - \beta_z)I_w) \quad (2.33)$$

where S denotes susceptible humans, I_w are patients infected with sensitive bacteria, I_z are patients infected with resistant bacteria, and the other parameters are given in Table 2.4. The replacement infection model denotes a scheme where there is no infection by both susceptible and resistant bacteria, one infection type can be replaced by another and neither strain can convert to the other (i.e. susceptible bacteria do not become resistant, they are instead replaced by resistant bacteria in a transmission event).

Parameter	Description	Typical Value
ϵ	Percentage of the population using antibiotics	0 -15%
β_w	Transmission rate of sensitive I_w strain	0.04
β_z	Transmission rate of sensitive I_z strain	0.015
γ	Innate recovery rate	0.01
γ'	Innate recovery rate from I_w	0.5

Table 2.4: Parameter Values from Spicknall et al. [128]

There is potential that one of these structures could be adapted to account for the transmission of AMR between cows in the dairy farm environment.

In recent reviews of mathematical models of AMR conducted by Leclerc et al. [121] and Birkegård et al. [134], it was found that most of the models of AMR surveyed are deterministic (33 out of 43 models reviewed by Leclerc et al. [121] and 29 out of 38 models reviewed by Birkegård et al. [134]). Furthermore, of the models reviewed in [121], all of the deterministic models were ODE models.

López-Lozano et al. [135] present an alternative approach to Hospital AMR modelling, using transfer function models for a time series analysis. They collected six months worth of data on antibiotic usage and AMR prevalence, and constructed a model to predict the interaction between the two. This work has been continued in various papers, including an analysis of AMR prevalence in Aberdeen over a four year period and the Hospital Vega Baja in Spain over 7 years [136–138].

Roberts et al. [139] model antibiotic resistance in rat burn wounds to investigate the effects of anti-adhesion and debridement therapies. A burn wound is inflicted on a rat, then the wound site is removed for study. The wound then consists of a layer of "host cells", which are covered by a layer of fluid, which in turn is partially covered by necrotic tissue. Anti-adhesion therapy inhibits the binding of bacteria to host cells and debridement is the act of cleaning the wound. Their model describes the development of antibiotic in the wound as cells bind and unbind to the host cell layer. Their model incorporates logistic growth and HGT, similar to the Baker and Volkova models [38,39], but also includes host-cell binding and unbinding, segregation (the division of plasmids when a cell reproduces), clearance (bacteria leaving the system through partial cover of the necrotic tissue) and uses an E_{max} model to model antibiotic killing of bacteria. The model predicts that through combination anti-adhesion-antibiotic-debridement therapy, antibiotic infections can be treated more effectively than using the treatments in isolation.

Another model model investigating the effects of combined treatments on bacterial populations is presented by Ternent et al. [140]. This model investigates the effects of antibiotic and anti-virulence treatments on a population of antibiotic-susceptible and resistant bacteria in the presence of phagocytes (immune system cells). Similar to the Roberts model [139], logistic growth and conjugation are modelled, alongside two E_{max} models to describe the effects of antibiotic and anti-virulence drugs. Phagocyte population size is modelled based on an immune response to the presence of bacteria. Ternent et al. [140] find that anti-virulence drugs are unlikely to be able to clear an infection in immunocompromised patients. However, if the physiological cost of antibiotic resistance is sufficiently high, combination therapy with antibiotics may be able to fully clear such infections

Conlin et al. [54] and Lambert et al. [141] both present evolutionary game theory models for bacterial behaviour. Conlin et al. consider a snowdrift game of increasing complexity to model the spread of AMR, whereas Lambert et al. model the growth dynamics of competing bacterial species with particular emphasis on cooperation mechanics within communities.

The Conlin et al. model assumes an infinite bacterial community is made up of β-lactamase producers (P) and non-producers (N), the resistant and susceptible members of the population, respectively. Pairs form randomly within the population, selection occurs based on competitor genotypes, the offspring are pooled and the parents die. With a payoff matrix shown in Table 2.5 they derive the average fitness of each genotype:

$$W(P) = wp + y(1-p) \tag{2.34}$$

$$W(N) = xp + z(1-p) \tag{2.35}$$

where p is the proportion of producers, w and y are the fitness of a P individual when paired with a partner of P or N, respectively and x and z is the fitness of an N individual when paired with a partner of P or N, respectively.

		Partner	
		P	N
Focal	P	w	y
	N	x	z

Table 2.5: Payoff Matrix for the Conlin et al. game [54]. P indicates a β-lactamase producing bacterium and N a non-producer.

These in turn lead to a recursion relation which can be used to track the proportion of producers over time:

$$p' = \frac{pW(P)}{pW(P) + (1-p)W(N)} \tag{2.36}$$

Under this system there are four possible outcomes:

1. Non-producer domination in the case $w < x$ and $y < z$
2. Producer domination in the case $w > x$ and $y > z$
3. Coexistence in the case $w < x$ and $y > z$
4. Bistability in the case $x > w$ and $y < x$

Simulations of these four outcomes are shown in Figures 2.4 to 2.7.

Similarly a differential equation model can be derived for p in a single well mixed population:

$$\frac{dp}{dt} = p(1-p)((w-x)p + (y-z)(1-p)) \tag{2.37}$$

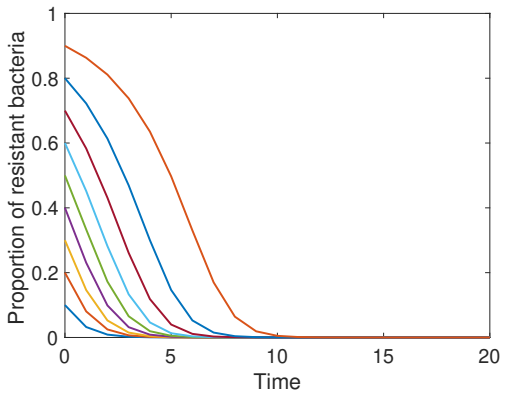


Figure 2.4: $x = 4$, $y = 1$, $w = 3$, $z = 4$

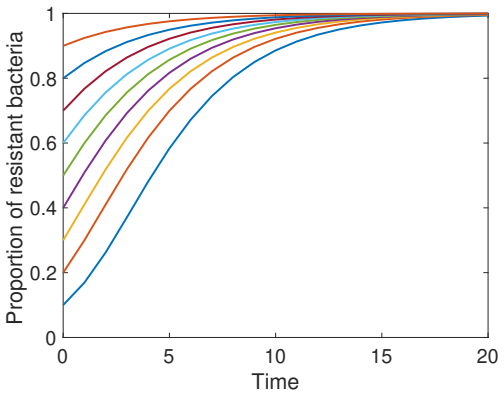


Figure 2.5: $x = 3$, $y = 2$, $w = 4$, $z = 1$

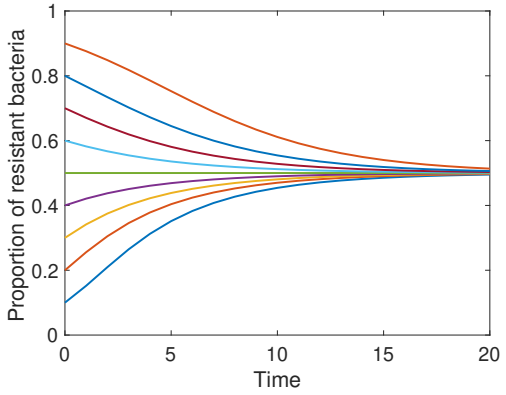


Figure 2.6: $x = 4$, $y = 2$, $w = 3$, $z = 1$

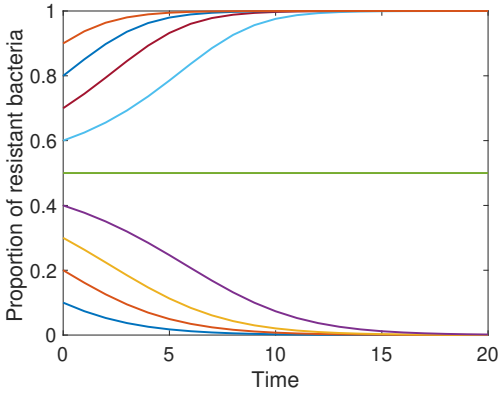


Figure 2.7: $x = 1$, $y = 2$, $w = 2$, $z = 3$

Realisations of the Conlin et al. model described in equation 2.36 showing the four possible configurations of the model: non-producer domination, producer domination, co-existence of producers and non-producers and bi-stability [54].

as before there are four possible outcomes following the same inequality dependent structure.

Evolutionary game theory provides an interesting framework for AMR modelling, under the assumption that resistance carries a cost to a competing bacteria. Furthermore, in the case where microbes produce β-lactamase as a resistance method, there is the potential evolutionary advantage for non-resistant bacteria surrounded by those producing β-lactamase.

Lastly, a simple model of the evolution of AMR is presented by Gullberg et al. [142] in environments where the concentration of antimicrobial agent is below the minimum inhibitory concentration. In a population where no resistant mutants initially exist, the Gullberg model gives the time to fixation of the resistance gene:

$$T_{50}^{0} = \frac{1}{uNs} + \frac{1}{s} \ln \left(\frac{sN}{uN + s} \right) \tag{2.38}$$

where u is the mutation rate, N is the population size and s is the fitness ad-

vantage in the presence of antibiotics. This model predicts the emergence of de novo resistant mutants that can take over a population of sensitive bacteria in between one-hundred and a thousand generations, these models are supported by competition experiments.

Gullberg et al.'s results bring some of the assumed knowledge about AMR into question, the basic premise of many models is that resistance only emerges under selective pressure and that, given the presumed cost of resistance, the emergence of AMR is reversible when that selective pressure is removed.

2.5.2 Modelling Considerations

In this thesis, three new models of AMR in the dairy slurry environment are developed, simulated and discussed. The first model builds on existing models from the literature, then the latter models build on that framework, each adding their own layer of model complexity. In mathematical modelling there is often a trade off between accuracy, model complexity and overparameterisation. Velten [143] describes a mathematical model as a combination of three things, a system (S), a question about the system, (Q), and a series of mathematical statements (M) which can be used to answer Q. As no mathematical model can perfectly represent a real-life system, is the best model then the simplest series M which accurately answers Q? Or is it M such that M best represents S? For example, though there are likely many strains of bacteria in dairy slurry, Baker et al.'s model only considers *E. coli*, as a sort of sentinel or marker organism for the prevalence of AMR at large, so in their design, they chose to prioritise simplicity rather than system accuracy. A further difficulty is that, in research areas where data is sparse or noisy, it can be difficult to know whether increased complexity is indeed improving prediction.

As noted by Knight et al. [144] and Birkegård et al. [134], the data in the field of AMR are indeed sparse, and more is required to develop mathematical tools that can help inform policy. In scenarios such as this, one of the uses of models can be to identify future directions for research and data collection. In this thesis, various techniques are used to identify possible areas of research, and specific consideration is given to suggestions for data collection.

2.6 Summary

Though there is a large body of work around the systems level processes of AMR, dating back to the early 1930s, there is limited knowledge about how all anthropogenic antimicrobial use has affected the environment and human health. This

appears particularly true for the use of antimicrobials in agriculture. Mathematical models of AMR are nearly all related to human health, with comparatively few models of AMR in agriculture. These models provide an interesting starting point for the investigation of this complicated problem, but ultimately there is still a requirement for a concerted data collection and modelling effort to truly understand the depth of the agricultural AMR risk.

Chapter 3

Should We Worry About Slurry?

The Should We Worry About Slurry? (SWWAS) project was a nine month data collection effort, funded by the EPSRC Bridging the Gaps initiative, to ascertain the variation in farming practices, antimicrobial use and prevalence of antimicrobial resistance (AMR) across Great British farms. SWWAS was conducted alongside an Agriculture and Horticulture Development Board (AHDB) project investigating feed efficiency on farms in Great Britain (GB). Fifteen farms were visited between April and July in 2017. Slurry was collected from each farm at two time points and the farmers were asked to conduct a survey on their farming practice. The collected samples were then analysed for the presence of extended-spectrum β-lactamase (ESBL) producing *E. coli*, colistin resistant *E. coli*, carbapenem resistant *E. coli* and cefotaxime resistance genes, concentration of heavy metals and other elements, and occurrence of antibiotic residues. SWWAS was a collaboration between the University of Nottingham School of Biosciences, the School of Mathematical Sciences, the Faculty of Engineering and the School of Pharmacy. The Animal and Plant Health Agency (APHA) were contracted to analyse slurry samples for the presence of *E. coli*.

In October 2016 the author and Dr Emma Gregson devised the concept for the project during a Bridging the Gaps competitive sandpit event. They then spent a week contacting potential stakeholders within the university, calculating project costs and putting together a presentation to give at the followup to the sandpit. They presented alongside three other groups and won a vote to be awarded £20,000 to undertake the project. Dr Gregson was the lead investigator for the project. Farms were chosen based on Dr Gregson's pre-existing relationship with them as part of the AHDB food efficiency project and all farmers involved in the SWWAS project gave consent for slurry sampling and analysis. Slurry samples were then collected by Dr Gregson and a team of assistants, which included the author on certain farm visits. Everyone involved in taking samples from the slurry undertook SCBA training. The samples were analysed for antimicrobial

resistance by APHA, for heavy metal concentration by researchers from the Food Water Waste group in the University of Nottingham Faculty of Engineering and for antibiotic residue concentrations by researchers in the University of Nottingham School of Pharmacy. The survey filled out by farm managers was co-written by the author and Dr Emma Gregson. The data analysis presented in this chapter was conducted by the author with supervision from Dr Gregson.

3.1 Project inspiration and vision

Though dairy slurry tanks have been recognised as a potential hot spot for AMR [31] little is known about the prevalence of AMR across farms or how it might be affected by individual farming practices [9]. Furthermore many factors may affect the prevalence and development of AMR, including the presence of antibiotics and heavy metals and other elements [64, 145]. Therefore a study of British farming practice, antibiotic usage, heavy metal concentration in slurry and AMR presence offered an opportunity to begin filling those knowledge gaps.

The goal of SWWAS was to identify risk factors within farming practices which might contribute to the development of AMR on the farm, as well as providing some insight into the variation in farm practice, antimicrobial use and heavy metal prevalence within the GB dairy industry. There have been various international multi-farm studies to evaluate the presence of AMR within the dairy industry, ranging from three or four farms [146, 147] to over twenty farms (up to 100) [148–151]. Brunton et al. [152] surveyed antimicrobial usage and waste milk disposal practices over 557 farms in England and Wales using a postal survey, but did not take any samples from the farms. As part of a large scale survey of ESBL *E. coli* in the UK, Day et al. analysed 97 samples from dairy slurry. Though it is not the largest study of resistant *E. coli* in dairy slurry, the SWWAS project is unique in the scope of its data collection, as it included farm practice and elemental analysis.

Farm practice and slurry tank characteristic data were collected to determine whether there was any link between farm variables and the presence of AMR. Antibiotic usage data was collected from farmers as more labile antibiotics might degrade quickly enough that they would not be recorded in the antibiotic residue analysis.

E. coli presence in slurry was monitored as part of this study as it is often regarded as a sentinel organism for AMR [153]. The resistance phenotypes tested for were ESBL producing *E. coli*, carbapenem resistant *E. coli* and colistin resistant *E. coli*. ESBL production was studied as it confers resistance to antibiotics used in both animal and human health, such as the penicillins and

cephalosporins [154]. Colistin and carbapenem resistance was studied as both are human-important last-resort antibiotics [19, 20, 155]. Resistance to either would indicate a dangerous trend in the development of on farm AMR. Ideally, more resistance phenotypes would have been studied, but due to budgetary restrictions the project was limited to ESBL production and colistin and carbapenem resistance.

Alongside the detection of ESBL production and carbapenem and colistin resistance phenotypes, the analysis performed by APHA also tested for the presence of CTX-M producing genes. CTX-M enzymes are extended-spectrum β-lactamases which confer resistance to cephalosporins and monobactam antibiotics [156], both of which are important for human health [157,158]. In particular CTX-M enzymes are characterised by their ability to break down cefotaxime, a third generation cephalosporin [156]. The presence of CTX-M producing *E. coli* in slurry has implications for both herd and environmental health, as it indicates the possibility of cattle gut-bacteria that are resistant to third generation cephalosporins and also may lead to the spreading of CTX-M producing *E. coli* onto pasture and arable land. Furthermore, there is a potential implication for human health, as third and fourth generation cephalosporins are regarded as "critically important antibiotics" by the World Health Organisation, based on the risks to human health of the development of resistance in animals [109, 154]. CTX-M production genes have also been linked to plasmids which also carry resistance genes for other antibiotic classes [159], and so may indicate the presence of multi-drug resistance.

Heavy metals concentrations were recorded as certain metals (including zinc and copper, which are often used in footbaths [28]) have antimicrobial properties and resistance to the effects of heavy metals can confer co-resistance to antibiotics [64, 65]. In particular, resistance mechanisms for heavy metals such as zinc, copper, silver and arsenic can confer resistance to β-lactam antibiotics [64]. Additionally, the UK government places restrictions on the concentrations of certain metals in agricultural soils [160]. The metal concentration data was also compared to these limits, to determine whether the metal concentrations in the slurry were ever above the legal limit.

The project provided an excellent opportunity to understand the sampling and availability of data in the field of agricultural AMR, as well as understanding the limitations and strengths of the data that exists in the literature. This knowledge then informs trust in the data and its used in modelling, model parameterisation and use in statistical evaluation.

Before beginning the study, it was expected that ESBL producing bacteria would be more commonly found in farms that used more antibiotics and had

higher concentrations of metals in the slurry. It was also expected that farms that disposed of antibiotic contaminated waste might be more likely to have resistant bacteria in the slurry. It was hoped that no colistin or carbapenem resistance would be found.

3.2 Materials and Methods

Slurry was collected from 15 dairy farms across the UK (the most southerly farm was located in Devon and the most northerly in Castle Douglas) between March and August 2017. Each farm was visited twice, and a slurry sample was taken at each visit. Four types of slurry store were used across the farms; over and underground slurry tanks, slurry lagoons and a biodigester. Slurry sampling locations were dependent on the tank design. In the case where tanks had access platforms, sampling was performed from these. Samples from lagoons were simply taken from the edge of the lagoon. In cases where it was not possible to sample from the tank directly, samples were taken from the tank outflow. Samples of $500-1000$ ml were taken in triplicate from two depths, where possible, representative of the liquid and solid phases, respectively.

Antibiotic usage data and farming practice information was collected using a questionnaire written by the author and Dr Gregson, and filled out by farmers or farm managers. The survey recorded herd size, farming system, food and bedding practice, slurry tank characteristics and antimicrobial usage. The full survey is in Appendix A.1. Slurry samples were stored in amber glass bottles and refrigerated before being sent for analysis. Heavy metal concentrations were quantified by researchers at the University of Nottingham School of Engineering using the methods detailed in [28]. Antibiotic quantification was performed by researchers in the University of Nottingham School of Pharmacy using the LC-ESI-MS/MS method based on that described by Baena-Nogueras et al. [37]. The full methods and report can be found in Appendix A.2. The samples were analysed for the presence of ESBL producing and carbapenem and colistin reistant *E. coli* by APHA. Selective growth media were used to detect ESBL resistant *E. coli* and PCR gene amplification and sequencing was used to detect cefotaxime resistance genes. The methods are given in Appendix A.3.

3.2.1 Statistical methods

Two methods were used to compare the the ESBL detection data with the survey results, elemental concentrations and antibiotic residue concentrations: Pearson correlation and Student's t-test.

The Pearson coefficient, ρ, measures the correlation between two random variables, X and Y, and is calculated as follows:

$$\rho = \frac{\mathrm{Cov}(X, Y)}{\sigma_X \sigma_Y} \tag{3.1}$$

where $\mathrm{Cov}(X, Y)$ is the covariance of X and Y and σ_X and σ_Y are the standard deviations of X and Y, respectively [161]. ρ ranges between -1 and 1, a positive value indicates a positive correlation (i.e. as X increases, Y increases) and a negative value indicates a negative correlation (as X increases, Y decreases). The greater the absolute value of ρ the stronger the correlation. Following [161]

- $0.90 < |\rho| \leq 1.00$ is considered a very strong correlation
- $0.70 < |\rho| \leq 0.90$ is considered a strong correlation
- $0.50 < |\rho| \leq 0.70$ is considered a moderate correlation
- $0.30 < |\rho| \leq 0.50$ is considered a weak correlation
- $0.00 < |\rho| \leq 0.30$ is considered a negligible correlation.

Given two data sets X and Y with means μ_X and μ_X, if X and Y are independent, have equal variance and the sample means are normally distributed, then Student's t-test can be used to determine whether or the difference between μ_X and μ_Y is statistically significant [162]. The Student's t-test can either be one or two-tailed. The one-tailed test is appropriate only if the means can differ in a single direction, so was not used here.

Throughout the analysis the null-hypothesis was that farms where ESBL *E. coli* was detected in the slurry did not differ from farms where ESBL *E. coli* was not detected. Overall, 66 correlation analyses were performed. Therefore, using a Bonferroni multiple-comparison correction would require a p value of 0.00075 for statistical significance.

3.3 Results and discussion

3.3.1 AMR Presence in slurry

Of the 30 samples tested, 11 were positive for *E. coli* growth pre-enrichment and post-enrichment 13 samples were positive for ESBL *E. coli* (5 on McC-CTX and 8 on CA-SEBL). Enrichment was used to grow the bacterial populations in the samples so that *E. coli* could be selected and ESBL resistance can be tested. In cases where *E. coli* were not found pre-enrichment, this indicates that the *E.*

coli concentration was below the limit of detection (100 CFU g^{-1}). 9 of the 15 farms investigated exhibited ESBL *E. coli* in their slurry samples on at least one of the visits, after enrichment. This is within the range of other studies across multiple farms: Schmid et al. [148] found that 86.7% of the cattle farms they sampled from in Bavaria displayed ESBL *E. coli*, whereas Hordijk et al. [149] found that 40% of the 20 dutch farms exhibited ESBL *E. coli*, but is considerably higher than the rates reported by Day et al. [163], who found that 28% of samples exhibted ESBL *E. coli*. No samples showed resistance to carbapenems or colistin. This is reassuring as both antibiotics are so called "last-line" or "last-resort" antibiotics [19, 20, 155] and hence are particularly important for human health.

Five different CTX-M resistance genes were detected across the farms: CTX-M-14, CTX-M-15, CTX-M-65, CTX-M-36 and CTX-M-8. Though most of these genes have been detected in agricultural settings and CTX-M-14 and CTX-M-15 are found relatively regularly in these types of studies [149–151, 163–167], it appears the CTX-M-65,36 and 8 have not before been detected on GB dairy farms. In fact, during a longtitudinal study at a UK dairy farm undertaken by Horton et al. [166], only CTX-M-1,14 and 15 were identified. Table 3.1 shows the results from each farm and visit. It should be noted here that in cases where ESBL was not detected, this does not necessarily mean it was not present at all in the slurry tank, just that it was not present in the sample that was taken. It seems likely that in many cases, the slurry is heterogenous, due to both the sheer size of the slurry tanks (see table 3.3) and phenomena such as solid settling within the tank. In later chapters, spatial models are developed to attempt to address this heterogeneity (see chapters 7 and 8).

	Growth of E. coli on agar media					
		ESBL Resistance (PE)		Carbapenem resistance (PE)		Colistin resistance (PE)
Farm ID	McC (BE)	McC-CTX	CA-ESBL	OXA-48	CARBA	McC-Col
1a	+	-	-	-	-	-
1b	-	-	+ (CTX-M-15)	-	-	-
2a	+	+	-	-	-	-
2b	-	-	+ (CTX-M-15)	-	-	-
3a	-	-	-	-	-	-
3b	-	-	-	-	-	-
4a	+	-	-	-	-	-
4b	+	-	+ (CTX-M-14)	-	-	-
5a	-	-	-	-	-	-
5b	-	-	-	-	-	-
6a	-	-	+ (CTX-M-14)	-	-	-
6b	-	-	-	-	-	-
7a	-	-	-	-	-	-
8a	+	-	-	-	-	-
9a	+	+	-	-	-	-
9b	-	-	-	-	-	-
10a (pre)	+	+	-	-	-	-
10b (pre)	-	-	-	-	-	-
10a (bio)	+	+	-	-	-	-
10b (bio)	-	-	-	-	-	-
11a	-	-	-	-	-	-
11b	-	-	-	-	-	-
12a	+	+ (CTX-M-65)	+ (CTX-M-65)	-	-	-
12b	-	-	+ (CTX-M-36)	-	-	-
13a	-	-	-	-	-	-
13b	-	-	-	-	-	-
14a	-	-	-	-	-	-
14b	+	-	+ (no seq)	-	-	-
15a	+	-	+ (CTX-M-8)	-	-	-
15b	-	-	-	-	-	-

Table 3.1: Results from the Two samples from each farm were analysed for the presence of ESBL *E. coli*, except in the case of farms 7 and 8, where only one sample was analysed. This was due to the choice to analyse samples from the pre-storage and biodigester on farm 10
. 43% of samples were positive for ESBL *E. coli*, equating to 60% of the farms being positive at at least one sample date. Here "a" and "b" refer to the first and second sample dates. In the case of farm 10 "pre" indicates samples taken from the storage pre-biodigester, and "bio" indicates samples taken directly from the biodigester. BE stands for Before Enrichment and PE for Post Enrichment.

3.3.2 Survey Results

The farms surveyed varied in herd size from 68 cows to 600, with a mean herd size of 291. The farms surveyed were divided into 5 farming categories, depending on grazing days and feeding approach. The five categories are shown in Table 3.2. Of the 15 farms surveyed, a third were System 5 farms, with Systems 3 and 1

being the next most common. The surveyed farms then represent a diverse set of feeding and housing approaches and it may be possible to determine whether housing and feeding practices have an effect on the development of AMR.

Descriptor	System 1	System 2	System 3	System 4	System 5
Calving pattern	Spring	Block/All year round	Block/All year round	All year round	All year round
Grazing days	274	183-274	91-182	0-90	Housed
Feeding approach	Grazed grass with limited supplementary concentrates. Silage and/or fodder crops fed during shortfalls in grazed forage	Grazed grass with more use of conserved forage and supplementary concentrates	Grazed grass with partial mixed ration and supplementary concentrates	Limited use of grazed grass. Total mixed ration, or partial mixed ration with supplementary concentrates	No use of grazed grass. Total mixed ration or partial mixed ration with higher use of supplementary concentrates
Farms Surveyed	3	1	4	2	5

Table 3.2: The requirements for each of the Farming Systems used in the study.

Farm ID	Container Type	Wall	Volume (m^3)	Covered/Open	Mixing Method	Tank Cleaning	Slurry Destination
1	Lagoon	Earth	591	Open	Tractor	None	Own fields
2	Tank	Metal	1637	Open	Mechanical	None	Arable/grassland
3	Lagoon	Concrete	3000	Open	Mechanical	None	Own fields
4	Lagoon	Concrete	810	Open	Mechanical	None	-
5	Underground tank	Concrete	920	Covered	Mechanical	None	Own fields
6	Tank	Metal	350	Open	Mechanical	2015	Own fields
7	Lagoon	Earth	19200	Open	Mechanical	None	-
8	Underground tank	Concrete	3500	Covered	Bubbler mixer	None	Own fields
9	Tank	Metal	2273	Open	Mechanical	None	Own fields
10	Biodigester	Metal	-	Open	-	none	Silage/arable
11	Tank	Metal	864	Open	None	None	Own fields
12	Lagoon	Earth	31823	Open	Mechanical	None	Own fields
13	Tank	Concrete	367	Semi enclosed	Mechanical	None	-
14	Lagoon	Concrete	4000	Open	Mechanical	None	Own fields
15	Tank	Metal	-	Open	Mechanical	None	-

Table 3.3: Details of slurry storage facilities on each of the 15 farms in the SWWAS project.

The tank slurry stores also varied widely in construction and maintenance, as shown in Table 3.3. Farm owners were asked about the type of slurry store they used, what it was made of, its size, whether it was covered or open, the method used for mixing, how regularly it was cleaned and where the slurry was deposited. The shape of the slurry stores was not recorded. Container type, materials and size were recorded to see whether there was any correlation between ESBL *E. coli* detection and tank design. Whether a tank is covered or open determines whether slurry is diluted by rainfall. The mixing method determines how well mixed the slurry is and whether or not a tank has regular cleaning may affect the persistence of AMR. Finally, the destination of the slurry was recorded, as it indicates where possible areas of risk for antibiotic or AMR contamination (though of course does not affect whether or not AMR develops).

Farm 10 had a bio-digester system with a pre-digester tank. The contents of both the pre-digester and the biodigester were analysed for this study. Interestingly, apart from on farm 6, none of the tanks had ever been cleaned, and on farm 6 it had last been cleaned 2 years before the SWWAS project data was collected. In general, slurry mixing only occurred during or prior to tank emptying, except in the case of farm 8, where it occurred nightly. The frequency with which the tank was filled ranged from once per week to a constant inflow, with a majority of respondents adding slurry to the store at least once a day. A question that was not asked was the age of the tanks, which, in hindsight, may have been an important omission, based on the results in Chapter 5, which indicate that the resistance profile of bacteria in a new tank differs from that of an older tank. This was not included in the SWWAS survey as this dynamic was not considered at the time. In the models discussed in the following chapters, the tank is considered to be cylindrical and metal sided, similar to the tank at the Sutton Bonington farm and some of the farms surveyed. Other aspects of the survey were used to set ranges for parameters related to herd size, tank cleaning and tank filling.

In most cases the final destination for the slurry was fields owned by the farmers, a practice that has been shown to increase the risk of antimicrobial resistance gene exposure to crops, farm workers and the environment at large [31, 168]. Eight of the fifteen farms disposed of waste milk (antibiotic contaminated milk) into the slurry tank and seven of the farms reported feeding waste milk to calves. There are recorded correlations between feeding waste milk to calves and fluoroquinolone resistance [155, 169]. In Brunton et al.'s study, 82% of farms reported feeding waste milk to calves [152]. There has been increased awareness of the risk of feeding waste milk due to recommendations from groups such as the Responsible Use of Medicines in Agriculture Alliance [170].

Across the fifteen farms, farm managers reported using 26 different antibiotics in the previous 12 months before filling out the survey, with some farms using as many as 15 different antibiotics. These antibiotics were used for mastitis treatment, calf treatment and dry-cow therapy. In some cases the antibiotics are being administered via combined medicines like Ubro Red, which contains Framycetin Sulfate, Penethamate Hydriodide and Procaine Penicillin. Six cleaning and animal hygiene chemicals are being used across the farms. A list of all medicines used across the farms is shown in Table 3.4. The antibiotic and chemical usage across the farms is shown in Figures 3.1 to 3.4

The most commonly reported antibiotic was streptomycin (or dihydrostreptomycin), which appears in some form in four different combined medicines used on the farms, Multiject, Tetra-Delta, Pen & Strep and Ubro Yellow, see Table 3.4. Brunton et al. [152] found that the most commonly used mastitis treat-

ments contained dihydrostreptomycin (around 37% of farms used it as their first choice), and treatments containing streptomycin or dihydrostreptomycin were also commonly used as second and third choices. Furthermore, a combination of dihydrostreptomycin and procaine penicillin was the most commonly used injectable antibiotic [152]. Of the other chemicals used (see Figures 3.3 and 3.4), formalin was the most common, and was used on 12 of the 15 farms, likely in footbaths. Of the six chemicals reported, there appears to be no recorded cases of co-resistance with antibiotics, except in the case of digicur, which contains copper and zinc [171], metals known to be selectors for antibiotic co-resistance [64]. Ideally the quantities of antibiotics and chemicals used would also be known, but this data can be very hard to acquire, as it is dependent on farm record keeping.

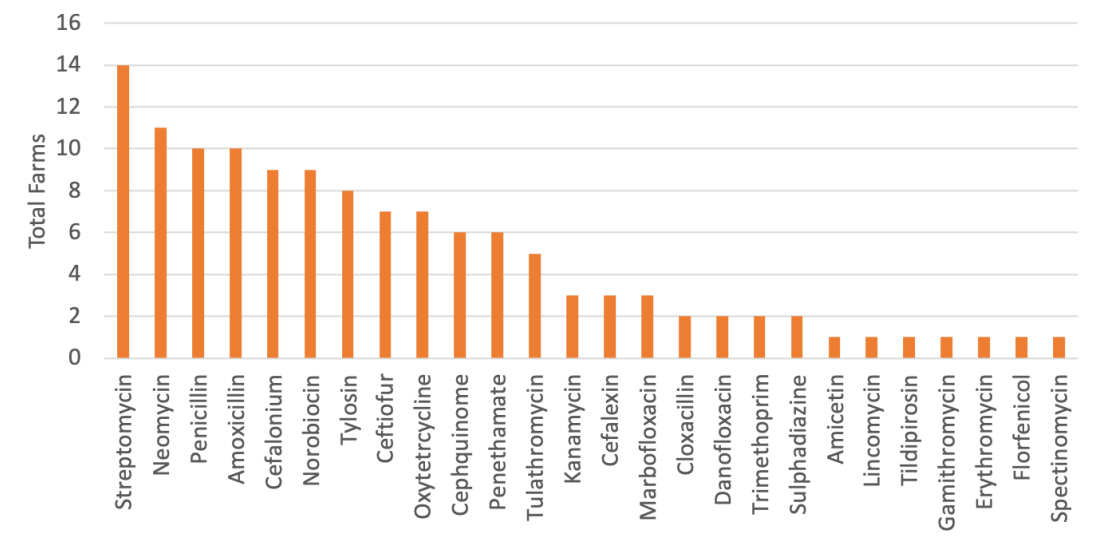


Figure 3.1: The 26 antibiotics farmers reported using within 12 months of the survey, collated by the number of farms that used them. Many of these antibiotics were used as part of combination medicines, see Table 3.4.

Analysis of the farm practice survey data alongside the AMR detection data yields interesting results, but more data would need to be collected to assert any statistical significance. The average herd size of farms where ESBL *E. coli* were detected was 361, compared to 196 on farms where resistance wasn't detected, a Students's two tailed t-test revealed this result to not be statistically significant ($p = 0.087$), similarly a correlation test showed a low correlation (0.47) with the same p value. The two tailed t-test was also used to compare differences in the tank volume and the days cows were housed per year, but both had p values > 0.6, so there was no statistically significant difference.

Surprisingly there was a low negative correlation between ESBL detection and whether or not antibiotic-contaminated waste milk was added to the tank ($\rho = -0.45$, $p = 0.099$). There was some assumption that the addition of antibiotic contaminated milk would increase the detection of ESBL *E. coli*. However, this

Medicine	Active ingredients
Multiject	Procaine Penicillin, Streptomycin, Neomycin and Prednisolone
Cobactan	Cefquinome
Betamox	Amoxicillin
Tetra-Delta	Dihydrostreptomycin, Neomycin, Novobiocin, Prednisolone, Procaine Penicillin
Norodine 24	Trimethoprim, Sulfadiazine
Pen & Strep	Procaine Penicillin, Dihydrostreptomycin Sulphate
Allomycin	Allomycin
Excenel	Ceftiofur
Cevaxel	Ceftiofur
Ceporex	Sodium Cefalexin
Naxcel	Ceftiofur
Marbox	Marbofloxacin
Cepravin	Cephalonium
A180	danofloxacin
Ubrolexin	Cefalexin, Kanamycin
Amoxypen	Amoxicillin Trihydrate
Engemycin	Oxytetracycline Hydrochloride
Synulox	Amoxicillin, Clavulanic Acid
Ubro Yellow	Dihydrostreptomycin Sulfate, Framycetin Sulfate, Penethamate Hydriodide, Prednisolone
Boflox	marbofloxacin
Tylan	Tylosin Phosphate
Tylan	Tylosin Phosphate
Zuprevo	Tildipirosin
Betamox	Amoxicillin
Framomycin	Framycetin Sulfate
Nuflor	Florfenicol
Draxxin	Tulathromycin
Alamycin	Oxytetracycline Dihydrate
Zactran	Gamithromycin
Noroclav	Amoxycillin Clavulanic Acid
Cepravin	Cephalonium
Ubro Red	Framycetin Sulfate, Penethamate Hydriodide, Procaine Penicillin
Ubrolexin	Cefalexin, Kanamycin
Cephaguard	Cefquinome
Excenel	Ceftiofur
Norodine	Trimethoprim, Sulfadiazine
Kloxerate	DC Cloxacillin
Zactran	Gamithromycin
Duphamox	Amoxicillin Trihydrate
Ubrolexin	Cefalexin, Kanamycin
A180	Danofloxacin

Table 3.4: Medicines used on the farms, as reported by farm managers, and their constituent antibiotics.

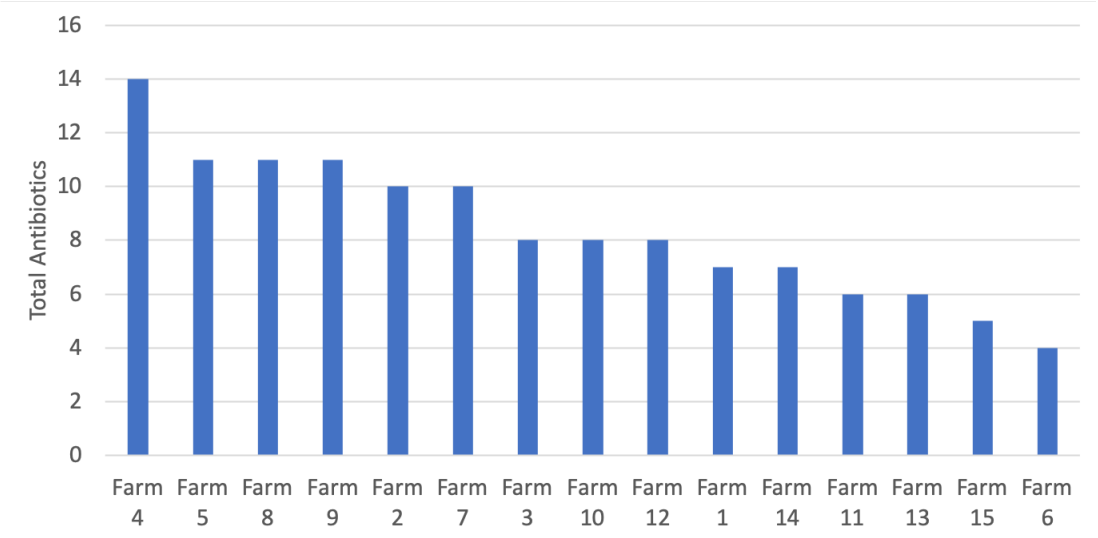


Figure 3.2: The total number of antibiotics each farm reported using within 12 months of the survey.

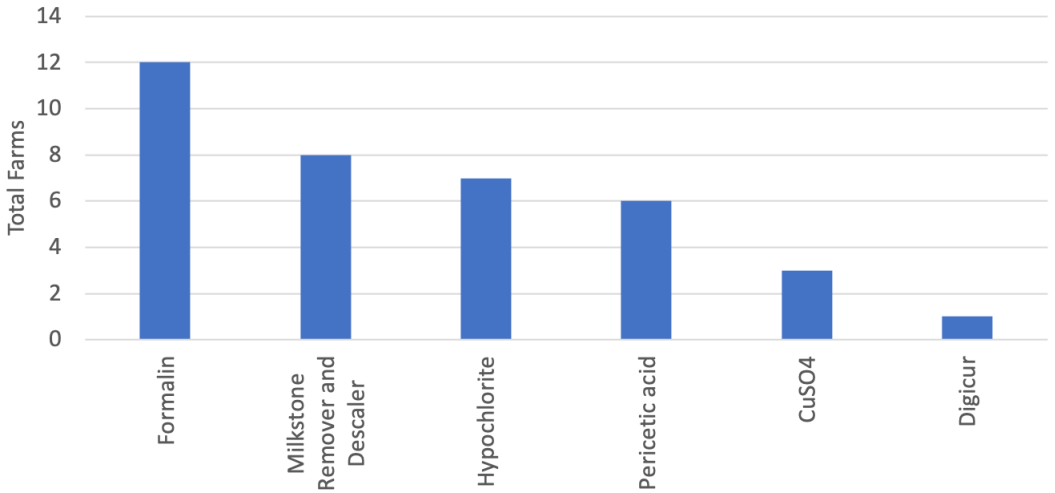


Figure 3.3: The six cleaning and herd hygiene chemicals that farmers reported using within 12 months of the survey, collated by the number of farms that used them.

may depend on which antibiotics are present in the milk. For example, if there is a high concentration of an antibiotic to which ESBL *E. coli* is susceptible in waste milk, this antibiotic might inhibit the growth of ESBL *E. coli* populations in the slurry. Very little correlation was found between the feeding of waste milk to calves and ESBL detection.

There was little-to-no correlation between the detection of ESBL *E. coli* and the total antibiotics reported, the store volume, the days housed (and hence the farming system) and the emptying frequency of the tank. The correlation analysis is shown in Figure 3.5.

3.3.3 Elemental analysis

The elements quantified in each of the slurry samples are show in Table 3.5. The elemental concentration distributions are shown in Figure 3.6. Potassium is by far the most abundant, followed by aluminium and iron, where silver and thallium are the least abundant. It should be noted that none of the elements were found to be above legal agricultural limits [160]. The co-selective agents found in the highest quantities were copper and zinc, potentially due to their use in footbaths [28]. Both copper and zinc were found in concentrations above their minimum co-selective concentrations (MCC) in sediment (fresh and dry weight) and manure (dry weight) [145]. Where MCC data is available, none of the other co-selective agents were found at concentrations above their MCC in sediment, soil or manure.

Ten of the metals tested (As, Fe, V, Cr, Al, Li, Cs, U, Tl) had low correlations with ESBL detection (correlation $\rho => 0.3$), but, once again, none were statistically significant ($p > 0.2$ in all cases). Of these 10, only As is a known co-selective agent and it also had the highest correlation score. Of the two known co-selective metals found above their MCC, copper had a correlation score of ρ =0.27 ($p = 0.35$) and zinc had a negative correlation of -0.16 ($p = 0.57$). Interestingly many of the metals were highly correlated with each other, implying that when slurries are metal rich they are potentially rich in many metals simultaneously, with copper being the main exception, these correlations are shown in Figure 3.7.

3.3.4 Antibiotic Residue

The samples were screened for nineteen antibiotics, shown in Table 3.6.

Of the nineteen antibiotics tested, seven were found above the limit of detection, these are shown in Table 3.7. The sample from farm 8 was not analysed, for reasons unknown to the author at the time of writing. None of the antibiotics were

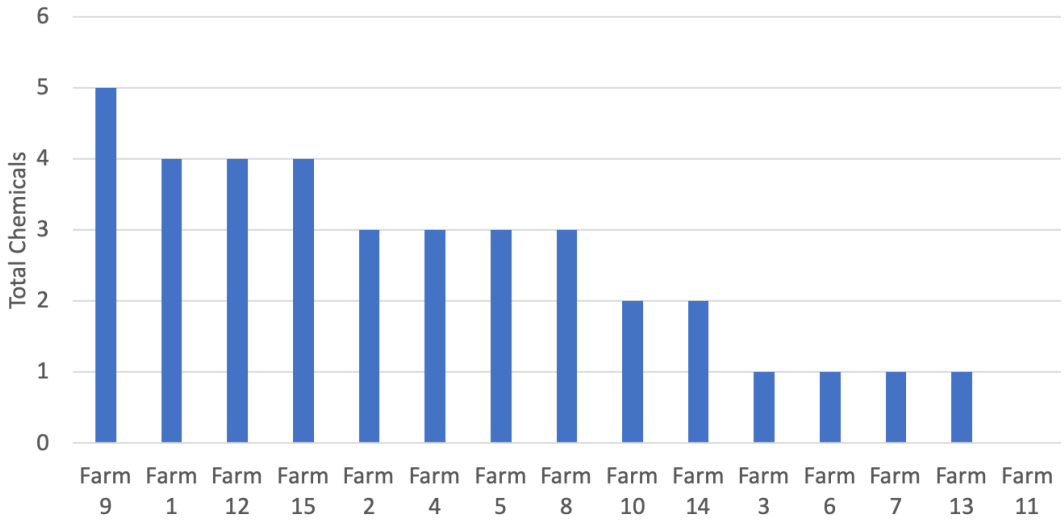


Figure 3.4: The total number of cleaning and herd hygiene chemicals used by each farm within 12 months of the survey.

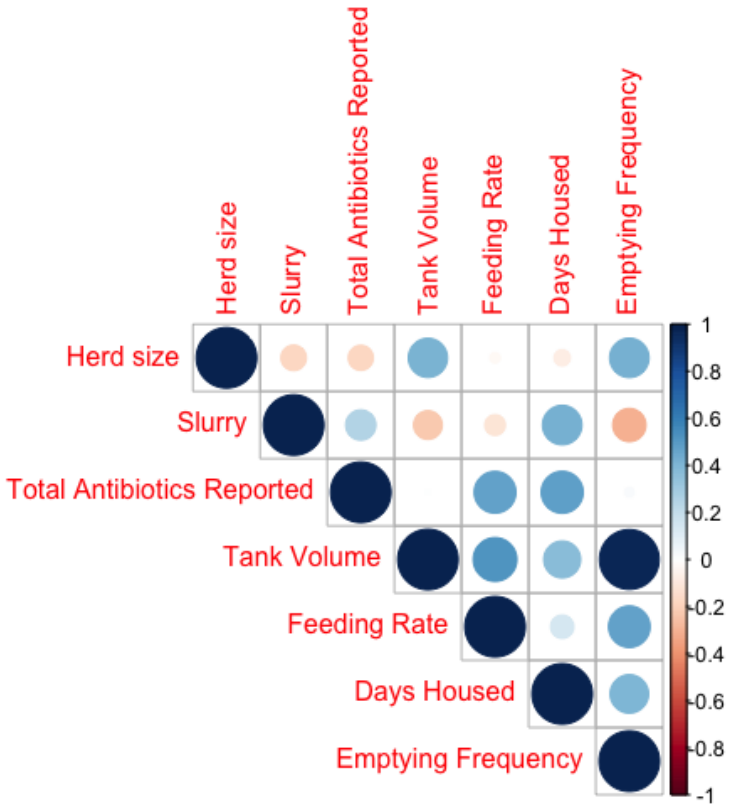


Figure 3.5: Correlations between recorded ESBL *E. coli* and farm practice factors. Here, the top row shows the Pearson coefficients for correlations between detected ESBL *E. coli* and farm practice factors. The remaining rows show the Pearson coefficients for correlations between the various farm practice factors. The colour bar and dot size indicate correlation strength.

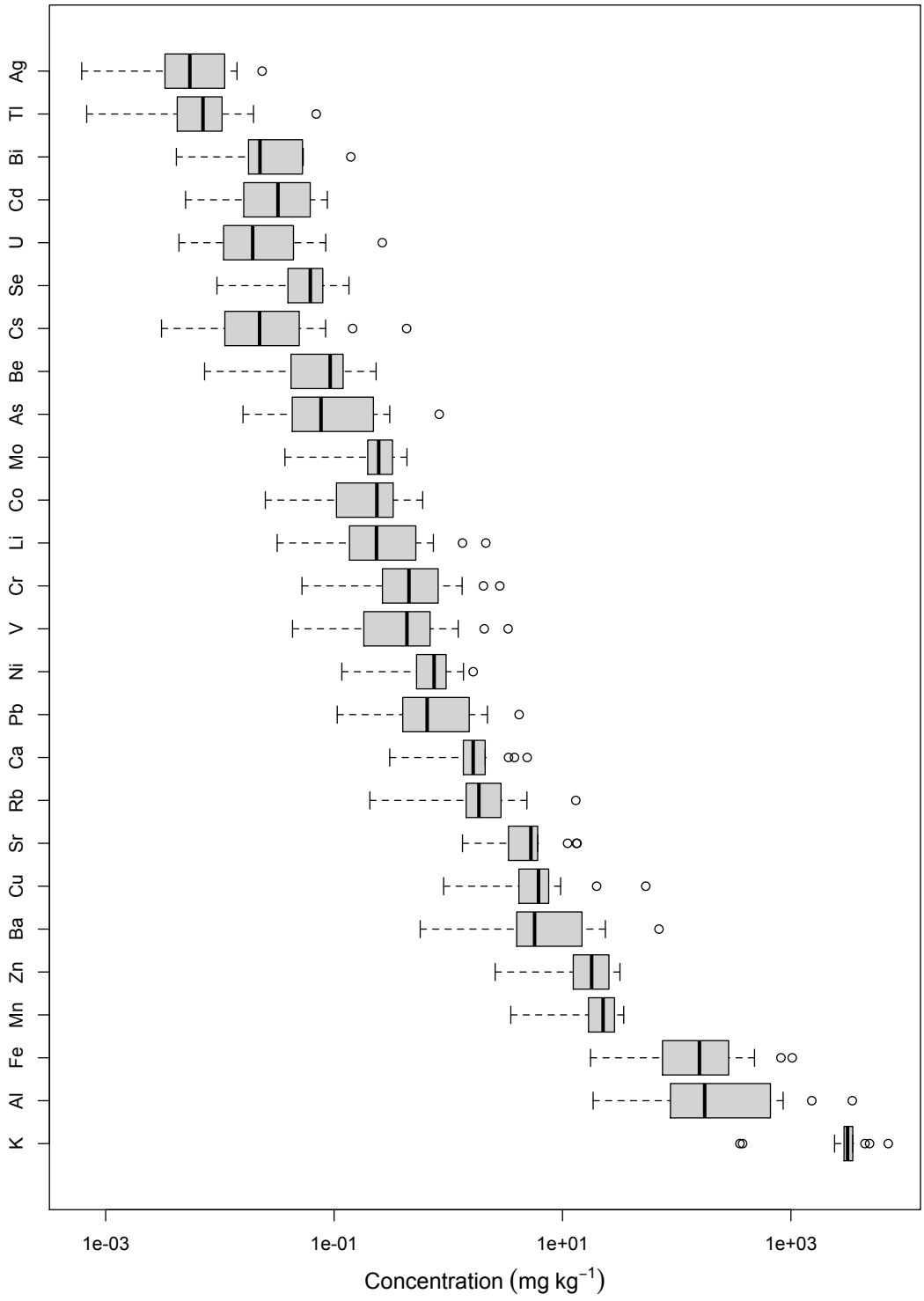


Figure 3.6: Heavy metal concentrations across the farms shown using box and whisker plots. Here, the boxes contain from the 25th to 75th percentile, the line within the box is the median. Whiskers are 1.5 times the interquartile range, and outliers are those points which lie outside that range.

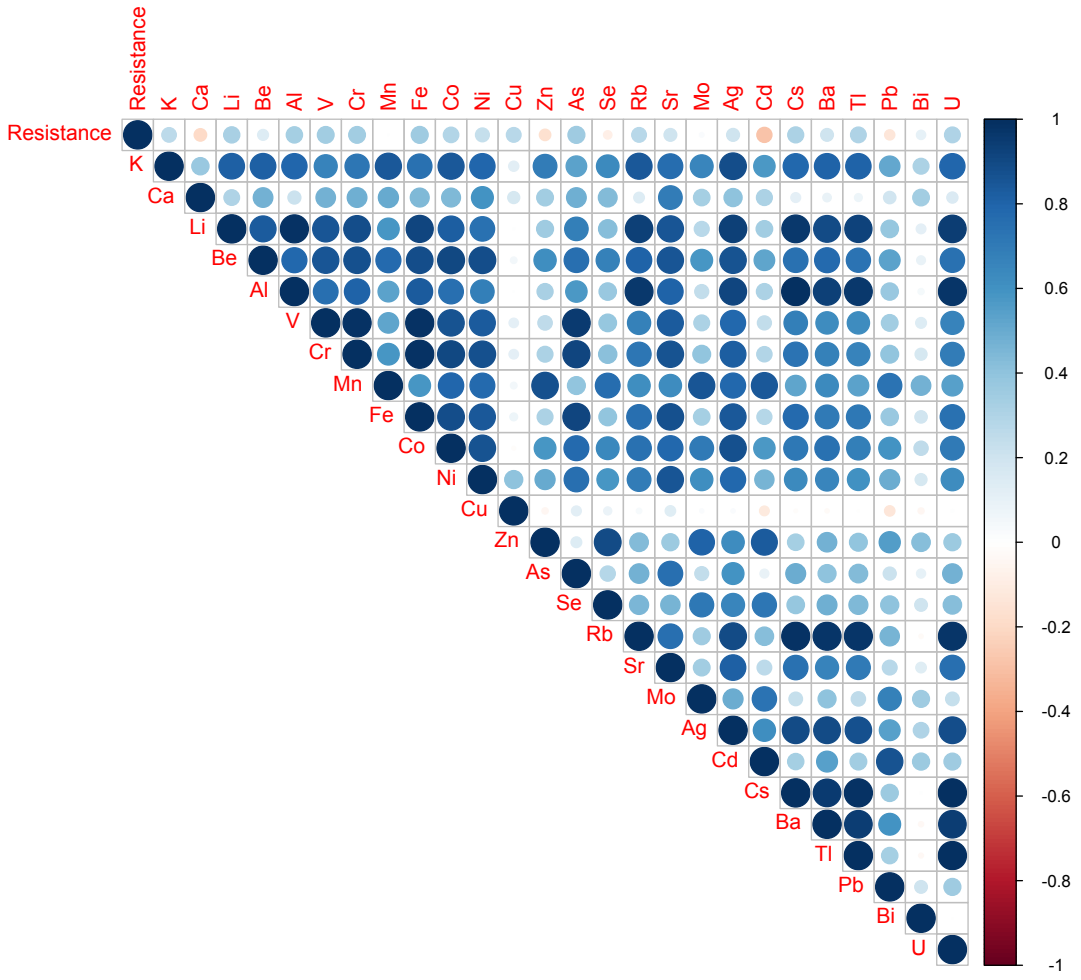


Figure 3.7: Correlations between recorded ESBL *E. coli* and elemental concentrations found in the slurry. Here the top row shows the Pearson coefficients for correlations between detected ESBL *E. coli* and the elemental concentrations found in slurry samples. The remaining rows show the Pearson coefficients for correlations between the detection of the various different elements. The colour bar and dot size indicate correlation strength.

Element	Symbol	Well characterised co-selective agent	Max Legal Agricultural Limit (mg kg^{-1})	Max Concentration Recorded (mg kg^{-1})
Boron	B	No	-	NQ
Sodium	Na	No	-	1290
Magnesium	Mg	No	-	989
Phosphorus	P	No	-	971
Sulphur	S	No	-	NQ
Potassium	K	No	-	7115
Calcium	Ca	No	-	4902
Titanium	Ti	No	-	NQ
Lithium	Li	No	-	2.131
Beryllium	Be	No	-	0.233
Aluminium	Al	No	-	3446
Vanadium	V	No	-	3.339
Chromium	Cr	Yes	400	2.824
Manganese	Mn	Yes	-	34.36
Iron	Fe	No	-	1026.73
Cobalt	Co	Yes	-	0.60
Nickel	Ni	Yes	75	1.65
Copper	Cu	Yes	135	53.56
Zinc	Zn	Yes	300	31.83
Arsenic	As	Yes	50	0.83
Selenium	Se	No	3	0.14
Rubidium	Rb	No	-	13.10
Strontium	Sr	No	-	13.4
Molybdenum	Mo	No	-	0.43
Silver	Ag	Yes	-	0.02
Cadmium	Cd	Yes	3	0.09
Caesium	Cs	No	-	0.43
Barium	Ba	No	-	69.94
Thallium	Tl	No	-	0.07
Lead	Pb	Yes	300	4.16
Bismuth	Bi	No	-	0.14
Uranium	U	No	-	0.26

Table 3.5: The elements quantified in the slurry samples from the SWWAS project. Co-selective characterisation data from [64] and [145]. Agricultural limits from [160].

found above lowest recorded MICs from the literature [172–176]. However, oxytetracycline and cefoperazone were found above the size adjusted MICs suggested by Bengtsson-Palme and Larsson [173]. Surprisingly cefoperazone was found on all but one of the farms, despite no farmer claiming to use it in the survey. Brunton et al. [152] record the use of cefoperazone as a mastitis treatment, though it is much less commonly used than other cephalosporins, such as cefquinome. In the analysis, cefoperazone was identified by retention time only and not compared to a chemical standard. Therefore, the analysis may have detected an antibiotic or substance with similar retention time. To identify the cases where antibiotics

Antibiotic	Family	Abbreviation	Limit of Quantification
Amoxicillin	Penicillin	AMX	0.2
Ampicillin	Penicillin	AMP	2
Cefalexin	Cephalosporin	CLX	0.4
Cefalotin	Cephalosporin	CLT	Monitored not quantified
Cefapirin	Cephalosporin	CPR	Monitored not quantified
Cefoperazone	Cephalosporin	CPZ	2
Cefquinome	Cephalosporin	CQM	2
Ceftiofur	Cephalosporin	CFT	0.4
Cloxacillin	Penicillin	CLOX	0.2
Enrofloxacin	Quinolone	ENR	Monitored not quantified
Florfenicol	Amphenicol	FLO	Monitored not quantified
Lincomycin	Lincosamides	LCM	0.02
Novobiocin	Quinolone	NOV	0.02
Oxytetracycline	Tetracycline	OTC	2
Penicillin-G	Penicillin	PEN	2
Sulfadiazine	Sulphonamide	SDZ	0.2
Sulfadoxine	Sulphonamide	SDX	Monitored not quantified
Trimethoprim	-	TMP	0.02
Tylosin	Macrolide	TYL	0.4

Table 3.6: The nineteen antibiotics screened for in the SWWAS project.

were used but not found or found but not used, a table was made to visualise the seven antibiotics which were quantified by pharmacy combined with the six antibiotics that farmers claimed to use and pharmacy tested for but didn't find, this is shown in Table 3.8.

In forty-eight cases antibiotics were used but no residues were found, this is not necessarily unusual, as it was unknown how recently these antibiotics had been used, as the survey recorded all antibiotics used in the previous twelve months. In thirty-three cases antibiotics were not used but residues were found, this was surprising, and either indicates that the survey had not been filled out thoroughly, or that there was some mistake in the residue analysis. In 13 cases antibiotics were used and residues were found. Lincomycin, oxytetracycline and cefoperazone make up 85% of the "not used but found" cases. Where norobiocin, oxytetracycline and penicillin make up 77% of "used and found" cases. Amoxicillin is the antibiotic which was most commonly "used but not found", which is potentially due to the relatively low persistence of β-lactams in manure [23] compared to other classes such as tetracyclines. Oxytetracycline has been shown to have a relatively long half-life in manure (17.7 days in dairy manure and 31.1 days in stored feedlot manure [23]). Unfortunately there is little data on the persistence of lincomycin and cefoperazone in slurry.

Overall the antibiotic residue results are surprising, as they do not match well

FARM	Lincomycin	Tylosin	Penicillin	Sulphadiazine	Oxytetracycline	Novobiocin	Cefoperazone
1	0.204	0	0	0	0	0	3.78
2	0	0	0	0.929	0	0.261	2.02
3	0.22	0	0	0	3.89	0.336	5.23
4	1.63	0	0	0	0	0	2.54
5	0.201	0	0	0	5.72	0	2.91
6	4.47	0	0	1.17	6.86	0.428	9.53
7	0	0	0	0	4.91	0.14	9.11
8							
9	0	0	0	0	11.8	0	7.69
10	0	0.664	5.04	2.05	38.4	0	8.69
11	0.3	0	3.53	0	14.9	0	2.62
12	0	0	1.45	0	3.85	0	4.38
13	4.33	0	0	0	0	1.28	6.85
14	0.237	0	4.11	0	10.4	0	6.06
15	0.344	0	18.3	0	0	1.84	0

Table 3.7: Antibiotics quantified in slurry. Concentrations in μg l^{-1}

.

FARM	Cefalexin	Ceftiofur	Cefquinome	Lincomycin	Tylosin
1	0	0	2	1	2
2	2	0	0	0	0
3	2	2	2	1	2
5	0	2	2	3	2
6	0	2	2	1	2
9	0	0	0	1	2
10	0	2	0	0	2
14					
15	2	2	0	0	0
16	0	0	0	0	3
18	0	0	2	1	0
19	0	2	0	0	0
21	0	0	0	1	0
23	0	0	2	1	0
24	0	0	0	1	0

FARM	Penicillin	Amoxicillin	Cloxacillin	Trimethoprim	Sulphadiazine
1	2	2	0	0	0
2	2	2	0	2	3
3	0	0	0	0	0
5	2	2	2	2	2
6	2	2	0	0	0
9	0	0	0	0	1
10	2	2	0	0	0
14					
15	2	2	0	0	0
16	3	2	0	0	1
18	1	0	0	0	0
19	3	0	0	0	0
21	0	2	2	0	0
23	3	0	0	0	0
24	1	2	0	0	0

FARM	Oxytetracycline	Norobiocin	Cefoperazone
1	0	0	1
2	0	1	1
3	1	3	1
5	2	2	1
6	1	0	1
9	1	1	1
10	3	3	1
14			
15	3	2	1
16	1	2	1
18	3	0	1
19	1	0	1
21	2	3	1
23	1	2	1
24	2	3	0

Table 3.8: Table showing antibiotics "used but not found" and "found but not used". 0 indicates "not used not found", 1 indicates "not used but found", 2 indicates "used and not found", 3 indicates "used and found". The "not used by found" case is the most concerning, as it either indicates a problem with the survey results, the sample analysis or that antibiotic residues are entering the tank from some other source or has been misidentified.

with the reported antibiotics used. This may be down to either survey and record keeping error or due to the analysis of the samples. Particularly concerning is the presence of cefoperazone in all but one of the samples analysed. Cephoperazone is a third-generation Cephalosporin and has particular importance to human health [155]. If it is entering the slurry tank from another source, it would important to determine the cause.

The data was analysed to determine whether there were correlations between the antibiotics used and found on the farms and the presence of ESBL *E. coli*. There were found to be no correlations that are statistically significant. There was also very little correlation between the number of antibiotics used and the detection of ESBL *E. coli*. The correlations between resistance and antibiotics reported (and the correlations of use between antibiotics reported) are shown in Figure 3.8. The strongest correlation is a negative correlation between ESBL detection and neomycin (ρ =-0.49, p = 0.062). This is potentially due to the ESBL *E. coli* sampled not having a resistance to neomycin. However, the second strongest correlation is that between ESBL detection and reported use of kanamycin (ρ =0.41, p = 0.13), which is a positive correlation. Both neomycin and kanamycin are aminoglycosides, so it might be expected that any bacteria which had developed resistance to one might have developed resistance to both (the standard modes of resistance to aminoglycosides are cell wall fortification and efflux pumps [177]). It is also interesting that there is little correlation between the reported use of β-lactam antibiotics such as the penicillins and cephalosporins and ESBL detection. In fact, there is a weak negative correlation between the reported use of ceftiofur and ESBL detection (ρ =-0.33, p = 0.2337). Analysis of detected antibiotic residue concentration alongside the detection of ESBL *E. coli* also yielded no statistically significant results. Though there are weak to negligible correlations between ESBL detection and tylosin, penicillin and sulphadiazine use. The correlations are shown in Figure 3.9.

3.4 Summary

Fifteen farms across Great Britain were visited between April and July 2017. At each farm Slurry samples were collected, these were analysed for the presence of ESBL *E. coli*, carbapenem resistant *E. coli*, colistin resistant *E. coli*, antibiotic residues and heavy metals and other elements. Due to budgetary constraints, no other antibiotic resistance phenotypes were analysed, meaning that the data does not account for resistance to many veterinary antibiotics. However, ESBL *E. coli* are resistant to herd and human-important antibiotics such as the penicillins and cephalosporins, and offer an indicator of the presence of resistance in the slurry.

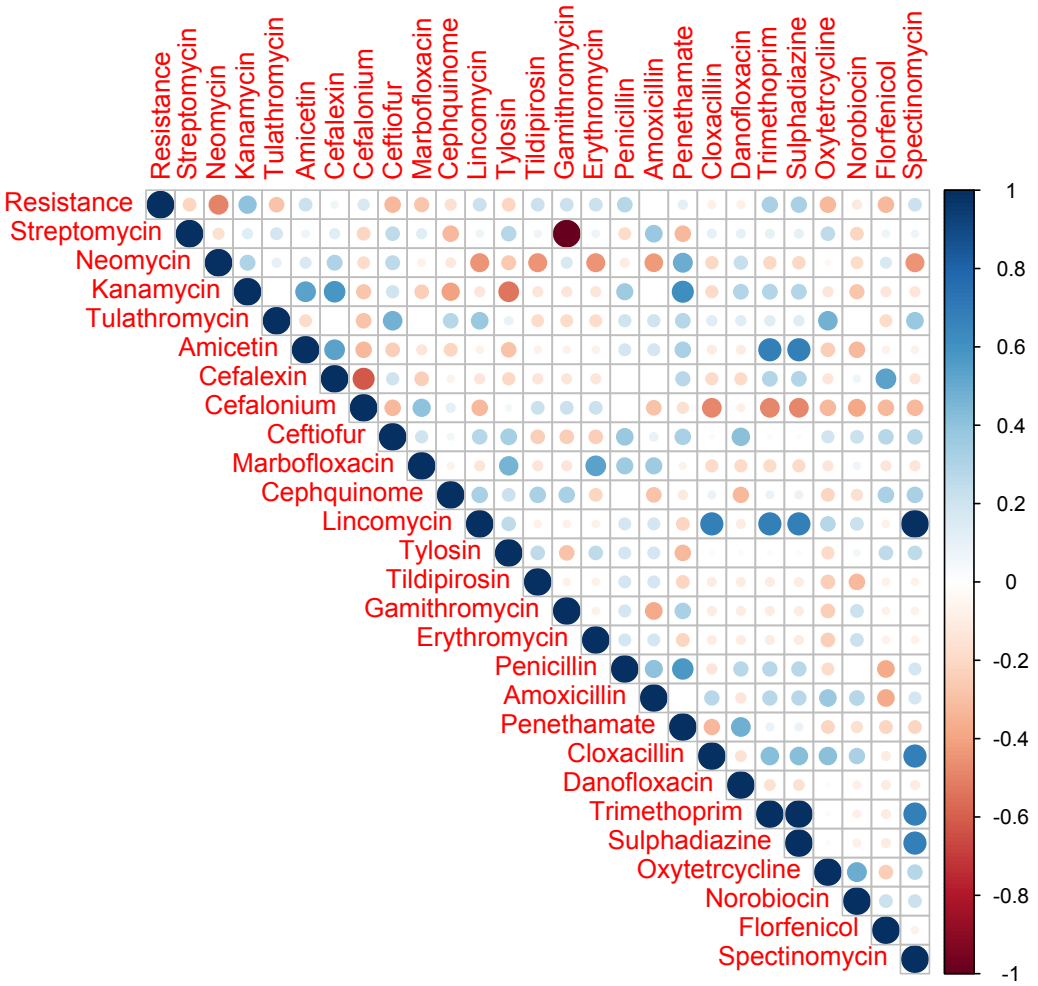


Figure 3.8: Correlations between recorded ESBL *E. coli* and reported use of antibiotics. Here the top row shows the Pearson coefficients for correlations between detected ESBL *E. coli* and reported use of antibiotics. The remaining rows show the Pearson coefficients for correlations between the reported use of the various reported antibiotics. The colour bar and dot size indicate correlation strength.

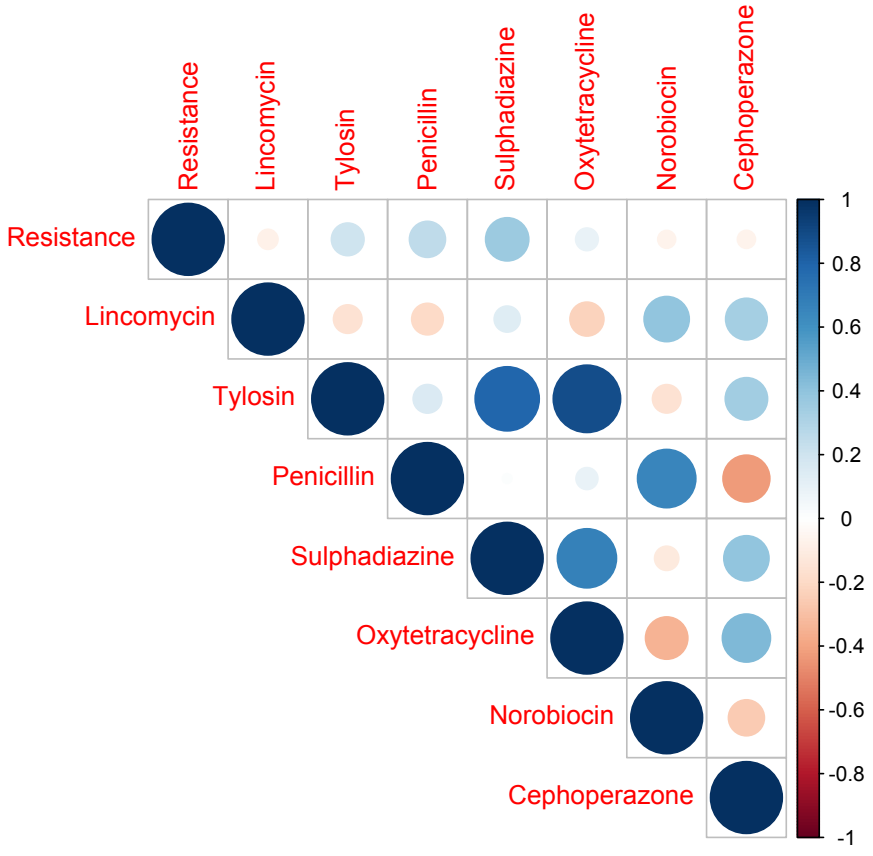


Figure 3.9: Correlations between recorded ESBL *E. coli* and antibiotic residues found in the slurry. Here the top row shows the Pearson coefficients for correlations between detected ESBL *E. coli* and antibiotic residue found in slurry samples. The remaining rows show the Pearson coefficients for correlations between the various antibiotic residues that were found in the slurry. The colour bar and dot size indicate correlation strength.

Each farm manager also completed a survey detailing farm and slurry storage practices. The resultant data provides an overview of the varied farm practices in the UK, alongside the distributions of heavy metals, minerals and antibiotics in dairy slurry.

ESBL *E. coli* were detected at over half of the farms tested, and genetic analysis revealed cefotaxime resistance genes that had not been recorded before in an agricultural setting on GB farms: CTX-M-8, CTX-M-36 and CTX-M-65. However, CTX-M-8 and CTX-M-65 have been recorded in other agricultural settings [178]. This indicates that the farm resistome is likely being influenced by the human or environmental resistomes. No colistin or carbapenem resistant *E. coli* were found. At all farms except farms 7 and 8, two samples were taken and analysed. Though ESBL *E. coli* were found at 9 out of 15 farms, on five of those farms ESBL *E. coli* were only detected in one sample. This could be due to sampling error, changes in microbial population or problems with sample transportation and analysis.

Antibiotic residues were found in all farms tested (farm 8 was not tested), and the two most regularly found antibiotics were oxytetracycline and cefoperazone. No antibiotics were found above their lowest recorded MICs [172–176]. Both bacteriolytic and bacteriostatic antibiotics were found in the slurry. Though cefoperazone was the most commonly found antibiotic, no farmer reported having used it within the last year. Following discussions with the lab that performed the antibiotic residue analysis, it became clear that cefoperazone was detected by retention time only and not corroborated using chemical standards. This indicates that where cefoperazone was detected, it may instead have been a different molecule, potentially one of the other cephalosporins that farmers reported using, such as cefalonium, cefquinome or cefalexin (see table 3.1).

Slurry samples were screened for 29 different heavy metals, 26 were found, 10 of which are known co-selective agents. Of the co-selective heavy metals found in the slurry both zinc and copper were found in concentrations above their MCCs for manure and sediments. A low correlation between ESBL presence and 10 metals was found, of those only one, arsenic, is a known co-selective agent. None of the metals were found in concentrations above legal agricultural limits.

The survey indicated that the project analysed samples from a wide variety of farms, with herd sizes ranging from 68 to 600 and using various grazing and calving patterns. Across the 15 farms, four types of slurry stores were used: lagoons, tanks, underground tanks and, on one farm, a biodigester. In total, farmers reported using 26 different antibiotics within the last year, with an individual farm maximum of 14 antibiotics. Streptomycin, neomycin and penicillin were the most commonly used antibiotics, though the quantities used are not known. Correla-

tions were found between ESBL *E. coli* presence and herd size and waste milk disposal into the slurry store (a negative correlation), though neither of these were found to be statistically significant. A summary of the results of the project is shown in Table 3.9.

The results were also analysed to determine whether there was any correlation between the findings and the detection of ESBL *E. coli*. Weak correlations were found between ESBL detection and herd size; disposal of waste milk into the slurry store; 10 of the elements analysed, including the known co-selective agent, arsenic; and reported neomycin (a negative correlation) and kanamycin use. However, it should be noted that none of these correlations were found to be statistically significant.

Small amounts of data are missing from nearly every element of the study: some farmer managers did not complete the survey; in two cases second visit samples were not analysed for the presence of ESBL *E. coli*; and one farm was omitted entirely from the analysis of antibiotic residues in slurry. The missing data combined with the small sample size of farms made it difficult to determine any statistically significant correlations between ESBL detection and any of the recorded factors. In the results presented here, missing values were omitted from the analysis, but as part of future work it might be possible to estimate the missing values, this could be done using a simple technique such as mean imputation (replacing the missing value with the mean of the observed values) or by using regression analysis to identify a likely value based on key known factors [179]. Additionally, the low number of samples compared to features of the data meant that predictive analysis methods, such as regression models or machine learning, were not possible to implement. In the case of a linear regression model, the number of features of the data is far greater than the number of samples. Developing a model would require choosing the features with no clear route to doing so. Methods like random forests are often very good at handling high-dimensional data [180], but in this case there weren't enough samples to properly divide into training and testing sets. One option for future work might be to increase the size of the data set by using synthetic data. Despite its shortcomings in terms of statistical analysis, the data provides useful insight for the development and parameterisation of mechanistic models. For example, it provides an overview of the sizes of farms; the sizes of slurry tanks; how regularly slurry stores are filled and emptied; and how regularly slurry stores are cleaned (practically never). It also gives an indication of which drivers of AMR are present in the slurry of GB farms. This knowledge is utilised in the development of models in the following chapters.

There are some methodological gaps within the study, most of which are due

Bacteria	
Farms where ESBL *E. coli* were found	60 %
Samples containing *E. coli* %	50%
Samples containing ESBL *E. coli* %	26.7%
Samples containing colistin resistant *E. coli* %	0%
Samples containing carbapenem resistant *E. coli* %	0%
CTX-M Genes	CTX-M-8 CTX-M-14 CTX-M-15 CTX-M-36 CTX-M-65
Farm Practice	
Max Herd Size	600
Min Herd Size	68
Mean Herd Size	290
Max Days Housed	365
Min Days Housed	45
Mean Days Housed	250
Max Store Size m^3	31823
Min Store Size m^3	350
Mean Store Size m^3	7226
Waste milk added to tank	9 farms
Waste milk fed to calves	7 farms
Antibiotics	
Max Reported Antibotics	14
Min Reported Antibiotics	4
Mean Reported Antibiotics	8
Most Common Reported Antibiotic	Streptomycin
Max Recorded Antibiotics	5
Min Recorded Antibiotics	2
Mean Recorded Antibiotics	3
Highest Total Concentration Antibiotic Residue	Oxytetracycline
Most Common Antibiotic Residue	Cefoperazone
Metals	
Highest Total Conccentration Metal	Al
Lowest Total Concentration metal	Ag
Metals above legal limits	None
Known Co-selective agents	8

Table 3.9: A summary table of findings from the SWWAS study.

to budget constraints and existing sample analysis protocol. Ideally it would have been possible to test *E. coli* for multiple resistances, rather than just for ESBL production, especially given that many veterinary antibiotics (for example oxytetracycline) have different modes of action to the β-lactam antibiotics. If possible, surveys would have been issued ahead of time and included questions on dates and quantities of antibiotic use, so that antibiotic analysis could be brought in line with reported usage. If possible, the study would have incorporated many more farms and sampled each farm more regularly over a longer timescale, increasing the depth and granularity of the data. This may have provided clearer patterns and correlations between resistance and farm practice. This was not possible as part of this initial study as the £20,000 funding was entirely used on the sample collection and analysis. Travel between farms was possible due to piggybacking on the existing AHDB food-efficiency project.

It was also difficult to establish a consistent sampling methodology across the various designs of slurry store. For example, the slurry in lagoons often had a high liquid content and was easily sampled by lowering a bucket into the lagoon, whereas, in the case of one particular slurry tank, the contents had formed a crust so thick that it could not be broken with a brick. Ideally, slurry would be sampled at at least two points: the store influent and effluent. This way it might be possible to analyse the effect of the tank on the development of AMR and the degradation of antibiotics. This might be difficult in the case of some stores, however, depending on how they are accessed for tank filling and emptying.

The limitations of the SWWAS project emphasise ongoing problems in the field of agricultural and environmental AMR, the lack of available data [9, 144] and the difficulty of collecting the "right" data. Despite these drawbacks, the project highlights that farm practice and the use of veterinary antibiotics may have some effect on the development and spread of AMR in slurry stores. The presence of AMR in the slurry of farms which spread their waste onto pasture and arable land further indicates that slurry stores may be a vector for AMR in the environment, as it has been recorded that field soil treated with dairy manure can be contaminated with antimicrobial resistance genes found on farms, and that those genes can persist for months after manure treatment [168, 181]. The project also provides useful knowledge around farm practice and antibiotic usage which can be used to develop conceptual and mathematical models of agricultural AMR. Ideally the SWWAS project would be extended into a longer term study with a more rigorous methodology based on the knowledge gaps identified during this pilot study.

Chapter 4

Conceptual Model

Conceptual models are tools used to summarise real-world systems, as a first step towards creating mathematical models. Conceptual models can be used to identify key processes that should be included in a mathematical model and to justify assumptions and simplifications. Furthermore, a conceptual model can be used to track which processes have been omitted from a mathematical model. This brief chapter outlines the known features, events and processes that may impact the prevalence and spread of antimicrobial resistance in the dairy slurry tank environment.

In this thesis, the conceptual model is used as a reference tool to indicate what is included and omitted in each of the three models in the following chapters. Hopefully acting as an aid for the reader to understand the model development process and the benefits and shortcomings of the various models.

4.1 A conceptual model of the prevalence and spread of antimicrobial resistance in the dairy slurry storage environment

4.1.1 Features

The Tank

Though slurry stores come in a variety of shapes and sizes, throughout the modelling in this thesis the store is considered to be a cylindrical tank constructed from an inactive material, with a three-million litre capacity, similar to the slurry tank at the University of Nottingham Sutton Bonington Campus. The sides of the tank are three metres tall and the tank has a diameter of 35.7 metres. There is a rotary mixer fixed to the side of the tank.

Tank influent

The tank influent comprises multiple waste products from the farm:

- Bovine manure and faeces [29]
- Waste milk from cows being treated with antibiotics (see Chapter 3)
- Waste footbath contents: footbaths can either be copper and zinc based or formalin based [28, 30]
- Parlour washings [29]

From the materials in the influent it is then possible to consolidate a list of substances which are of interest for modelling the development of and spread of AMR within the tank:

- Bacteria (in bovine manure and faeces) [33]
- Antibiotics (in bovine manure and faeces and waste milk) [32]
- Suspended and settling solids (from faeces, suspended within the general liquid phase) [182]
- Heavy metals (in waste footbath contents) [28]
- Other biocides (in waste footbath contents) [30]

Tank effluent

Tank effluent is slurry removed from the tank (after some period of storage), usually via an effluent pipe.

4.1.2 Events

Tank filling

Based on the findings of the SWWAS project (see Chapter 3), in most cases, slurry is added to the tank at least daily and some farms have a constant filling mechanism to transport manure and the other constituent parts of farm slurry to the tank.

Tank emptying

Tank emptying occurs semi regularly and depends on the time of year and the volume of slurry in the tank [183]. In Nitrate Vulnerable Zones (NVZ) there is a muck spreading closed period between October and February, and spreading is not allowed when land is flooded or frozen [106, 184, 185]. This means that tanks are emptied frequently during summer months and rarely during the winter.

Mixing

Based on the findings of the SWWAS project (see Chapter 3), most stores undergo mechanical mixing when emptying. The Sutton Bonington farm slurry tank has a rotor mixer added to the side of the tank, for example.

Cleaning

Based on the findings of the SWWAS project (see Chapter 3), most slurry stores are rarely (and generally never) cleaned.

4.1.3 Processes

Bacteria and antibiotics

- Bacteriolytic antibiotics can kill bacteria [61]
- Bacteriostatic antibiotics can halt bacterial growth [61]
- Bacteria can develop resistance to antibiotics via antimicrobial resistance genes [186]
- At high enough concentrations, antibiotics can cause environmental pressure which leads to the selection of antimicrobial resistance genes within a bacterial community [142]

Bacteria and heavy metals

- Heavy metals have antibacterial properties [64]
- Bacteria can develop resistance to heavy metals [64]
- Heavy metal resistance may also confer co-resistance to antibiotics (horizontal gene transfer) [64]

Antibiotics, metals, biocides and suspended solids

- Antibiotics, metals and biocides can sorb to suspended solids [72]
- Solids settling

Other factors potentially affecting the life cycle of bacteria and the development and spread of AMR

- Antibiotic degradation, volatilisation and ionisation [69, 70]
- Bacterial growth and natural death [38, 187]
- Temperature effects [188]
- Seasonality [117]
- Fluid flow through the tank (during filling and emptying)

A summary of the features, events and processes that occur in the tank is given in Table 4.1. In the following chapters, three new models of AMR in the slurry tank environment are developed. At the beginning of chapters 5, 7 and 8, there is a version of table 4.1 showing the features, events and processes that are included or omitted in each of the models. In some cases, a feature, or event or process, will be omitted from all three models. These are still included in the conceptual model to highlight modelling shortcomings and possibilities for future work.

Features
Tank:
Height
Diameter
Volume
Material
Influent:
Bovine manure and faeces
Bacteria
Antibiotics
Suspended and settling solids
Heavy metals
Other biocides
Rain water
Parlour washings
Effluent
Events
Filling
Emptying
Mixing
Cleaning
Processes
Bacteriolytic antibiotics and bacteria
Bacteriostatic antibiotics and bacteria
Horizontal gene transfer
Sorption
Solid settling
Antibiotic degradation
Bacterial growth and death
Temperature effects
Seasonality
Fluid flow

Table 4.1: A summary of the features, processes and events which may contribute to the development and spread of AMR in the slurry tank.

Chapter 5

A model of multidrug-resistance in the dairy slurry tank

This chapter details the development of a new ordinary differential equation (ODE) model of antimicrobial resistance (AMR) proliferation and persistence in the Sutton Bonington slurry tank. The model draws from models developed by Baker et al. and Volkova et al. [38, 39], but incorporates additional bacterial and farm process dynamics. The model comprises six coupled ODEs which describe the concentrations of two antibiotics, one susceptible strain and three resistant strains of *E. coli*. The model is simulated for various scenarios and sensitivity and stability analyses are performed.

The antibiotics used in agriculture can be broadly defined as either bacteriolytic (those that kill bacteria) and bacteriostatic (those that inhibit the reproduction of bacteria), it is possible that reducing one of these types may be an effective way of controlling AMR. There is evidence that the evolution of resistance development against drug combinations can be explained by co-resistance or co-sensitivity to those drugs [189] and though there have been studies of the interactions between bacteriolytic and bacteriostatic antibiotics and their respective efficacies when treating bacterial infections [190–192], this possibility has not been investigated in slurry before, and it is a key part of this work to try and predict the differential impact of such potential reductions.

Existing mathematical models of AMR in agriculture often model the emergence of a single resistant pathogen (or treat all pathogens as a homogenous group) [17,38,39,120]. The single pathogen is often considered only in the context of a single antibiotic (or single antibiotic class), and does not take into account the use of other antimicrobials or the wider environmental context, including the impact of farm practice.

Dairy slurry tanks are replete with many different bacterial strains and various different antibiotics. These antibiotics are generally either bacteriolytic, such

as penicillins and cephalosporins [49, 193], or bacteriostatic, such as the tetracyclines [193], and bacteria can acquire separate resistance methods for different antibiotics via resistance plasmids [194] and other genetic material [42] through the process of horizontal gene transfer (HGT). Furthermore, multidrug-resistance (MDR) is known to be common in dairy slurry [195]. Despite this, little is currently known about how the different types of antibiotic contribute to the development of MDR or how farm process factors affect the persistence and spread of AMR. This prompts the development of a mathematical model that is intended to predict the evolution of *E. coli* within a slurry tank, that are capable of both bacteriolytic and bacteriostatic-resistance, and can be resistant to one or the other type of antibiotic, or resistant to both. The model also incorporates tank emptying effects, to determine their influence on the development of AMR.

ODE modelling was chosen as it offers a simple framework for modelling the processes in the slurry tank by utilising a combination of widely accepted biological modelling approaches [196,197], concepts from previous models of AMR [38,39,139,140] and reaction kinetics equations [196]. Due to the lack of available data [9,134], statistical modelling approaches such as a machine learning were not viable. Due to the high bacterial concentrations considered ($> 1 \times 10^6$CFU l^{-1}), an approach such as agent-based modelling would have been computationally expensive. Similarly, due to these high concentrations, an assumption was made that stochastic effects would be smoothed and could be accounted for using a deterministic model [198].

The features, events and processes that are included and omitted in the model presented in this chapter are shown in Table 5.1. This table is intended to provide a guide for understanding the model presented in this chapter in the wider context of the real world problem and reasons are given for omissions.

5.1 Model Development

The Baker and Volkova models [38, 39] provided a useful starting framework for the new ODE model, as their models incorporate bacterial growth and the effects of antibiotics on bacterial reproduction, HGT and the effect of influent concentrations of antibiotics and bacteria, all of which are key processes in the conceptual model presented in chapter 4. Furthermore, the outputs of the Volkova model were found to match well with experimental data from their model system (a cow stomach) [39]. However, both models only include a single antibiotic and omit explicit bacterial death, both natural and due to antibiotics. The Baker model [38], the only model of AMR in the slurry tank at the time of writing, also omits tank emptying effects. When developing the model presented in this

Features

Included	Omitted
Tank	
Volume Material (non-reactive)	Height (assumed spatially homogeneous) Diameter (assumed spatially homogeneous)
Influent	
Bovine manure and faeces Bacteria (*E. coli* as sentinel organism) Antibiotics	Suspended and settling solids (assumed spatially homogeneous) Heavy metals (simplicity) Other biocides (simplicity) Rain water (assumed that tank is covered) Parlour washings (simplicity)
Effluent	

Events

Included	Omitted
Filling	
Emptying	
Mixing (assumed constant and homogeneous)	
	Cleaning (rare based on results from chapter 3)

Processes

Included	Omitted
Bacteriolytic antibiotics and bacteria	
Bacteriostatic antibiotics and bacteria	
Horizontal gene transfer	
	Sorption (suspended and settling solids omitted)
	Solid settling (suspended and settling solids omitted)
Antibiotic degradation	
Bacterial growth and death	
	Temperature effects (evidence that temperature does not affect *E. coli* in slurry [188])
Seasonality (seasonal emptying regime used)	
	Fluid flow (assumed spatially homogeneous)

Table 5.1: A summary of the features, processes and events from the conceptual model in chapter 4 that are included or omitted in the model presented in this chapter.

chapter, the effects of bacteriostatic and bacteriolytic antibiotics, explicit bacterial cell death and tank filling and emptying were incorporated alongside growth and HGT.

In their model, Baker et al. [38] model the quantities of antibiotic and bacteria, to convert the model equations to instead model the concentration throughout the tank (assuming the tank is well-mixed), the quotient rule was used. Let A_q (μg) and B_q (CFU) be the quantities of an antibiotic and bacterial strain, respectively. Taking the the equation for antibiotic in the tank over time from Baker et al. [38]:

$$A_q(t) = \left(A_1 - \frac{\theta}{\gamma}\right) e^{-\gamma t} + \frac{\theta}{\gamma} \tag{5.1}$$

where A_1 is the initial quantity of antibiotics in the system, θ is the antibiotic inflow rate and γ is the degradation rate of antibiotics. Equation 5.1 can easily be written as an ODE:

$$\frac{dA_q}{dt} = -\gamma \left(A_1 - \frac{\theta}{\gamma}\right) e^{-\gamma t} = -\gamma A_q + \theta. \tag{5.2}$$

The volume of slurry in the tank is given by

$$V(t) = V_1 + \lambda(t) - \omega(t) \tag{5.3}$$

where V_1 is the initial volume, $\lambda(t)$ is the quantity of slurry inflow and $\omega(t)$ is the outflow from the tank (which is not included in Baker et al.'s model [38]). To incorporate this into the ODE in equation 5.2 an emptying term is added to describe the removal of antibiotics in the effluent:

$$\frac{dA_q}{dt} - \gamma A_q + \theta - \omega' \frac{A_q}{V(t)} \tag{5.4}$$

where $\omega'(t)$ is the outflow rate from the tank and $A_q/V(t)$ is the concentration of A_q in the tank. To convert this equation to model concentration let A be the concentration of antibiotic, so that $A = A_q/V(t)$, then

$$\frac{dA}{dt} = \frac{d}{dt}\left(\frac{A_q}{V(t)}\right) = \frac{A_q' V(t) - A_q V'(t)}{V(t)^2} = \frac{A_q'}{V(t)} - A\frac{V'(t)}{V(t)}. \tag{5.5}$$

Substituting in equation 5.4 and using $V'(t) = \lambda'(t) - \omega'(t)$ gives

$$\frac{dA}{dt} = \frac{\theta}{V(t)} - A\left(\gamma + \frac{\lambda'(t)}{V(t)}\right). \tag{5.6}$$

Using the same process it is possible to derive the general concentration equation for for some bacteria, $B = B_q/V(t)$, where B_q is the quantity of bacteria in

the tank. The Baker et al. model for bacterial growth contains a growth term, G, a gene transfer term, τ, and the inflow to the tank, Λ. Adding a bacterial death term (which incorporates both natural and antibiotic induced death), Δ, and an outflow term, gives equations of the form

$$\frac{dB_q}{dt} = \left(G - \tau - \Delta - \frac{\omega'(t)}{V(t)}\right) B_q + \Lambda. \tag{5.7}$$

Similar to equation 5.5,

$$\frac{dB}{dt} = \frac{B'_q}{V(t)} - B\frac{V'(t)}{V(t)} \tag{5.8}$$

then substituting in equation 5.7 gives

$$\frac{dB}{dt} = \left(G - \tau - \Delta - \frac{\omega'(t)}{V(t)}\right) B + \frac{\Lambda}{V(t)} - B\frac{\lambda'(t) - \omega'(t)}{V(t)} \tag{5.9}$$

and finally simplifying gives

$$\frac{dB}{dt} = \left(G - \tau - \Delta - \frac{\lambda'(t)}{V(t)}\right) B + \frac{\Lambda}{V(t)}. \tag{5.10}$$

5.1.1 Model Design and Parameterisation

The Slurry Tank

The volume of slurry within the tank ($V(t)$) is modelled using equation 5.3. During initial simulations it is assumed that the tank fills at a constant rate, has infinite capacity and is never emptied, as a simple first case and following the Baker model [38]. This gives $\lambda(t)$=λt where λ is the rate of inflow and $\omega(t) = 0$. Following the calculations in [38], the rate of influent to the tank is given by $\lambda = 613\text{lh}^{-1}$, to simulate a 200 cow herd. When slurry tanks are emptied there is often a small amount of slurry left in the tank, for consistency with Baker et al. [38], the minimum quantity of slurry in the tank is chosen to be 150000 l, so $V(t) = 150000 + \lambda t$. This approach was chosen as a first case due to its simplicity and its potential for approximating very large slurry stores, such as lagoons. An alternative method would have been to maintain a constant volume of slurry within the tank, though this requires an assumption of constant emptying. Later in the analysis, periodic filling and emptying regimes are considered and the steady states of the constant volume case are discussed.

Antibiotics

Though the modes of action of bacteriostatic and bacteriolytic antibiotics vary within their respective classes, the resultant effects of each class remain the same.

In the case of bacteriostatic antibiotics reproduction is inhibited, slowing population growth, this is modelled by modifying a logistic growth term using a Hill function, following [38] and [39]. Bacteriolytic antibiotics on the other hand lead to cell death via lysis, which can be modelled by incorporating a death term into the equations, based on Michaelis-Menten kinetics [199] (this modelling approach could also apply to bactericidal antibiotics in general). Both dynamics were included in the model, in order to analyse whether reproduction inhibition or cell death had a greater effect on the development and survival of resistant bacteria. Rather than modelling each of the possible antibiotics in the slurry tank, antibiotics are grouped by their effect for simplicity. However, the model could be used to model the interactions between the bacteria and two specific antibiotics.

The total antibiotic inflow rate was set to $3422\mu\text{gh}^{-1}$ following [38]. For simplicity it is assumed that the total rate of antibiotic inflow is split evenly between bacteriolytic and bacteriostatic antibiotics so that $\theta_s = \theta_l = 1711\mu\text{gh}^{-1}$. As described in [38, 39, 199], both bacteriostatic and bacteriolytic antibiotics undergo first order degradation at constant rates (γ_s, γ_l, respectively). Van Epps and Blaney [200] found that the half life of the bacteriostatic antibiotic Oxytetracycline varied between 3 and 31 days in beef and dairy cattle manure compost, specifically 9.8 and 17.7 days in the two dairy manure samples. The antibiotic trimethoprim is bacteriostatic on its own but becomes bacteriolytic in the presence of sulphonamides, with which it is often combined, has a half life in manure amended soils varying between 2.3 and 197 days, depending on soil type and whether the system was anaerobic or aerobic, in general the half life was shorter in the anaerobic case [201]. Though the half life of cephalosporins (a widely used bacteriolytic antibiotic [49, 202]) has not been recorded in dairy slurry, Jiang et al. [203] found that cephalosporins have half-lives varying between 2.7 and 18.7 days in lake surface water. For simplicity it is assumed that both bacteriostatic and bacteriolytic antibiotics decay at the same rate and have a half life of 10 days, equating to a rate of decay of $\gamma_s = \gamma_l = 0.0029\text{h}^{-1}$. These parameters were allowed to vary during sensitivity analysis.

Bacteria

For this model, *Escherichia coli* (*E. coli*) was chosen as the model organism. *E. coli* is found in dairy cow manure [204], is a common cause of mastitis in dairy cows [205] and is often regarded as a sentinel organism for monitoring AMR [153]. However, there are likely high levels of microbial diversity in the slurry tank and this model can be adjusted to simulate the growth of other bacteria. The model is specific to *E. coli* due to parameter choices and the omission of temperature effects on bacterial population following [188].

The growth of bacterial communities is classically modelled using logistic growth [197]. Following [38, 39], microbial growth is modelled using a logistic growth term, modified by a Hill function, which accounts for the effects of bacteriostatic antibiotics. Though the specific growth rate of *E. coli*, r, has not yet been reported for dairy slurry, [206] found that the growth rate of *E. coli* in manure amended soils varied between 0.05 and 0.6 h^{-1}; Kim et al. [207] found that rifampin resistant *E. coli* had a growth rate of 0.33 h^{-1} in a 2:1 compost and water growth media; and [38] note that faster growth rates have been recorded in laboratory conditions (up to 0.9 h^{-1}) in [208] and [209], and a value of 0.5 h^{-1} has previously been used to model the growth of *E. coli* in activated sludge [210]. Using this information and following [38], in this model, $r = 0.5$ h^{-1}.

In the model, bacteria can become resistant to either or both antibiotics, allowing for the emergence of MDR [48]. Rather than consider stochastic transfer events, these are homogenised into a constant rate of horizontal gene transfer (HGT), following [38, 139, 140]. It is assumed that the strains of bacteria can acquire new genetic elements which confer resistance through HGT [48]. The plasmid and gene dynamics are simplified here, assuming that the relevant genes for resistance to both antibiotics have become associated on a single mobile genetic element (in the case of susceptible bacteria becoming multidrug resistant with no intermediate resistances being acquired). It was also assumed that plasmids carrying individual resistance genes are compatible [211], so both resistance genes can be received on separate plasmids.

In Baker et al.'s model, the rate of HGT is described using a "force of transfer" term:

$$\frac{\beta}{N(t)}R(t), \tag{5.11}$$

where β is the rate of horizontal gene transfer, $N(t)$ is total number of bacteria at time t and R is the number of resistant bacteria at time t. Ternent et al. [140] and Roberts et al [139] use a slightly different term, which can be derived using chemical reaction kinetics. For a reaction of the type

$$A + B \xrightarrow{k} B + C, \tag{5.12}$$

where A and B are chemical reactants and C is the reaction product, the reaction kinetics for C can be described mathematically by employing the law of mass action which results in the differential equation

$$\frac{d[C]}{dt} = k[A][B] \tag{5.13}$$

where $[X]$ is the concentration of chemical X [196]. Under the assumption that

the conversion of susceptible bacteria to resistant bacteria is irreversible (once new genetic elements have been acquired), the interaction between the two microbial strains could be considered as a reaction equation:

$$S + R \xrightarrow{k_\beta} 2R, \tag{5.14}$$

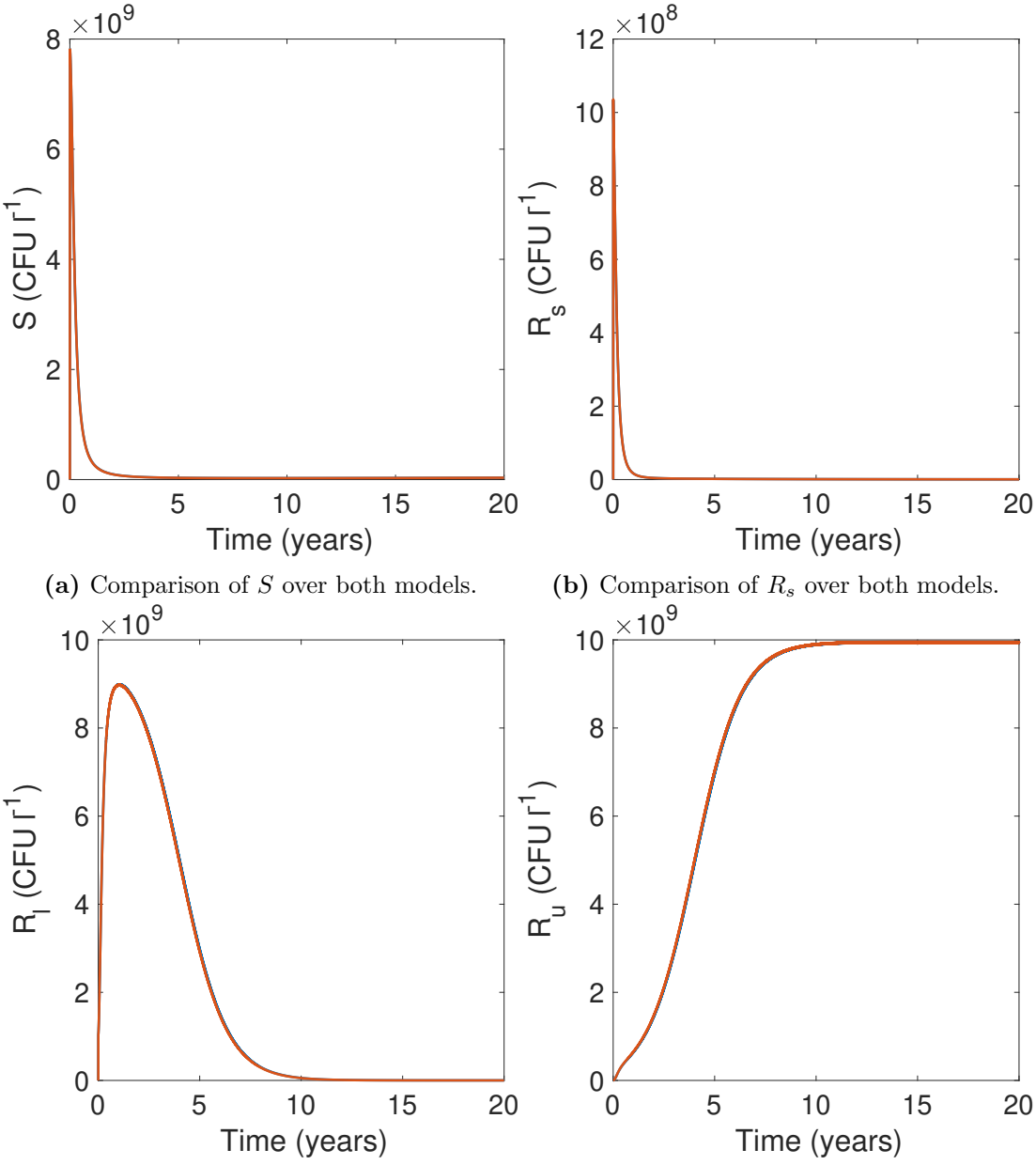
where S and R are the susceptible and resistant strains of bacteria, respectively and k_β is the rate of HGT. Positing that this stands for all three strains of resistant bacteria in the model, then using equation 5.13 allows an alternative formulation for modelling HGT in the new model. For example, the transfer of bacteriolytic, bacteriostatic and multidrug-resistance genes to susceptible bacteria via HGT can be modelled with the term

$$S(\beta_s R_s + \beta_l R_l + \beta_u R_u) \tag{5.15}$$

where S is the concentration of susceptible bacteria, R_s, R_l and R_u are the concentrations of bacteriostatic-resistant, bacteriolytic-resistant and multidrug-resistant bacteria, respectively, and β_s, β_l and β_u are the HGT rates for bacteriostatic, bacteriolytic and super resistant bacteria, respectively (each with dimensions of l(CFU h)$^{-1}$). Both the force of transfer and mass action terms best capture conjugation, but potentially omit transduction and transformation effects [121]. Figure 5.1 shows each of the simulations for each microbial strain side by side. The mean absolute percentage error (MAPE) was calculated to quantify the difference between the two models. At most the models differ by $\approx 2\%$ on average over the full 20 year time period, see Table 5.2. It is evident from Figures 5.1a to 5.1d that, under typical parameter values (see Table 5.3), the new model behaves very similarly to the original, to the point where it is almost indiscernible. Figure 5.2 shows the difference in bacterial concentration between the two models (here the force of transfer model is subtracted from the mass action model). In general the largest discrepancies are at the start of the simulations. The difference between the models fluctuates as they are simulated, leading to the varying line thickness in Figure 5.2. Though the differences in the first five years appear large (approaching a magnitude 1×10^8), it should be noted that these differences are less than 1% of the total bacterial concentration. As the reaction kinetics approach simplifies the HGT term without having a large impact on the model behaviour, it was used instead of the force of transfer term from [38].

Microbial Strain	S	R_s	R_l	R_u
MAPE	1.9251	0.3413	2.2056	0.6280

Table 5.2: Mean average percentage error (MAPE) values comparing the similarity of the two models.



(a) Comparison of S over both models.

(b) Comparison of R_s over both models.

(c) Comparison of R_l over both models.

(d) Comparison of R_u over both models.

Figure 5.1: Comparison plots of the four microbial strains using the the mass action model (see equation 5.15) and the force of transfer model (see equation 5.11). The two models behave very similarly, so much so that it is hard to distinguish between them.

The three rates of HGT, β_s, β_l and β_u are all initially set to 10^{-14}, based on the mass-action rate of transfer given in [123], which is equivalent to between 10^{-11} and 10^{-18} $(\text{CFU/l})^{-1}\text{h}^{-1}$. The chosen mass-action rates of transfer are slower than

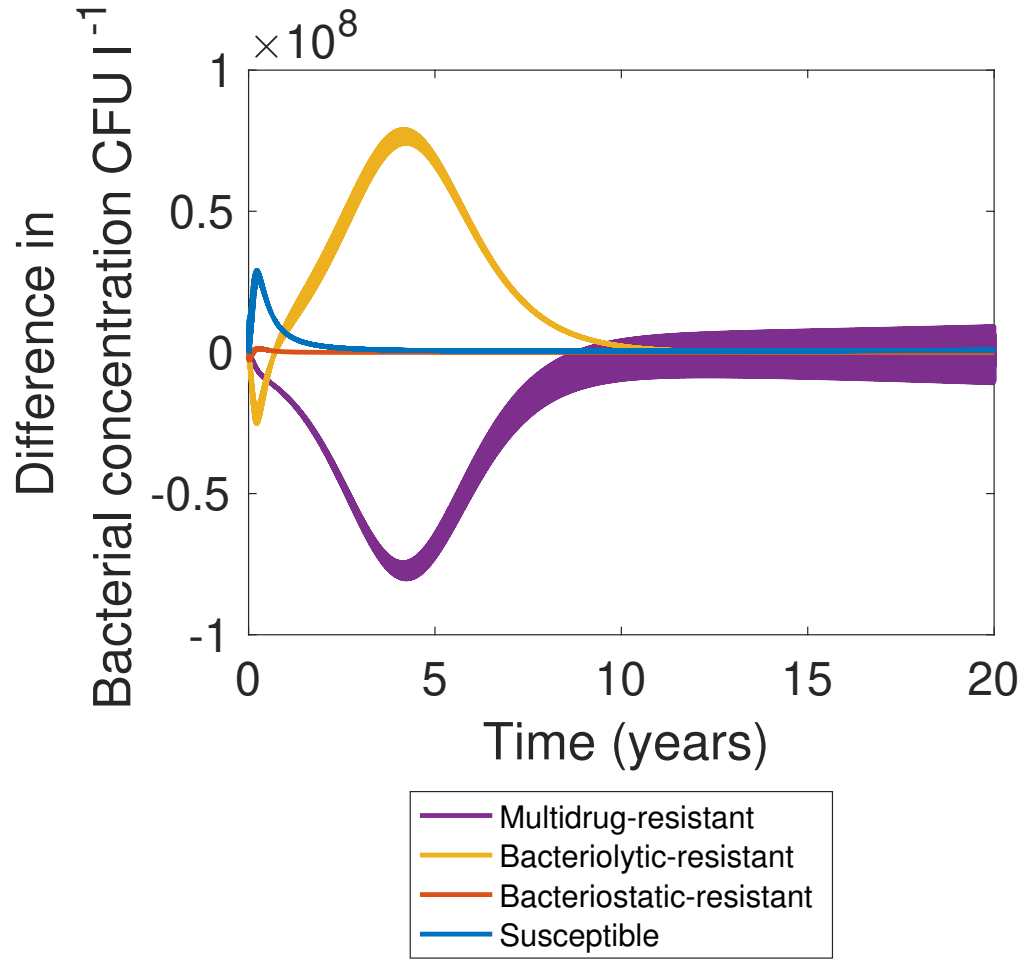


Figure 5.2: The difference in bacterial concentrations between the mass action model (see equation 5.15) and the force of transfer model (see equation 5.11). Here the force of transfer model is subtracted from the mass action model. The varying line thickness arises due to fluctuations in the difference between the models.

the relative rates of HGT used in [39] and [38] (10^{-13} and 4×10^{-13}, respectively) but well within the range of possible values described in [123]. During sensitivity testing β_u, β_l and β_s were allowed to vary to investigate the impact of faster and slower genetic transfer.

Minimum inhibitory concentrations (MIC) vary greatly between antibiotics. The MIC of bacteriostatic antibiotics, (MIC_s), is assumed to be 8 μg l^{-1}, based on the size adjusted MIC for Erythromycin, a bacteriostatic antibiotic used in agriculture [212], reported in [173] and slightly higher than the adjusted MIC for oxytetracycline, another commonly used veterinary antibiotic. The size adjusted MIC is a corrected value for the lowest recorded MIC in the EUCAST database, based on calculations performed by Bengtsson-Palme and Larsson [173]. The

MIC of bacteriolytic antibiotics (MIC_l) is set to 4 μg l^{-1}, the size adjusted MIC of bacteriolytic veterinary antibiotic ampicillin [173, 193, 212]. This MIC is also a similar order of magnitude to several cephalosporin antibiotics, bacteriolytic antibiotics which frequently used in agriculture [49, 173, 212]. This discrepancy in MIC values between bacteriolytic and bacteriostatic antibiotics means that a lower concentration of bacteriolytic antibiotics are required to inhibit the bacteria in the slurry tank. However, sensitivity analysis later in the chapter indicates that increasing MIC_l does not greatly affect the eventual distribution of bacterial phenotypes.

It was assumed that bacteria incur a relative fitness cost for resistance to each type of antibiotic [50]. Furthermore it was assumed that these costs, α_s, α_l and α_u, are all equal, i.e. no extra cost is incurred by multidrug-resistant bacteria, due either to selective pressure reducing the cost of MDR, or the presence of a compensatory mutation [50–52]. Furthermore, the resistance fitness costs are all constant and within the range for *E. coli* described in [50] at $\alpha_s = \alpha_l = \alpha_u = 0.1$.

It was assumed that bacteria can die from both natural causes and from exposure to bacteriolytic antibiotics [213]. Following [187], it is assumed that natural death occurs at a constant rate and the natural death rate for susceptible and resistant bacteria are denoted by δ_S and δ_R, respectively. Following [214–216] and [187] the natural death rates for susceptible and resistant bacteria, δ_S and δ_R, are set to 0.001h^{-1}. For bacteria susceptible to bacteriolytic antibiotic, following [199], the antibiotic induced death rate is described using Michaelis-Menten kinetics:

$$\Delta_A = \delta_l \frac{A_l}{MIC_l + A_l}, \tag{5.16}$$

where δ_l is the rate at which antibiotic kills bacteria at MIC, A_l is the concentration of bacteriolytic antibiotic and MIC_l is the minimum inhibitory concentration of the bacteriolytic antibiotic which will inhibit 50% of bacteria. The time to kill kinetics of various veterinary antibiotics on *E. coli* have been studied in Mueller Hinton broth and agar by [213]. The bacteria was exposed to eight times the MIC of enrofloxacin, danofloxacin, erythromycin, tilmicosin, penicillin G, ceftiofur and tetracycline. Norcia et al. report per hour proportional death rates of between ~ 0 and 0.3. Initially, δ_l was set to 0.01, assuming a low death rate due to bacteriolytic antibiotic. However, as enrofloxacin and penicillin are both used in dairy agriculture [212] and have $\delta_l \approx 0.3$ at eight times MIC, δ_l was varied between 0 and 1 during sensitivity analysis. In the case of bacteriolytic-resistant *E. coli*, Palaniappian and Holley [217] were not able to record an MIC for a multi-resistant strain of *E. coli* for two bacteriolytic antibiotics, ampicillin and penicillin, tested up to 512000μg l^{-1}. Due to this, the bacteriolytic antibiotic driven death term is

omitted in the cases of bacteriolytic-resistant and multidrug-resistant *E. coli*.

Baker et al. [38] report *E. coli* concentrations between 2 and 6×10^4 CFU ml^{-1} in dairy slurry, consistently within the same range reported in [218]. Furthermore, the proportion of drug resistant strains of *E. coli* in healthy lactating dairy cows is estimated to be approximately 40% [204]. Using these values, assuming there are no MDR bacteria present in the cows and based on data from [38], the influent concentration of bacteria is given by $\nu = 6 \times 10^7 \text{CFUl}^{-1}$ and and the proportions of bacteriostatic, bacteriolytic and multidrug-resistant bacteria in the inflow, respectively, $\rho_s = \rho_l = 0.2$ and $\rho_u = 0$, so that the total proportion of resistant bacteria in the inflow is 0.4.

Though temperature has been shown to affect the survival of pathogens in slurry, Kearney et al. [219] recorded no difference in *E. coli* population decimation time between samples stored in 4°C and 17°C cattle slurry. Similarly Biswas et al. [188] showed that *E. coli* populations in slurry (which ranged between 30°C and 50°C) had increased survivability at varying temperatures compared to *Salmonella spp.* and *Listeria monocyogenes*, with *E. coli* populations only declining slightly over the incubation period. Due to this temperature dependence is omitted from the model, though it may be important to have a temperature dependent death rate when modelling other bacteria.

All parameter definitions and typical values are shown in Table 5.3. Though, where possible, parameter values have been taken from studies of slurry and manure [38, 200], the lack of available data meant that parameters often had to be selected based on recorded values in other media, such as manure amended soils [206], compost and water [207] or even *in vitro* studies [123]. In other cases, parameter values (such as resistance fitness costs) were chosen based on meta-analyses [50] or, in the case of MIC values, the EUCAST database [172]. Some parameters are even drawn from assumptions made by previous models, for example the antibiotic influent rate which is taken from [38]. This means that, though it is possible to determine model behaviours and sensitivity to parameters, the accuracy of individual simulations is unknown. In the following chapter, parameter inference is performed alongside data from the Sutton Bonington farm in order to determine more accurate parameter values.

5.1.2 Mathematical model

The model is made up of six coupled differential equations, two of which describe the concentrations of bacteriostatic and bacteriolytic antibiotics (A_s and A_l), respectively, and four that describe susceptible (S), bacteriostatic-resistant (R_s), bacteriolytic-resistant (R_l) and multidrug-resistant (R_u) bacteria.

Parameter	Description	Typical Value	Reference
r	Specific growth rate of *E. coli*	0.5 h^{-1}	[38]
β_s	Bacteriostatic-resistance gene transfer term	10^{-14} $lCFU^{-1}h^{-1}$	[38, 39, 123]
β_l	Bacteriolytic-resistance gene transfer term	10^{-14} $lCFU^{-1}h^{-1}$	[38, 39, 123]
β_u	MDR gene transfer term	10^{-14} $lCFU^{-1}h^{-1}$	[38, 39, 123]
λ	Rate of slurry inflow to tank	$613lh^{-1}$	[38]
ν	Concentration of bacteria in slurry inflow	6×10^7 CFU l^{-1}	[38, 218]
ρ_s	Proportion of bacteriostatic-resistant bacteria in inflow	0.2	[204]
ρ_l	Proportion of bacteriolytic-resistant bacteria in inflow	0.2	[204]
ρ_u	Proportion of multidrug-resistant bacteria in inflow	0.0	[204]
α_s	Bacteriostatic-resistance fitness cost as a fraction of r	0.1	[38, 50]
α_l	Bacteriolytic-resistance fitness cost as a fraction of r	0.1	[38, 50]
α_u	MDR fitness cost as a fraction of r	0.1	[38, 50]
V_1	Initial volume of slurry in the tank	150,000 l	[38]
θ_s	Rate of bacteriostatic antibiotic inflow	1711 μg h^{-1}	[38]
θ_l	Rate of bacteriolytic antibiotic inflow	1711 μg h^{-1}	[38]
E_{max}	Maximum effect of antibiotics on bacterial growth	2	[38, 39]
H	Hill coeficient in E_{max} model	2	[38, 39]
MIC_R	MIC for bacteriostatic-resistant bacteria	2000 μg l^{-1}	[38]
MIC_s	MIC for bacteriostatic-sensitive bacteria	8 μg l^{-1}	[173]
MIC_l	MIC for bacteriolytic-sensitive bacteria	4 μg l^{-1}	[173]
μ	Carrying capacity of liquid slurry	10^{10} CFU l^{-1}	[38]
γ_s	Decay rate of bacteriostatic antibiotics	0.0029 h^{-1}	[38]
γ_l	Decay rate of bacteriolytic antibiotics	0.0029 h^{-1}	[38]
δ_S	Natural death rate of susceptible bacteria	0.001 h^{-1}	[187]
δ_R	Natural death rate of resistant bacteria	0.001 h^{-1}	[187]
δ_l	Antibiotic driven death rate of bacteriolytic-susceptible bacteria	0.01 h^{-1}	[213]

Table 5.3: Typical parameter values used for initial simulations of the model.

Model Equations

The equations for the antibiotics are as follows:

$$\frac{dA_s}{dt} = \underbrace{\frac{\theta_s}{V(t)}}_{\text{Inflow}} - A_s \left(\underbrace{\gamma_s}_{\text{Degradation}} + \underbrace{\frac{\Lambda'(t)}{V(t)}}_{\text{Volume change}} \right) \tag{5.17}$$

and, similarly,

$$\frac{dA_l}{dt} = \frac{\theta_l}{V(t)} - A_l \left(\gamma_l + \frac{\Lambda'(t)}{V(t)} \right). \tag{5.18}$$

The ODEs for the four strains of bacteria are

$$\begin{aligned} \frac{dS}{dt} = \underbrace{r\left(1 - \frac{N}{\mu}\right) E_S S}_{\text{Modified logistic growth}} - \overbrace{S(\beta_s R_s + \beta_l R_l + \beta_u R_u)}^{\text{Gene transfer}} + \underbrace{\Lambda'(t)(1-\rho)\frac{\nu}{V(t)}}_{\text{Inflow}} - \\ \overbrace{\frac{\Lambda'(t)S}{V(t)}}^{\text{Volume}} - \underbrace{\delta_S S}_{\text{Natural death}} - \overbrace{\delta_l S \frac{A_l}{MIC_l + A_l}}^{\text{Antibacterial death}} \end{aligned} \tag{5.19}$$

$$\begin{aligned} \frac{dR_s}{dt} = r(1-\alpha_s)\left(1 - \frac{N}{\mu}\right) E_R R_s + R_s(\beta_s S - \beta_l R_l - \beta_u R_u) + \\ \Lambda'(t)\rho_s \frac{\nu}{V(t)} - \frac{\Lambda'(t)R_s}{V(t)} - \delta_R R_s - \delta_l R_s \frac{A_l}{MIC_l + A_l} \end{aligned} \tag{5.20}$$

$$\begin{aligned} \frac{dR_l}{dt} = r(1-\alpha_l)\left(1 - \frac{N}{\mu}\right) E_S R_l + R_l(-\beta_s R_s + \beta_l S - \beta_u R_u) + \\ \Lambda'(t)\rho_l \frac{\nu}{V(t)} - \frac{\Lambda'(t)R_l}{V(t)} - \delta_R R_l \end{aligned} \tag{5.21}$$

and

$$\begin{aligned} \frac{dR_u}{dt} = r(1-\alpha_u)\left(1 - \frac{N}{\mu}\right) E_R R_u + R_s R_l(\beta_s + \beta_l) + \beta_u R_u(S + R_s + R_l) + \\ \Lambda'(t)\rho_u \frac{\nu}{V(t)} - \frac{\Lambda'(t)R_u}{V(t)} - \delta_R R_u. \end{aligned} \tag{5.22}$$

Here N, $V(t)$, E_S, E_R, ρ and Λ are given by

$$N = S + R_s + R_l + R_u \tag{5.23}$$

$$V(t) = V_1 + \Lambda(t) - \omega(t) \tag{5.24}$$

$$E_S = 1 - \frac{E_{max} A_s^H}{MIC_s^H + A_s^H} \tag{5.25}$$

$$E_R = 1 - \frac{E_{max} A_s^H}{MIC_R^H + A_s^H} \tag{5.26}$$

$$\rho = \rho_s + \rho_l + \rho_u \tag{5.27}$$

$$\Lambda(t) = \lambda t. \tag{5.28}$$

The initial conditions for bacteriolytic and bacteriostatic antibiotic are $A_s(0) = A_l(0) = 0$, respectively. Similarly the initial conditions for the four strains of bacteria are $S(0) = R_s(0) = R_l(0) = R_u(0) = 0$. The ODE45 MATLAB solver was used to solve the equations in MATLAB_R2019a. ODE45 is a nonstiff, medium accuracy solver recommended by MATLAB as first choice when solving ODEs [220].

5.2 Results and Discussion

In this section the model is simulated under various conditions and analysis is performed to determine the effect of the parameters on the development of AMR. As a simple first case, the model is simulated with constant inflow of slurry and no tank emptying. The model was then simulated with no direct transfer of multidrug-resistance, and then with an increased cost of multidrug-resistance, to test the model output under alternative conditions. Various emptying regimes, including a seasonal emptying regime which mimics that used on UK farms [106, 184, 185], were then tested to determine the effects of tank emptying on the development of AMR. A one-way sensitivity analysis was performed to determine key parameters and their effects on multidrug resistance. This was followed by a two-way analysis of some of those key parameters. Finally a stability analysis was performed to identify the steady states of the system.

Figure 5.3 shows a simulation of the model under typical parameter values as in Table 5.3. After ten years, multidrug-resistant bacteria dominate the tank and the number of bacteria in the tank has reached the carrying capacity. After approximately one year, the tank is dominated by bacteriolytic resistant bacteria and the community of susceptible bacteria makes up around 5% of the total bacteria in the tank. This is similar to the timescales in [38], where susceptible bacteria in the tank are largely removed after 300 days.

In the infinite filling case, multidrug-resistance dominating the tank, as seen in Figure 5.3 is not, in fact, the long term behaviour of the system. If the model is simulated over hundreds of years (likely much longer than the lifespan of a slurry tank), susceptible bacteria begin to become the most prevalent strain. This can

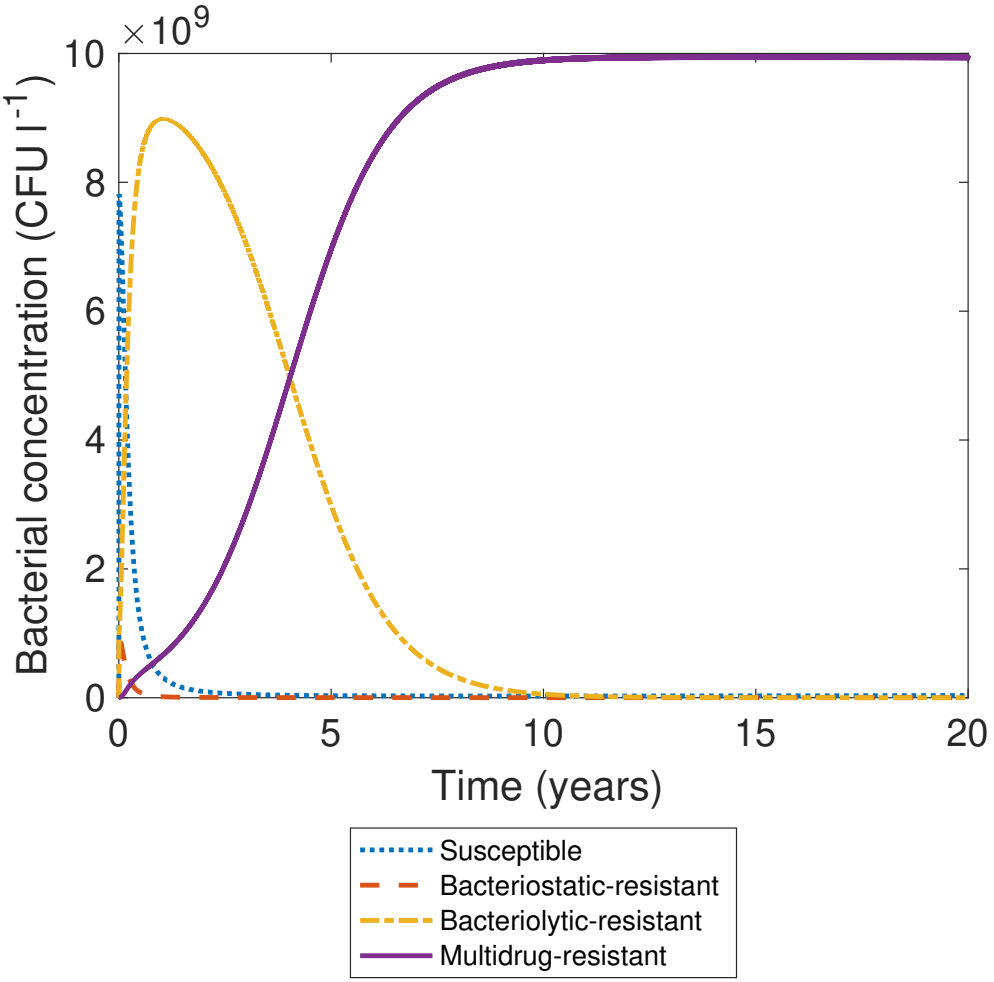


Figure 5.3: A simulation of the model described by equations 5.17 to 5.22, using the parameter values given in Table 5.3.

be seen in Figure 5.4. It will be shown later in this chapter that susceptible bacteria dominating the tank is, in fact, a steady stable state of the infinite filling scenario. This is likely due to the lack of environmental pressure from antibiotics; as the volume of slurry in the tank increases, the concentration of antibiotic decreases to become almost negligible. This means that, though multidrug resistant bacteria dominate the tank at the beginning of the simulations, as the antibiotic concentration decreases, the cost of resistance no longer outweighs the advantages of resistance.

The scale of the genetic transfer terms for the simulation shown in Figure 5.3 can be seen in Figure 5.5. This shows pathways the bacteria follow as they gain resistance to either type of antibiotic. As HGT of a certain genetic element is dependent on the prevalence of bacteria with that genetic element, once multidrug resistant bacteria dominate the tank, transfer events associated with multidrug

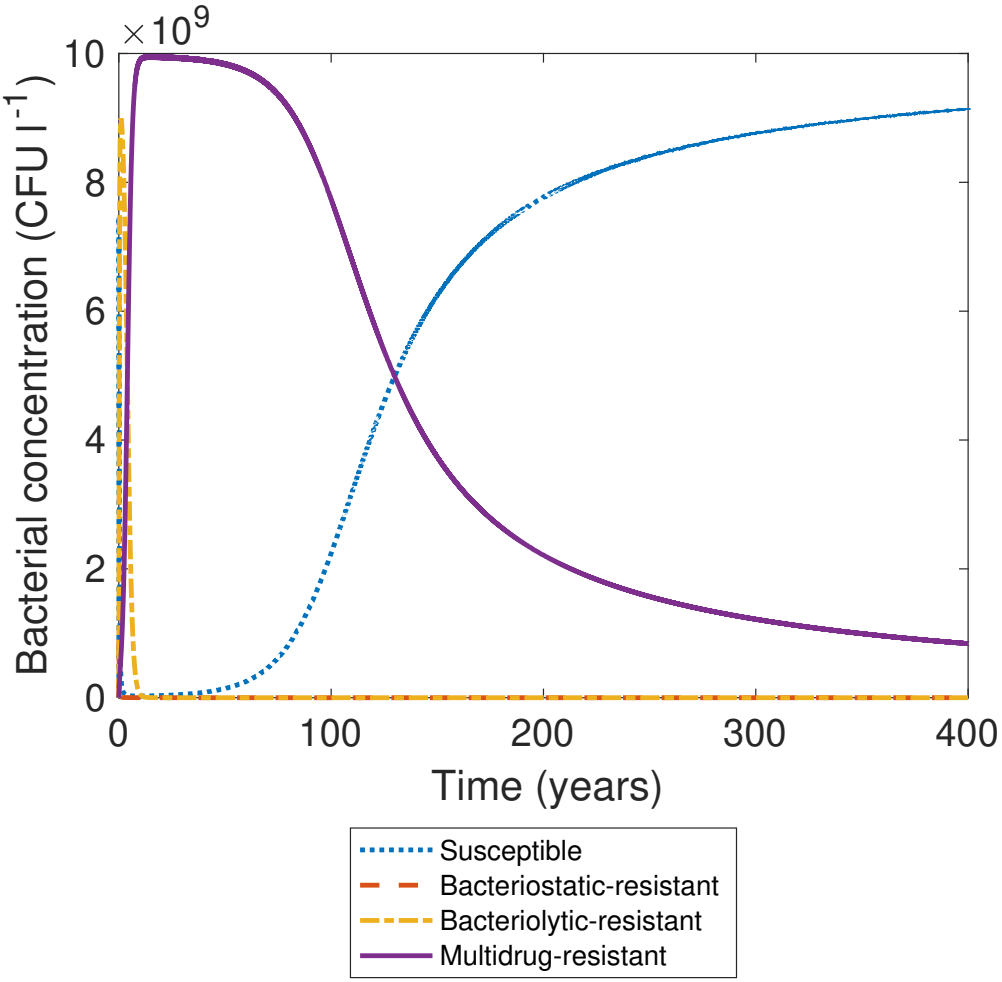


Figure 5.4: The model described by equations 5.17 to 5.22, simulated for 400 years, using parameter values given in Table 5.3.

resistance become most common. In the first year of the simulation, the most prevalent pathway is $S \rightarrow R_l$, after which it becomes $R_l \rightarrow R_u$ as the R_l concentration in the tank increases. Eventually the transfer terms become dictated by the influent concentrations of S, R_s and R_l as R_u dominates the tank.

Certain scenarios using alternative parameter values have also been considered to ensure the model behaves as expected. Figure 5.6 shows the bacterial concentrations when the rate of multidrug-resistant gene transfer, β_u, is equal to zero and the other parameters are as in Table 5.3. Here it is assumed that there is no mobile genetic element that can directly transfer MDR to a bacterium, instead MDR can only be acquired through the acquisition of the two separate genetic elements which confer bacteriostatic and bacteriolytic-resistance. This results in bacteriolytic-resistant bacteria dominating the tank, while less than 10% of the bacterial population are multidrug-resistant. In this case a small proportion of the

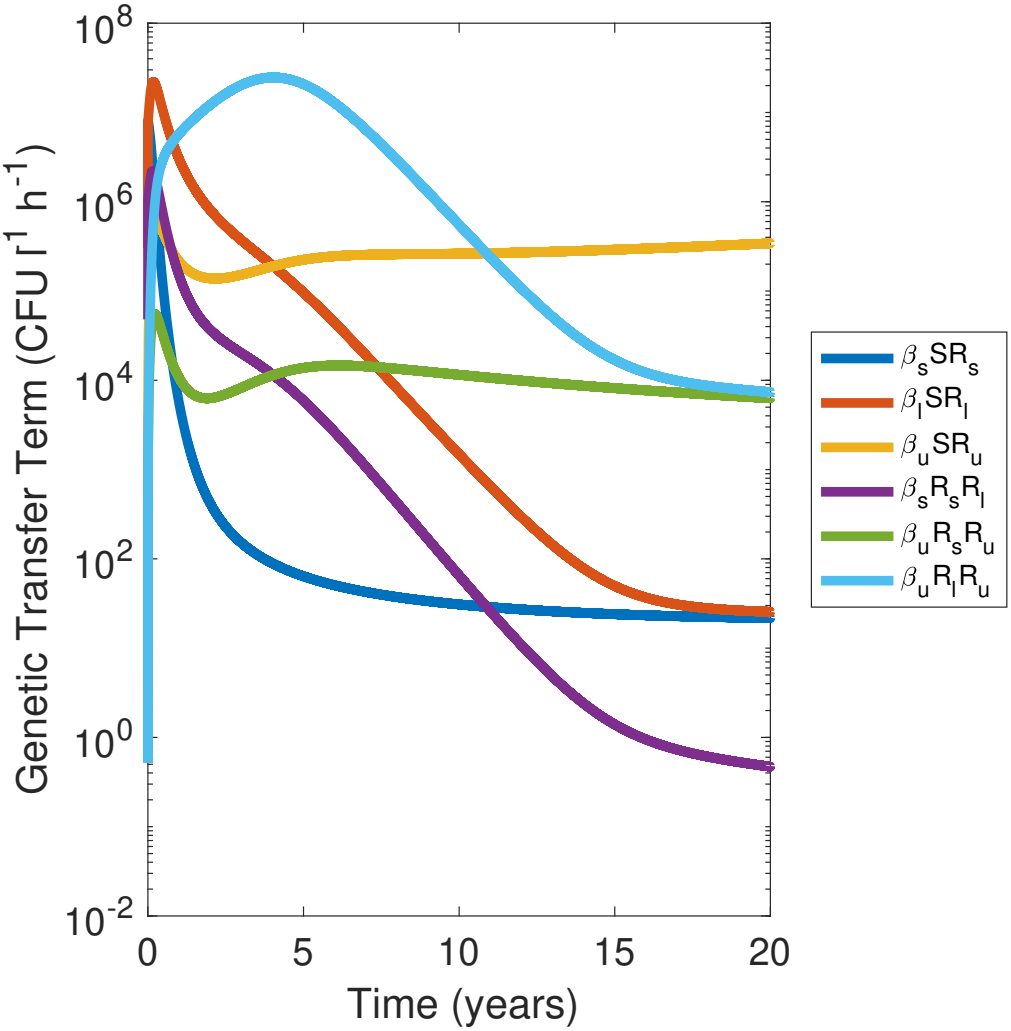


Figure 5.5: The Resistance transfer terms for the model simulation shown in 5.3, plotted on a log scale.

tank acquires MDR whilst bacteriolytic bacteria make up the greatest proportion in the tank. This simulation may not be reflective of real-world circumstances, as it is known that ARGs accumulate on plasmids [186, 194] and that in the presence of both types of antibiotic there is a biological advantage to acquiring both resistance genes, it is very unlikely that β_u would be zero.

Figure 5.7 shows the bacterial concentrations in the tank when the physiological cost of maintaining MDR, α_u, is increased from 0.1 to 0.2 to simulate stacking resistance costs (i.e. $\alpha_u = \alpha_l + \alpha_s$). It has been assumed up until this point that the physiological cost of being resistant to a single antibiotic is the same as the physiological cost of being resistant to both from a microbial growth perspective, as if MDR was accompanied with a compensatory mutation which mitigated the cost of being resistant to both antibiotics [50, 221]. It is also likely that there would be selective pressure to keep the cost of resistance low. In this new sce-

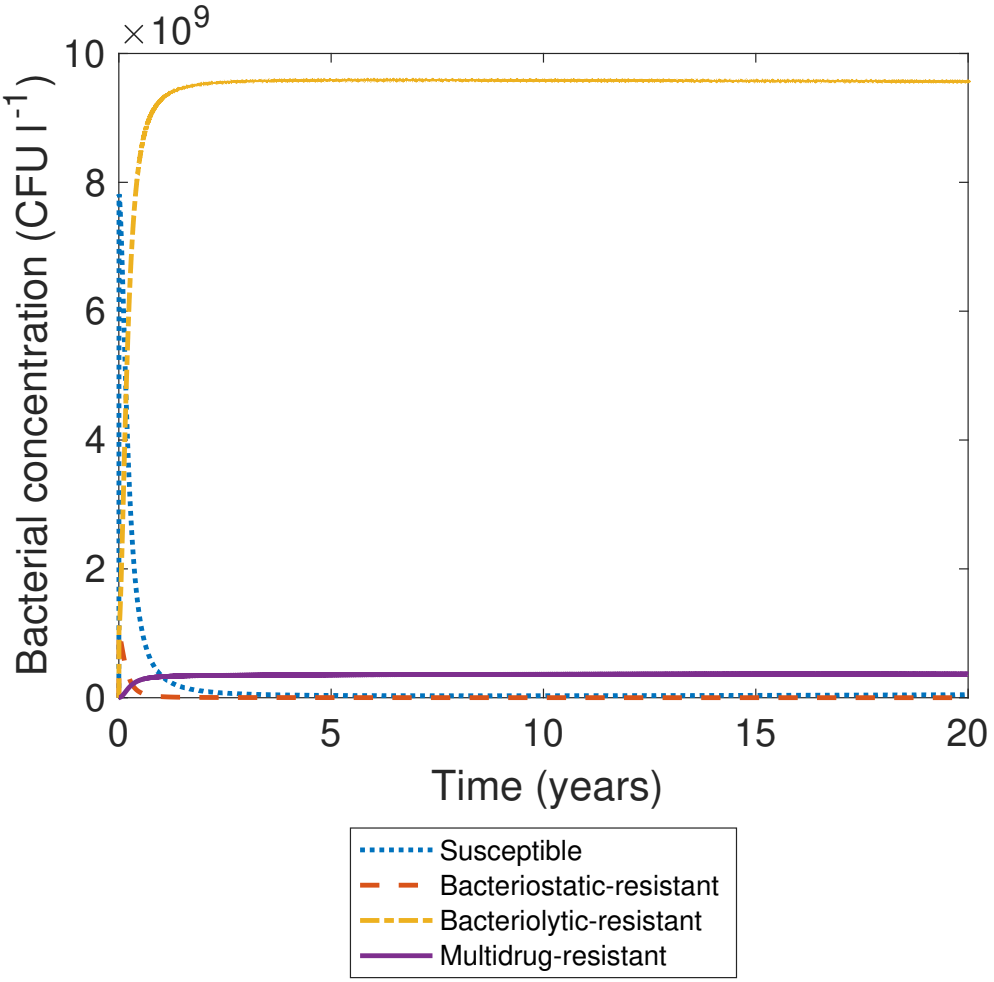


Figure 5.6: A simulation of the model described by equations 5.17 to 5.22, using the parameter values given in Table 5.3 and setting the rate of MDR transfer, β_u, to zero.

nario it is assumed there is no compensatory mutation, so that being resistant to both strains of antibiotic causes the relative fitness cost to the microbial population to double. In this scenario, similar dynamics to those in Figure 5.6 arise as bacteriolytic-resistant bacteria become the dominant strain within the tank. However, the multidrug-resistant population decrease over time in this scenario.

5.2.1 Effects of altering the tank emptying regime

An aspect that differentiates the current model from existing models in the literature is the inclusion of a tank emptying. Thus far, the volume function, $V(t) = V_1 + \lambda t$, has been used (setting the emptying term $\omega(t) = 0$), following [38]. In effect simulating an infinite capacity slurry tank. Instead consider a regular, instantaneous emptying regime, whereby the tank fills for a set number

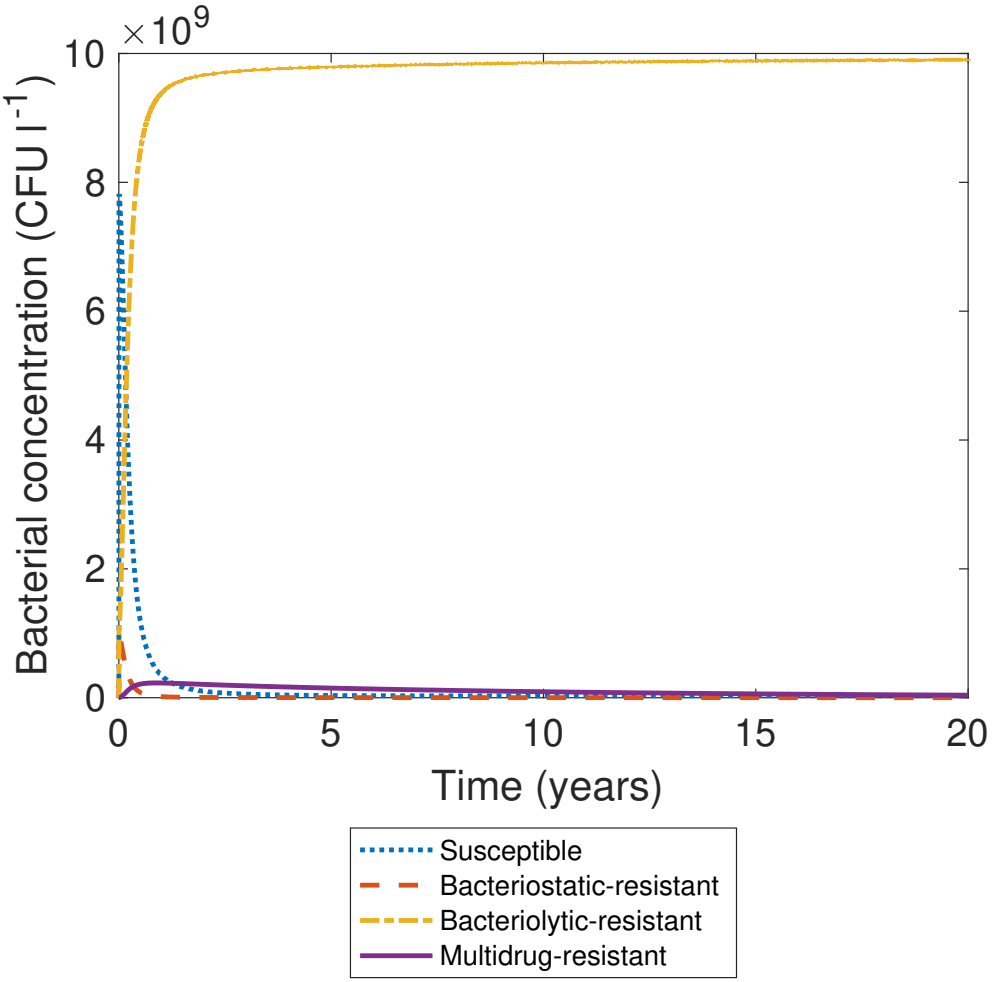


Figure 5.7: A simulation of the model described by equations 5.17 to 5.22, using the parameter values given in Table 5.3 and setting the relative cost of MDR, α_u, to 0.2.

of hours, τ_e, then is emptied to its original volume and not cleaned as the results from the Should We Worry About Slurry project also indicate that tank cleaning happens very rarely (see Chapter 3). It also disregards the possible influence of resistant biofilms which could be employing multiple resistance mechanisms [222]. With this in mind tank emptying is modelled without cleaning and for simplicity it is assumed that emptying is instantaneous, so that

$$\omega(t) = \lambda\tau_e \text{floor}\left(\frac{t}{\tau_e}\right) \tag{5.29}$$

where τ_e is the time between tank emptyings, i.e.

$$V(t) = V_1 + \lambda t - \omega(t) = V_1 + \lambda(t \bmod (\tau_e)) \tag{5.30}$$

where mod is the modulo function, which finds the remainder when dividing one number by another. A range of V_1 and τ_e values were chosen to simulate the conditions in a farm slurry tank which has a capacity of three million litres.

To simulate the filling and emptying of the tank on a working UK farm, a seasonal emptying regime was implemented, based on government guidance for NVZs (every week 1st May to 31st October and every 90 days in the other months, accounting both for the muck spreading closed period between October and February and for those times when the land is more likely to be flooded or frozen [106, 184, 185]) leads to multidrug-resistant bacteria dominating the tank within 5 years, as shown in Figure 5.8. In the no-emptying case it took 10 years for multidrug-resistant bacteria to dominate the tank (though the no-emptying case is unrealistic). This indicates that implementing an emptying regime has an effect on the speed at which MDR develops, despite having little effect on the eventual proportion of multidrug-resistant bacteria in the tank. Figure 5.9a shows the antibiotic concentration in the no-emptying case and Figure 5.9c shows the antibiotic concentration in the seasonal emptying case. Figures 5.9b and 5.9d show the slurry volume in the no-emptying and seasonal emptying cases, respectively. By emptying the tank regularly, a higher concentration of antibiotic is maintained due to the reduced slurry volume, driving up resistance through environmental pressure.

The model was simulated with varying V_1 and τ_e over 20 years, the minimum recommended lifespan of a slurry store [223]. Changing the emptying regime in this way leads to the final proportion of multidrug-resistant bacteria varying between 0.976 and 0.992, so that multidrug-resistant bacteria dominate the tank regardless of emptying regime. To determine the effects of tank emptying regime on the rate of development of MDR bacteria, the time at which multidrug-resistant bacteria make up 95% of the total population was plotted against increasing initial volume, V_1, and increasing time to empty, τ_e. These values were chosen to show the effects of altering the emptying schedule. Figure 5.10a shows that as τ_e and V_1 increase so does the time to reach 95% MDR. This indicates that farm practice may well an influence on the way in which AMR persists and spreads within the slurry tank. The time at which multidrug-resistant bacteria make up 95% of the population under an NVZ seasonal emptying regime is marked on Figure 5.10a. Figure 5.10b shows the relationship between the initial tank volume and the time to 95% MDR. The higher the initial volume, the longer it takes for multidrug-resistant bacteria to dominate the tank.

Current legislation dictates that slurry can only be spread between 1st February and 31st October, and only during those times is the ground is not frozen or at risk of flooding [184], meaning that the slurry store is emptied more frequently

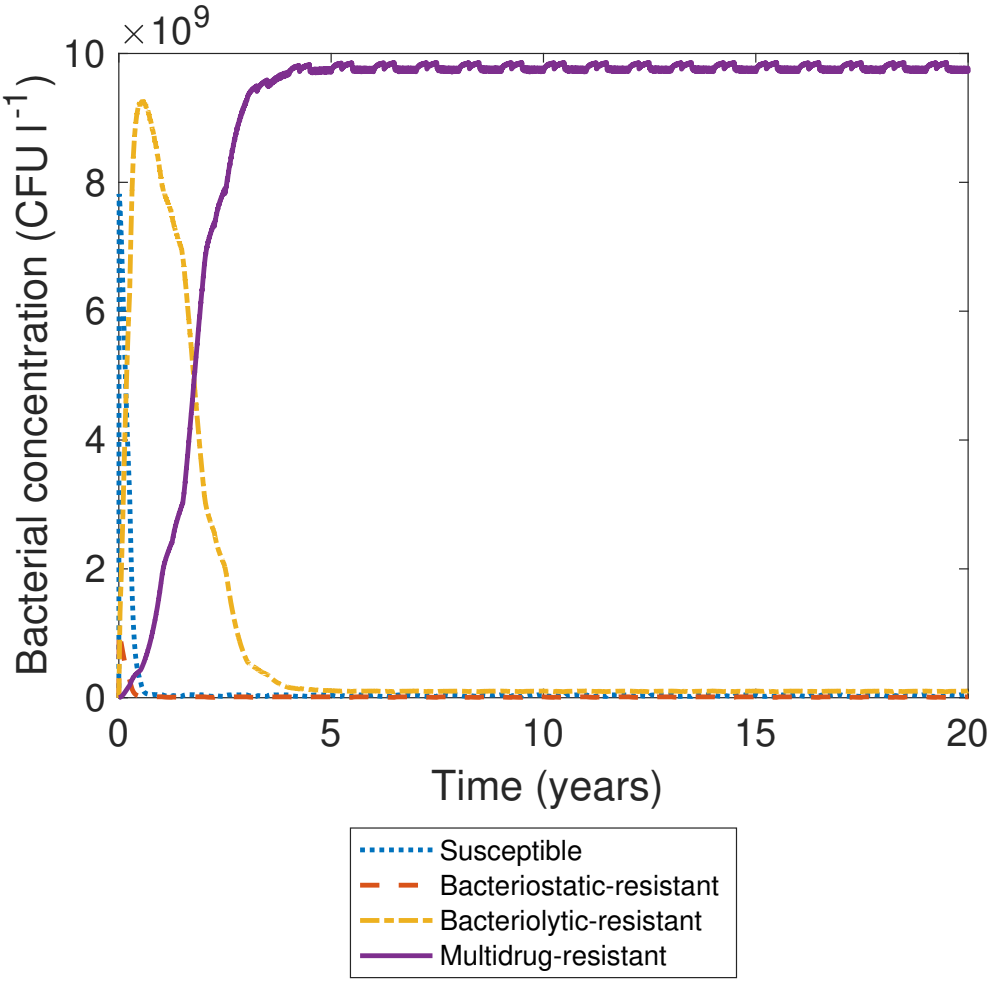
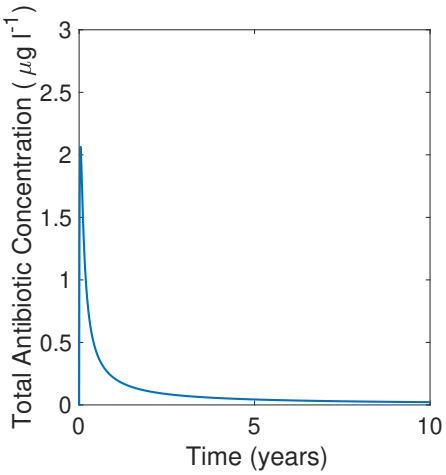


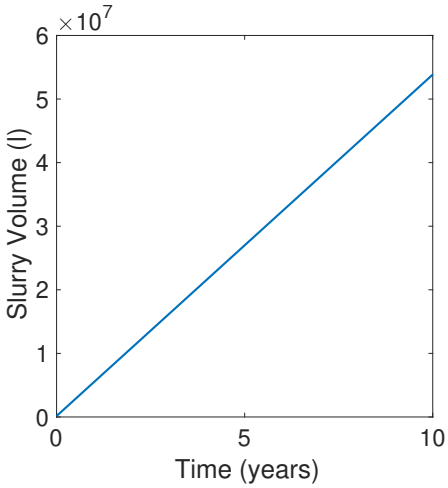
Figure 5.8: A simulation of the model described by equations 5.17 to 5.22, using the parameter values given in Table 5.3. In this simulation, the volume of slurry is calculated using a seasonal emptying regime; the tank is emptied every week 1st May to 31st October and every 90 days in the other months.

during the summer months. According to the simulations, if the tank is emptied to 150,000 litres and a seasonal emptying regime is used, then it takes just under four years for multi-drug resistant bacteria to make up 95% of the population in the tank, as shown in Figure 5.10a. Alternatively, if the minimum volume of slurry in the tank is maintained at around 1.5 million litres, the time to MDR dominance could be increased to seven years without having to alter the rate at which the tank is emptied, see Figure 5.10b.

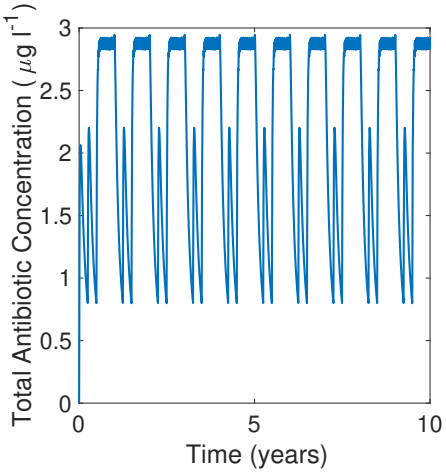
This presents am opportunity for AMR stewardship and intervention. If the tank is emptied completely and then throughly cleaned, this is the equivalent of running the model up to time τ_e and then restarting it completely. In this case it is possible to specify an acceptable resistant proportion within the tank and



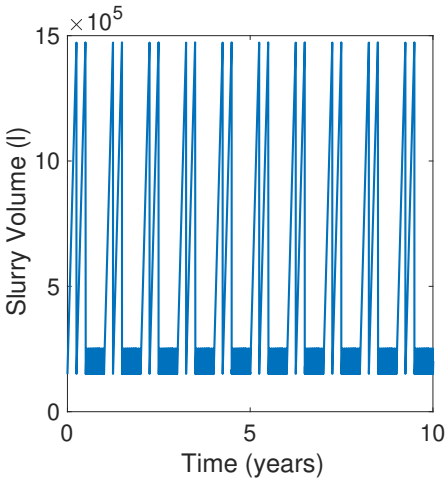
(a) Total antibiotic concentration under a no-emptying regime



(b) Slurry volume under a no-emptying regime.



(c) Total antibiotic concentration under a seasonal emptying regime.



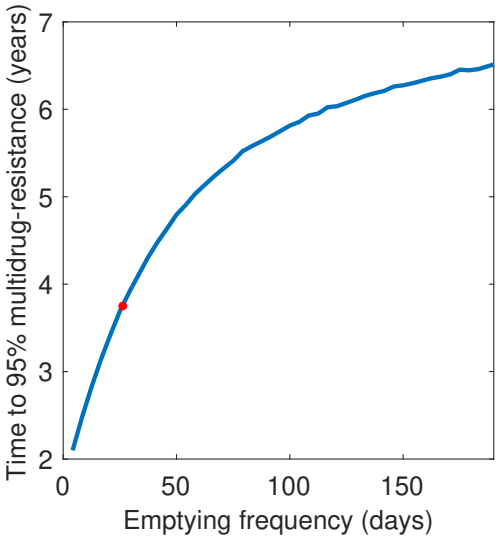
(d) Slurry volume under a seasonal emptying regime

Figure 5.9: Plots of the total antibiotic concentration in the slurry ($A_l + A_s$) and the total volume of slurry in the tank, using the parameter values given in Table 5.3, under no-emptying and seasonal emptying regimes.

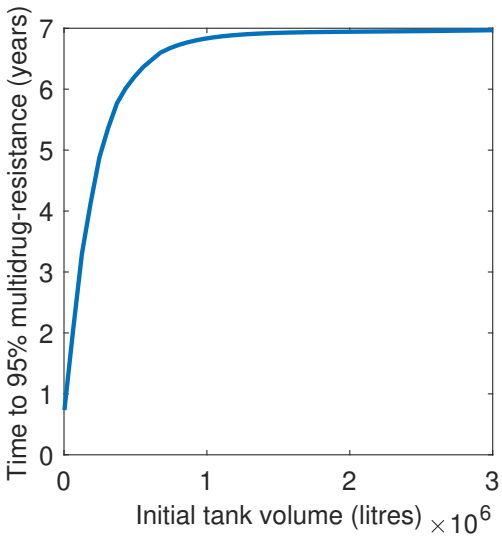
choose τ_e such that the concentration of multidrug resistant *E. coli* never exceeds that proportion. Figure 5.11 shows the appropriate values of τ_e as the multidrug resistant proportion increases. As an example, say that the maximum tolerable proportion of multidrug resistant bacteria was 0.5, then the tank would need to be emptied and fully cleaned after approximately 1.5 years of use.

5.2.2 Sensitivity Analysis

In order to provide a more precise analysis of how model parameters affect the output of the model, one-way sensitivity analysis was conducted. This is a process that allows the investigation of the sensitivity of a model's output to its individual input parameters [224]. Sensitivity scores, S_X, where X is the parameter being



(a) Varying the time between tank emptying, τ_e.



(b) Varying the initial tank volume, V_1.

Figure 5.10: Effects of varying the time between tank emptying, τ_e, and the initial tank volume, V_1, on the time to reach 95% multidrug-resistant bacteria, R_u, within the tank. The dot in 5.10a indicates the time to 95% MDR using the seasonal emptying frequency. A seasonal emptying regime is being used in 5.10b.

changed, were calculated for fifteen model parameters as shown in Table 5.4, the model output being measured was the proportion of multidrug-resistant bacteria in the tank. Here the sensitivity measure, S_X, is defined by

$$S_X = \frac{\Delta P_{SR}/P_{SR}}{\Delta X/X} \tag{5.31}$$

where P_{SR} is the proportion of multidrug-resistant bacteria in the tank at the end of a typical parameter value simulation, X is the parameter being changed and ΔX and ΔP_{SR} represent the change in the parameter value and the resulting change in the model output, respectively [38, 225]. S_X was calculated for each parameter at 100 points evenly spaced across the parameter ranges given in Table 5.4. Two regimes were considered for sensitivity analysis: a simulation with no tank emptying and a simulation with tank emptying every week between 1st May and 31st October and every 90 days in the other months. Both simulations ran for an in-model time of 20 years as this is the minimum recommended lifespan of a slurry store [223]. Though it should be noted it is likely that some farm practices would change over this timescale.

Figure 5.12 shows boxplots of the sensitivities for all thirteen parameters in the no emptying regime. The parameters to which the model is most sensitive are the relative cost of MDR (α_u), the relative cost of bacteriolytic-resistance (α_l) and the inflow rate of bacteriolytic antibiotic (θ_l). The model is also sensitive to

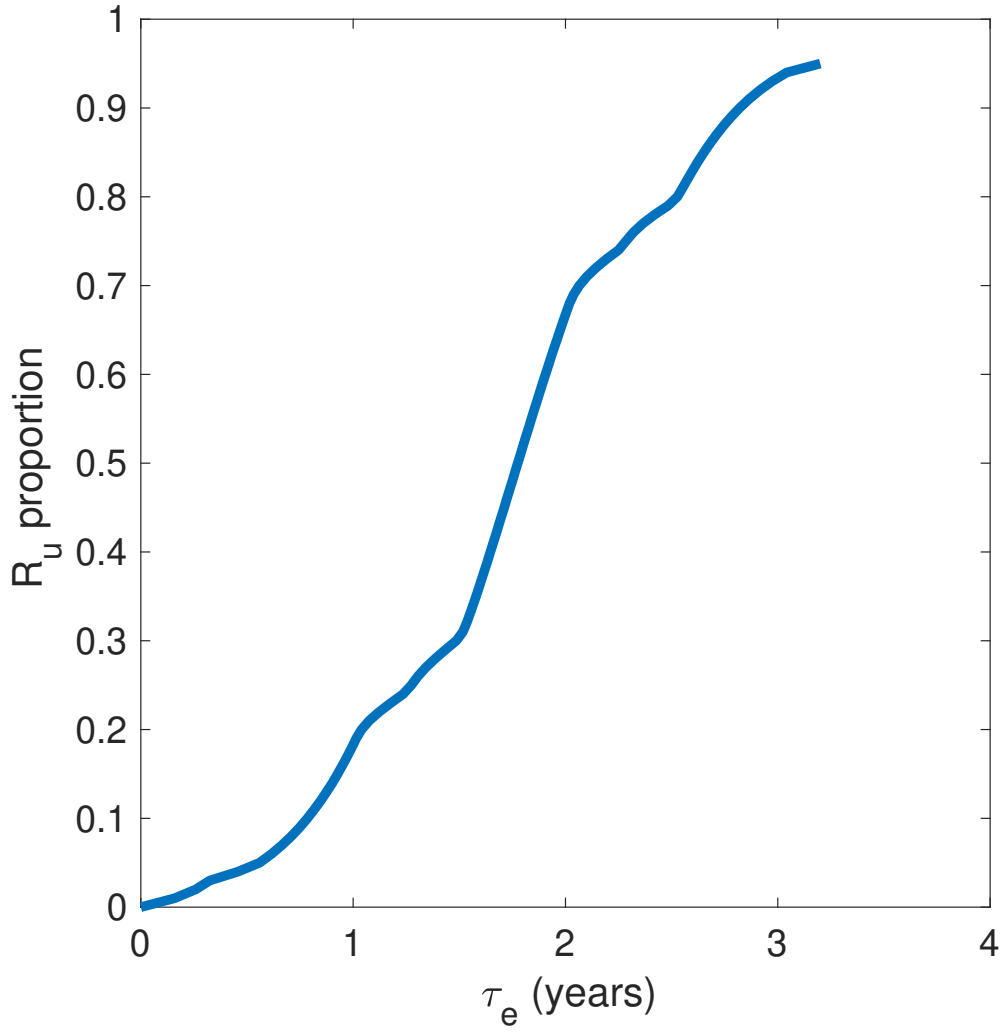


Figure 5.11: Plot of the time at which an intervention would need to occur, τ_e, to stop the multidrug proportion exceeding a given limit. This was simulated using the parameter values given in Table 5.3. The volume of slurry is calculated using a seasonal emptying regime; the tank is emptied every week 1st May to 31st October and every 90 days in the other months.

the bacteriolytic MIC (MIC_l) and the decay rate of bacteriolytic antibiotic (γ_l), indicating that it is the parameters relating to bacteriolytic antibiotics that most affect the development of multidrug-resistant bacteria. Figure 5.13 shows how changing each parameter affects the proportion of multidrug-resistant bacteria. There is also some sensitivity to the death rate of resistant bacteria, δ_R. It is clear that those parameters to which the model is most sensitive have the largest effect on the proportion of R_u bacteria. Increasing the costs of bacteriolytic resistance or MDR (α_l and α_u, respectively) decreases the total multidrug-resistant community. In the case of α_u this occurs at around $\alpha_u = 0.2$, indicating that within the model this is a maximum tolerable cost of MDR. A 20% fitness cost is within recorded ranges for *E. coli* [53]. Similarly, increasing the death rate of resistant

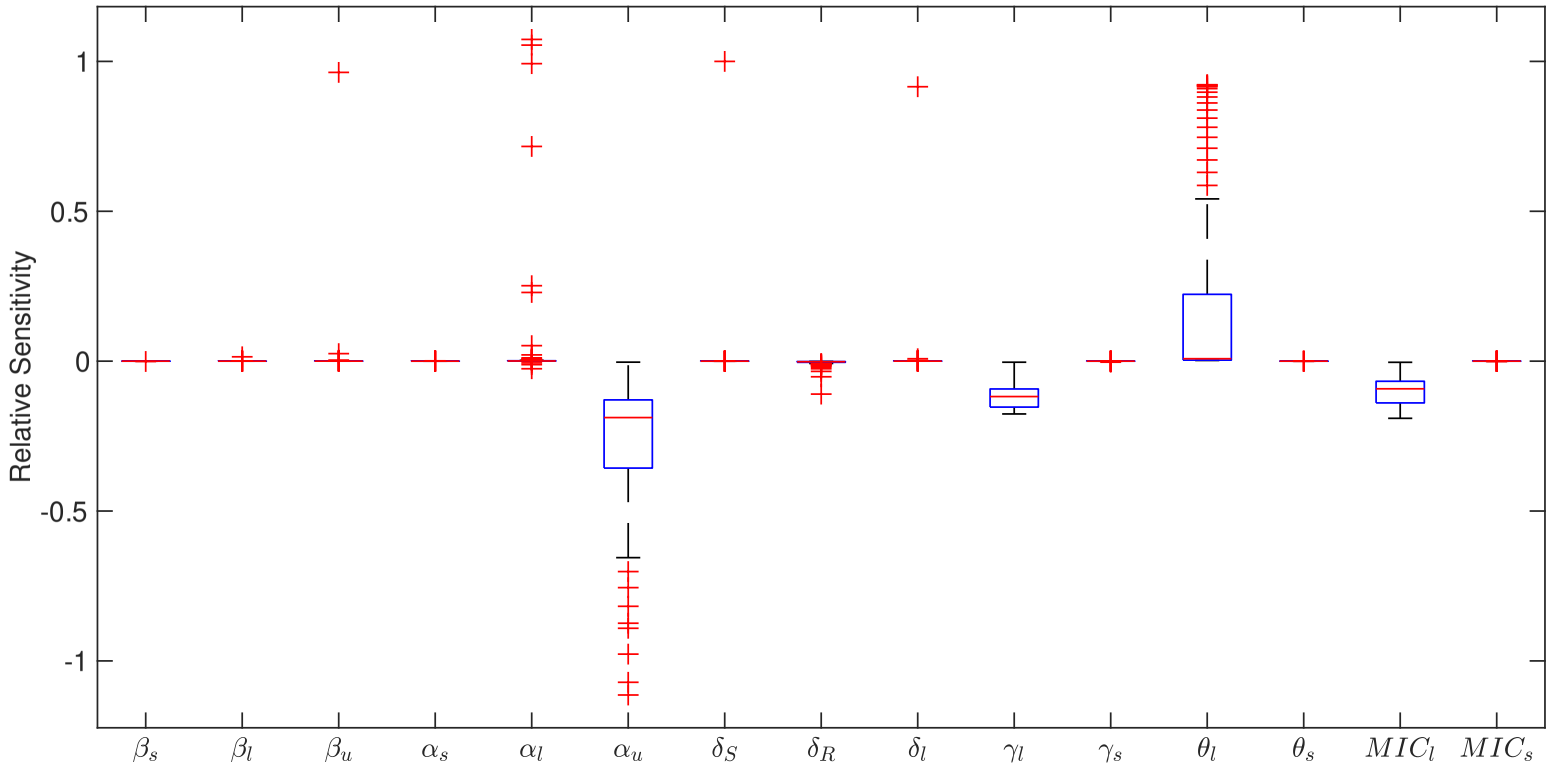


Figure 5.12: Sensitivity analysis of the model parameters where proportion of multidrug-resistant bacteria after 20 years is the output of interest under the no emptying regime. Here the boxplots show the results of calculating equation 5.31 for various parameter values. See Table 5.4 for parameter definitions and ranges. The system is particularly sensitive to α_u, the relative cost of multidrug-resistance and θ_l the inflow rate of bacteriolytic antibiotic. It is also sensitive to other parameters relating to bacteriolytic antibiotics. Here, the boxes contain from the 25th to 75th percentile, the line within the box is the median. Whiskers are 1.5 times the interquartile range, and outliers are those points which lie outside that range.

Parameter	Description	Range	Reference
β_s	Bacteriostatic-resistance gene transfer term	$0 - 10^{-12}$ lCFU^{-1}h^{-1}	[38, 123]
β_l	Bacteriolytic-resistance gene transfer term	$0 - 10^{-12}$ lCFU^{-1}h^{-1}	[38, 123]
β_u	MDR gene transfer term	$0 - 10^{-12}$ lCFU^{-1}h^{-1}	[38, 123]
α_s	Bacteriostatic-resistance fitness cost as a fraction of r	$0 - 1$	Full mathematically plausible range
α_l	Bacteriolytic-resistance fitness cost as a fraction of r	$0 - 1$	Full mathematically plausible range
α_u	MDR fitness cost as a fraction of r	$0 - 1$	Full mathematically plausible range
δ_S	Natural death rate of susceptible bacteria	$0 - 1$ h^{-1}	[213]
δ_R	Natural death rate of resistant bacteria	$0 - 1$ h^{-1}	[213]
δ_l	Antibiotic driven death rate of bacteriolytic-susceptible bacteria	$0 - 1$ h^{-1}	[213]
γ_l	Decay rate of bacteriolytic antibiotics	$0 - 0.029$ h^{-1}	[119]
γ_s	Decay rate of bacteriostatic antibiotics	$0 - 0.029$ h^{-1}	[119]
θ_l	Rate of bacteriolytic antibiotic inflow	$0 - 3422$ lh^{-1}	[38]
θ_s	Rate of bacteriostatic antibiotic inflow	$0 - 3422$ lh^{-1}	[38]
MIC_l	MIC for bacteriolytic-sensitive bacteria	$0 - 250$ μg l^{-1}	[173]
MIC_s	MIC for bacteriostatic-sensitive bacteria	$0 - 250$ μg l^{-1}	[173]

Table 5.4: The parameters considered for sensitivity testing and the ranges used.

bacteria (δ_R) causes a complete removal of multidrug-resistant bacteria. This can be seen in Figure 5.13, but is not particularly clear in Figure 5.12, likely due to the discretisation of the parameter range. Increasing the inflow of bacteriolytic antibiotic (θ_l) increases the population of multidrug-resistant bacteria, due to increased selective pressure. Whereas increasing the MIC of bacteriolytic antibiotic (MIC_l) decreases the number of multidrug-resistant bacteria. As the MIC increases the effect of the antibiotic on the susceptible bacteria decreases, allowing them to live for longer in the tank. Figure 5.14 shows the relative sensitivities of the fifteen parameters under a seasonal emptying regime (every week 1st May to 31st October and every 90 days in the other months). In this scenario the system's sensitivity to α_l, θ_l, MIC_l and γ_l decreases, while the system remains similarly sensitive to the natural death rate of resistant bacteria, δ_R.

Sensitivity analysis of this model indicates that the mechanisms that most affect the proportion of multidrug-resistant bacteria in the slurry tank are the concentration of bacteriolytic antibiotic and the relative cost of resistance to bacteria. This indicates that the ramifications of the use of bacteriolytic antibiotics in farming, such as penicillins and cephalosporins, should be investigated. In their study of drug combination therapy and resistance development, Munck et al.'s results appear to indicate that evolution of resistance to combinations of bacteriostatic and bacteriolytic antibiotics is, in general, slightly higher than in combinations of just bacteriostatic or bacteriolytic antibiotics. However, whether

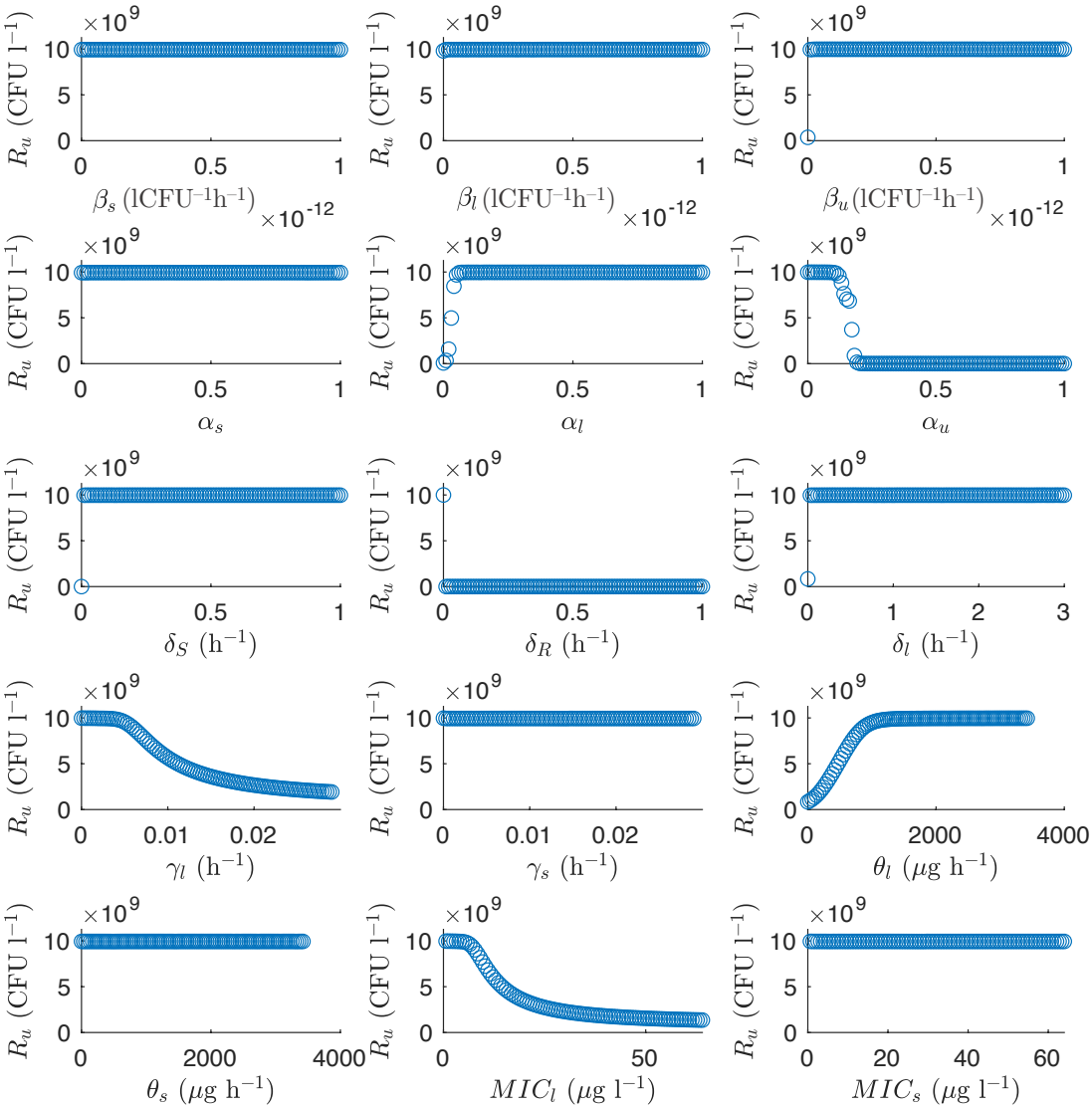


Figure 5.13: The proportion of multidrug-resistant bacteria, R_u, after 20 years as each of the parameters in Table 5.4 varies. This is based on simulations of the model described by equations 5.17 to 5.22. The remaining parameter values are as in Table 5.3.

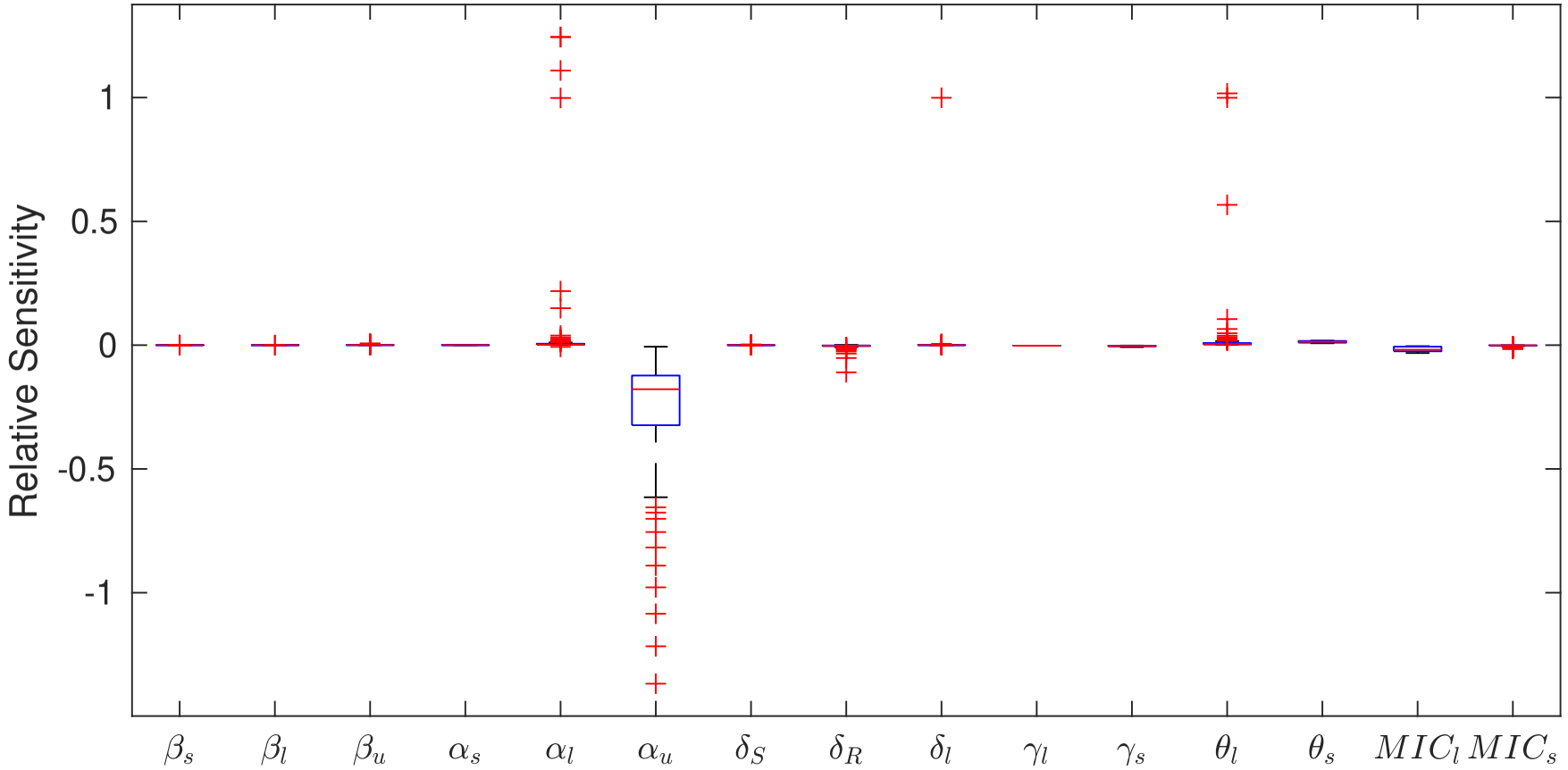


Figure 5.14: Sensitivity analysis of the model parameters where proportion of multidrug-resistant bacteria after 20 years is the output of interest and a seasonal emptying regime is used. Here the boxplots show the results of calculating equation 5.31 for various parameter values. See Table 5.4 for parameter definitions and ranges. Compared to the infinite tank simulations the system is much less sensitive (see Figure 5.12), but α_u, the relative cost of multidrug-resistance remains the most parameter to which the model is most sensitive. Similarly, the system is also sensitive to θ_l, the inflow rate of bacteriolytic antibiotic, and α_l the cost of bacteriolytic-resistance. Here, the boxes contain from the 25th to 75th percentile, the line within the box is the median. Whiskers are 1.5 times the interquartile range, and outliers are those points which lie outside that range.

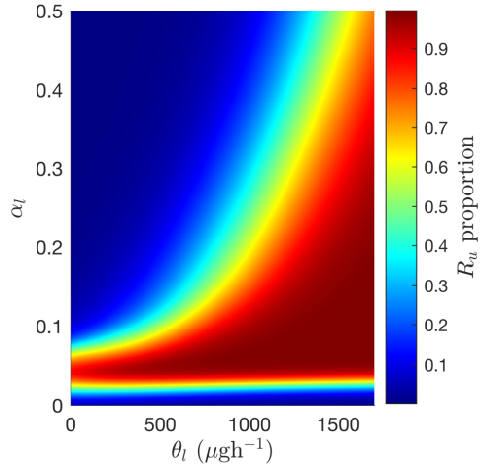
this resistance development was sensitive to the relative concentrations of bacteriolytic and bacteriostatic antibiotic was not tested. Some studies suggest that, in certain circumstances, bacteriolytic (or bactericidal) antibiotics have a greater efficacy for treating infections than bacteriostatic antibiotics [190]. If this is reflected in the slurry environment then it may not be surprising that bactericidal antibiotics exert greater environmental pressure, increasing the rates of resistance. Other studies have shown that there is not a significant difference between the efficacy of bacteriostatic and bacteriolytic antibiotics [192], and that differences are likely due to other factors such as dosing and pharmacokinetics. Therefore, it seems that it would have been difficult to predict beforehand that the model would have been more sensitive to bacteriolytic parameters than bacteriostatic.

5.2.3 Bacteriolytic and Bacteriostatic Antibiotics

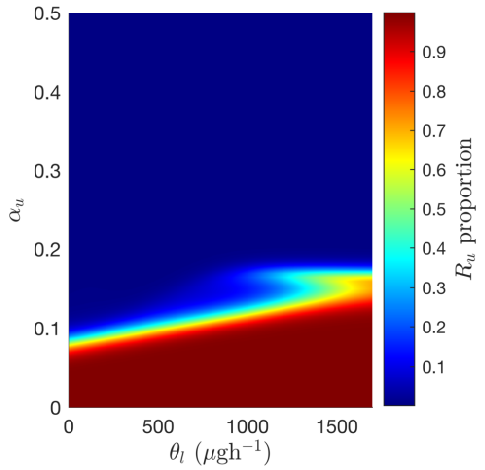
Sensitivity analysis indicates that some of the parameters to which the model is most sensitive are those related to the properties of the bacteriolytic antibiotic. As one-at-a-time sensitivity analysis shows the effects of changes to one parameter, heatmaps have been used to show the effect of altering the bacteriolytic antibiotic parameters in tandem with the cost of bacteriolytic and multidrug-resistance under a no-emptying regime, and with a seasonal emptying regime, show in Figure 5.15.

Figure 5.15a shows the effects of varying α_l and θ_l simultaneously under an no-emptying regime. For α_l <0.05 the growth of bacteriolytic-resistant bacteria is uninhibited and they dominate the tank, meaning that $P_{SR} \approx 0$. As α_l increases, higher quantities of antibiotic need to be introduced into the system to apply enough environmental pressure to select for multidrug-resistant bacteria. Varying α_u alongside θ_l under a no emptying regime shows that, as θ_l increases, the bacterial tolerance for the cost of MDR increases until once α_u reaches a threshold value of approximately 0.2; see Figure 5.15b. When $\alpha_u > 0.2$ $P_{SR} \approx 0$ for all values of θ_l, with the increased relative cost for the growth of multidrug-resistant bacteria counteracting the selective pressure of the antibiotic. Subbiah et al. [53] recorded fitness costs between 0.09 and 0.25 for *E. coli* carrying plasmids that conferred resistance to extended spectrum cephalosporins. Vogwill and Maclean [226] found that for cell-wall alteration, target-site alteration, β-lactamase production and efflux pump resistance mechanisms, the cost of resistance ranged between approximately 0.05 and 0.2, depending on the conferred mechanism (though this was not specific to *E. coli*). These results indicate that a fitness cost of 0.2 is possible, though it is relatively high.

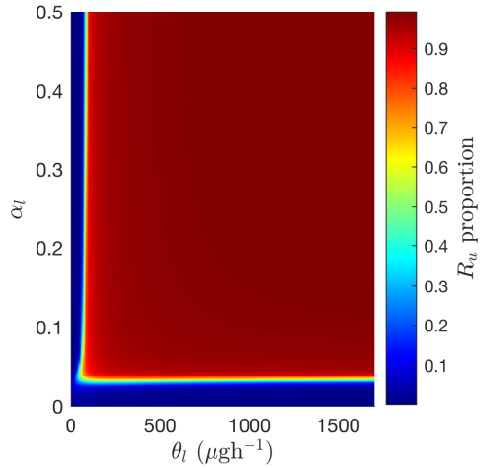
When α_l and θ_l are varied simultaneously under an seasonal emptying regime,



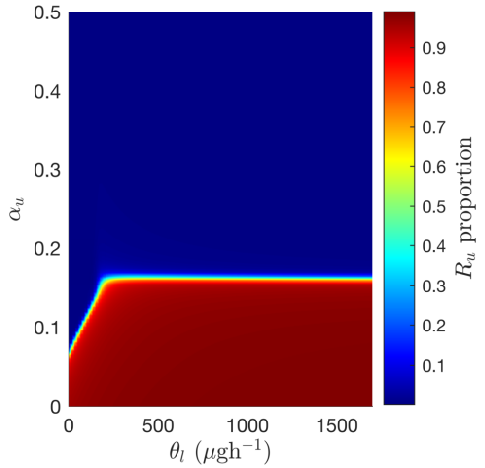
(a) Relative cost of bacteriolytic-resistance, α_l, plotted against the inflow rate of bacteriolytic antibiotic, θ_l under a no-emptying regime.



(b) Relative cost of MDR, α_u, plotted against the inflow rate of bacteriolytic antibiotic, θ_l under a no-emptying regime.



(c) Relative cost of bacteriolytic-resistance, α_l, plotted against the inflow rate of bacteriolytic antibiotic, θ_l under a seasonal emptying regime.



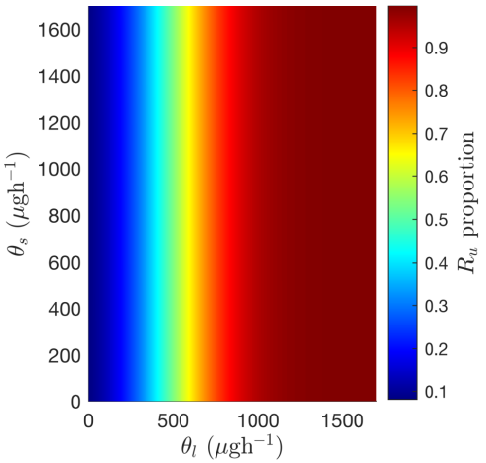
(d) Relative cost of MDR, α_u, plotted against the inflow rate of bacteriolytic antibiotic, θ_l under a seasonal emptying regime.

Figure 5.15: Heatmaps showing the multidrug-resistant proportion, R_u, in the tank after 20 years when varying the relative cost of bacteriolytic-resistance, α_l, and the relative cost of MDR, α_u against the inflow rate of bacteriolytic antibiotic, θ_l under no-emptying and seasonal emptying regimes. This is based on simulations of the model described by equations 5.17 to 5.22. The remaining parameter values are as in Table 5.3.

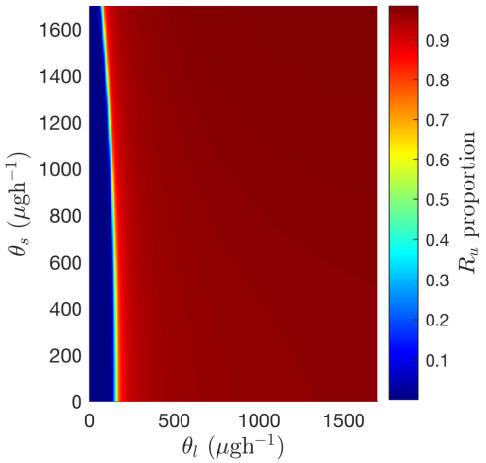
as shown in Figure 5.15c, it is shown that, even for rates of bacteriolytic inflow of less than 100μg h^{-1} the MDR can develop even when the relative cost of bacteriolytic resistance is 0.5. In the no-emptying case, for the same inflow rate of bacteriolytic antibiotic, the development of MDR required the cost of bacteriolytic resistance to be around 0.05; for $\alpha_l > 0.1$ multidrug-resistant bacteria did not dominate the tank. This change is likely because under the seasonal emptying

regime the long term concentration of antibiotic is increased and there is more selective pressure on the bacteria in the tank. Figure 5.15d shows the R_u proportion as α_u and θ_l vary. The bacterial tolerance for the cost of MDR increases as θ_l increases up to around $\theta_l = 250\mu$g h^{-1}, and then remains reaches a threshold value of around $\alpha_u = .18$.

Figure 5.16 shows the R_u proportion after 20 years for varying θ_l and θ_s under no-emptying and seasonal emptying regimes. From this figure it is very clear that the inflow rate of bacteriostatic antibiotic has little effect on the eventual proportion of multidrug-resistant bacteria. On the other hand increasing the inflow rate of A_l has a marked influence on the R_u proportion. This is not to say however that θ_s has no effect on the system: in fact, as θ_s decreases the time it takes for R_u to dominate the tank increases.



(a) Inflow rate of bacteriostatic antibiotic, θ_s, plotted against the inflow rate of bacteriolytic antibiotic, θ_l under a no-emptying regime.



(b) Inflow rate of bacteriostatic antibiotic, θ_s, plotted against the inflow rate of bacteriolytic antibiotic, θ_l under a seasonal emptying regime.

Figure 5.16: Heatmaps showing the multidrug-resistant proportion in the tank after 20 years when varying the inflow rate of bacteriostatic antibiotic, θ_s, and the inflow rate of bacteriolytic antibiotic, θ_l under a no-emptying regime and a seasonal emptying regime. This is based on simulations of the model described by equations 5.17 to 5.22. The remaining parameter values are as in Table 5.3.

5.3 Stability Analysis

In this section the steady states of the model described by equations 5.17 to 5.22 are identified and the stable steady states are found. When investigating the steady states of the model, it is important to consider the effects of the tank volume, $V(t)$; in the case that $V(t)$ is following a filling and emptying cycle, it is not possible to find any steady states for the model. This means there are two

options to consider:

- the tank fills indefinitely and $\lim_{t\to\infty} V(t) \to \infty$
- the tank volume remains the constant and $V(t) = V_1$.

Both options lead to analytic solutions for the antibiotic equations, so that finding the model steady states is a case of solving four coupled non-linear equations. Neither of these filling regimes are realistic, but they can be used to illustrate how antibiotic concentration and volume might affect the steady states of a more realistic rendering of the model.

5.3.1 Indefinite filling

In the case where the tank fills indefinitely, $V \to \infty$ as $t \to \infty$, and the equation for bacteriostatic antibiotic is then given by

$$\lim_{t\to\infty} \frac{dA_s}{dt} = -\gamma_s A_s. \tag{5.32}$$

Solving this equation using gives

$$\lim_{t\to\infty} A_s = \lim_{t\to\infty} Ce^{-\gamma_s t} = 0, \tag{5.33}$$

where C is a constant of integration, so as $t \to \infty$, $A_s \to 0$. Similarly, in the case $\lim_{t\to\infty} V(t) \to \infty$, $\lim_{t\to\infty} A_l = 0$. By setting $V(t) \to \infty$ in equations 5.19 to 5.22, letting $A_s = A_l = 0$ and letting the derivatives equal zero, the equations to solve to find the steady state are:

$$f_1 = r\left(1 - \frac{N}{\mu}\right) S - S(\beta_s R_s + \beta_l R_l + \beta_u R_u) - \delta_S S = 0 \tag{5.34}$$

$$f_2 = r(1-\alpha_s)\left(1 - \frac{N}{\mu}\right) R_s + R_s(\beta_s S - \beta_l R_l - \beta_u R_u) - \delta_R R_s = 0 \tag{5.35}$$

$$f_3 = r(1-\alpha_l)\left(1 - \frac{N}{\mu}\right) R_l + R_l(-\beta_s R_s + \beta_l S - \beta_u R_u) - \delta_R R_l = 0 \tag{5.36}$$

$$f_4 = r(1-\alpha_u)\left(1 - \frac{N}{\mu}\right) R_u + R_s R_l(\beta_s + \beta_l) + \beta_u R_u(S + R_s + R_l) - \delta_R R_U = 0 \tag{5.37}$$

It is not possible to solve these equations analytically, but using a numerical solver the steady states can be found. Under typical parameter conditions, as shown in Table 5.3, there are five possible steady states where all strains are non-negative:

- $\xi_1 = \{S = 0, R_s = 0, R_l = 0, R_u = 0\}$
- $\xi_2 = \{S = 9.98 \times 10^9, R_s = 0, R_l = 0, R_u = 0\}$
- $\xi_3 = \{S = 0, R_s = 9.98 \times 10^9, R_l = 0, R_u = 0\}$
- $\xi_4 = \{S = 0, R_s = 0, R_l = 9.98 \times 10^9, R_u = 0\}$
- $\xi_5 = \{S = 0, R_s = 0, R_l = 0, R_u = 9.98 \times 10^9\}$

To test the stability of each of the steady states the Jacobian matrix was calculated:

$$\mathbf{J}(S, R_s, R_l, R_u) = \begin{bmatrix} \frac{\partial f_1}{\partial S} & \frac{\partial f_1}{\partial R_s} & \frac{\partial f_1}{\partial R_l} & \frac{\partial f_1}{\partial R_u} \\ \frac{\partial f_2}{\partial S} & \frac{\partial f_2}{\partial R_s} & \frac{\partial f_2}{\partial R_l} & \frac{\partial f_2}{\partial R_u} \\ \frac{\partial f_3}{\partial S} & \frac{\partial f_3}{\partial R_s} & \frac{\partial f_3}{\partial R_l} & \frac{\partial f_3}{\partial R_u} \\ \frac{\partial f_4}{\partial S} & \frac{\partial f_4}{\partial R_s} & \frac{\partial f_4}{\partial R_l} & \frac{\partial f_4}{\partial R_u} \end{bmatrix}. \tag{5.38}$$

The Jacobian is then evaluated at each of the steady states and the eigenvalues are calculated. If all the eigenvalues are negative then the steady state is stable. Of the five steady states above ξ_2 is the only stable state, with eigenvalues $\lambda_2 = \{-0.499, -2 \times 10^-7, -2 \times 10^-7, -2 \times 10^-7\}$. The steady state ξ_1 is an unstable node, as all of the eigenvalues associated with it are positive. ξ_3 and ξ_4 are 2-2 saddle points (2 positive and 2 negative eigenvalues) and ξ_5 is a 3-1 saddle (3 negative and 1 positive eigenvalue) [227]. Though during simulation, the model approaches ξ_5, it tends to ξ_2 over long timescales.

Indefinite filling with fixed antibiotic concentration

When simulating the system using the parameter values given in Table 5.3, the system approaches steady state ξ_5 before eventually tending to ξ_2. To test the dependence of the stable manifold on antibiotic concentration, the indefinite filling system was adjusted to included constant antibiotic concentrations, A_s and A_l, the system of equations to solve is then given by

$$f_1 = r\left(1 - \frac{N}{\mu}\right) E_s S - S(\beta_s R_s + \beta_l R_l + \beta_u R_u) - \delta_S S - \delta_l S \frac{A_l}{MIC_l + A_l} = 0 \tag{5.39}$$

$$f_2 = r(1-\alpha_s)\left(1 - \frac{N}{\mu}\right) E_r R_s + R_s(\beta_s S - \beta_l R_l - \beta_u R_u) - \delta_R R_s - \delta_l R_s \frac{A_l}{MIC_l + A_l} = 0 \tag{5.40}$$

$$f_3 = r(1-\alpha_l)\left(1 - \frac{N}{\mu}\right) E_s R_l + R_l(-\beta_s R_s + \beta_l S - \beta_u R_u) - \delta_R R_l = 0 \tag{5.41}$$

$$f_4 = r(1-\alpha_u)\left(1 - \frac{N}{\mu}\right) E_r R_u + R_s R_l(\beta_s + \beta_l) + \beta_u R_u(S + R_s + R_l) - \delta_R R_U = 0. \tag{5.42}$$

As the values of A_s and A_l change, so too do the number and stability of the steady states. In most cases there are 5 mathematically plausible steady states, but certain combinations of A_s and A_l result in seven mathematically plausible steady states. Of these, generally one state is also stable, though in some combinations there are no stable steady states and in others there are 2. The number of physically plausible steady states and stable steady states as A_s and A_l vary is shown in Figures 5.17 and 5.18.

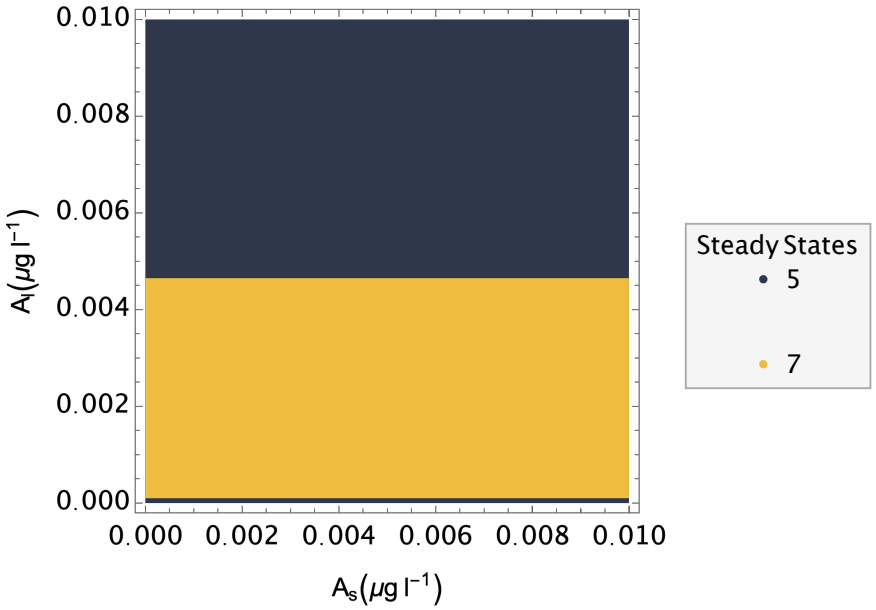


Figure 5.17: The number of steady states as A_s and A_l vary. These were calculated by solving equations 5.39 to 5.42, using the parameter values given in 5.3.

Figure 5.19 shows the stable steady states of S and R_u as A_s and A_l vary between 0 and 0.01 μg l^{-1}. As shown in figure 5.18 there are regions with 0, 1 and 2 stable steady sates. In the region with two stable steady states, one of the stable states has greater than zero concentration of both S and R_u and in the other R_u dominates.

Figure 5.20 shows the stable steady states when $A_s = A_l$ and they vary between 0 and 1. For $A_s = A_l < 0.005$, there is is a stable steady state split between S and R_u, and for $A_s = A_l > 0.005$, R_u dominates the tank.

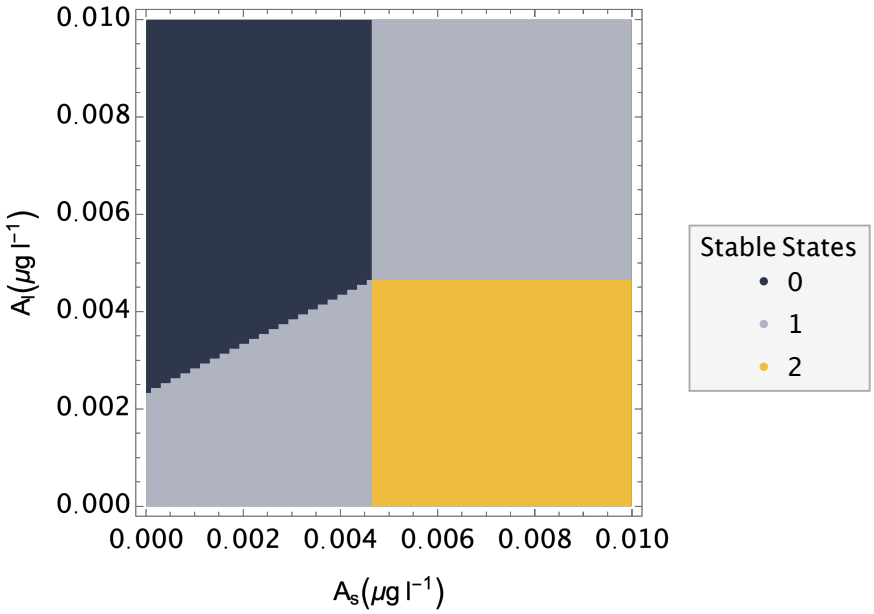
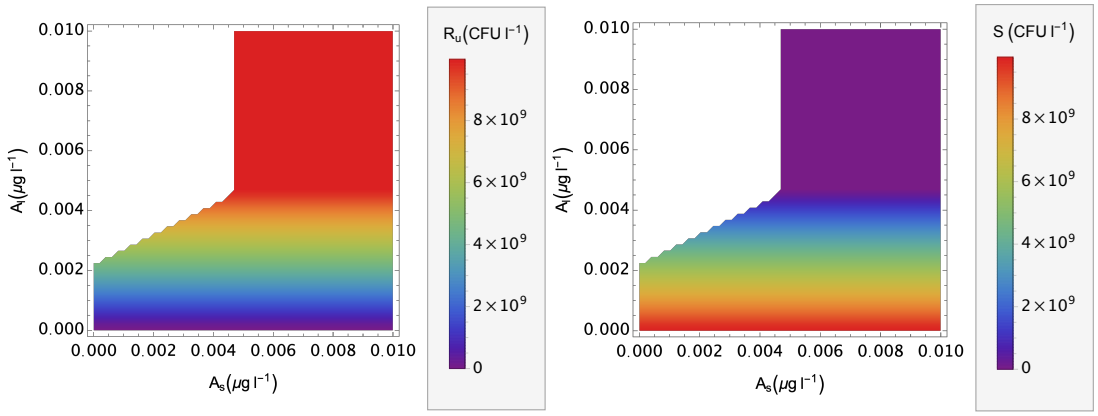
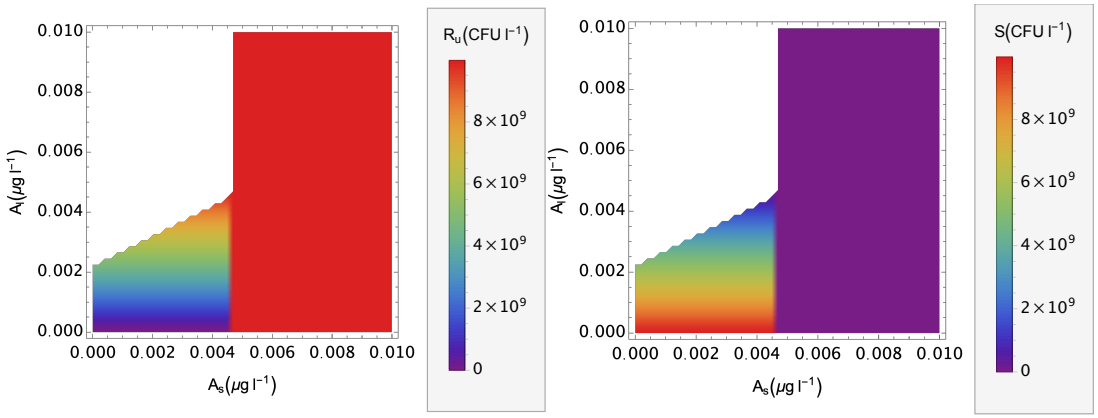


Figure 5.18: The number of stable steady states as A_s and A_l vary. These were calculated by solving equations 5.39 to 5.42, using the parameter values given in 5.3.



(a) R_u stable steady states showing S and R_u mixed state.

(b) S stable steady states showing S and R_u state.



(c) R_u stable steady states showing R_u dominant state.

(d) S stable steady states showing R_u dominant state.

Figure 5.19: Stable steady states of S and R_u as A_s and A_l vary. These were calculated by solving equations 5.39 to 5.42, using the parameter values given in 5.3.

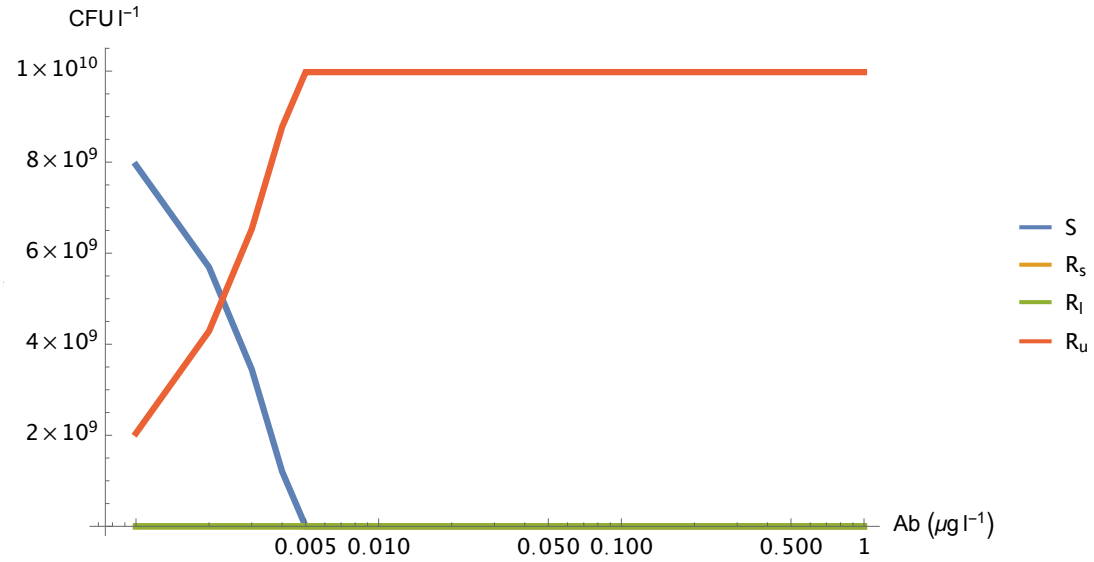


Figure 5.20: The steady states as the antibiotic concentration varies, here $Ab = A_s = A_l$. These were calculated by solving equations 5.39 to 5.42, using the parameter values given in 5.3.

5.3.2 Constant tank volume

In the constant tank volume case, the influent and effluent rates ($\lambda'(t)$ and $\omega'(t)$, respectively) are equal, so the volume is given by $V(t) = V_1$. There are then two scenarios to consider, $\lambda'(t) = \omega'(t) = 0$, and $\lambda'(t) = \omega'(t) \neq 0$.

Zero inflow and outflow

In the case where $\lambda'(t) = \omega'(t) = 0$, there is no antibiotic or bacteria entering the tank. The antibiotic concentration in the long term can be calculated by solving the antibiotic ODEs as in equation 5.32, so that, once again, as $t \to \infty$, A_s and $A_l \to 0$. Therefore, as $t \to \infty$, the equations to solve are the same as in the infinite filling case, see equations 5.34 to 5.37. Therefore the long term behaviour is the same as discussed in the previous section and is determined by the initial conditions of bacteria within the tank, as no new substances enter the tank over time.

Equal inflow and outflow

In the case where $\lambda'(t) = \omega'(t) \neq 0$, the long term concentration of antibiotic in the tank can be calculated by solving both the antibiotic equations and then sending $t \to \infty$. For bacteriostatic antibiotic the equation to solve is:

$$\frac{dA_s}{dt} = \frac{\theta_l}{V_1} - A_s\left(\gamma_s + \frac{\lambda}{V_1}\right), \tag{5.43}$$

which gives

$$A_s = \frac{\theta_s}{V_1\gamma_s + \lambda} + C\exp\left(\frac{-(\lambda + \gamma_s V_1)t}{V_1}\right), \tag{5.44}$$

where C is the constant of integration, dependent on the initial conditions. Using equation 5.44 the long-time concentration of antibiotic can is given by

$$\lim_{t\to\infty} A_s \to \frac{\theta_s}{V_1\gamma_s + \lambda} = A_s^* \tag{5.45}$$

and similarly

$$\lim_{t\to\infty} A_l \to \frac{\theta_l}{V_1\gamma_l + \lambda} = A_l^*. \tag{5.46}$$

Substituting $V(t) = V_1$, A_s^* and A_l^* into equations 5.19 to 5.22 and setting the derivatives to 0, leads to the system of equations to solve to find the steady states:

$$f_1 = r\left(1-\frac{N}{\mu}\right)E_S^*S - S(\beta_s R_s + \beta_l R_l + \beta_u R_u) + \lambda(1-\rho)\frac{\nu}{V_1} - \frac{\lambda S}{V_1} - \delta_S S - \delta_l S\frac{A_l^*}{MIC_l + A_l^*} = 0 \tag{5.47}$$

$$f_2 = r(1-\alpha_s)\left(1-\frac{N}{\mu}\right)E_R^*R_s + R_s(\beta_s S - \beta_l R_l - \beta_u R_u) + \lambda\rho_s\frac{\nu}{V_1} - \frac{\lambda R_s}{V_1} - \delta_R R_s - \delta_l R_s\frac{A_l^*}{MIC_l + A_l^*} = 0 \tag{5.48}$$

$$f_3 = r(1-\alpha_l)\left(1-\frac{N}{\mu}\right)E_S^*R_l + R_l(-\beta_s R_s + \beta_l S - \beta_u R_u) + \lambda\rho_l\frac{\nu}{V_1} - \frac{\lambda R_l}{V_1} - \delta_R R_l = 0 \tag{5.49}$$

$$f_4 = r(1-\alpha_u)\left(1-\frac{N}{\mu}\right)E_R^*R_u + R_s R_l(\beta_s + \beta_l) + \beta_u R_u(S + R_s + R_l) + \lambda\rho_u\frac{\nu}{V_1} - \frac{\lambda R_u}{V_1} - \delta_R R_U = 0, \tag{5.50}$$

where

$$E_S^* = 1 - \frac{E_{max}A_s^{*H}}{MIC_S^H + A_s^{*H}} \tag{5.51}$$

$$E_R^* = 1 - \frac{E_{max}A_s^{*H}}{MIC_R^H + A^{*H}}. \tag{5.52}$$

Solving this system of equations leads to a single physically plausible steady state for each value of V_1. Calculating the eigenvalues of the Jacobian at each of these steady states shows that they are also stable. The stable steady state for varying V_1 is shown in figure 5.21. For $V_1 \lessapprox 1000$ the bacterial populations do not grow to the carrying capacity and susceptible bacteria make up the majority of the bacteria in the tank. This steady state arises as the slurry is flushed through the tank faster than the bacteria can grow, meaning that each strain remains at approximately its influent concentration. Some HGT does occur, as $R_u > 0$. For $1000 \lessapprox V_1 \lessapprox 10^{8.5}$, multidrug-resistant bacteria dominate the tank. Based on the range of tank sizes presented in Chapter 3, all practical tank sizes are likely within this range. For $V_1 \gtrapprox 10^{8.5}$ the system approaches the dynamics of the infinite-filling steady steady state analysis, where susceptible bacteria dominate the tank and R_s, R_l and R_u decrease as V_1 increases. As V_1 increases, both A_s^* and A_l^* decrease. Therefore, it is likely that S comes to dominate the system as V_1 increases due to the decrease in antibiotic concentration.

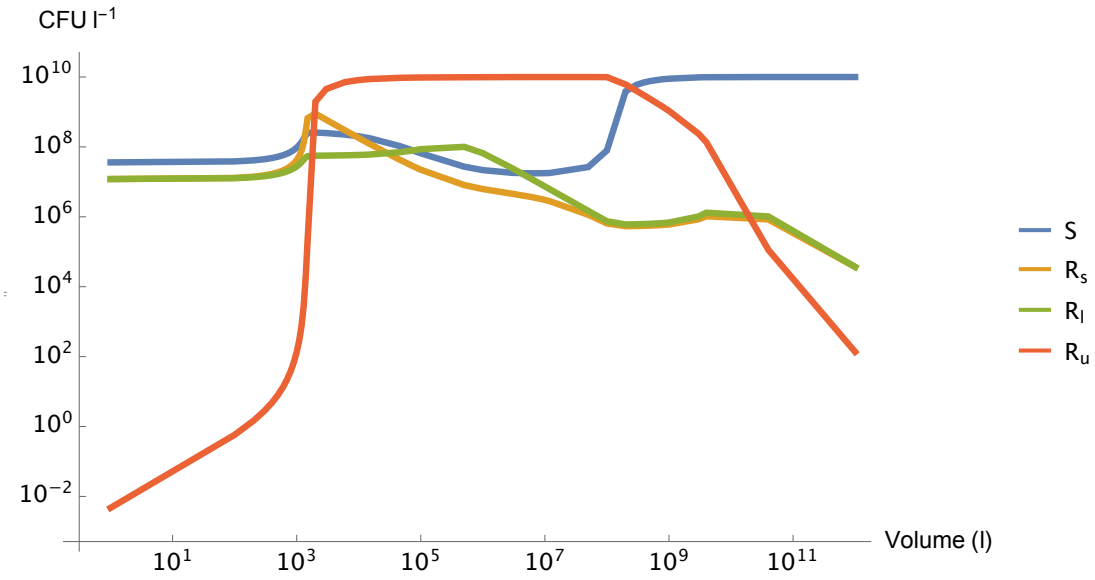


Figure 5.21: The steady state as V_1 varies in the constant filling and emptying scenario using typical parameter values. These were calculated by solving equations 5.47 to 5.50, using the parameter values given in 5.3.

In the previous section it was shown that, under typical parameter conditions (as in Table 5.3), α_u has a cut-off value of ~ 0.2, above which R_u does not dominate the tank in both the ongoing filling and seasonal emptying cases. The effects of increased α_u can also be seen in the steady state analysis of the fixed-volume system with $\alpha_u = 0.2$, see figure 5.22. For $V_1 \lessapprox 1000$ the system behaves similarly to the $\alpha_u = 0.1$ case. For larger volumes, instead of R_u dominating the tank, as in Figure 5.21, the steady state moves from R_s dominating the tank, to R_u, to R_l and finally to S as V_1 increases.

5.3.3 Discussion and recommendations for future work

This model of AMR in the dairy slurry tank predicts the emergence of widespread MDR after less than a decade of use. It also predicts that changes in agricultural practice could delay the rate at which MDR develops and shows that farm practice is an important consideration for those modelling AMR in agricultural settings. The key results from the model are that the emptying regime affects the rate of development of AMR, that bacteriolytic antibiotics appear to contribute more to the development of multidrug resistant bacteria than bacteriostatic antibiotics. The model also predicts that the fitness cost of resistance plays a large factor in the development of resistance, as posited by Ternent et al. [140].

The model indicates that although altering the tank emptying regime does not affect the proportion of multidrug-resistant bacteria in the long term, it does change the speed at which model equilibrium is reached. This is interesting from

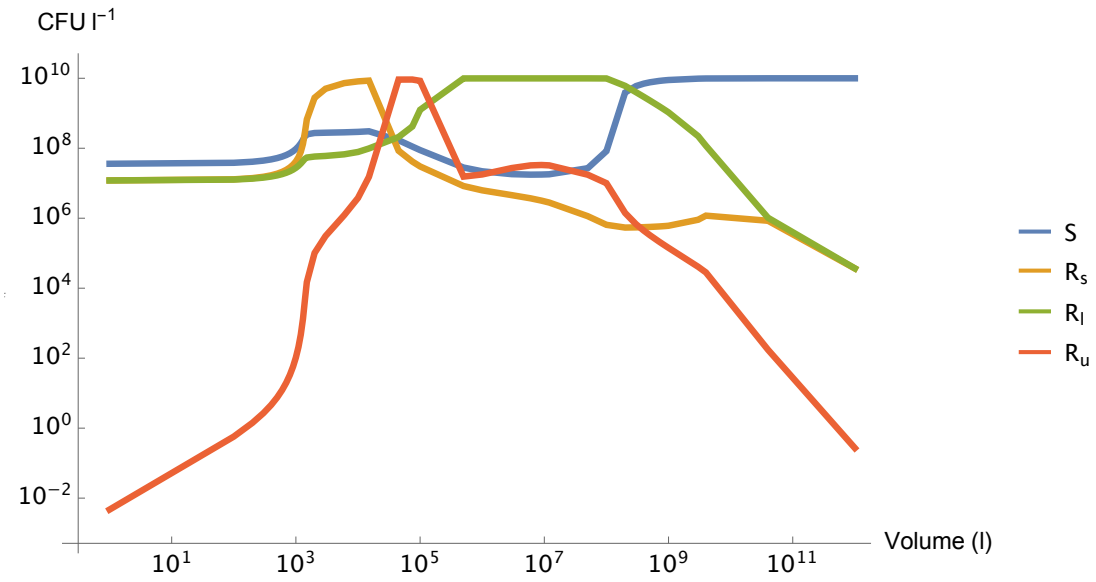


Figure 5.22: The steady state as V_1 varies in the constant filling and emptying scenario with $\alpha_u = 0.2$. These were calculated by solving equations 5.47 to 5.50, using the parameter values given in 5.3.

a farm practice perspective as it implies that it is safer to store slurry in higher volumes for longer periods of time and when it is removed, only to remove it in small quantities.

To better understand the model behaviour a sensitivity analysis was performed to determine which parameters most affect the model output. Two scenarios were considered: a simulation with no tank emptying regime, and one with seasonal tank emptying. In both cases the system is most sensitive to the relative costs of multidrug and bacteriolytic-resistance α_u and α_l, and to the inflow rate of bacteriolytic antibiotic, θ_l, as indicated by one and two way sensitivity analyses. This brings about another possible implication for farm practice, indicating that reduced usage of bacteriolytic antibiotics would decrease the number of multidrug-resistant bacteria much more effectively than reducing the quantity of bacteriostatic antibiotics used on farms. Thus, the model appears to advise two possible channels for research into the way that farm practices affect the persistence and spread of AMR within the slurry tank; the storage and emptying regime (as the model indicates that longer slurry storage times could lead to a slowed development of multidrug resistance) and the administration of bacteriolytic antibiotics such as β-lactam antibiotics, for example penicillin, or cephalosporins to the herd. A larger multivariate sensitivity analysis was not performed, as two-way analyses were used to identify interactions between key parameters identified in the one-way analysis. However, this omission may have led to underestimating the significance of certain parameters, and so a multivariate sensitivity analysis is proposed for further work.

When considering the cost of resistance, it has generally assumed that the cost of MDR, α_u, is the same as the cost of resistance to a single type of antibiotic, either due to a compensatory mutation [50, 221] or the fact that the cost of resistance is likely to be under selective pressure; a version of the resistance gene which incurs a low fitness cost will outcompete those with higher fitness costs. Sensitivity and stability analyses have shown that α_u has a direct effect on whether multidrug resistance dominates the tank environment, so determining the true cost of MDR in the slurry tank may be important.

One method of antimicrobial stewardship that has been used in clinical settings to take advantage of AMR fitness costs is antibiotic cycling [228]. Antibiotic cycling is a prescription strategy where prescribed antibiotics are replaced over time by alternative antibiotics with a different mechanism of resistance. The aim of this is to mitigate the advantages of resistance to one type of antibiotic and thus take advantage of the resistance fitness cost. It has been shown that cycling can slow down the development of resistance and therefore may have applications in agriculture [229]. It might be possible to test the effects of antibiotic cycling on slurry tanks using a tank facsimile in a laboratory study.

It is important that the effects of slurry storage on the spread of AMR are further investigated. Our model has shown that both the volume of slurry left in the tank and the frequency at which the tank it is emptied affect the rate at which MDR develops. A longitudinal survey and analysis of AMR in slurry at the point of land application after various storage times is recommended. Furthermore slurry stores vary in design, from clay-lined lagoons to steel towers or concrete stores [29]; there is currently little knowledge on how the storage design might affect the development of AMR. During the analysis of the model it has been assumed that the slurry tank is never cleaned or disinfected, based on the results of the SWWAS study (see Chapter 3). If it is, this could delay the process of multidrug-resistant development, as, from a modelling perspective, it would be the same as restarting the model at day zero. However, if resistant biofilms [222] develop in the tank and are not fully cleaned away, they could potentially act as a seed for resistance in the tank, as biofilms are known to promote HGT of ARGs [230, 231]. Another farm practice factor which requires more investigation is the effect of heavy metal co-resistance on bacterial populations in slurry, given the widespread use of copper and zinc footbaths in the UK [28, 232]. Though it is well known that metals can contribute to the development and spread of AMR, it has also been shown that heavy metals can impede selection for resistance, in the case of ciprofloxacin and zinc [233]. A future model could consider cases in which heavy metals both contribute and detract from the development of AMR.

There are various environmental factors that have been shown to have an

impact on the development of AMR. The temperature and pH of the slurry will likely affect microbial growth in bacteria other than *E. coli* [114] and there is evidence that there is seasonal variation in AMR spread in swine agriculture [115–117]. It was assumed that the tank is covered so that slurry dilution by rainfall is negligible. As not all tanks are covered [29], there is potentially significant dilution to the slurry via rainfall which may slow the rate at which resistance develops, as it would reduce the overall antibiotic concentration. Though the model incorporates farm practice elements these environmental factors have not been considered, which may play a crucial role in agricultural AMR.

Though throughout this model it has been assumed that the slurry is well mixed, given that slurry stores have large capacities, often millions of litres (especially in the case of slurry lagoons, see Chapter 3), the tanks are not continuously stirred, and the input to the tank is changeable, this is unlikely to be the case. The well mixed assumption may lead to a quicker development of AMR, as bacteria are assumed to be always interacting with antibiotics, and experiencing selective pressure. A next step might be an extension of this model that takes into account spatial factors.

All factors affecting HGT were consolidated into a scalar rate coefficient. However, there is evidence that HGT occurs with a degree of stochasticity [234] and therefore may be better modelled under a stochastic framework [121]. Furthermore, neither acquisition of extracellular DNA released by dead bacteria or transduction of DNA by phage [43] are considered in this model. These omissions could affect the rate at which multidrug resistance develops, and the resistance profiles of the population over time.

The development of MDR in the model is particularly sensitive to the inflow rate of bacteriolytic antibiotic (see Figures 5.12, 5.14 and 5.16). As the half-life of bacteriolytic antibiotic and the relative cost of bacteriolytic-resistance increase, the multidrug-resistant population in the tank increased, see Figure 5.13. This implies that the chemical properties of the antibiotics being used also have an effect on whether or or not MDR develops. It is possible that policy or prescription recommendations could be put into place to limit the prescribing of certain antibiotic types, as has already occurred with third and fourth generation cephalosporins, which have been banned for use in egg production under the British Egg Industry Council code of practice [109].

Though there are few studies to which the model can be compared, it generates comparable results to the experimental study conducted by Mulamattathil et al. [235], which sampled fecal coliform bacteria from a water reticulation system near a chicken meat processing plant. Their findings show population-wide resistance developing over similar timescales to that of the model, alongside stable

populations of multidrug-resistant bacteria, similar to the tail end of the simulation shown in Figure 5.3. Though the system sampled from is quite different to our model system, in that it comprises multiple water storage facilities, the similarities between the results are encouraging, as they indicate that the resistance development timescales in the model are seen in real-world scenarios. As the study does not sample only *E. coli*, temperature may play some part in the development of resistance at each of the sampling points. Furthermore, the fluctuations in resistance to specific antibiotics shown in [235] indicate that an interesting extension to the model would be to incorporate resistance to multiple specific bacteriolytic and bacteriostatic antibiotics with different modes of action. In addition, Gullberg et al. [142] found that in certain E. coli strains, when exposed to varying concentrations of ciprofloxacin, resistant bacteria could outnumber susceptible by over 100 to 1 after 60 generations of growth over 24 hours, though the speed of growth was found to vary with strain and antibiotic concentration. This indicates that it is plausible that resistant bacteria can dominate systems in which selective pressure is exerted by antibiotics. To test the outputs of our model in more detail, time series data from dairy slurry storage facilities will need to be acquired and analysed; such data is not yet available.

5.4 Summary

A model of the spread and persistence of antimicrobial resistance in an *E. coli* population in a dairy farm slurry tank was developed. The model incorporates bacteriolytic and bacteriostatic antibiotics and four strains of *E. coli*: a strain susceptible to both antibiotics, a strain resistant to bacteriolytic antibiotics, a strain resistant to bacteriostatic antibiotics and a "multidrug-resistant" strain which is resistant to both antibiotics. The increased complexity of this model compared to its predecessors ([38] and [39]), due to the inclusion of tank emptying dynamics and bacteriostatic and bacteriolytic antibiotics, has led to new avenues for investigation and data collection at very little extra computational cost. It has been shown that tank emptying regime may affect the rate at which AMR develops. Additionally it has been shown that bacteriolytic antibiotics parameters have more effect on the spread of MDR than bacteriostatic antibiotics.

Chapter 6

Parameter estimation for the ODE model

In this chapter, likelihood-based methods were used to estimate parameters in the ordinary differential equation (ODE) model discussed in Chapter 5. Though the parameters for the ODE model were chosen carefully from the literature, there are cases where certain phenomena have not been recorded in the dairy slurry environment (for example, horizontal gene transfer (HGT)). To remedy this, data from a working dairy farm was used to estimate certain parameter values of the model.

Two methods of inference were used, the frequentist approach of Maximum Likelihood Estimation (MLE) and a Bayesian Inference approach, the Metropolis Hastings algorithm.

The data used was collected as part of the EVAL-FARMS project [36] and by Baena Nogueras et al. [37]. Three data sets were available, all based on samples taken from the slurry tank at the University of Nottingham Sutton Bonington Campus Dairy Farm:

- Presumptive *E. coli* counts from samples taken between February 2017 and February 2018, on four different *E. coli* growth media [36]
- Antibiotic concentration data from samples taken between October 2017 and October 2018, for 20 different veterinary antibiotics [37]
- *E. coli* resistance phenotype data; *E. coli* strains were tested for resistance to 17 different veterinary antibiotics between May 2017 and December 2017 [36].

The antibiotic concentration data were used to infer the inflow rates of bacteriostatic and bacteriolytic antibiotic, θ_s and θ_l, and the degradation rates of

bacteriostatic and bacteriolytic antibiotic γ_s and γ_l, which are the four key parameters in the antibiotic concentration model. This analysis was performed first as the antibiotic equations are not dependent on any parameters from the bacterial equations.

The *E. coli* counts data were used to infer the the carrying capacity of liquid slurry, μ, at the Sutton Bonington farm. Based on the results of the model in chapter 5, the bacterial population grows to approximately the carrying capacity. This data set comprises presumed total concentrations of *E. coli* in slurry, and so it was assumed that these concentrations approximated the carrying capacity. The carrying capacity was inferred both using antibiotic parameters from the literature and and using the inferred antibiotic parameters.

Finally, the resistance phenotype data were used to infer both the degradation and inflow rates of antibiotics (θ_s, θ_l, γ_s and γ_l, as before) and the HGT rates of bacteriostatic, bacteriolytic and multidrug-restance, β_s, β_l and β_u, respectively. This data was used to infer the antibiotic parameters as a test of the parameterisation of the model from the literature. I.e., if the bacterial equations were accurately parameterised, then it should be possible to infer the antibiotic parameters, as these would be dictating the behaviour of the system. The HGT parameters were then inferred as they are of particular interest to researchers of AMR [121] and horizontal gene transfer was shown by Baker et al. [38] to be important to the development of AMR over short timescales. The HGT parameters were inferred both using antibiotic and carrying capacity parameters from the literature and those that were inferred in this chapter. The reason only these parameters were chosen was to avoid overfitting.

In this chapter

- the three datasets will be presented
- the model equations will be reintroduced
- the statistical methods will be introduced
- the observational models for each data set will be defined
- the parameters of interest will be inferred from the data and the results discussed in relationship to the literature.

6.1 The Data

In this section the three data sets are introduced.

6.1.1 Antibiotic Concentration

Baena Nogueras et al. [37] collected slurry samples from the Sutton Bonington slurry tank between 3 October 2017 and 31 October 2018 over 10 dates. These samples were then analysed for the presence of 20 veterinary antibiotics, shown in Table 6.1.

Name	Class	Mode of Action	Max in Slurry (μg l^{-1})
Penicillin-G	Penicillin	Bacteriolytic [193]	-
Amoxicillin	Penicillin	Bacteriolytic [193]	-
Ampicillin	Penicillin	Bacteriolytic [193]	-
Cloxacillin	Penicillin	Bacteriolytic [193]	-
Cephalexin	1st Gen Cef	Bacteriolytic [49]	-
Cephalotin	1st Gen Cef	Bacteriolytic [49]	-
Cephoperazone	3rd Gen Cef	Bacteriolytic [49]	-
Cefquinome	4th Gen Cef	Bacteriolytic [49]	0.18
Ceftiofur	3rd Gen Cef	Bacteriolytic [49]	-
Cephapirin	1st Gen Cef	Bacteriolytic [49]	-
Cefotaxime	3rd Gen Cef	Bacteriolytic [49]	-
Oxytetracycline	Tetracycline	Bacteriostatic [193]	33.82
Enrofloxacin	Fluoroquinolone	Bactericidal [193]	-
Novobiocin	Aminocoumarin	Both [236]	8.84
Florfenicol	Fenicol	Bacteriostatic [237]	6.26
Tylosin	Macrolide	Bacteriostatic [238]	0.01
Lincomycin	Lincosamide	Bacteriostatic [239]	-
Sulfadiazine	Sulfonamide	Bacteriostatic [239]	0.63
Sulfadoxine	Sulfonamide	Bacteriostatic [239]	-
Trimethoprim		Bacteriolytic [191, 239, 240]	3.48

Table 6.1: Antimicrobials tested by Baena Nogueras et al. [37] in the SB slurry tank.

Of 20 antibiotics tested, 9 antibiotics were found above the limit of detection in that time period: the bacteriolytic antibiotics cefquinome and cefapirin [49], the bacteriostatic antibiotics oxytetracycline [193], florfenicol [237], tylosin [238], sulfadiazine [239] and sulfadoxine [239]. Novobiocin and Trimethoprim were also found above the limit of detection. Novobiocin is bacteriostatic at low concentrations and bacteriolytic at high concentrations [236] and is bacteriostatic against *E. coli*, excluding certain mutant strains [241]. Trimethoprim is bacteriostatic on its own, but bactericidal in combination with sulphonamides [240]. It has also been shown to have cell wall inhibition properties [191]. In this analysis novobiocin is considered to be bacteriostatic and trimethoprim is considered to be bacteriolytic, as it was only found above the limit of detection when sulfadiazine was also present. The antibiotic concentrations were consolidated into the combined bacteriostatic and bacteriolytic concentrations so that they could be directly compared with the output of the mathematical model. The concentrations of all antibiotics over time are shown in Table 6.2 and the concentrations of bacteriolytic and bacteriostatic antibiotic are shown in Table 6.3. Of the seven

antibiotics found above the limit of quantification by Baena Nogueras et al. [37], four were also found in analysis of slurry samples from the SWWAS project (see Chapter 3): oxytetracycline, novobiocin, sulphadiazine and tylosin.

Compounds	03/10/2017	20/11/2017	19/02/2018	24/04/2018	18/09/2018	24/09/2018	28/09/2018	03/10/2018	22/10/2018	31/10/2018
Cefquinome	0.18	0	0	0	0	0	0	0	0	0
Cephapirin	0	0	1.94	0	0	0	0	0	0	0
Oxytetracycline	33.82	12.45	9.67	8.2	3.26	1.25	17.14	6.15	5.01	5.88
Novobiocin	1.56	0.25	1.54	0.54	0.55	8.84	1.06	0.62	0.68	0.86
Florfenicol	6.26	0	0	2.27	0	0	0	0	0	0
Tylosin	0	0	0	0.01	0	0	0	0	0	0
Sulfadiazine	0.58	0	0.63	0.31	0	0	0	0	0	0
Sulfadoxine	0.1	0	0	0	0	0	0	0	0	0
Trimethoprim	3.48	0	0.13	0.14	0	0	0	0	0	0

Table 6.2: The concentration of antibiotics found at above detection limits in the slurry (μg l^{-1}). Here a zero value implies that the quantity of antibiotic in the slurry at that sampling point was below the limits of detection.

Date	Bacteriostatic (μg l^{-1})	Bacteriolytic(μg l^{-1})
03/10/2017	42.3±2.6	3.7± 1.8
20/11/2017	12.7±4.0	0.0± 0.0
19/02/2018	11.8±0.9	2.1± 1.4
24/04/2018	11.3±1.9	0.1± 0.1
18/09/2018	3.8±1.1	0.0± 0.0
24/09/2018	10.1±1.6	0.0±0.0
28/09/2018	18.2±2.4	0.0± 0.0
03/10/2018	6.8±1.9	0.0± 0.0
22/10/2018	5.7±0.5	0.0± 0.0
31/10/2018	6.7±1.1	0.0± 0.0

Table 6.3: Bacteriostatic and Bacteriolytic concentrations from [37].

Bacteriolytic antibiotics were consistently found at lower concentrations than bacteriostatic at each point in the sampling period (see Table 6.3). In fact, at seven out of the ten sampling dates, no bacteriolytic antibiotic was detected. Based on the sensitivity analysis in chapter 5, this would affect the expected proportion of multidrug resistant *E. coli* (R_u) in the slurry tank. Figure 5.13 in chapter 5 indicates that for both lower inflow rates and higher degradation rates of bacteriolytic antibiotic, the R_u population sized was reduced and did not entirely dominate the tank. This is seen in the bacterial phenotype data below (see section 6.1.3).

6.1.2 Microbial Counts

This data set comprises the presumptive concentrations of *E. coli* found in the slurry tank as cultured on TBX, MacConkey Agar (MAC), TBX+AMP16 and TBX/CTX plates. Here the TBX+AMP16 and TBX/CTX are selecting for ampicillin and cefotaxime resistance, respectively, and TBX and MAC are considered "non-selective" growth media for AMR. On some collection dates there

is not data for all four plate types. Figure 6.1 shows the log concentration of the presumptive counts on 14 dates where data was available for at least the TBX, MacConkey Agar and TBX+AMP16 growth media. In general MAC and TBX plates show higher counts than TBX+AMP16 and the counts on the TBX/CTX plates is often below or close to the statistical limit of detection (300 CFU ml^{-}1), which was determined by the method used by EVAL-FARMS researchers [36]).

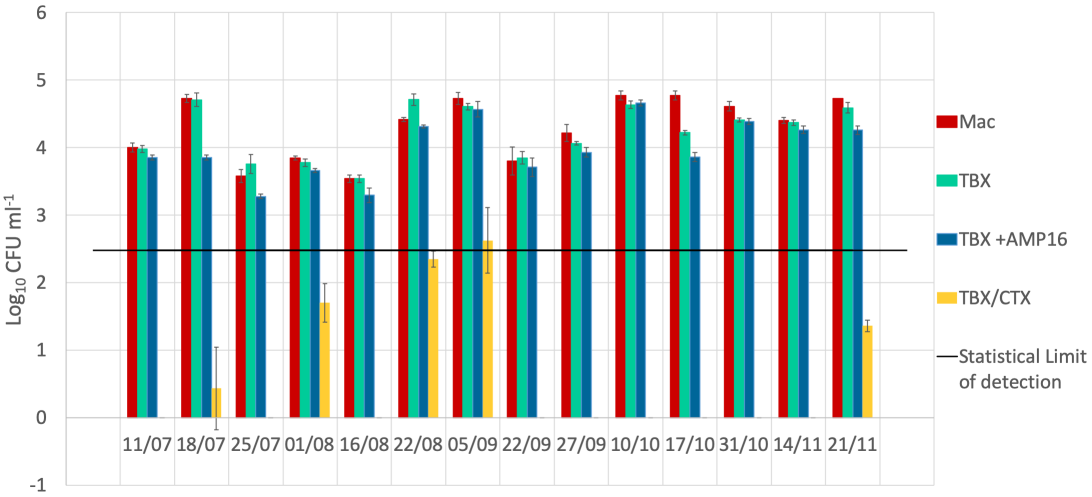


Figure 6.1: Presumptive *E. coli* Counts on MacConkey agar (Mac) TBX plates, TBX plates with added ampicillin (TBX+AMP16), TBX plates with added cefotaxime (TBX/CTX). The limit of detection (300 CFU ml^{-}1) was determined by the methods used by EVAL-FARMS researchers [36].

For parameter estimation, the data from the non-selective plates was taken at all available dates. Data from the TBX+AMP16 and TBX/CTX plates was not used as, to estimate the carrying capacity, it was important that ampicillin and cefotaxime susceptible bacteria not be omitted. The total counts for MAC and TBX plates, and the dates on which samples were collected, are shown in Table 6.4.

It is assumed that *E. coli* populations grow to match the carrying capacity of the slurry, as was seen in the simulations from Chapter 5. Under this assumption it is possible to use the data in Table 6.4 to estimate the average carrying capacity of the slurry, μ, over the time period the data was collected. Though the actual carrying capacity might vary in time due to changes in the tank influent, μ was treated as constant for these calculations.

6.1.3 Bacterial phenotype data

This data set details the phenotypic resistances of *E. coli* found in the slurry tank between May 2017 and December 2017 over 21 sampling dates. On each date a

MAC Collection date	*E. coli* (CFU l^{-1})	TBX Collection Date	*E. coli* (CFU l^{-1})
28/02/2017	7.50E+06	11/07/2017	9.55E+06
17/05/2017	3.17E+08	18/07/2017	5.08E+07
11/07/2017	1.00E+07	25/07/2017	5.68E+06
18/07/2017	5.32E+07	01/08/2017	5.95E+06
25/07/2017	3.78E+06	16/08/2017	3.45E+06
01/08/2017	7.03E+06	22/08/2017	5.11E+07
16/08/2017	3.45E+06	05/09/2017	4.04E+07
22/08/2017	2.60E+07	22/09/2017	7.04E+06
05/09/2017	5.30E+07	27/09/2017	1.15E+07
22/09/2017	6.30E+06	10/10/2017	4.29E+07
27/09/2017	1.65E+07	17/10/2017	1.66E+07
10/10/2017	5.91E+07	31/10/2017	2.55E+07
17/10/2017	5.91E+07	14/11/2017	2.34E+07
31/10/2017	4.07E+07	21/11/2017	3.87E+07
14/11/2017	2.51E+07	12/12/2017	1.48E+07
21/11/2017	5.33E+07	25/01/2018	1.96E+07
12/12/2017	1.93E+07	19/02/2018	5.52E+07

Table 6.4: Presumptive counts of *E. coli* in the SB slurry tank, cultured on MacConkey Agar (MAC) and TBX plates [36].

number of *E. coli* strains were grown on growth media and tested for resistance to 17 different antibiotics. Both full resistances and intermediate resistances were reported. Strains were grown on TBX plates, MacConkey agar plates and MacConkey and TBX plates with ampicillin (to selectively grow ampicillin resistant bacteria). The 17 antibiotics are shown in Table 6.5.

Name	Class	Mode of action	% resistance
Ampicillin	Penicillin	Bacteriolytic [193]	33.45
Amoxicillin-clavulanic acid	Penicillin & β-lactamase inhibitor	Bacteriolytic [193]	4.88
Aztreonam	Monobactam	Bactericidal [193]	9.76
Chloramphenicol	Phenicol	Bacteriostatic [242]	5.92
Ceftazidime	3rd Gen Cef	Bacteriolytic [49]	28.22
Ciprofloxacin	Flouroquinolone	Bacteriolytic [193]	18.82
Cefpodoxime	3rd Gen Cef	Bacteriolytic [49]	40.77
Colistin	Polymixin	Bacteriolytic [243]	4.18
Cefotaxime	3rd Gen Cef	Bacteriolytic [49]	31.01
Nitrofurantoin	Nitrofuran	Bacteriostatic [244]	9.76
Cefoxitin	2nd Gen Cef	Bacteriolytic [49]	2.44
Imipenem	Carbapenem	Bactericidal [245]	2.79
Nalidixic acid	Quinolone	Bactericidal [193]	7.32
Streptomycin	Amino-glycoside	Bactericidal [246]	19.51
Trimethoprim-sulfamethoxazole	Combination	Bacteriolytic [191, 239, 240]	6.27
Tetracyclines	Tetracycline	Bacteriostatic [193]	8.01
Azithromycin	Macrolide	Bacteriostatic [247]	9.41

Table 6.5: Antimicrobials quantified by EVAL-FARMS in the SB slurry tank. Percentage resistance refers to the percentage of bacterial strains cultured that were resistant to each antibiotic, from a total of 287 strains.

For the purposes of model fitting, the strains grown on selective plates (MacConkey and TBX plates with ampicillin) were removed from the dataset, as including these would skew the proportion of susceptible strains at each time point. This brought the total number of sampling dates down to 17. The resistance phenotypes were then consolidated into into "susceptible", "bacteriolytic-resistant", "bacteriostatic-resistant" and "multidrug-resistant" categories, so that they could be compared with the model output. Table 6.6 shows the number of susceptible and resistant strains cultured at each sampling date.

Date	Susceptible	Bacteriostatic	Bacteriolytic	Multidrug	Total strains
16/05/2017	8	0	14	0	22
22/05/2017	6	0	4	11	21
11/07/2017	0	0	6	4	10
18/07/2017	3	0	3	4	10
04/07/2017	1	0	8	1	10
25/07/2017	1	0	5	4	10
01/08/2017	1	0	3	6	10
16/08/2017	1	1	17	19	38
22/08/2017	3	0	6	15	24
05/09/2017	2	0	5	3	10
22/09/2017	5	0	19	9	33
27/09/2017	8	2	14	11	35
10/10/2017	4	0	4	6	14
17/10/2017	4	1	1	3	9
31/10/2017	3	0	7	7	17
14/11/2017	5	1	0	3	9
12/12/2017	2	1	0	3	6

Table 6.6: Bacterial phenotype data showing the number of strains of each phenotype on the collection dates, from EVAL-FARMS [36].

The three data sets were then used to infer parameters from the ODE model from 5, which is reintroduced in the next section.

6.2 Methods

6.2.1 The mathematical model

The aim of this chapter is to use the three data sets to infer key parameters in the ODE model developed in chapter 5. This model describes the interactions between an *E. coli* population and two types of antibiotic (bacteriolytic and bacteriostatic) within a dairy slurry tank environment. The *E. coli* in the tank can be susceptible, resistant to either antibiotic or resistant to both. As in chapter

5, the bacterial equations are given by:

$$\frac{dS}{dt} = r\left(1-\frac{N}{\mu}\right)E_S S - S(\beta_s R_s + \beta_l R_l + \beta_u R_u) + \lambda(1-\rho)\frac{\nu}{V(t)} - \frac{\lambda S}{V(t)} - \delta_S S - \delta_l S\frac{A_l}{MIC_l + A_l} \tag{6.1}$$

$$\frac{dR_s}{dt} = r(1-\alpha_s)\left(1-\frac{N}{\mu}\right)E_R R_s + R_s(\beta_s S - \beta_l R_l - \beta_u R_u) + \lambda\rho_s\frac{\nu}{V(t)} - \frac{\lambda R_s}{V(t)} - \delta_R R_s - \delta_l R_s\frac{A_l}{MIC_l + A_l} \tag{6.2}$$

$$\frac{dR_l}{dt} = r(1-\alpha_l)\left(1-\frac{N}{\mu}\right)E_S R_l + R_l(-\beta_s R_s + \beta_l S - \beta_u R_u) + \lambda\rho_l\frac{\nu}{V(t)} - \frac{\lambda R_l}{V(t)} - \delta_R R_l \tag{6.3}$$

$$\frac{dR_u}{dt} = r(1-\alpha_u)\left(1-\frac{N}{\mu}\right)E_R R_u + R_s R_l(\beta_s + \beta_l) + \beta_u R_u(S + R_s + R_l) + \lambda\rho_u\frac{\nu}{V(t)} - \frac{\lambda R_u}{V(t)} - \delta_R R_u. \tag{6.4}$$

Where S, R_s, R_l and R_u are the concentrations of susceptible, bacteriostatic resistant, bacteriolytic resistant and multi-drug resistant *E. coli*, respectively, and N, $V(t)$, E_S, E_R and ρ are given by

$$N = S + R_s + R_l + R_u \tag{6.5}$$

$$V(t) = V_1 + \lambda t - \omega(t) \tag{6.6}$$

$$E_S = 1 - \frac{E_{max}A_s^H}{MIC_s^H + A_s^H} \tag{6.7}$$

$$E_R = 1 - \frac{E_{max}A_s^H}{MIC_R^H + A_s^H} \tag{6.8}$$

$$\rho = \rho_s + \rho_l + \rho_u \tag{6.9}$$

$$\tag{6.10}$$

In equation 6.6, $\omega(t)$ is the quantity of slurry leaving the tank. The other parameters are as described in chapter 5 and are defined in Table 6.7.

The equations for antibiotic concentration in the slurry tank are given by:

$$\frac{dA_s}{dt} = \frac{\theta_s}{V(t)} - A_s\left(\gamma_s + \frac{\lambda}{V(t)}\right) \tag{6.11}$$

and

$$\frac{dA_l}{dt} = \frac{\theta_l}{V(t)} - A_l\left(\gamma_l + \frac{\lambda}{V(t)}\right). \tag{6.12}$$

Parameter	Description	Typical Value	Reference
r	Specific growth rate of E. coli	0.5 h^{-1}	[38]
β_s	Bacteriostatic-resistance gene transfer term	10^{-14} $lCFU^{-1}h^{-1}$	[38, 39, 123]
β_l	Bacteriolytic-resistance gene transfer term	10^{-14} $lCFU^{-1}h^{-1}$	[38, 39, 123]
β_u	MDR gene transfer term	10^{-14} $lCFU^{-1}h^{-1}$	[38, 39, 123]
λ	Rate of slurry inflow to tank	$613lh^{-1}$	[38]
ν	Concentration of bacteria in slurry inflow	6×10^7 CFU l^{-1}	[38, 218]
ρ_s	Proportion of bacteriostatic-resistant bacteria in inflow	0.2	[204]
ρ_l	Proportion of bacteriolytic-resistant bacteria in inflow	0.2	[204]
ρ_u	Proportion of multidrug-resistant bacteria in inflow	0.0	[204]
α_s	Bacteriostatic-resistance fitness cost as a fraction of r	0.1	[38, 50]
α_l	Bacteriolytic-resistance fitness cost as a fraction of r	0.1	[38, 50]
α_u	MDR fitness cost as a fraction of r	0.1	[38, 50]
V_1	Initial volume of slurry in the tank	150,000 l	[38]
θ_s	Rate of bacteriostatic antibiotic inflow	1711 μg h^{-1}	[38]
θ_l	Rate of bacteriolytic antibiotic inflow	1711 μg h^{-1}	[38]
E_{max}	Maximum effect of antibiotics on bacterial growth	2	[38, 39]
H	Hill coeficient in E_{max} model	2	[38, 39]
MIC_R	MIC for bacteriostatic-resistant bacteria	2000 μg l^{-1}	[38]
MIC_s	MIC for bacteriostatic-sensitive bacteria	8 μg l^{-1}	[173]
MIC_l	MIC for bacteriolytic-sensitive bacteria	4 μg l^{-1}	[173]
μ	Carrying capacity of liquid slurry	10^{10} CFU l^{-1}	[38]
γ_s	Decay rate of bacteriostatic antibiotics	0.0029 h^{-1}	[38]
γ_l	Decay rate of bacteriolytic antibiotics	0.0029 h^{-1}	[38]
δ_S	Natural death rate of susceptible bacteria	0.001 h^{-1}	[187]
δ_R	Natural death rate of resistant bacteria	0.001 h^{-1}	[187]
δ_l	Antibiotic driven death rate of bacteriolytic-susceptible bacteria	0.01 h^{-1}	[213]

Table 6.7: Typical parameter values used for initial simulations of the model given by equations 6.1 to 6.12.

Where A_s and A_l are the concentrations of bacteriostatic and bacteriolytic antibiotic, respectively, θ_s and θ_l are the inflow rates of bacteriostatic and bacteriolytic antibiotic, respectively, γ_s and γ_l are the decay rates of bacteriostatic and bacteriolytic antibiotics, respectively, $V(t)$ is the volume of slurry in the tank at time t and λ is the inflow rate of slurry to the tank.

6.2.2 Methods of inference

Here, brief summaries of MLE and the Metropolis Hastings algorithm are given.

Maximum Likelihood Estimation

MLE is a method used to estimate parameter values in a given model by maximising a likelihood function. It is one of the most common approaches used for parameter estimation [248].

Let $\mathbf{y} = \{y_1, y_2, ..., y_n\}$ be a set of observed data points, it is assumed that $\mathbf{y}$ is distributed according to some observational model, M, with model parameters $\theta = \{\theta_1, \theta_2, ..., \theta_{np}\}$ and probability density function f_M, so that

$$\mathbf{y} \sim M(\theta). \tag{6.13}$$

The probability density function $f_M(\mathbf{y}|\theta)$ then describes the probability that $\mathbf{y}$ is observed, given the values of θ. Furthermore, in the case that the y_i are statistically independent, $f_M(\mathbf{y}|\theta)$ is given by

$$f_M(\mathbf{y}|\theta) = f_M(y_1|\theta)f_M(y_2|\theta)...f_M(y_n|\theta) = \prod_{i=1}^{n} f_M(y_i|\theta). \tag{6.14}$$

The likelihood function is defined as $L(\theta) = f_M(\mathbf{y}|\theta)$, and calculates the likelihood that θ has a given value, given the fixed data set $\mathbf{y}$. Maximising $L(\theta)$ with respect to θ then returns the value of θ which is most likely, given the observed data [248,249]. This is then the method for inferring parameters using MLE. Often, for the sake of numerical stability, the log-likelihood is maximised ($ll(\theta) = \log(L(\theta))$).

Bayesian Inference

The aim of Bayesian inference, in basic terms, is to take an assumed or estimated distribution of parameter values, the prior distribution, and then to improve that estimation by reducing the uncertainty of the parameters to find a posterior distribution [248].

Definining $\mathbf{y} = \{y_1, y_2, ..., y_n\}$ and $\theta = \{\theta_1, \theta_2, ..., \theta_{np}\}$ as before, it is possible

to write Baye's Theorem for probability distributions:

$$\pi(\theta|\mathbf{y}) = \frac{\pi(\mathbf{y}|\theta)\pi(\theta)}{\pi(\mathbf{y})} \tag{6.15}$$

where $\pi(\theta|\mathbf{y})$ is the posterior distribution of θ (the distribution being sought), $\pi(\mathbf{y}|\theta)$ is the likelihood function, $\pi(\theta)$ is the prior distribution (what is believed about the θ before analysis) and $\pi(\mathbf{y})$ is the marginal likelihood, a normalising constant of the density of the posterior distribution. The marginal likelihood is given by

$$\pi(\mathbf{y}) = \int \pi(\mathbf{y}|\theta)\pi(\theta)d\theta, \tag{6.16}$$

the integral of the prior distribution multiplied by the likelihood function over all possible values of θ. Equation 6.15 implies that the posterior distribution is proportional to the likelihood times the prior density. The posterior distribution can tell us a lot about the parameter set θ, including the predicted mean values, but also the probability that elements of θ are greater or less than a certain given value.

Markov Chain Monte Carlo and the Metropolis Hastings algorithm

Markov Chain Monte Carlo (MCMC) methods are a class of algorithms that can be used to sample from probability distributions. This sampling method can be used to infer parameter values for a model, given an existing data set. For a parameter set θ, with an established prior distribution, MCMC methods generate a posterior distribution by using the likelihood function to update the prior [250, 251]. This allows estimation of the density, mean, variance, and probabilities of θ.

In this thesis, the MCMC method used is a single-site-update Metropolis Hastings algorithm [251]. The random walk, single-site-update Metropolis Hastings algorithm takes as its inputs a set of observed data, $\mathbf{y} = y_1, y_2, ..., y_n$, which, as before, is assumed to be distributed $\mathbf{y} \sim M(\theta)$; and a model $M(\theta)$.

The algorithm begins with an initial guess for each θ_i, θ_i^0, then at each iteration, j, of the algorithm ($j \in \{1, 2, 3, ...\}$), for each θ_i in θ

- Calculate the likelihood $\pi(\mathbf{y}|\theta_i^j)$ (determined by the chosen model, M)
- Generate a candidate value θ_i^{can}, by sampling from a normal distribution: $N(\theta_i^0, \sigma^2)$

- Select θ_i^{can} with probability

$$\min\left(1, \frac{\pi(\mathbf{y}|\theta_i^{can})\pi(\theta_i^{can})}{\pi(\mathbf{y}|\theta_i^{j})\pi(\theta_i^{j})}\right) \tag{6.17}$$

- If θ_i^{can} is selected, assign $\theta_i^j = \theta_i^{can}$.

This system iterates until it converges to the posterior distribution. The output is then a matrix of the selected values of θ at each iteration:

$$\mathbf{\Theta} = \begin{bmatrix} \theta_1^1 & \theta_1^2 & \dots & \theta_1^k \\ \theta_2^1 & \theta_2^2 & \dots & \theta_2^k \\ \vdots & \vdots & \ddots & \vdots \\ \theta_{np}^1 & \theta_{np}^2 & \dots & \theta_{np}^k \end{bmatrix}. \tag{6.18}$$

Traditionally, a number of columns are removed from $\mathbf{\Theta}$, as these represent a so called "burn in period" as the algorithm approaches the posterior distribution for the parameter set. In the case of this thesis, the results of the first 5000 iterations were removed. The resulting matrix can be used to provide numerical approximations of the posterior distribution for each θ_i, by creating a histogram using the corresponding row in $\mathbf{\Theta}$.

Both MLE and MCMC methods were used in this chapter as both have advantages and disadvantages. MLE is generally quicker than the Metropolis Hastings algorithm but provides only a single point estimate of the parameters. On the other hand, the Metropolis Hastings algorithm generates an estimated posterior distribution of each parameter inferred, meaning it is possible to calculate probabilities that a parameter would take a certain value. However, the Metropolis Hastings method requires a prior distribution which needs to be determined from existing data. It can be difficult to generate an informative prior in situations where the existing data is sparse.

Microbial Count Statistical Model

The microbial counts data in Table 6.4 was used to infer a functional carrying capacity for dairy slurry from the SB dairy tank. Let $\mathbf{C^{obs}} = \{C_i^{obs}, t = 1, 2, ..n\}$ be the observed presumptive concentration recorded at each time point and $\mathbf{C^{mod}} = \{C_i^{mod}, t = 1, 2, .., n\}$ be the total concentration of bacteria predicted in the model at each time point from the data. It is assumed that the observations differ from the model outputs by some error quantity. The observational model to be fitted is then

$$\mathbf{C^{obs}} = \mathbf{C^{mod}} + \epsilon \tag{6.19}$$

where $\epsilon = \{\epsilon_i, i = 1, 2, .., n\}$ is a vector of errors that are assumed to be random variables. Here, the distribution of the errors is so unknown, but for simplicity it is assumed that ϵ_i is distributed normally for all i, so that $\epsilon_i \sim N(0, \sigma_C^2)$, where σ_C is the standard deviation of the error.

Assuming that $\epsilon_i \sim N(0, \sigma_C^2)$ and that ϵ_i are independent for all i, and $\theta_{MC} = \mu$ is the carrying capacity to be inferred, the likelihood function is given by

$$L_{MC}(\theta_{MC}) = \prod_{i=1}^{n} f(C_i^{obs}) = \prod_{i=1}^{n} \frac{1}{\sigma\sqrt{2\pi}} \exp\left(-\frac{1}{2\sigma_C^2}(C_i^{mod} - C_i^{obs})^2\right) \tag{6.20}$$

and the log-likelihood is given by

$$l_{MC}(\theta_{MC}) = log(L(\theta_{MC})) = -n\log(\sigma) - \frac{n}{2}\log(2\pi) - \frac{1}{2\sigma^2}\sum_{i=1}^{n}(C_i^{mod} - C_i^{obs})^2. \tag{6.21}$$

The function to be maximised is then the log-likelihood up to proportionality:

$$ll_{MC}(\theta_{MC}) = log(L(\theta_{MC})) = -\frac{1}{2\sigma^2}\sum_{i=1}^{n}(C_i^{mod} - C_i^{obs})^2. \tag{6.22}$$

Designating the presumptive count data from both TBX and MacConkey Agar growth mediums $\mathbf{C_{TBX}^{obs}}$ and $\mathbf{C_{Mac}^{obs}}$ the functions to maximise are

$$ll_{TBX}(\mu) = \frac{1}{2\sigma^2}\sum_{i=1}^{n}(C_i^{mod} - C_{TBX_i}^{obs})^2. \tag{6.23}$$

and

$$ll_{Mac}(\mu) = \frac{1}{2\sigma^2}\sum_{i=1}^{n}(C_i^{mod} - C_{Mac_i}^{obs})^2. \tag{6.24}$$

Antibiotic Concentration Statistical Model

The concentrations of bacteriostatic and bacteriolytic antibiotics were summed over each sampling date to give $\mathbf{A_s^{obs}} = \{A_{s1}^{obs}, A_{s2}^{obs}, ..., A_{s10}^{obs}\}$ and $\mathbf{A_l^{obs}} = \{A_{l1}^{obs}, A_{l2}^{obs}, ..., A_{l10}^{obs}\}$, the observed concentrations of bacteriostatic and bacteriolytic antibiotic at each sampling date, respectively, with units of μg l^{-1}.

Once again it is assumed that each observation differs from the model output by some error. The observational model is given by

$$A_{st}^{obs} = A_{st}^{mod} + \epsilon_{i_{A_s}} \tag{6.25}$$

$$A_{lt}^{obs} = A_{lt}^{mod} + \epsilon_{i_{A_l}} \tag{6.26}$$

$$\tag{6.27}$$

where $\epsilon_{i_{A_s}} \sim N(0, \sigma^2_{A_s})$ and $\epsilon_{i_{A_l}} \sim N(0, \sigma^2_{A_l})$. Assuming that $\epsilon_{i_{A_s}}$ and $\epsilon_{i_{A_l}}$ are independent for all i, and following the same procedure as in functions 6.32 to 6.34 the log-likelihoods up to proportionality for A_s and A_l are given by

$$ll(\theta_s, \gamma_s) = -\frac{1}{2\sigma^2_{A_s}} \sum_{i=1}^{n} (A^{mod}_{st} - A^{obs}_{st})^2 \tag{6.28}$$

and

$$ll(\theta_l, \gamma_l) = -\frac{1}{2\sigma^2_{A_l}} \sum_{i=1}^{n} (A^{mod}_{lt} - A^{obs}_{lt})^2. \tag{6.29}$$

Defining $\theta_{AB} = \{\theta_s, \gamma_s, \theta_l, \gamma_l\}$, the quantity to maximise over all time points is then

$$ll_{AB}(\theta_{AB}) = ll(\theta_s, \gamma_s) + ll(\theta_l, \gamma_l) = -\frac{1}{2\sigma^2_{A_s}} \sum_{i=1}^{n} (A^{mod}_{st} - A^{obs}_{st})^2 - \frac{1}{2\sigma^2_{A_l}} \sum_{i=1}^{n} (A^{mod}_{lt} - A^{obs}_{lt})^2. \tag{6.30}$$

Bacterial Phenotype Statistical Model

Under the assumption that this data represents a random sample of the *E. coli* population in the slurry tank over the 17 discrete time points, the data is treated as set of multinomial experiments of n_t trials, where n_i is the number of strains at the time point t ($t = 1 : 17$). The Multinomial distribution, $\text{Mult}(n, \{p_1, p_2, ..., p_m\}$, describes n independent samples from a distribution with m possible outcomes, where the probability of selecting outcome i has probability p_i. Here it is assumed that at each sampling time, t, n_t bacterial strains were sampled from the slurry and each sample could be susceptible (S), bacteriostatic resistant (R_s), bacteriolytic resistant (R_l) or multidrug resistant (R_u). The observational model is thus assumed to be

$$\mathbf{y}_t \sim \text{Mult}(n_t, \{S^p_t, R^p_{st}, R^p_{lt}, R^p_{ut}\}) \tag{6.31}$$

where $\mathbf{y}_t = \{y_{1t}, y_{4t}, y_{3t}, y_{4t}\}$ is the vector of results at time t, such that y_{1t} is the number of susceptible *E. coli* strains cultured at time t, y_{2t} is the number of bacteriostatic resistant *E. coli* strains cultured at time t, y_{3t} is the number of bacteriolytic resistant *E. coli* strains cultured at time t and y_{4t} is the number of multi-drug resistant *E. coli* strains cultured at time t; n_t is the number of *E. coli* strains cultured at time t, and $S^p_t, R^p_{st}, R^p_{lt}$ and R^p_{ut} are the proportions of Susceptible, bacteriostatic resistant, bacteriolytic resistant and multi-drug resistant bacteria at time t.

Let $\mathbf{M}_t = \{M_{1t}, M_{2t}, M_{3t}, M_{4t}\} = \{S^p_t, R^p_{st}, R^p_{lt}, R^p_{ut}\}$, then the likelihood is

given by

$$L_B(\theta_B) = f(\mathbf{y}_t^{obs}|\mathbf{M}_t) = \frac{n_t!}{\prod_{i=1}^{4} y_{ti}!} \prod_{i=1}^{4} M_{ti}^{y_{ti}} \tag{6.32}$$

and the log-likelihood is

$$ll(\theta_B) = log(L_B(\mathbf{M}_t)) = \log(4!) - \sum_{i=1}^{4} \log(y_{ti}!) + \sum_{i=1}^{4} y_{ti} \log(M_{ti}) \tag{6.33}$$

The quantity to maximise over the all time points is then

$$ll_B(\theta_B) = \sum_{t=1}^{t_{end}} \log(l(\mathbf{M}_t)) = \log(4!) - \sum_{i=1}^{4} \log(y_{ti}!) + \sum_{i=1}^{4} y_{ti} \log(M_{ti}). \tag{6.34}$$

6.3 Results and Discussion

Estimating the antibiotic parameters

In this section the inflow rates (θ_s and θ_l) and degradation rates (γ_s and γ_l) of bacteriostatic and bacteriolytic antibiotic were inferred. To estimate $\theta_{AB} = \{\theta_s, \gamma_s, \theta_l, \gamma_l\}$ in equations 6.11 and 6.12 using the antibiotic concentration data, the goal is to maximise $ll_{AB}(\theta_{AB})$ (see Equation 6.30), where A_{st}^{obs} is the data collected by Baena Nogueras et al.. The Metropolis hastings algorithm was also used to sample from the posterior of the parameters of interest.

To test how well MLE was able to infer the parameters of interest, it was tested using synthetic data. To generate the synthetic data the antibiotic ODE model was run using standard parameters for 9432 hours (the time between the first and last data points from Baena Nogueras et al. [37]), then n = 101,21 and 11 evenly spaced time steps were chosen throughout the data and gaussian noise was added to the data at each time step. In this way, the synthetic data matches the observational model as

$$A_{st}^{syn} = A_{st}^{mod} + \epsilon_{i_{A_s}} \tag{6.35}$$

$$A_{lt}^{syn} = A_l st^{mod} + \epsilon_{i_{A_l}}. \tag{6.36}$$

Here A_{st}^{syn} and A_{lt}^{syn} are the synthetic concentrations of bacteriostatic and bacteriolytic antibiotic and $\epsilon_{i_{A_s}}$ and $\epsilon_{i_{A_l}}$ are both distributed $N(0, \sigma^2)$. The variance, σ^2, was allowed to vary between 0.1 and 1.

In total there were 15 different conditions for the simulated data sets (three sample sizes and five possible values of σ^2). Data was simulated 10 times for each of the different conditions. The log-likelihood function was maximised using the optim function in R, over the four parameters for each simulated data set

and then the mean inferred parameter value and the standard deviation were calculated for each of the 15 conditions. The results are shown in Table 6.8. In general γ_s is well fairly estimated even at the highest σ^2 and the lowest number of time points (though the standard deviation does increase as σ^2 increases and n decreases). γ_l is less well estimated as n decreases and σ^2 increases. As the governing equations are the same for both antibiotics this must be due to the initial conditions. Similarly θ_s is fairly well estimated across all tests, the mean estimated parameter is always within plus or minus 10% of the original value. However for $n = 11$ and $\sigma^2 > 0.2$, the mean predicted value of θ_l is far from the original, with a very large standard deviation. In the $n = 11$ and $\sigma^2 = 1$ case, the mean predicted value is an order of magnitude too large, this was likely caused by a single outlier in the inference results.

σ^2	data points (n)	γ_s	γ_s SD	γ_l	γ_l SD	θ_s	θ_s SD	θ_l	θ_l SD
NA	9432	0.0029	NA	0.0029	NA	1711	NA	1711	NA
0.1	101	0.00291	0.00001	0.00291	0.00016	1718.9	12.9	1710.9	47.6
0.2	101	0.00291	0.00005	0.00286	0.00019	1714.8	39.5	1681.3	69.2
0.3	101	0.00292	0.00008	0.00297	0.00056	1703.6	59.3	1718.9	162.2
0.5	101	0.00286	0.00008	0.00266	0.00066	1747.1	59.8	1672.2	207.5
1	101	0.00301	0.00021	0.00237	0.00089	1856.0	161.3	1583.8	328.7
0.1	20	0.00293	0.00005	0.00289	0.00033	1728.9	29.1	1710.5	101.6
0.2	20	0.00288	0.00010	0.00304	0.00093	1741.9	79.1	1736.7	275.1
0.3	20	0.00302	0.00015	0.00318	0.00116	1731.8	125.6	1771.5	408.2
0.5	20	0.00286	0.00032	0.00279	0.00071	1713.4	235.8	1671.3	225.6
1	20	0.00266	0.00043	0.00144	0.00094	1562.0	335.0	1293.4	366.8
0.1	11	0.00296	0.00017	0.00279	0.00047	1741.8	90.6	1651.3	157.1
0.2	11	0.00280	0.00027	0.00271	0.00066	1642.3	138.8	1679.9	213.9
0.3	11	0.00272	0.00029	0.00637	0.00521	1564.9	120.9	2945.6	1755.7
0.5	11	0.00317	0.00061	0.00526	0.00652	1841.2	357.0	2497.7	2244.6
1	11	0.00281	0.00087	0.06297	0.18838	1612.5	455.6	27089.1	80398.2

Table 6.8: Parameter estimation of bacteriostatic and bacteriolytic rate of degradation (γ_s and γ_l, respectively) and rate of inflow (θ_s and θ_l, respectively) with varying number of simulated data points, n, and varying noise variance, σ^2. Here "SD" indications the standard deviation of the inferred parameter value.

The likelihood was then maximised over the four parameters against the data from Baena Nogueras et al. to attempt to infer the parameter values for the SB slurry tank. The values which maximise the likelihood are $\gamma_s = 1.115 \times 10^{-4}$, $\gamma_l = 6.494 \times 10^{-2}$, $\theta_s = 5.868 \times 10^3$ and $\theta_l = 1.367 \times 10^3$. The degradation rate of bacteriostatic antibiotic, γ_s is the same order of magnitude as the degradation rate of Oxytetracycline in pig slurry recorded in [252]. Massé et al. report a half-life of 17.7 days for oxytetracycline in dairy manure and 31.1 days in stored feedlot manure, which equates to a degradation rates of 0.0017 h^{-1} and 9.3×10^{-4} h^{-1}, both nearly an order of magnitude larger than the predicted value of γ_s [23]. The predicted degradation rate of bacteriolytic antibiotic, γ_l, indicates a predicted half life of approximately 10 hours, which is in line with the results reported by

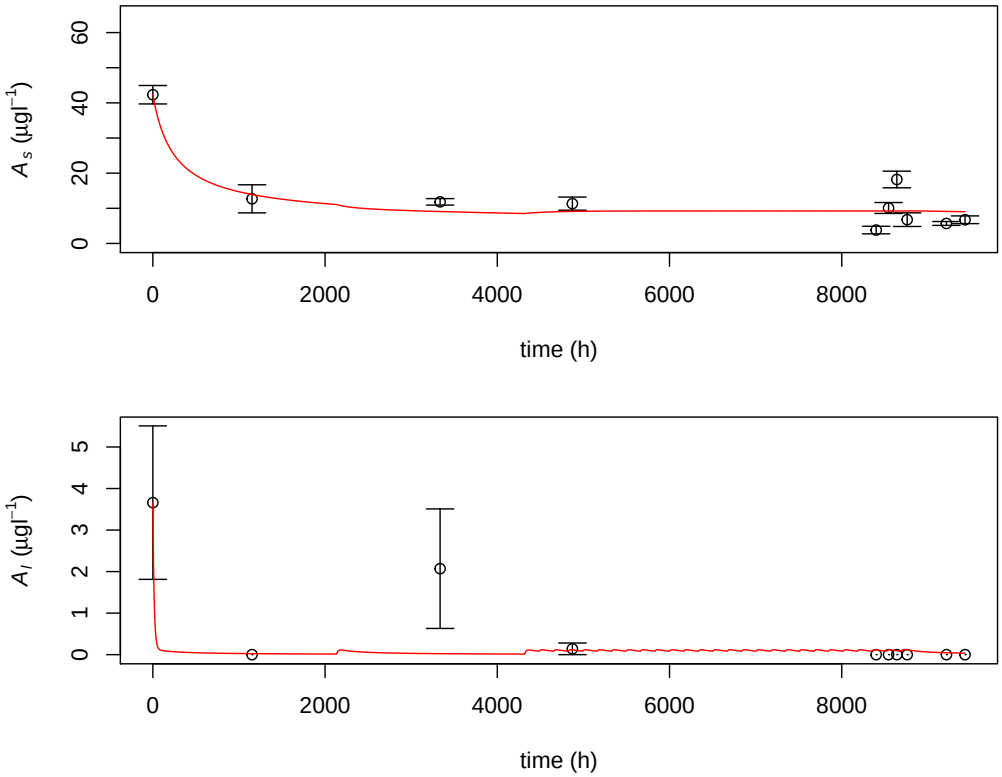


Figure 6.2: Graph of A_s and A_l usin bacteriostatic and bacteriolytic rate of degradation (γ_s and γ_l, respectively) and rate of inflow (θ_s and θ_l, respectively) which maximise the log likelihood (equation 6.30), plotted alongside the data collected by Baena Nogueras et al. [37]. Model values are generated using equations 6.11 and 6.12.

Baena Nogueras et al. [37] for several penicillin and cephalosporin antibiotics. The antibiotic equations simulated with the inferred parameters is shown in Figure 6.2, the mean squared error is 8.50. The inflow rates of antibiotic are within the same order of magnitude as values proposed by Baker et al., though θ_s is somewhat larger than expected. This could be due to antibiotic sources that have not previously been considered in the parameterisation, such as antibiotics in the dairy manure.

The simulation of the A_l model is in general good, with the exception of one outlier whereas in the A_s case the initial fit is relatively good, but there are more outliers at the end of the timescale (see Figure 6.2).

A random walk MCMC algorithm was used to estimate the posterior distributions of each of the four parameters. The trace plots are shown in Figure 6.3 and histograms representing the posterior distributions of the four parameters are shown in Figure 6.4.

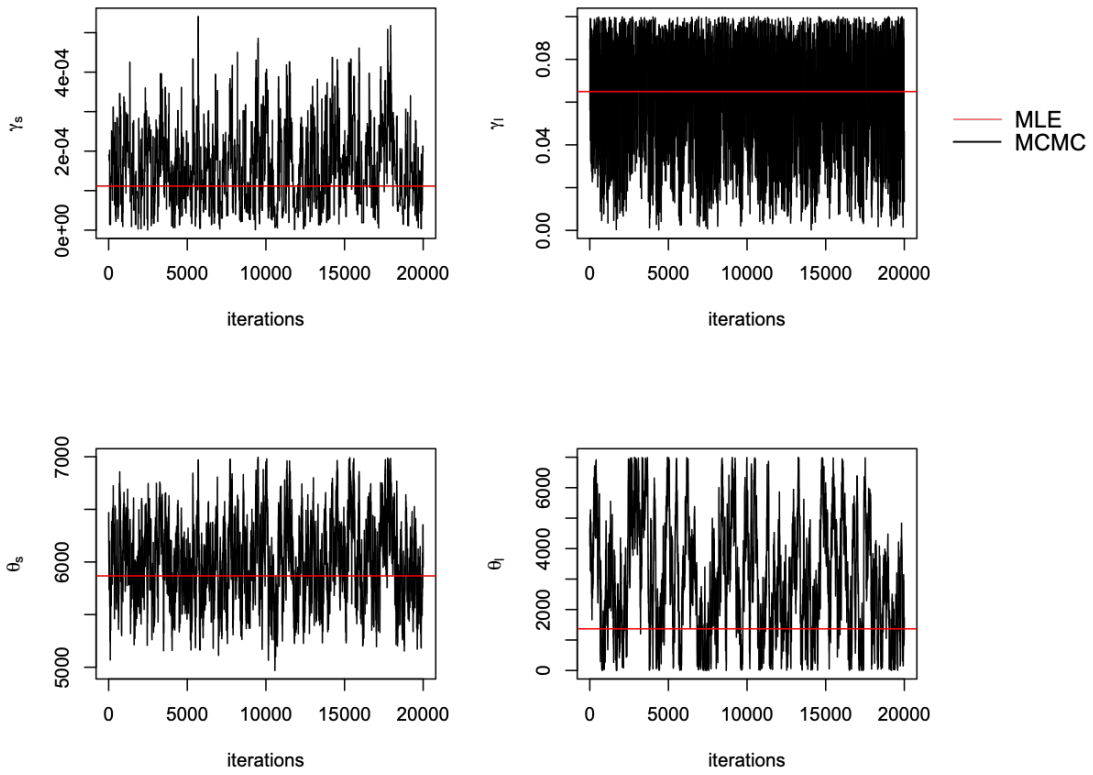


Figure 6.3: MCMC trace plots for the antibiotic parameters using the antibiotic concentration data. These plots were generated using the Metropolis Hastings algorithm to infer bacteriostatic and bacteriolytic rate of degradation (γ_s and γ_l, respectively) and rate of inflow (θ_s and θ_l, respectively) using the data from [37]. The MLE values were also calculated the data from [37], by maximising equation 6.30.

6.3.1 Estimating the carrying carrying capacity of liquid slurry

Using the bacterial counts data it may be possible to estimate a functional carrying capacity for the SB Farm slurry by comparing the total concentration of bacteria in the model to the total bacteria in slurry. The parameter values used to simulate the model are shown in the previous section, in Table 6.7. It was also assumed that between 1st October and 31st March the tank is emptied every three months and is emptied weekly during the other months, as in chapter 5.

The carrying capacity, μ, which maximises $ll_{TBX}(\mu)$ is $\mu_{TBX} = 2.6{\times}10^7$. The value of μ which maximises $ll_{Mac}(\mu)$ is $\mu_{Mac} = 4.7{\times}10^7$. Figure 6.5 shows the model run with $\mu = \mu_{TBX}$ against $\mathbf{C^{obs}_{TBX}}$ and Figure 6.5 shows the model run with $\mu = \mu_{Mac}$ against $\mathbf{C^{obs}_{Mac}}$. Using the values of $\gamma_s = 1.115 \times 10^{-4}$, $\gamma_l = 6.494 \times 10^{-2}$, $\theta_s = 5.868 \times 10^3$ and $\theta_l = 1.367 \times 10^3$, as inferred in the previous subsection, leads to the same values of of $\mu_{TBX} = 2.6{\times}10^7$ and $\mu_{Mac} = 4.7{\times}10^7$.

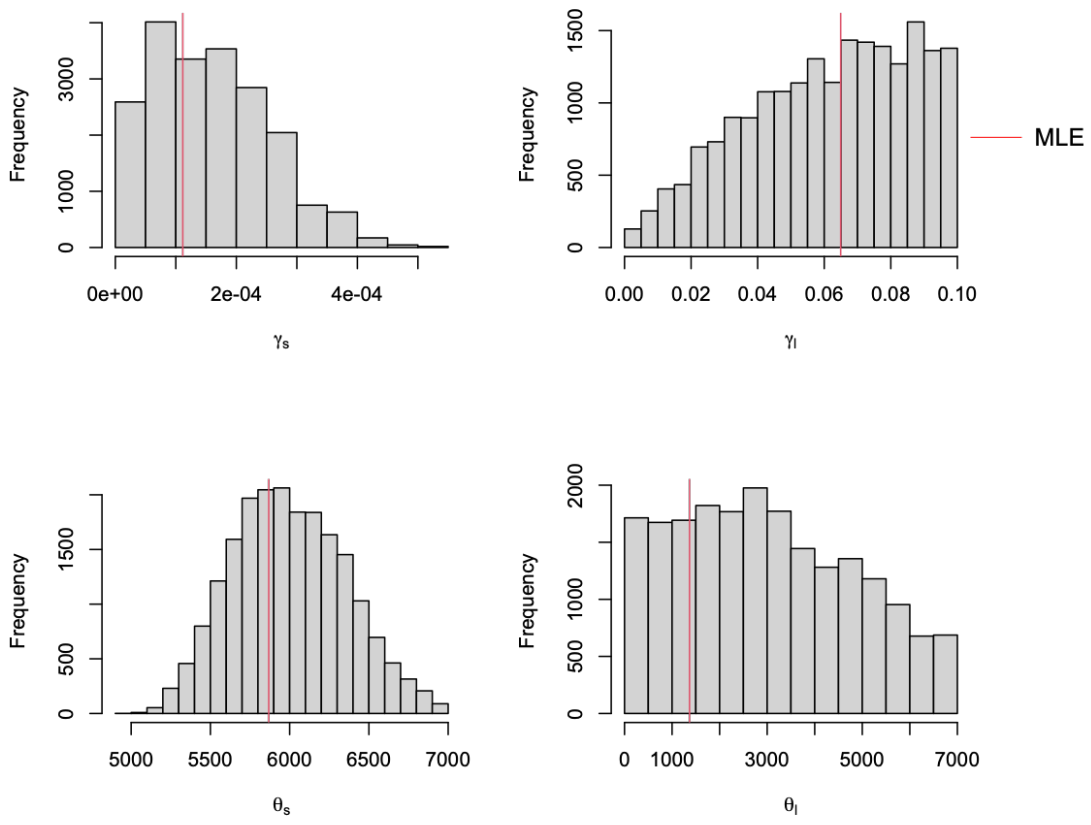


Figure 6.4: MCMC Histograms for the antibiotic parameters using antibiotic concentration data from [37]. These plots were generated using the Metropolis Hastings algorithm to infer bacteriostatic and bacteriolytic rate of degradation (γ_s and γ_l, respectively) and rate of inflow (θ_s and θ_l, respectively) using the data from [37]. The MLE values were also calculated the data from [37], by maximising equation 6.30.

This is likely because the antibiotic concentrations don't appear to affect the total bacterial population size.

These results are particularly interesting as the concentration of antibiotic in the inflow is assumed to be $\nu = 6 \times 10^7 \text{CFU l}^{-1}$. Baker et al. [38] report ν ranging between 2 and $6 \times 10^7 \text{CFU l}^{-1}$, similar to the concentrations found in sewage by Rheinthaler et al. [218]. Under the assumption that, as in the model, the total concentration *E. coli* in the slurry tank is close to the carrying capacity, and both μ_{TBX} and μ_{Mac} are less than $6 \times 10^7 \text{CFU l}^{-1}$, this implies that *E. coli* in the tank are not proliferating or thriving, but in fact decreasing in number within the slurry tank. This could be due to a decreased carrying capacity compared to bovine waste, competition with other organisms for nutrients or the slurry tank not providing optimum conditions for *E. coli* to grow.

MCMC was used to sample from the posterior distributions of μ_{Mac} and μ_{TBX}. Interestingly both algorithms converged to a single value, within one 10000th of

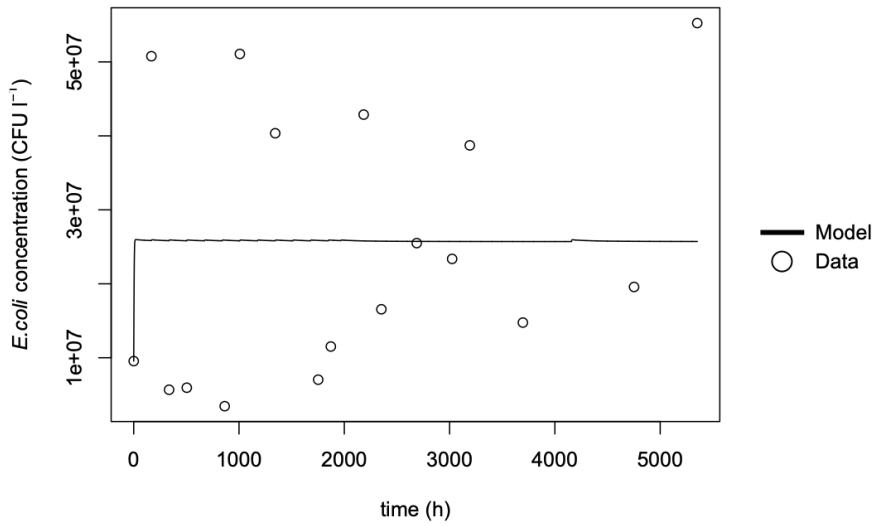


Figure 6.5: The concentration of bacteria predicted by the model using likelihood maximising μ_{TBX}, plotted against the presumptive counts of *E. coli* found on the TBX plates from [36]. The MLE value was calculated by maximising equation 6.23 using data from [36].

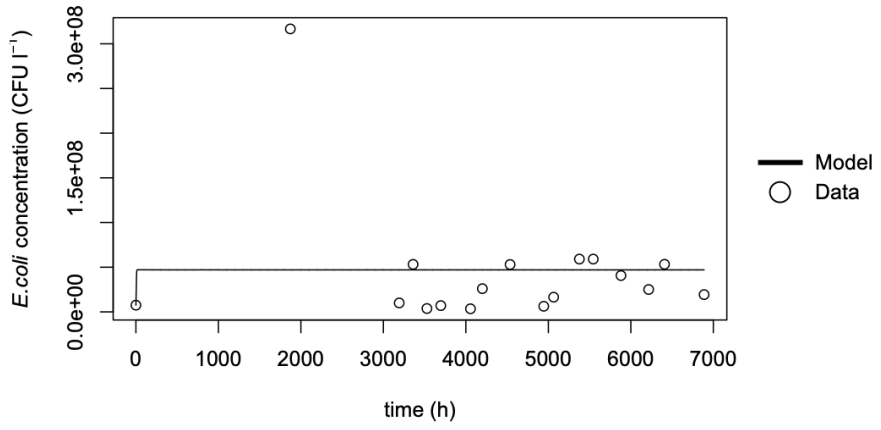


Figure 6.6: The concentration of bacteria predicted by the model using likelihood maximising μ_{Mac}, plotted against the presumptive counts of *E. coli* found on the MacConkey agar plates from [36]. The MLE value was calculated by maximising equation 6.24 using data from [36].

the MLE inferred values (2.6×10^7 for μ_{TBX} and 4.7×10^7 for μ_{Mac}). This is shown in Figures 6.7 and 6.8.

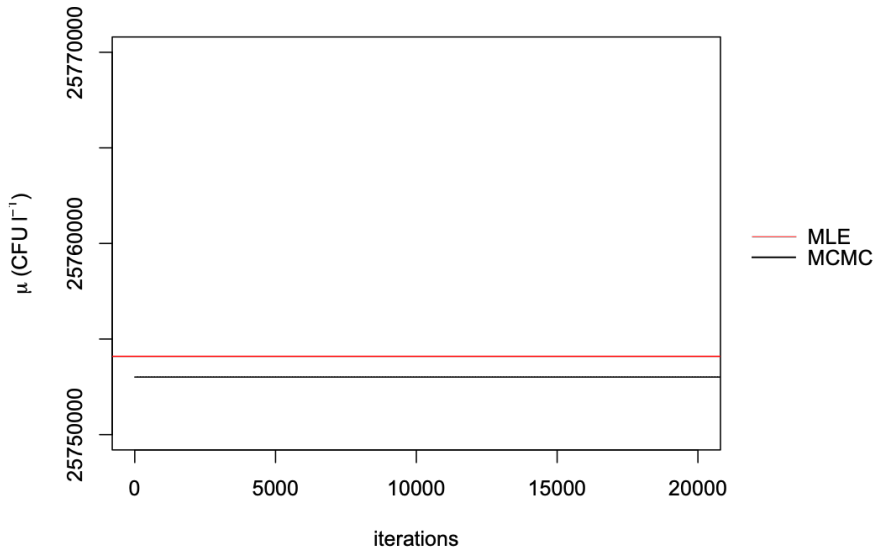


Figure 6.7: The likelihood maximising value of μ_{TBX}, plotted against the MCMC trace plot from the Metropolis Hastings algorithm. The MLE value was calculated by maximising equation 6.23 using data from [36]. The graph shows that the MLE value is relatively close to the MCMC value.

6.3.2 Estimation of the antibiotic parameters using the bacterial phenotype data

In theory, if the bacterial parameters from the literature are well chosen, it should be possible to infer the antibiotic concentrations from the phenotype data. Hence, as a test of the bacterial parameter values from the literature, the bacterial phenotype data was used to estimate the antibiotic parameters by setting $\theta = \{\theta_s, \theta_l, \gamma_s, \gamma_l\}$ and maximising the bacterial phenotype log-likelihood,

$$ll_B(\theta) = \log(4!) - \sum_{i=1}^{4} \log(y_{ti}!) + \sum_{i=1}^{4} y_{ti} \log(M_{ti}). \tag{6.37}$$

Some adjustments were made to the assumed minimum inhibitory concentrations, based on the concentration data from [37]. As oxytetracycline is the most prominent bacteriostatic antibiotic in the tank and according to the European Committee on Antimicrobial Susceptibility Testing (EUCAST) database has a lowest recorded MIC of 125 μ_g l^{-1}, and a highest recorded MIC of 64000 μ_g l^{-1} in *Listeria monocytogenes* (no data was available for *E. coli* in the database). How-

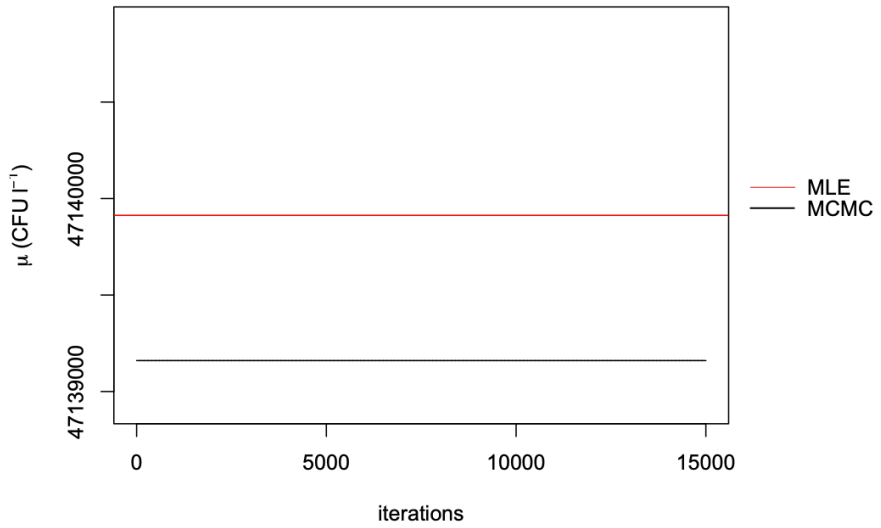


Figure 6.8: The likelihood maximising value of μ_{Mac}, plotted against the MCMC trace plot from the Metropolis Hastings algorithm. The MLE value was calculated by maximising equation 6.23 using data from [36]. The graph shows that the MLE value is relatively close to the MCMC value.

ever, the lowest recorded MIC for tetracycline (another antibiotic in the tetracycline family) in *E. coli* was also 125 μ_g l^{-1}. Therefore MIC_S was set to 125 μ_g l^{-1} and MIC_R was adjusted to 64000 μ_g l^{-1}. In the case of bacteriolytic antibiotics, the three found present were Cefquinome, Cefapirin and Trimethoprim (in combination with sulphonamides). Trimethoprim-sulfamethoxazole has a lowest recorded MIC of 2 μ_g l^{-1} (in *Listeria monocytogenes*) and a lowest recorded MIC in *E. coli* of 8 μ_g l^{-1}. EUCAST does not currently have data available for Cefquinome or Cefapirin, but The department for Environment Food and Rural Affairs (DEFRA) recorded MICs of Cefquinome between 8 and 2000 μ_g l^{-1} [38]. As trimethoprim was found to be present at the most time points in the antibiotic concentration data, MIC_l was set to 8 μ_g l^{-1}. Furthermore, the carrying capacity μ was set to 4.7×10^7, following the inference of μ_{TBX} and μ_{Mac}. The full set of parameters used to infer the antibiotic parameters is given in Table 6.9

The θ which maximised equation 6.38 was $\gamma_s = 1.015$ $\gamma_l = 2.089 \times 10^{-44}$ $\theta_s = 2.169 \times 10^7$ and $\theta_l = 8.358 \times 10^9$.

These values of θ_s, θ_l, γ_s and γ_l are far outside of the expected ranges discussed in the previous chapters and the literature. They imply very quick degradation of bacteriostatic antibiotic, almost no degradation of bacteriostatic antibiotic and a very large concentration of both types of antibiotic in the inflow. Figure 6.9 shows

Parameters being estimated

Parameter	Description	Initial Value	Reference
γ_s	Decay rate of bacteriostatic antibiotics	0.0029 h^{-1}	[38]
γ_l	Decay rate of bacteriolytic antibiotics	0.0029 h^{-1}	[38]
θ_s	Rate of bacteriostatic antibiotic inflow	1711 μg h^{-1}	[38]
θ_l	Rate of bacteriolytic antibiotic inflow	1711 μg h^{-1}	[38]

Fixed Parameters

Parameter	Description	Typical Value	Reference
r	Specific growth rate of *E. coli*	0.5 h^{-1}	[38]
β_s	Bacteriostatic-resistance gene transfer term	10^{-14} $lCFU^{-1}h^{-1}$	[38, 39, 123]
β_l	Bacteriolytic-resistance gene transfer term	10^{-14} $lCFU^{-1}h^{-1}$	[38, 39, 123]
β_u	MDR gene transfer term	10^{-14} $lCFU^{-1}h^{-1}$	[38, 39, 123]
λ	Rate of slurry inflow to tank	$613lh^{-1}$	[38]
ν	Concentration of bacteria in slurry inflow	6×10^7 CFU l^{-1}	[38, 218]
ρ_s	Proportion of bacteriostatic-resistant bacteria in inflow	0.2	[204]
ρ_l	Proportion of bacteriolytic-resistant bacteria in inflow	0.2	[204]
ρ_u	Proportion of multidrug-resistant bacteria in inflow	0.0	[204]
α_s	Bacteriostatic-resistance fitness cost as a fraction of r	0.1	[38, 50]
α_l	Bacteriolytic-resistance fitness cost as a fraction of r	0.1	[38, 50]
α_u	MDR fitness cost as a fraction of r	0.1	[38, 50]
V_1	Initial volume of slurry in the tank	150,000 l	[38]
MIC_R	MIC for bacteriostatic-resistant bacteria	64000 μg l^{-1}	EUCAST
MIC_s	MIC for bacteriostatic-sensitive bacteria	125 μg l^{-1}	EUCAST
MIC_l	MIC for bacteriolytic-sensitive bacteria	8 μg l^{-1}	DEFRA
E_{max}	Maximum effect of antibiotics on bacterial growth	2	[38, 39]
H	Hill coeficient in E_{max} model	2	[38, 39]
MIC_R	MIC for bacteriostatic-resistant bacteria	64000 μg l^{-1}	EUCAST
MIC_s	MIC for bacteriostatic-sensitive bacteria	125 μg l^{-1}	EUCAST
MIC_l	MIC for bacteriolytic-sensitive bacteria	8 μg l^{-1}	DEFRA
μ	Carrying capacity of liquid slurry	10^{10} CFU l^{-1}	[38]
MIC_R	MIC for bacteriostatic-resistant bacteria	64000 μg l^{-1}	EUCAST
MIC_s	MIC for bacteriostatic-sensitive bacteria	125 μg l^{-1}	EUCAST
MIC_l	MIC for bacteriolytic-sensitive bacteria	8 μg l^{-1}	DEFRA
δ_S	Natural death rate of susceptible bacteria	0.001 h^{-1}	[187]
δ_R	Natural death rate of resistant bacteria	0.001 h^{-1}	[187]
δ_l	Antibiotic driven death rate of bacteriolytic-susceptible bacteria	0.01 h^{-1}	[213]

Table 6.9: The parameter values used to estimate the antibiotic parameters using the bacterial phenotype data.

the fit of the model to the bacterial phenotype data, the mean squared error is 0.039. Qualitatively, the model predicts the proportions of each strain reasonably well over the time period, though the mean squared error higher than in some later approximations. However, these estimates of the bacterial parameters lead to a very poor fit with the antibiotic data (with a mean squared error of 8.9×10^{13}), see Figure 6.10. This indicates that there are other parameters in the antibiotic equations that are not well chosen in the case of the SB slurry tank and so need to be inferred.

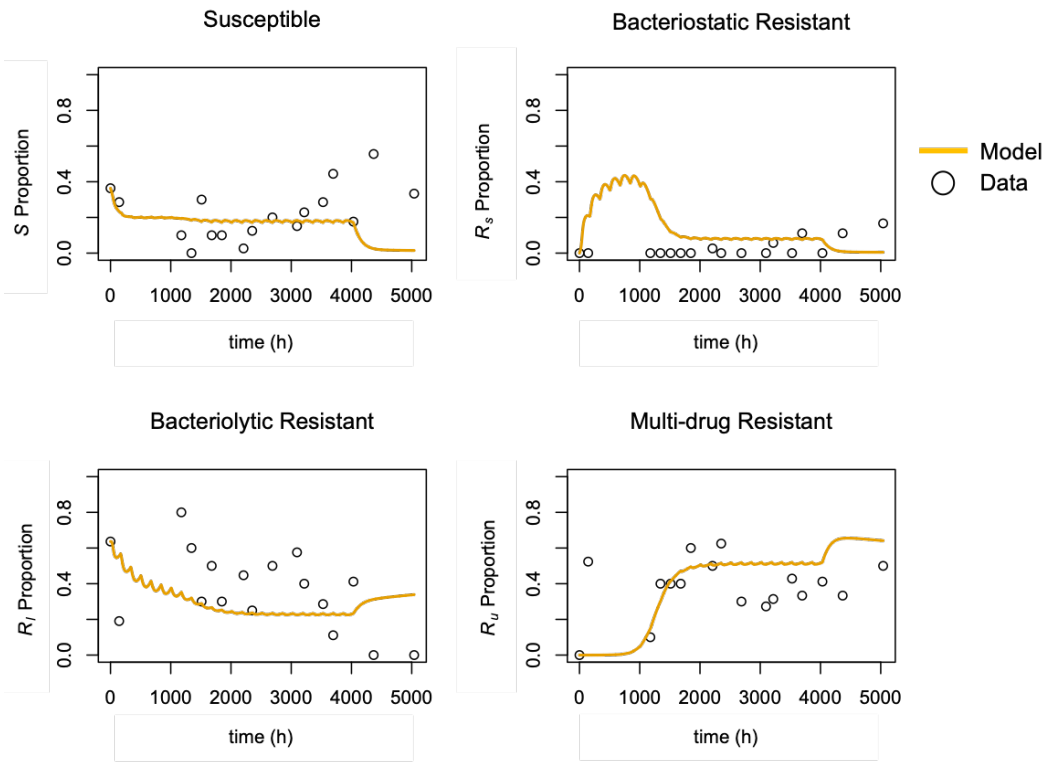


Figure 6.9: S, R_s, R_l and R_u proportion (lines) using θ_s, θ_l, γ_s and γ_l inferred from the bacterial phenotype data from [36] using MLE (equation 6.30), plotted against the bacterial phenotype data.

As the predictions here were so far from expected values, and the fits to both bacterial phenotype and antibiotic concentration data were so poor, an MCMC analysis was not performed. The parameters inferred in subsection 6.3 gave a much better fit for the antibiotic data and were much closer to the expected values of these parameters. This analysis indicates that the bacterial parameters from the literature do not match the processes occurring in the Sutton Bonington Slurry Tank, and that parameter estimation will also be important for the bacterial parameters.

In the following subsection the horizontal gene transfer parameters (β_s, β_l and β_u) are inferred using the bacterial phenotype data. The fixed model parameters

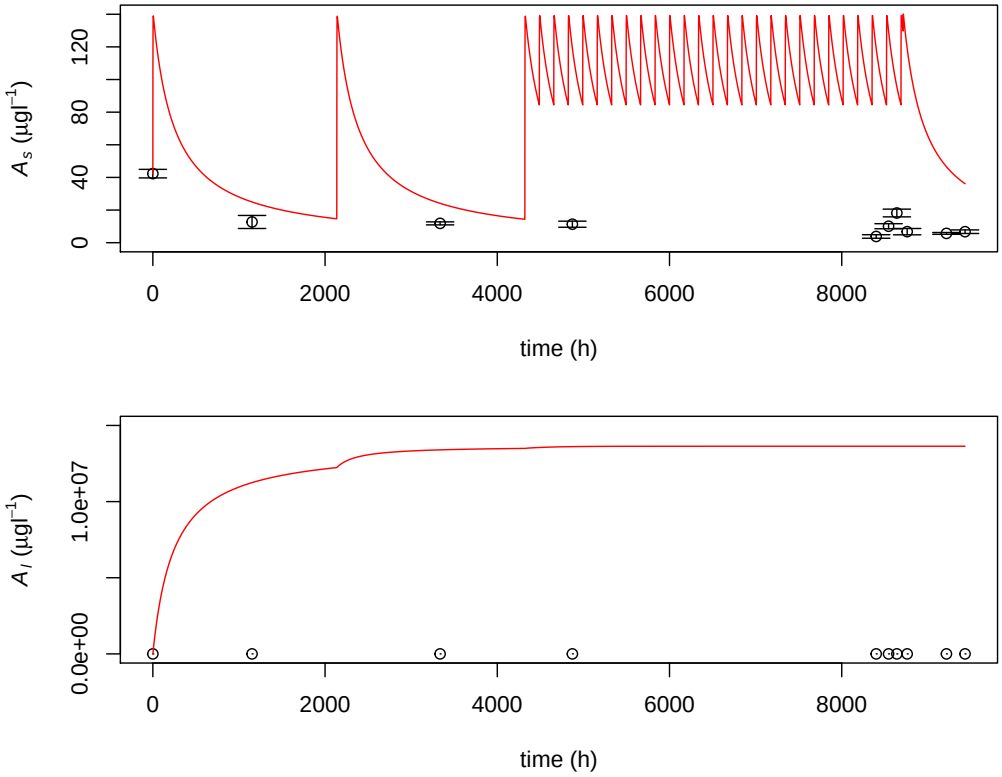


Figure 6.10: Graph of A_s and A_l using θ_s, θ_l, γ_s and γ_l inferred from the bacterial phenotype data from [36] using MLE (equation 6.30), plotted alongside the data collected by Baena Nogueras et al.

are taken both from the literature and from the previous inference done in this chapter.

6.3.3 Estimating the horizontal gene transfer parameters

As there are nearly 20 parameters which could be inferred, some choices need to be made as which ones should be the focus of the investigation. Parameters could be inferred in groups, β_s, β_l and β_u or δ_S, δ_R and δ_l, for example. Alternatively it might be possible to infer the parameters to which the model was shown to be most sensitive in the previous chapter, α_l, α_u and δ_R or to run new sensitivity analysis over the length of time that samples were collected for to determine which parameters make the most difference in the short term.

In this instance the parameters which were inferred were β_s, β_l and β_u, as Baker et al. found that the rate of horizontal gene transfer was one of the parameters their model was most sensitive to over a short time period. All other parameters in the model were fixed. These parameters were inferred both using the original parameters from the literature discussed in the previous chapter and with the likelihood maximising values of $\mu = 4.7 \times 10^7$, $\gamma_s = 1.115 \times 10^{-4}$, $\gamma_l = 6.494 \times 10^{-2}$, $\theta_s = 5.868 \times 10^3$ and $\theta_l = 1.367 \times 10^3$. In the latter case the MICs were also adjusted as discussed in subsection 6.3.2.

Inferring the parameters using literature parameter values

Initially the β parameters were inferred using only the parameter values drawn from the literature. These are shown in Table 6.10. As in the case of the antibiotics, simulated data sets were generated to see how well the likelihood maximising parameters were estimated. Data was generated by running the model with $\beta_s = \beta_l = \beta_u = 10^{-14}$, then drawing n samples from a multinomial distribution probabilities given by the proportions of S, R_s, R_l and R_u over a set number of data points. Both n and the number of data points were varied. The results of this test are shown in Table 6.11. In general, the estimated values were around the right order of magnitude, even in the low n, low data points cases.

The bacterial phenotype data was used to estimate the three horizontal gene transfer rates by setting $\theta_{\mathbf{B}} = \{\beta_s, \beta_l, \beta_u\}$ and maximising

$$ll_B(\theta_{\mathbf{B}}) = \log(n!) - \sum_{i=1}^{4} \log(y_{ti}!) + \sum_{i=1}^{4} y_{ti} \log(M_{ti}). \tag{6.38}$$

The value of $\theta_{\mathbf{B}}$ which maximised $ll_B(\theta_{\mathbf{B}})$ was ${\theta_{\mathbf{B}}}^* = \{\beta_s = 1.137 \times 10^{-12}, \beta_l =$

Parameters being estimated

Parameter	Description	Initial Value	Reference
β_s	Bacteriostatic-resistance gene transfer term	10^{-14} lCFU^{-1}h^{-1}	[38, 39, 123]
β_l	Bacteriolytic-resistance gene transfer term	10^{-14} lCFU^{-1}h^{-1}	[38, 39, 123]
β_u	MDR gene transfer term	10^{-14} lCFU^{-1}h^{-1}	[38, 39, 123]
Fixed Parameters			
Parameter	Description	Typical Value	Reference
r	Specific growth rate of *E. coli*	0.5 h^{-1}	[38]
λ	Rate of slurry inflow to tank	613lh^{-1}	[38]
ν	Concentration of bacteria in slurry inflow	6×10^7 CFU l^{-1}	[38, 218]
ρ_s	Proportion of bacteriostatic-resistant bacteria in inflow	0.2	[204]
ρ_l	Proportion of bacteriolytic-resistant bacteria in inflow	0.2	[204]
ρ_u	Proportion of multidrug-resistant bacteria in inflow	0.0	[204]
α_s	Bacteriostatic-resistance fitness cost as a fraction of r	0.1	[38, 50]
α_l	Bacteriolytic-resistance fitness cost as a fraction of r	0.1	[38, 50]
α_u	MDR fitness cost as a fraction of r	0.1	[38, 50]
V_1	Initial volume of slurry in the tank	150,000 l	[38]
θ_s	Rate of bacteriostatic antibiotic inflow	1711 μg h^{-1}	[38]
θ_l	Rate of bacteriolytic antibiotic inflow	1711 μg h^{-1}	[38]
E_{max}	Maximum effect of antibiotics on bacterial growth	2	[38, 39]
H	Hill coeficient in E_{max} model	2	[38, 39]
MIC_R	MIC for bacteriostatic-resistant bacteria	2000 μg l^{-1}	[38]
MIC_s	MIC for bacteriostatic-sensitive bacteria	8 μg l^{-1}	[173]
MIC_l	MIC for bacteriolytic-sensitive bacteria	4 μg l^{-1}	[173]
μ	Carrying capacity of liquid slurry	10^{10} CFU l^{-1}	[38]
γ_s	Decay rate of bacteriostatic antibiotics	0.0029 h^{-1}	[38]
γ_l	Decay rate of bacteriolytic antibiotics	0.0029 h^{-1}	[38]
δ_S	Natural death rate of susceptible bacteria	0.001 h^{-1}	[187]
δ_R	Natural death rate of resistant bacteria	0.001 h^{-1}	[187]
δ_l	Antibiotic driven death rate of bacteriolytic-susceptible bacteria	0.01 h^{-1}	[213]

Table 6.10: Parameter values used when inferring the β parameters from the bacterial phenotype data from [36].

$4.336 \times 10^{-61}, \beta_u = 3.528767 \times 10^{-25}\}$. Here β_s is within the range described by Reinthaler et al. [218] and β_l and β_u are very small, indicating almost no transfer of bacteriolytic or multi-drug resistant genes. The proportions of S, R_s, R_l and R_u are shown in Figure 6.11. The mean squared error between the data and the

n	data points	β_s	sd	β_l	sd	β_u	sd
100	101	1.71E-13	5.40E-13	1.47E-07	4.65E-07	7.61E-06	8.60E-06
100	101	1.23E-14	8.21E-15	8.15E-15	5.46E-15	8.69E-15	8.90E-15
50	101	1.10E-14	6.99E-15	8.39E-15	5.70E-15	1.29E-14	1.46E-14
25	101	5.56E-15	7.44E-15	1.27E-14	1.10E-14	2.17E-14	2.89E-14
10	101	6.25E-15	1.08E-14	1.04E-14	8.68E-15	3.92E-14	4.90E-14
5	101	1.96E-15	3.61E-15	1.79E-14	2.12E-14	2.54E-14	2.83E-14
100	21	6.34E-15	6.63E-15	1.14E-14	1.03E-14	1.61E-14	2.23E-14
50	21	9.36E-15	1.13E-14	1.58E-14	1.81E-14	7.65E-15	1.12E-14
25	21	7.69E-15	1.09E-15	1.71E-14	2.76E-14	2.40E-14	2.47E-14
10	21	4.10E-15	8.80E-15	7.96E-15	1.16E-14	3.20E-14	6.07E-14
5	21	8.94E-15	1.88E-14	2.61E-14	5.04E-14	3.29E-14	9.15E-14

Table 6.11: Parameter estimation for the horizontal gene transfer rates of bacteriostatic, bacteriolytic and multidrug resistance (β_s, β_l and β_u, respectively) using simulated data generated with the parameters in Table 6.10, with varying numbers of *E. coli* strains per sample, n, and varying total data points.

model is 0.041. Qualitatively, the model predicts the S proportion very poorly over the time frame, the predictions for R_s, R_l and R_u appear slightly better.

An MCMC Metropolis Hastings algorithm was run to predict the distributions of $\theta_{\mathbf{B}}$, the trace plots and histograms are shown in Figures 6.12 and 6.13, respectively. For β_s the likelihood maximising value sits near the mean of the distribution. For β_l and β_u both posterior distributions have a strong positive skew, with most values near to 0.

Inferring the β parameters using inferred antibiotic parameters

Unfortunately it was not possible to use the actual antibiotic concentrations when simulating the bacterial concentrations, as the sample dates did not match up. However, it was possible to estimate the rates of HGT by using the previously inferred parameters from the antibiotic concentration and microbial count data: $\mu = 4.7 \times 10^7$, $\gamma_s = 1.115 \times 10^{-4}$, $\gamma_l = 6.494 \times 10^{-2}$, $\theta_s = 5.868 \times 10^3$ and $\theta_l = 1.367 \times 10^3$. As these best describe the true to life system, as far as is known. The full set of parameters for these calculations is shown in Table 6.12.

Following the procedure outlined above, simulated data was generated with $\beta_s = \beta_l = \beta_u = 10^{-14}$. Using these simulated data sets, maximising the MLE led to unreliable estimates of the known parameters. In nearly all cases at least one parameter was estimated to be five orders of magnitude smaller than its known value. This analysis is shown in Table 6.13. This is possibly due to the optimisation algorithm finding a local maximum of equation 6.34, leading to a poor estimation of the parameters.

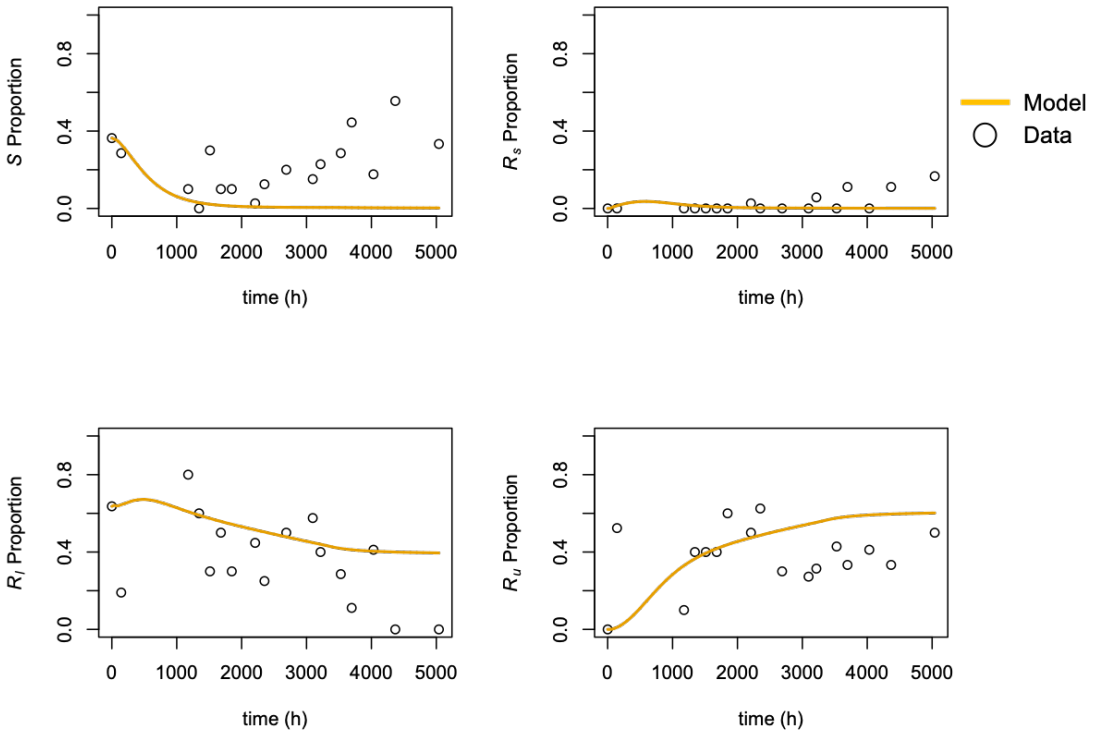


Figure 6.11: Predicted S, R_s, R_l and R_u proportion (lines) plotted alongside the bacterial phenotype data (points) from [36]. Here the horizontal gene transfer parameters are the likelihood maximising values (equation 6.34) of the horizontal gene transfer rates of bacteriostatic, bacteriolytic and multidrug resistance (β_s, β_l and β_u, respectively), using parameter values from Table 6.10.

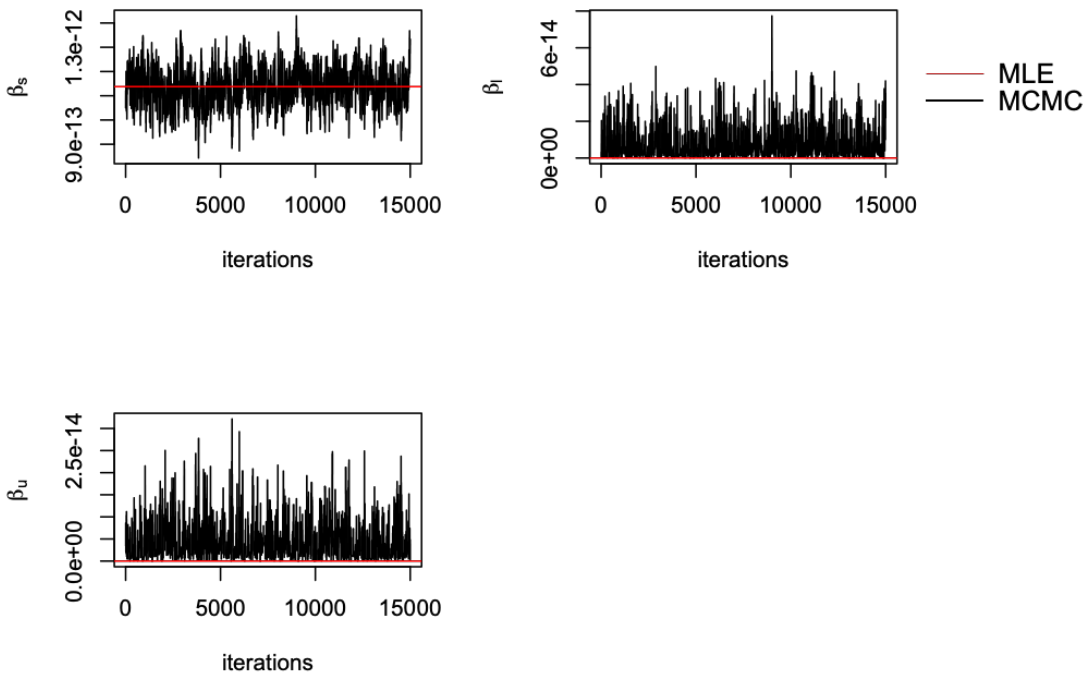


Figure 6.12: Trace plots of the β parameters generated using the original parameters, as in Table 6.10. These plots were generated using the Metropolis Hastings algorithm to infer the horizontal gene transfer rates of bacteriostatic, bacteriolytic and multidrug resistance (β_s, β_l and β_u, respectively) using the data from [36]. The MLE values were also calculated using the data from [36], by maximising equation 6.34.

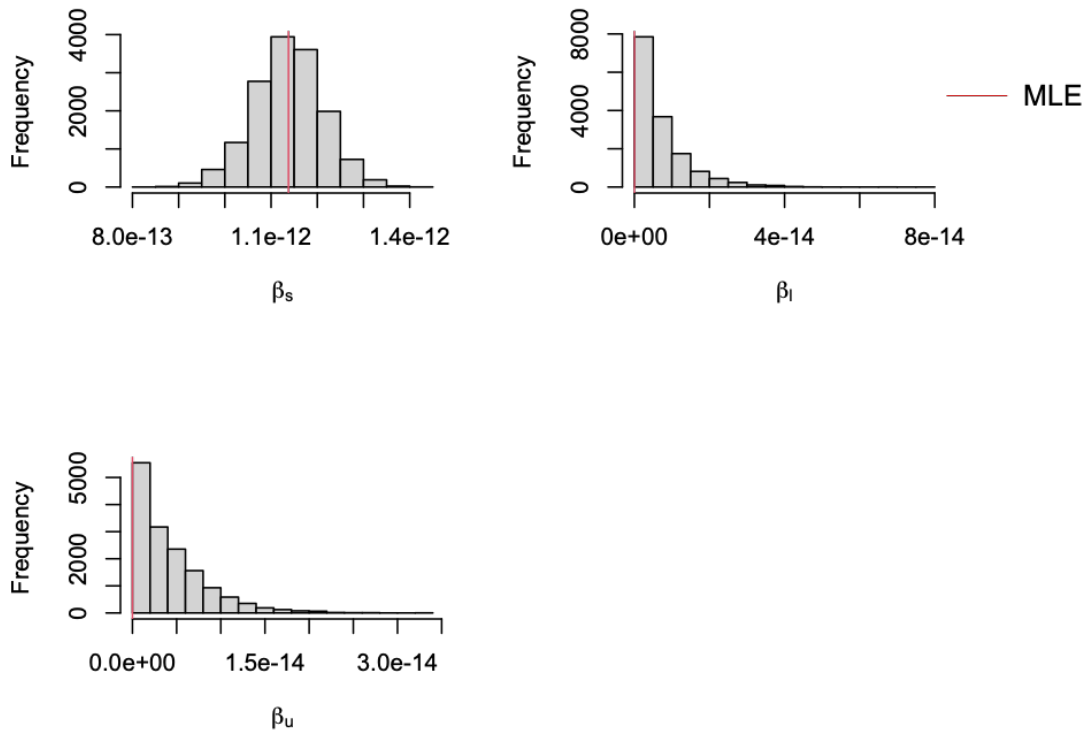


Figure 6.13: Histograms of the β parameters posterior distributions, generated using the original parameters as in Table 6.10. These plots were generated using the Metropolis Hastings algorithm to infer the horizontal gene transfer rates of bacteriostatic, bacteriolytic and multidrug resistance (β_s, β_l and β_u, respectively) using the data from [36]. The MLE values were also calculated using the data from [36], by maximising equation 6.34.

Parameters being estimated

Parameter	Description	Initial Value	Reference
β_s	Bacteriostatic-resistance gene transfer term	10^{-14} lCFU^{-1}h^{-1}	[38, 39, 123]
β_l	Bacteriolytic-resistance gene transfer term	10^{-14} lCFU^{-1}h^{-1}	[38, 39, 123]
β_u	MDR gene transfer term	10^{-14} lCFU^{-1}h^{-1}	[38, 39, 123]
Fixed Parameters			
Parameter	Description	Typical Value	Reference
r	Specific growth rate of *E. coli*	0.5 h^{-1}	[38]
λ	Rate of slurry inflow to tank	613lh^{-1}	[38]
ν	Concentration of bacteria in slurry inflow	6×10^7 CFU l^{-1}	[38, 218]
ρ_s	Proportion of bacteriostatic-resistant bacteria in inflow	0.2	[204]
ρ_l	Proportion of bacteriolytic-resistant bacteria in inflow	0.2	[204]
ρ_u	Proportion of multidrug-resistant bacteria in inflow	0.0	[204]
α_s	Bacteriostatic-resistance fitness cost as a fraction of r	0.1	[38, 50]
α_l	Bacteriolytic-resistance fitness cost as a fraction of r	0.1	[38, 50]
α_u	MDR fitness cost as a fraction of r	0.1	[38, 50]
V_1	Initial volume of slurry in the tank	150,000 l	[38]
θ_s	Rate of bacteriostatic antibiotic inflow	5.868×10^3 μg h^{-1}	Inference
θ_l	Rate of bacteriolytic antibiotic inflow	1.367×10^3 μg h^{-1}	Inference
E_{max}	Maximum effect of antibiotics on bacterial growth	2	[38, 39]
H	Hill coeficient in E_{max} model	2	[38, 39]
MIC_R	MIC for bacteriostatic-resistant bacteria	64000 μg l^{-1}	EUCAST
MIC_s	MIC for bacteriostatic-sensitive bacteria	125 μg l^{-1}	EUCAST
MIC_l	MIC for bacteriolytic-sensitive bacteria	8 μg l^{-1}	DEFRA
μ	Carrying capacity of liquid slurry	4.7×10^7 CFU l^{-1}	Inference
γ_s	Decay rate of bacteriostatic antibiotics	1.115×10^{-4} h^{-1}	Inference
γ_l	Decay rate of bacteriolytic antibiotics	6.494×10^{-2} h^{-1}	Inference
δ_S	Natural death rate of susceptible bacteria	0.001 h^{-1}	[187]
δ_R	Natural death rate of resistant bacteria	0.001 h^{-1}	[187]
δ_l	Antibiotic driven death rate of bacteriolytic-susceptible bacteria	0.01 h^{-1}	[213]

Table 6.12: Parameter values used based on inference from the previous sections, used to infer the horizontal gene transfer parameters β_s, β_l and β_u.

n	data points	β_s	sd	β_l	sd	β_u	sd
100	101	1.71E-20	5.40E-20	1.47E-14	4.65E-14	7.61E-13	8.60E-13
50	101	3.52E-14	1.11E-13	2.56E-27	7.78E-27	5.94E-12	1.66E-11
25	101	9.98E-27	1.55E-26	1.30E-26	1.67E-26	5.67E-13	8.21E-13
10	101	1.33E-22	4.20E-22	4.86E-24	1.53E-23	1.17E-11	2.32E-11
5	101	4.89E-21	1.03E-20	7.24E-21	1.53E-20	4.00E-11	2.13E-11
100	21	1.51E-28	3.88E-28	8.97E-27	1.46E-26	5.57E-12	1.67E-11
50	21	9.53E-16	3.01E-15	2.25E-20	7.10E-20	1.83E-11	3.17E-11
25	21	1.37E-19	4.32E-19	2.41E-13	7.63E-13	9.07E-11	2.25E-11
10	21	7.66E-13	2.42E-12	8.55E-13	1.84E-12	1.68E-11	2.50E-11
5	21	1.61E-18	3.34E-18	5.19E-12	9.04E-12	2.95E-11	3.14E-11

Table 6.13: Parameter estimation for the horizontal gene transfer rates of bacteriostatic, bacteriolytic and multidrug resistance (β_s, β_l and β_u, respectively) using simulated data generated with the parameters in Table 6.12, with varying numbers of *E. coli* strains per sample, n, and varying total data points.

Maxmising the likelihood using the real data leads to the predicted values of $\beta_s = 5.24 \times 10^{-10}$, $\beta_l = 5.334 \times 10^{-10}$ and $\beta_u = 8.155 \times 10^{-20}$ indicating approximately equal HGT of bacteriostatic and bacteriolytic resistance and very little multi-drug resistance. The model was simulated using these parameters and is shown alongside the phenotype data in Figure 6.14. The mean squared error between the data and the model is 0.035, an improvement compared to simulating the model with parameter values from the literature. Here the fit appears relatively good for the first 3-4 thousand hours of data, and then the model diverges from the data, especially in the case of S and R_l.

The Metropolis Hastings MCMC algorithm was used to determine the posterior distribution of the β parameters. The trace plots and histograms are shown in Figures 6.15 and 6.16, respectively, the likelihood maximising values are shown by the red line. The likelihood maximising value is only around the mean of the distribution in the case of β_l.

Taking the mean value of the posterior distributions gives $\theta_{\mathbf{MCMC}} = \{\beta_s = 1.465 \times 10^{-10}$, $\beta_l = 5.048 \times 10^{-10}$, $\beta_u = 5.410 \times 10^{-11}\}$. Calculating the MLE using these values gives $ll(\theta_{MCMC})$ = -111.9898, which is larger than $ll(\theta_{MLE})$ = -114.8328, indicating that the optimisation algorithm did indeed get stuck at a local maxima when calculating the MLE. The values in $\theta_{\mathbf{MCMC}}$ are all larger than those predicted in [123] by one order of magnitude. As Zhong et al.'s work was conducted *in vivo*, it may be possible that in the dairy slurry environment specifically, HGT occurs at faster rates. Interestingly, the predicted values of β_s and β_l are very similar, where β_u is an order of magnitude smaller, implying that the transfer of multi-drug resistance occurs more slowly. As, within the model, the conference of multi-drug resistance genes requires genetic material where both bacteriolytic and bacteriostatic resistance genes are present, this seems plausible.

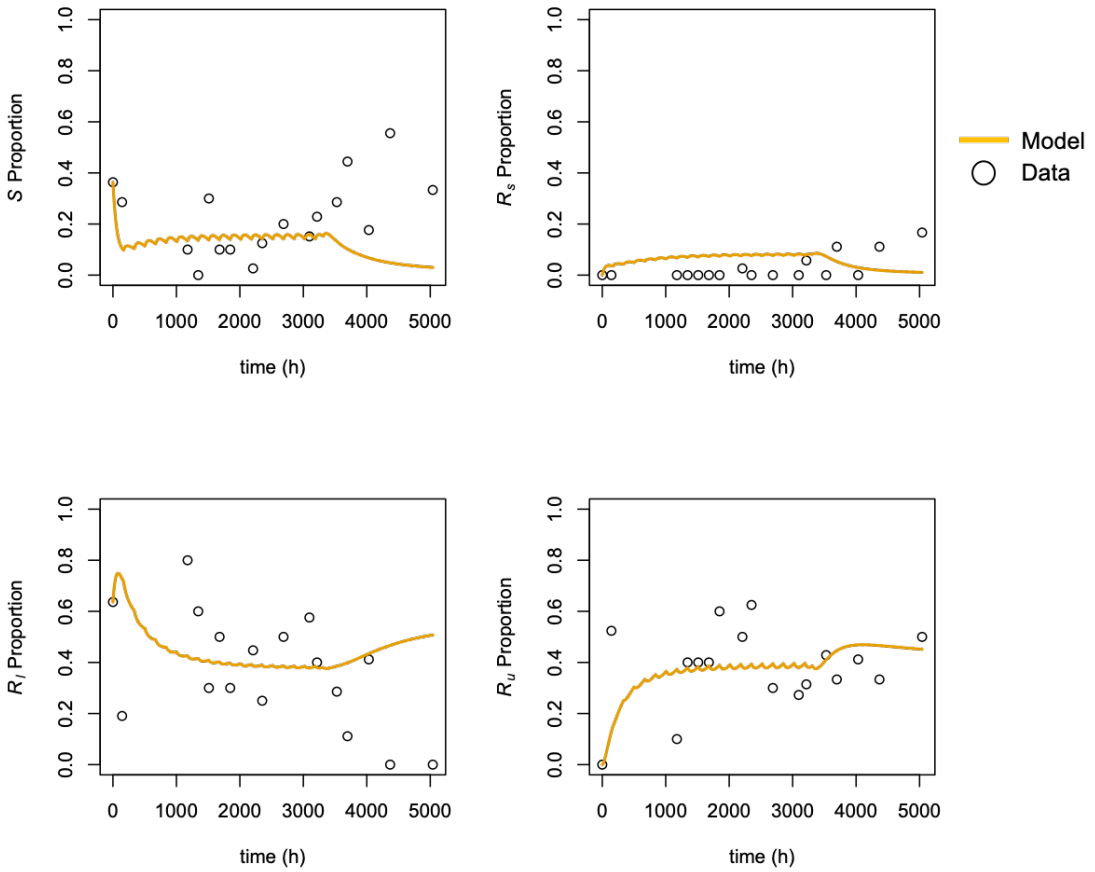


Figure 6.14: Predicted S, R_s, R_l and R_u proportion (lines) plotted alongside the bacterial phenotype data (points) from [36]. Here the horizontal gene transfer parameters are the likelihood maximising values (equation 6.34) of the horizontal gene transfer rates of bacteriostatic, bacteriolytic and multidrug resistance (β_s, β_l and β_u, respectively), using parameter values from Table 6.12.

The model was simulated using θ_{MCMC} and is shown alongside the phenotype data in Figure 6.17. The mean squared error between the data and the model is 0.033, an improvement compared to the model simulations shown in Figures 6.11 and 6.14. As before, the model appears to approximate the proportions of all bacterial strains relatively well for the first 3000 hours and, in this simulation, the fit has improved for R_l compared to Figure 6.14.

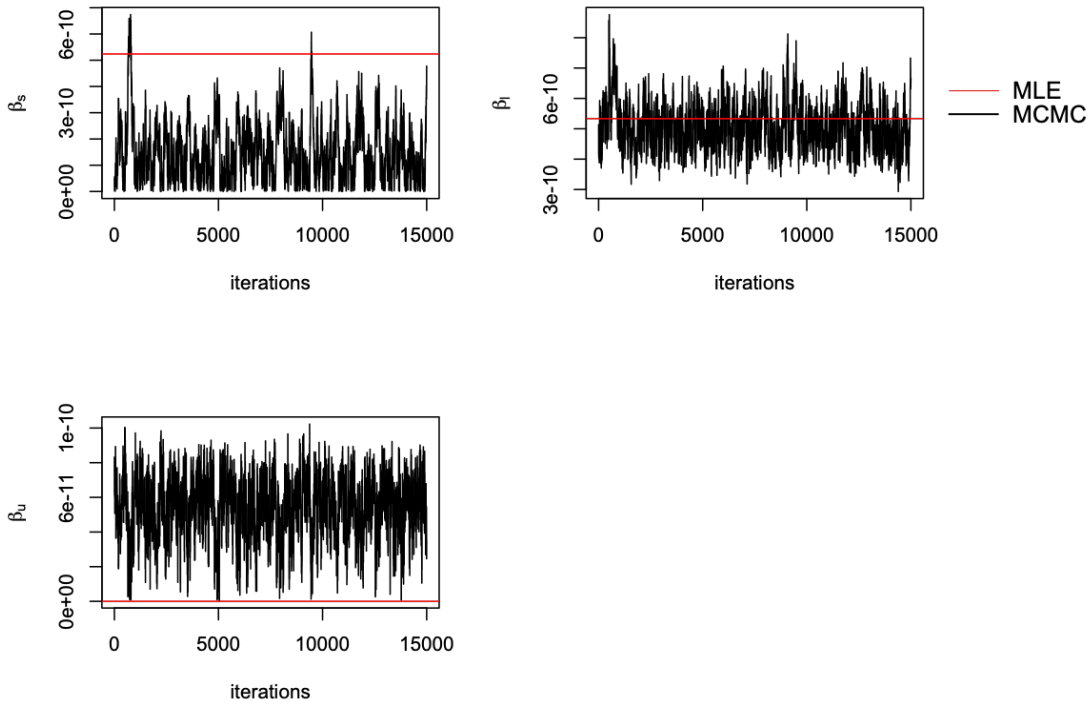


Figure 6.15: Trace plots of the β parameters generated using the original parameters, as in Table 6.12. These plots were generated using the Metropolis Hastings algorithm to infer the horizontal gene transfer rates of bacteriostatic, bacteriolytic and multidrug resistance (β_s, β_l and β_u, respectively) using the data from [36]. The MLE values were also calculated using the data from [36], by maximising equation 6.34.

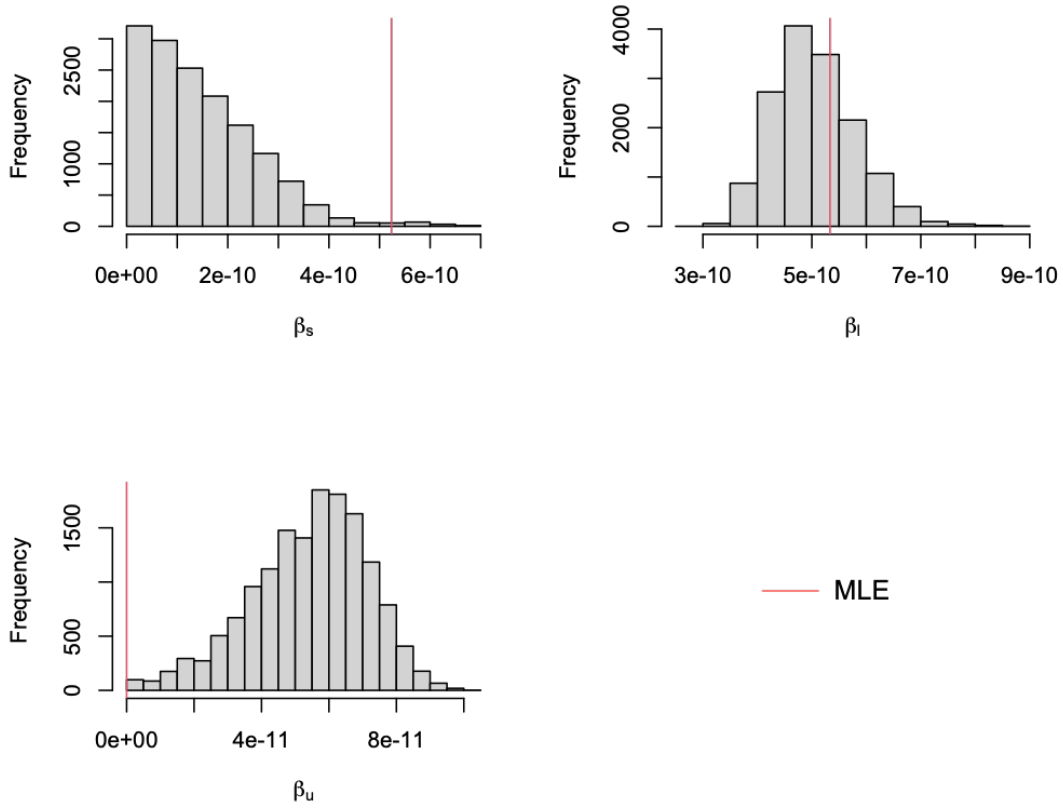


Figure 6.16: Histograms of of the β parameters generated using the original parameters, as in Table 6.12. These plots were generated using the Metropolis Hastings algorithm to infer the horizontal gene transfer rates of bacteriostatic, bacteriolytic and multidrug resistance (β_s, β_l and β_u, respectively) using the data from [36]. The MLE values were also calculated using the data from [36], by maximising equation 6.34.

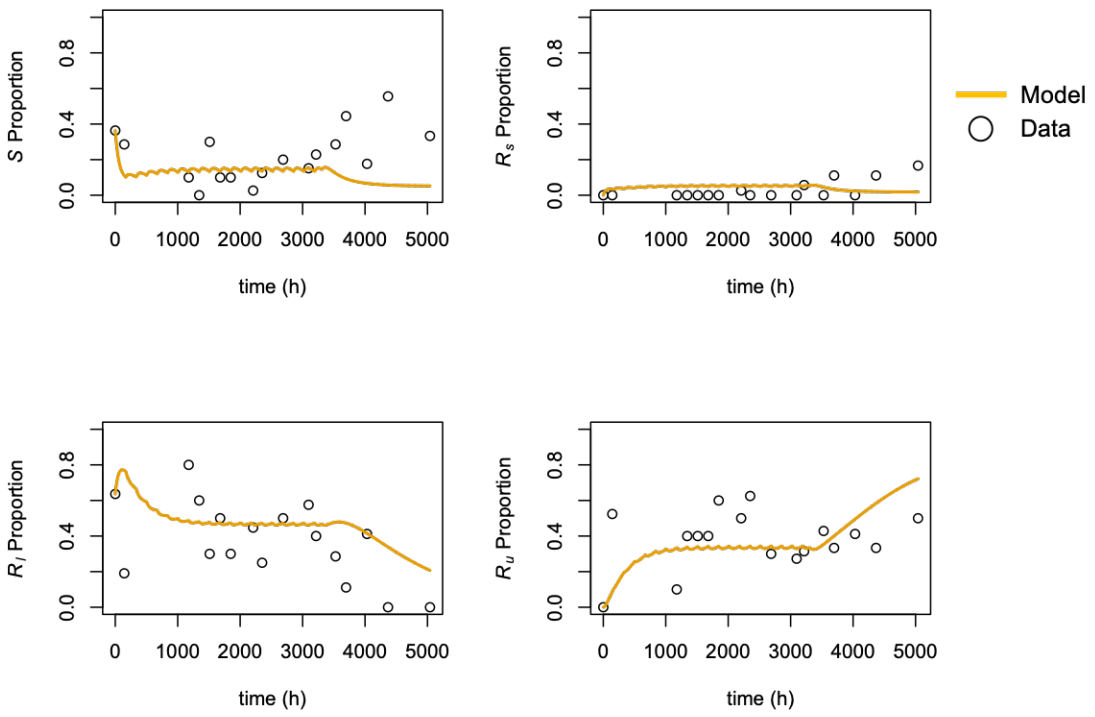


Figure 6.17: Predicted S, R_s, R_l and R_u proportion (lines) plotted alongside the bacterial phenotype data (points) from [36]. Here the horizontal gene transfer parameters are the means of the posterior distributions of the horizontal gene transfer rates of bacteriostatic, bacteriolytic and multidrug resistance (β_s, β_l and β_u, respectively), generated by the Metropolis Hasting algorithm, using parameter values from Table 6.12.

6.4 Summary

Maximum likelihood estimation and Bayesian inference were used to estimate parameters in the ODE model developed in chapter 5 using three data sets: microbial concentration, antibiotic concentration and bacterial phenotype. A summary of the results is shown in Table 6.14.

Target Parameters	Input data and parameter set	Simulated data results	Likelihood Maximising values and Posterior Ranges	Comment
μ	Microbial counts data Parameters from literature (ch 5)		$\mu_{Mac} = 4.7 \times 10^7$ $\mu_{TBX} = 2.6 \times 10^7$	Given the influent concentration of *E. coli* from Baker et al. ($\nu = 6 \times 10^6$) [38], this result implies that bacteria are not proliferating or thriving in the tank but in fact remaining steady or slightly decreasing.
θ_s, θ_l, γ_s, γ_l	Antibiotic Concentration data Parameters from literature (ch 5)	θ_s and γ_s well estimated, lower estimation quality of θ_l and γ_l	$\gamma_s = 1.115 \times 10^{-4}$ Range: $0-5\times10^{-4}$ $\gamma_l = 6.494 \times 10^{-2}$ Range: $0 - 0.10$ $\theta_s = 5.868 \times 10^3$ Range: $5000-7000$ $\theta_l = 1.367 \times 10^3$ Range: $0 - 7000$	γ_s is same order of magnitude as the degradation rate of Oxytetracycline [252], order of magnitude lower than in [23]. γ_l, in line with the results reported by Baena Nogueras et al.. θ_s and θ_l within the same order of magnitude as values proposed by Baker et al.
	Bacterial Phenotype Data Parameters from literature (ch 5)		$\theta_s = 1.015$ $\theta_l = 2.089 \times 10^{-44}$ $\gamma_s = 2.169 \times 10^7$ $\gamma_l = 8.358 \times 10^9$	θ_s, θ_l, γ_s and γ_l outside expected range. Implies very quick degradation of bacteriostatic antibiotic, almost no degradation of bacteriostatic antibiotic and a very large concentration of both types of antibiotic in the inflow. No MCMC calculation performed.
β_s, β_l, β_u	Bacterial phenotype data Parameters from literature (ch 5)	Estimated values at right order of magnitude even in low n, low data case	$\beta_s = 1.137 \times 10^{-12}$ Range: $8 \times 10^{-13} - 1.5 \times 10^{-12}$ $\beta_l = 4.336 \times 10^{-61}$ Range: $0 - 1.5 \times 8^{-14}$ $\beta_u = 3.529 \times 10^{-25}$ Range: $0 - 1.5 \times 3^{-14}$	β_s in line with results from [123]. β_l and β_u very small, indicating little transfer of bacteriolytic or multi-drug resistant genes. Fit is relatively good for all strains except for S.
	Bacterial phenotype data Parameters from literature (ch 5), μ, θ_s, θ_l, γ_s and γ_l inferred from counts data and AB conc data	Unreliable estimates due to possible local minimum	$\beta_s = 5.24 \times 10^{-10}$ Range: $0 - 7 \times 10^{-10}$ $\beta_l = 5.334 \times 10^{-10}$ Range: $2 \times 10^{-10} - 9 \times 10^{-10}$ $\beta_u = 8.155 \times 10^{-20}$ Range: $0 - 10 \times 10^{-11}$ e	Approximately equal HGT of bacteriostatic and bacteriolytic resistance and very little multi-drug resistance fit is relatively good for the first 3-4 thousand hours of data, and then the model diverges from the data. Taking mean of posterior distributions leads to higher MLE, indicating local max found during optimisation algorithm.

Table 6.14: Summary table of parameter estimation results.

The microbial concentration data from EVAL-FARMS was used to estimate μ, the carrying capacity of *E. coli* in liquid slurry. The value proposed in [38] was $\mu = 1\times10^{10}$CFU l^{-1}, which is based on the assumption that the carrying capacity will not inhibit bacterial dynamics. The concentrations of *E. coli* found in the slurry tank ranged between approximately 3×10^6 and 6×10^7 CFU l^{-1}. This

variation is possibly due to the makeup of the slurry in the influent changing over time. Maximum likelihood estimation predicted $\mu_{Mac} = 2.6 \times 10^7$ and $\mu_{TBX} = 4.7 \times 10^7$. Both of these results, and in fact the highest recorded concentration of slurry are less than the presumed inflow concentration, $\nu = 6 \times 10^7$CFU l^{-1}. If correct, this indicates that *E. coli* communities are not thriving within the slurry tank, but are remaining at similar concentrations as in the influent, or slightly decreasing. Maule [216] reports that *E. coli* O157 (a toxin producing strain of *E. coli*) survives less well in cattle slurry than in solid faeces. This could explain the slight decrease in the *E. coli* population modelled here. To test the theory, slurry samples could be collected at the point of entry to the tank and analysed for *E. coli* concentration. It is possible that the functional carrying capacity for *E. coli* changes as the makeup of the influent changes or depending on weather, as such the constant capacity used in the model is used as a best estimate, rather than as indicative of the real time changes in the tank.

Four antibiotic parameters were estimated, the decay rates of the two antibiotics, θ_s and θ_l and the the rates of antibiotic inflow into the tank θ_s and θ_l using time series data of antibiotic concentration in the tank. Bacteriostatic antibiotics were found to persist for longer and at higher concentrations in the tank. This is not particularly surprising as the antibiotic found at highest concentration in the slurry tank was the bacteriostatic antibiotic oxytetracycline, which is known to have a relatively long half-life in bovine manure [23]. On the other hand, veterinary bacteriolytic antibiotics such as the penicillins and cephalosporins have been shown by Baena-Nogueras et al. [37] to have much shorter half-lives in dairy slurry, which would explain why they are often found at much lower concentrations in the tank. The estimated parameters could be confirmed by testing antibiotic concentrations at the point of entry to the slurry tank.

The bacterial phenotype data was used to estimate the three rates of horizontal gene transfer, β_s, β_l and β_u. Using typical parameter conditions (as discussed in chapter 5) the predicted values indicated almost no transfer of genetic material conferring either bacteriolytic or multidrug resistance. This may be possible, given the low concentration of bacteriolytic antibiotic in the slurry tank, but didn't lead to a very good fit of the model to the data. On the other hand, using the previously inferred values of μ_{Mac}, θ_s, θ_l, γ_s and γ_l, then taking the mean of the resultant posterior distributions for β_s, β_l and β_u led to a better fit to the data. In this case the inferred parameters are outside the range predicted by Zhong et al. [123], but this could be due to the slurry medium. Alternatively, it might not be the gene transfer parameters that are driving the development of the *E. coli* population in the slurry tank over this timescale.

Though all four of the key parameters in the antibiotics equations were in-

ferred, there are over twenty parameters in the bacterial equations. A small number of these were selected to avoid overfitting. However, many of the parameter values are unknown or have not been recorded in the slurry environment. Alongside data collection to determine some of the unknown parameters, it may be useful to attempt to infer other bacterial model parameters to determine whether they offer a better fit to the data.

Another limitation of this work is that, alongside the large parameter space, there were relatively few data points in each of the data sets (less than twenty in each case). The use of simulated data indicated that, especially in the case of the antibiotic parameters, as the number of data points decreased, so did the quality of the inference. Furthermore, the data was not concurrent, with only around two months overlap between the antibiotic concentration data and the bacterial phenotype data. Meaning that the inferred antibiotic values may not match the antibiotic concentration during the time at which the bacterial phenotype data was collected.

A small scale study utilising a facsimile of a slurry tank which was able to fix certain parameters (for example influent antibiotic and bacterial concentrations and influent flow rate), could lead to better estimation of other parameters of interest. This could then be used to better model the real-world slurry tank system.

Chapter 7

Modelling the effects of sorption on antimicrobial resistance

The slurry tank at Bonington has a capacity of 3 million litres, a fairly common size for slurry tanks (see Chapter 3). Though the tank has a rotary mixer affixed to the wall, when the level of slurry in the tank is relatively low, a sump of deposited solids is visible. This indicates that the slurry is not well mixed. This prompts the development of two temporospatial models of AMR in the slurry tank. In this chapter, solids settling and sorption dynamics are incorporated into the model and the spread of AMR is allowed to vary in the vertical direction.

Up to now the models of AMR in the slurry tank have assumed that slurry is well mixed and have ignored suspended solids and particulate matter within the tank. The presence of bovine faeces, footbath contents and waste bedding will contribute to the existence of suspended solids within the slurry. These solids will then settle within the tank, antibiotics and heavy metals may sorb to the settling solids which will affect the bioavailability of the antimicrobials. A mathematical model of the prevalence and spread of AMR in the slurry tank which incorporates antimicrobial sorption and solid settling could give a greater insight into the dynamics within the slurry tank.

In general, models of solid settling and sedimentation use a one-dimensional layered approach to solve the equations for solid concentration [40, 254–256], which can be discontinuous [256]. The model selected to simulate settling in the slurry tank is the Takács model [40], which divides the settling vessel into 10 layers. At the inflow of the tank, antibiotics, bacteria and solids flow in, and the contents of the tank flow out from an outflow pipe at the bottom of the tank. In each layer it is assumed that antibiotics can sorb to the solids and that bacteria interact with each other and the antibiotics. Figure 7.2 shows the interactions between bacteria, antibiotics and settling solids in the tank. In this chapter, as in previous chapters, the bacterial population in question is *E. coli*,

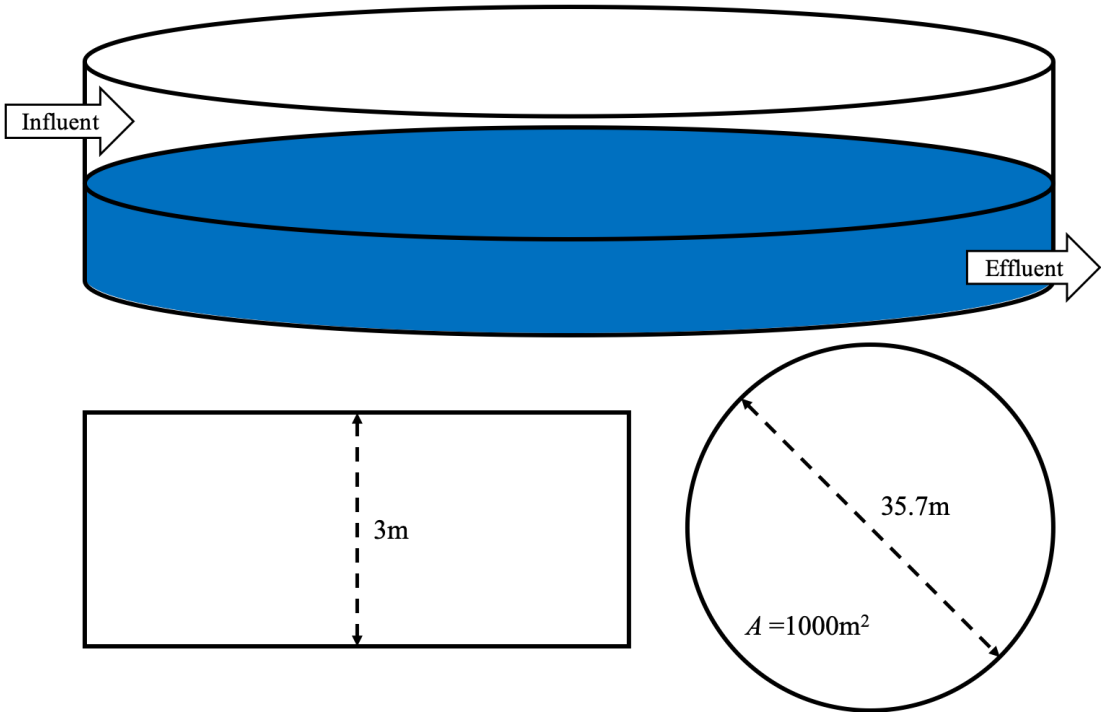


Figure 7.1: A simple schematic of a cylindrical slurry tank with a capacity of three-million litres (not to scale). These dimensions replicate the slurry tank at Sutton Bonington but could be adjust to model other commercially available cylindrical slurry tanks [253].

established via parameterisation. Slurry flows downwards in the tank from the inlet to the outlet and antibiotics, bacteria and solids are drawn downwards in the flow. Additionally, solids in each layer are settling due to gravity.

There are various models of antibiotic sorption in soils [257, 258], activated sludge [259] and marine sediments [260]. Commonly used models include the linear model and the Freudlich model. The linear model is given by

$$C_W = K_d C_S, \tag{7.1}$$

where C_W is the equilibrium mass of sorbed antibiotic per gram of solid, K_d is the partition coefficient and C_S is the equilibrium concentration of antibiotic in the liquid phase. The Freudlich model is given by

$$C_W = K_f C_S^n, \tag{7.2}$$

where C_W and C_S are as before, K_f is a measure of sorption strength and n is an indicator of sorption linearity [260], with $n = 1$ indicating a linear relationship. Similarly, bacterial sorption to solids has been measured using linear isotherms and also using first order kinetics within ODEs [261]. Roberts et al. used a similar approach to model bacterial binding to wound tissue [139].

To test the effects of sorption on the model outputs, the model was simulated with parameters from the literature, parameters inferred in chapter 6 and a one way sensitivity analysis was performed.

The features, events and processes that are included and omitted in the model presented in this chapter are shown in Table 7.1.

7.1 Methods

To model the settling dynamics in the tank, a modified version of the Takács settling model was designed and simulated. Antibiotics were modelled using ordinary differential equations and the proportion of antibiotics which sorbed to solids was calculated using partition coefficients. The prevalence and spread of AMR bacteria was modelled using differential equations based on a discretised advection-diffusion reaction system and the ODE model discussed in chapter 5. The Takács model [40] was selected as it is relatively simple to simulate and is used as part of the benchmark model of wastewater treatment plants, as determined by the IWA Task Group on Benchmarking of Control Strategies for Wastewater Treatment Plants [262]. The Takács model does suffer from some mathematical inconsistencies, which are discussed later in this chapter. The model is also modified slightly, to account for the design of the slurry tank. At the time of writing, it appears that there are no models of dairy slurry sedimentation and settling.

7.1.1 Modified Takács Settling Model

In wastewater treatment and engineering there are generally considered to be four types of settling [40]:

- Type 1: Discrete settling.
- Type 2: Flocculent settling.
- Type 3: Hindered or zone settling
- Type 4: Compression settling

Discrete settling is the settling of particles that settle individually with no flocculating (clumping) between particles and very little particle interaction as they settle, for example: sand in a dilute suspension. Flocculent settling describes particles in dilute suspension which clump together (flocculate), causing them to settle at increasing velocities as they grow in mass. At intermediate concentrations the forces between particles can impede the rate of settling of neighbouring

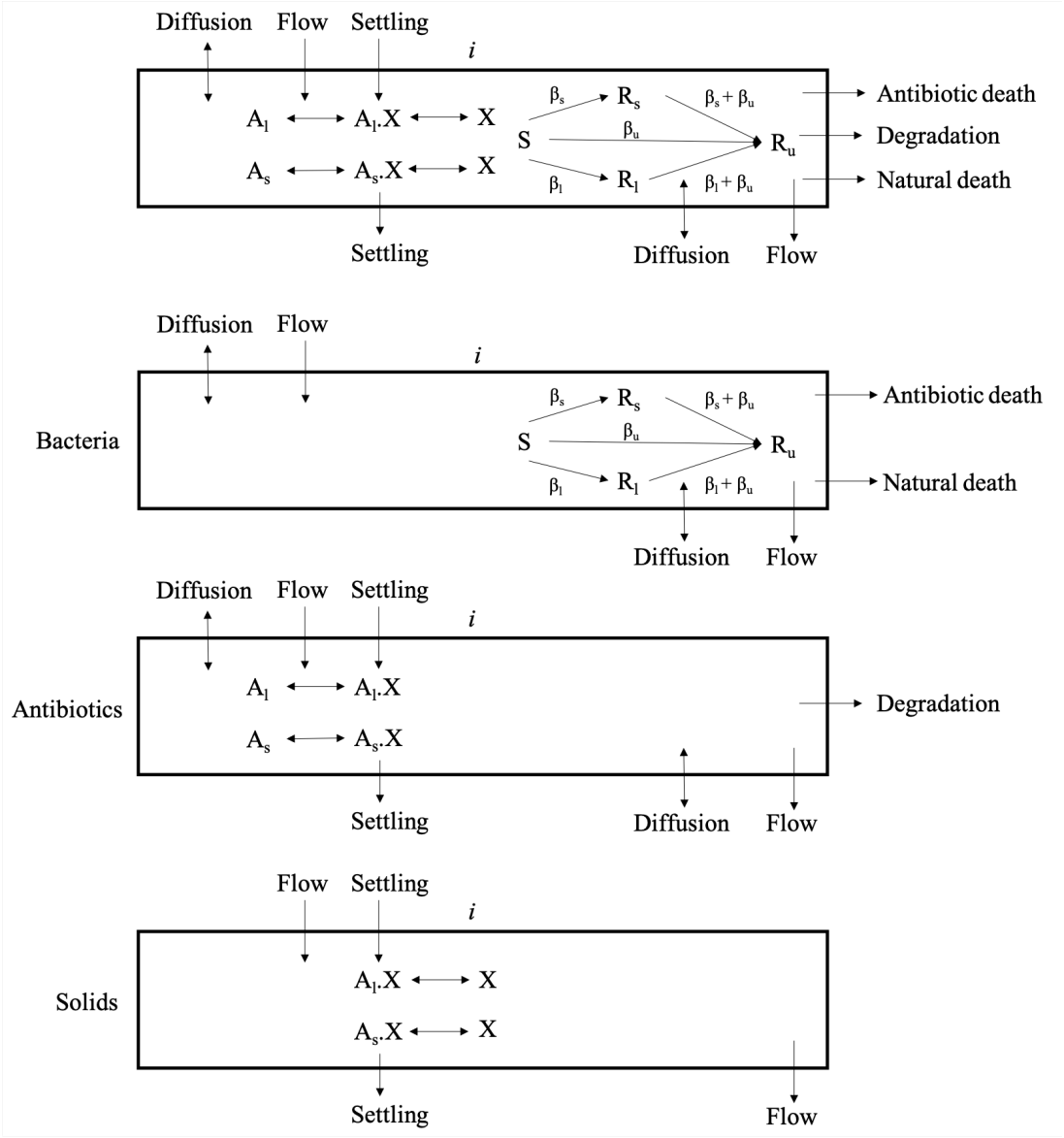


Figure 7.2: Tank interactions schematic at layer i. Here X is suspended solids, A_s and A_l are bacteriostatic and bacteriolytic antibiotics, respectively; S, R_s, R_l and R_u are susceptible, bacteriostatic-resistant, bacteriolytic-resistant and multidrug-resistant *E. coli*, respectively; and β_s, β_l and β_u are the horizontal gene transfer rates for bacteriostatic-resistance, bacteriolytic-resistance and multidrug-resistance, respectively. Here a dot indicates sorption of a substance to the settling solids. For example $As.X$ indicates bacteriostatic antibiotic sorbed to solids.

Features

Included	Omitted
Tank	
Height	Diameter (homogenous in x and y dimensions)
Volume	
Material (non-reactive)	
Influent	
Bovine manure and faeces	Heavy metals (simplicity)
Bacteria (*E. coli* as sentinel organism)	Other biocides (simplicity)
Antibiotics (bacteriostatic and bacteriolytic)	Rain water (assumed that tank is covered)
Suspended and settling solids	Parlour washings (simplicity)
Effluent	

Events

Included	Omitted
Filling (constant)	
Emptying (constant)	
	Mixing (substances are distributed by fluid flow)
	Cleaning (rare based on results from chapter 3)

Processes

Included	Omitted
Bacteriolytic antibiotics and bacteria	
Bacteriostatic antibiotics and bacteria	
Horizontal gene transfer	
Sorption (to settling solids)	
Solid settling	
Antibiotic degradation	
Bacterial growth and death	
	Temperature effects (evidence that temperature does not affect *E. coli* in slurry [188])
	Seasonality (emptying and filling are constant)
Fluid flow (driven by tank inlet and outlet)	

Table 7.1: A summary of the features, processes and events which are included and omitted in the settling model presented in this chapter, based on the conceptual model described in Chapter 4.

partners, this is zone-settling. At high concentrations particles are in constant contact with one and another, thus settling occurs via the compression of the mass of particles as more particles are added to the system. The four types of settling can occur simultaneously in a single system as settling occurs and the particle concentration increases.

Slurry tank influent likely contains both small, non-flocculating particles such as sand bedding and also larger flocculant particles such as bovine manure. Therefore a model needed to be chosen which accounts for both discrete and flocculent settling dynamics.

The continuity equation for solid flux [263] is given by:

$$\frac{\partial X}{\partial t} + \frac{\partial F}{\partial z} = 0 \tag{7.3}$$

where X is the solid concentration and F is the flux.

The Takács model [40] describes the solid-liquid separation process in wastewater plant clarifiers. Wastewater enters the clarifier at a feed-layer. Low solids concentration effluent is then extracted from the top of the clarifier and high solids concentration wastewater is removed from the bottom of the clarifier, effluent extraction drives fluid flow throughout the system. The solids concentration in the tank is then determined by advective flux due to fluid flow and settling flux due to gravity. To simulate the model, the clarifier is separated into 10 distinct layers and the settling velocity of each layer is described using a double exponential modified Vesilind equation, which accounts for both unhindered and hindered settling:

$$v_{s,i} = v_0 \exp(-r_h(X_i - X_{min})) - v_0 \exp(-r_p(X_i - X_{min})), \tag{7.4}$$

$$0 \leq v_{s,i} \leq v_0', \tag{7.5}$$

where $v_{s,i}$ is the velocity of the solids in layer i. Here v_0 is the maximum theoretical settling velocity and v_0' is the maximum realistic settling velocity; r_p and r_h are Takács settling parameters associated with settling of low-concentration, slow settling components and with hindered settling components, respectively; X_i is the concentration of solids in layer i; $X_{min} = f_{ns}X_{in}$, is the minimum possible suspended solids concentration in the effluent, calculated using influent concentration of solids, X_{in}, and the non-settleable fraction f_{ns}. The first exponential term describes the settling of larger flocculating particles in the hindered settling zone, and second term is used to adjust the velocity to account for the slower settling of small particles.

From a modelling perspective, the system described by the Takács model

differs from the slurry tank in two major ways; generally the inflow to the slurry tank is at the top of the system, and no effluent is extracted from the top of the tank. Therefore the model was adjusted to account for these differences. The tank is divided into n equal layers and the feed layer is assumed to be the top layer of the tank (see Figure 7.3). Following Takács et al., the model equations are given by:

$$Z\frac{dX_1}{dt} = \frac{Q_{in}X_{in}}{A} - v_{dn}X_1 - J_{s,1}, \tag{7.6}$$

$$Z\frac{dX_i}{dt} = v_{dn}(X_{i-1} - X_i) + J_{s,i-1} - J_{s,i}, \text{ for } i = 1 : n-1 \tag{7.7}$$

$$Z\frac{dX_n}{dt} = v_{dn}(X_{n-1} - X_n) + J_{s,n-1}, \tag{7.8}$$

where X_i is the suspended solids concentration in layer i, Z is the depth of each layer, Q_{in} is the influent flow rate, A is the surface area of the tank, $v_{dn} = Q_{in}/A$ is the downwards fluid velocity and $J_{s,i}$ is the solid flux due to settling.

It can be shown that the Takács model approximates equation 7.3. Consider the continuum limits of equations 7.6 to 7.8 as $n \to \infty$ and $Z \to 0$. Using the approximation $X_i = X(z,t)$, where z is the vertical coordinate, and similarly $J_i = J(z,t)$, $X_{i\pm1} = X(z \pm Z, t)$ and $J_{i\pm1} = J(z \pm Z, t)$. Using standard Taylor expansions $X(z \pm Z, t)$ and $J(z \pm Z, t)$ can be written as

$$X(z \pm Z, t) = X(z,t) \pm ZX'(z,t) + \mathcal{O}(Z^2) \tag{7.9}$$

and, similarly,

$$J(z \pm Z) = J(z,t) \pm ZJ'(z,t) \pm \mathcal{O}(Z^2). \tag{7.10}$$

Substituting equations (7.9) and (7.10) in equation (7.7) gives

$$Z\frac{\partial X}{\partial t} = v_{dn}(X(z,t) - ZX'(z,t) - X(z,t)) + J(z,t) - ZJ'(z,t) - J(z,t) + \mathcal{O}(Z^2) \tag{7.11}$$

$$= Z(v_{dn}X'(z,t) - J'(z,t)) + \mathcal{O}(Z^2). \tag{7.12}$$

Dividing both sides through by Z and taking the limit as $Z \to 0$ gives

$$\frac{\partial X}{\partial t} = -\frac{\partial X}{\partial z} - \frac{\partial J}{\partial z}. \tag{7.13}$$

In the case of the layers at the boundaries of the ($i = 1$ and $i = n$) a similar process can be applied. As X_{in} represents the inflow of solids into layer 1 via bulk movement, it can be interpreted as X_0. Given that there is no settling into layer 1, $J(z-Z,t) = 0$; using the Taylor expansion this gives $J(z,t) = ZJ'(z,t)+(O)(Z^2)$.

Combining this with $Q_{in}/A = v_{dn}$, equation (7.6) can be rewritten as

$$Z\frac{\partial X}{\partial t} = v_{dn}(X(z,t) - ZX'(z,t) - X(z,t)) - ZJ'(z) + (O)(Z^2) \tag{7.14}$$

$$= Z(v_{dn}X'(z,t) - J'(z,t)) + \mathcal{O}(Z^2), \tag{7.15}$$

which, as before, tends to equation (7.13) as $Z \to 0$. At layer n there is no settling into layer $n+1$, so $J(z,t) = 0$. Therefore, from the Taylor expansion, $J_{n-1} = J(z - Z, t) = -ZJ'(z,t) \pm \mathcal{O}(Z^2)$. Substituting this into equation (7.8) at layer n we have

$$Z\frac{\partial X}{\partial t} = Z(v_{dn}X'(z,t) - J'(z,t)) + \mathcal{O}(Z^2) \tag{7.16}$$

which, once again, tends to equation (7.13) as $Z \to 0$. As $v_{dn}X(z,t)$ describes the bulk movement flux of solids and $J(z,t)$ describes the flux of solids due to settling, $v_{dn}X(z,t) + J(z,t) = F(z,t)$, where F is the total flux, and equation (7.13) is clearly the same as the continuity equation shown in equation (7.3).

Following Takács *et al.* [40], $J_{s,i}$ is defined as:

$$J_{s,i} = \max\{\min(v_{s,i}X_i, v_{s,i+1}X_{i+1}), 0\} \tag{7.17}$$

where $v_{s,i}$ is once again given by:

$$v_{s,i} = v_0 \exp(-r_h(X_i - X_{min})) - v_0 \exp(-r_p(X_i - X_{min})) \tag{7.18}$$

$$0 \leq v_{s,i} \leq v_0'. \tag{7.19}$$

Here equation (7.17) is the Stenstrom flux constraint, which is based on the assumption that the settling mass flux into layer i cannot exceed the flux that layer i is capable of transferring to layer $i+1$ [256, 264].

There are some downsides to using the modified Takács model with a fixed layer volume to represent the slurry tank. It requires the assumption that the filling and emptying of the tank is simultaneous, to maintain the volume of slurry in each layer. A future model could incorporate varying layer volume or increasing and decreasing layer numbers as the tank fills and empties. Many of the parameters need to be experimentally determined, which there has not been the opportunity to do in this case. Furthermore, ten layers is a relatively coarse discretisation of the tank. Another downside is that the model parameterisation is very system-sensitive, as shown by the model fitting performed by Takács *et al.* [40]. As the Takács parameters for the dairy slurry tank system are unknown, parameters were chosen based on those used by Takács *et al.* [40] and Abusam

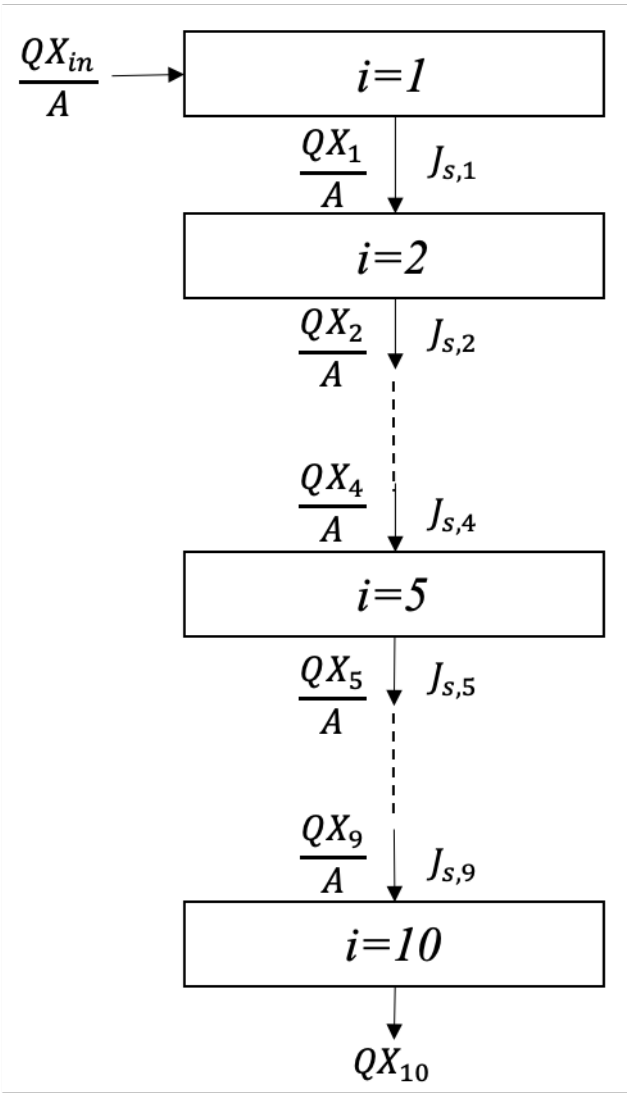


Figure 7.3: Tank settling schematic. Here Q is the influent flow rate of slurry, X_{in} is the concentration of solids in the influent, A is the cross-sectional area of each layer and $J_{s,i}$ is the settling flux of solids from layer i to layer $i+1$.

and Keesman [255]: $r_p = 4.3\times10^{-3}\text{m}^3\text{g}^{-1}$, $r_h = 4.6\times10^{-4}\text{m}^3\text{g}^{-1}$, $f_{ns} = 2.5\times10^{-3}$, $v_0 = 712\ \text{md}^{-1}$ and $v_0' = 340\ \text{md}^{-1}$. Definitions for these parameters are given in table 7.2. Both Takács *et al.* [40] and Abusam and Keesman [255]'s parameters are tuned for sludge in secondary clarifiers, so how accurate these parameters are to the slurry system is hard to determine. Later in the chapter, these parameters were varied during sensitivity analysis to determine their effects on the model.

Slurry enters the tank at a rate of 0.613 m^3h^{-1}, based on the calculations in [38], the tank is assumed to have a capacity of 3000m^2 (or three-million litres), with sides 3m tall. As part of the EVAL-FARMS project [36], The Food Water Waste group at Nottingham recorded total suspended solids (TSS) concentrations between 17760 gm^{-3} and 52300 gm^{-3} in the tank. Drawing on this X_{in} was set to 30000gm^{-3}. The full set of parameter values and their definitions is shown in

table 7.2

Parameter	Description	Typical Value	Reference
A	Surface area of the tank	1000 m^2	3000 m^3 tank
Z	Height of the tank	3 m	3000 m^3 tank
Q_{in}	Influent flow rate to the tank	14.712 m^3d^{-1}	[38]
v_{dn}	Downward fluid velocity in the tank	1.4712×10^{-2} m^3d^{-1}	Q_{in}/A
X_{in}	Influent suspended solids concentration	$30000gm^{-3}$	[36]
X_{min}	Minimum suspended solids concentration in effluent	$f_{ns} \times X_{in}$ gm^{-3}	[40]
X_i	Suspended solids concentration in layer i	gm^{-3}	[40]
f_{ns}	Non-settleable fraction of influent suspended solids	2.5×10^{-3}	[40]
r_p	Takács settling parameter for low concentration and slow settling components in suspenstion	$4.3 \times 10^{-3}m^3g^{-1}$	[255]
r_h	Takács settling parameter for low concentration and slow settling components in suspension	$4.6 \times 10^{-4}m^3g^{-1}$	[255]
v_0	Maximum theoretical settling velocity	712 md^{-1}	[40]
v_0'	Maximum practical settling velocity	340 md^{-1}	[40]

Table 7.2: Typical parameter values used for the modified Takács settling model, given by equations 7.6 to 7.8.

7.1.2 Antibiotic Modelling

Modelling the available antibiotic concentration throughout the tank required modelling the sorption of antibiotic to the settling solids. One option is to include the adsorption and desorption explicitly within the model. The other is to assume that adsorption and desorption are at equilibrium and calculate the proportion of biologically available antibiotic at any one time, using either partition coefficients or adsorption isotherms, as discussed in Chapter 2. The antibiotics also undergo degradation, move across layers by diffusion and move by bulk fluid flow. The antibiotic equations are based on a spatial discretisation of the advection-diffusion-reaction equation in one dimension:

$$\frac{\partial R}{\partial t} = D_R \nabla^2 R - \mathbf{u} \cdot \nabla R + F_R, \tag{7.20}$$

where R is the concentration of some substance of interest, D_R is the diffusion coefficient of R, $\mathbf{u}$ is the velocity field and F_R is the reaction term.

After discretisation, following the model developed by Baker et al. [38] and In the case where there was no sorption the equations for an antibiotic are given

by:

$$\frac{dA_1}{dt} = -\gamma A_1 - \frac{v_{dn}}{Z}(A_1 - A_{in}) + \frac{D_A}{Z^2}(A_2 - A_1) \tag{7.21}$$

$$\frac{dA_i}{dt} = -\gamma A_i - v_{dn}\frac{A_i - A_{i-1}}{Z} + \frac{D_A}{Z^2}(A_{i+1} - 2A_i + A_{i-1}), \text{ for } i = 2:9 \tag{7.22}$$

$$\frac{dA_{10}}{dt} = -\gamma A_{10} - v_{dn}\frac{A_{10} - A_9}{Z} + \frac{D_A}{Z^2}(A_9 - A_{10}) \tag{7.23}$$

where A_i is the concentration of antibiotic in layer i, θ is the concentration of antibiotic in the influent, γ is the degradation rate of the antibiotic and D_A is the diffusion coefficient for this antibiotic.

The chosen approach for modelling the sorption of bacteriostatic and bacteriolytic antibiotics (A_s and A_l) respectively is to use the partition coefficient, K_d ($\mathrm{m^3 g^{-1}}$). The K_d describes the equilibrium ratio of chemical concentration in the solid phase C_S (mg/kg) to chemical concentration in the liquid phase C_W ($\mathrm{mg/m^3}$) so that

$$K_d = \frac{C_S}{C_W}. \tag{7.24}$$

If the total concentration of a chemical, C_{tot}, is known the K_d can be used to determine the available fraction, f_a [74]. Using $C_{tot} = C_W + C_S X$, where X ($\mathrm{g/m^3}$) is the concentration of solids obtained using equations 7.6 to 7.8,

$$f_a = \frac{C_W}{C_{tot}} = \frac{C_W}{C_W + C_S X} = \frac{1}{1 + X C_S / C_W} = \frac{1}{1 + K_d X}. \tag{7.25}$$

Let A_{si}^f and A_{li}^f denote the available concentrations of bacteriostatic and bacteriolytic antibiotic in layer i, respectively, and K_{ds} and K_{dl} be the partition coefficients of bacteriostatic and bacteriolytic antibiotic. Then

$$A_{si}^f = \frac{A_{si}}{1 + K_{ds} X_i} \tag{7.26}$$

and

$$A_{li}^f = \frac{A_{li}}{1 + K_{dl} X_i} \tag{7.27}$$

where A_{si} and A_{li} are the total concentrations of antibiotics in layer i, calculated using equations (7.21) to (7.23). Though no studies have been done to determine the partition coefficient of veterinary antibiotics in dairy farm slurry, studies have been done to determine the K_d of antibiotics in pig manure [74, 265, 266] and in soils and manure attenuated soils [258, 267–272]. Loke et al. [74] reported the K_d of oxytetracycline in swine manure as 8.317×10^{-5} $\mathrm{m^3\ g^{-1}}$, as oxytetracycline made up the majority of bacteriostatic antibiotics found in the Sutton Bonington slurry tank [37], this is used as the proposed value of K_{ds}. Though the action

of trimethoprim is bacteriostatic, in combination with sulphonamides it is bacteriolytic, and in the SB slurry tank it was only found when sulphonamides were also present, therefore the value of K_{dl} is set to 8.63×10^{-6} m^3 g^{-1}, following the value reported by Zhang et al. [272] for the K_d of trimethoprim in wastewater treatment plant effluent, which they also found to be similar to its K_d in soils. The full set of parameter values for the modelling of antibiotics is shown in Table 7.3.

7.1.3 Bacterial equations

As before, the bacterial dynamics are described by the advection-diffusion-reaction equation (see equation (8.15)), discretised across the layers of the tank, resulting in 40 coupled ODEs, for susceptible, bacteriostatic resistant, bacteriolytic resistant and multi-drug resistant bacteria.

$$\frac{dB_1}{dt} = Q_{in}\frac{B_{in}}{V} - v_{dn}\frac{B_1}{Z} + \frac{D_B}{Z^2}(B_2 - B_1) + G_{B_1} \tag{7.28}$$

$$\frac{dB_i}{dt} = -v_{dn}\frac{B_i - B_{i-1}}{Z} + \frac{D_B}{Z^2}(B_{i+1} - 2B_i + B_{i-1}) + G_{B_i}, \text{ for } i = 2:9 \tag{7.29}$$

$$\frac{dB_{10}}{dt} = -v_{dn}\frac{B_{10} - B_9}{Z} + \frac{D_B}{Z^2}(B_9 - B_{10}) + G_{B_{10}} \tag{7.30}$$

where $B = \{S,\ R_s,\ R_l,\ R_u\}$, the concentrations of susceptible, bacteriostatic resistant, bacteriolytic resistant and multidrug resistant bacteria, respectively, the subscript i refers to the concentration of each strain of bacteria in layer i and the subscript in refers to the influent concentration; D_B is the diffusion coefficient of the bacteria. Here G_{B_i} represents the bacterial reaction terms in layer i. These are based on those from the model described in chapter 5 and are given by

$$G_{S_i} = r\left(1 - \frac{N}{\mu}\right)E_{S_i}S_i - S_i(\beta_s R_{si} + \beta_l R_{li} + \beta_u R_{ui}) - \delta_S S_i - \delta_l S_i \frac{A_{li}^f}{MIC_l + A_{li}^f}, \tag{7.31}$$

$$G_{R_{si}} = r(1-\alpha_s)\left(1 - \frac{N}{\mu}\right)E_{R_i}R_{si} + R_{si}(\beta_s S_i - \beta_l R_{li} - \beta_u R_{ui}) - \delta_R R_{si} - \delta_l R_{si}\frac{A_{li}^f}{MIC_l + A_{li}^f}, \tag{7.32}$$

$$G_{R_{li}} = r(1-\alpha_l)\left(1 - \frac{N}{\mu}\right)E_S R_{li} + R_{li}(-\beta_s R_{si} + \beta_l S_i - \beta_u R_{ui}) - \delta_R R_{l_i} \tag{7.33}$$

and

$$G_{R_{ui}} = r(1-\alpha_u)\left(1 - \frac{N}{\mu}\right)E_R R_{ui} + R_{si}R_{li}(\beta_s + \beta_l) + \beta_u R_{ui}(S_i + R_{si} + R_{li}) - \delta_R R_{ui}, \tag{7.34}$$

where

$$E_{S_i} = 1 - \frac{E_{max} A_{si}^{fH}}{MIC_S^H + A_{si}^{fH}} \tag{7.35}$$

$$E_R = 1 - \frac{E_{max} A_{si}^{fH}}{MIC_R^H + A_{si}^{fH}}. \tag{7.36}$$

These dynamics are based on the model presented in chapter 5, and describe the growth, horizontal gene transfer and death of a population of bacteria in the presence of bacteriolytic and bacteriostatic antibiotic. Parameter definitions and typical values are shown in Table 7.3.

Determining antibiotic and bacterial diffusion coefficients in slurry (D_A and D_B, respectively) was difficult, as little prior research has been done into the diffusive properties of antibiotics and bacteria in dairy slurry. Therefore, diffusion coefficient values from other media were chosen to approximate the model system. Soriano et al. [273] calculated the diffusion coefficients of five veterinary antibiotics in water at infinite dilution (a state of very low solute concentration) and reported a range of $0.84 \times 10^{-8} - 1.2 \times 10^{-8} \mathrm{m^2 s^{-1}}$. Though the antibiotic diffusion coefficient is likely different in slurry, $D_A = 1 \times 10^{-8} \mathrm{m^2 s^{-1}} = 3.6 \times 10^{-5} \mathrm{m^2 h^{-1}}$ was chosen as an initial estimate. In the case of *E. coli*, "diffusion" is interpreted as a measure of cell motility as an artefact of the cell's brownian motion, or the "random motility coefficient" (RMC) [274]. Ford et al. [275, 276] predict a RMC of $1.1 - 1.5 \times 10^{-5} \mathrm{cm^2 s^{-1}}$ in vitro. In their model of bacteria spread in water, Zhang uses a RMC value of $8.3 \times 10^{-6} \mathrm{cm^2 s^{-1}}$ [277]. Phillips and Quinn [278] report values between $1 \times 10^{-7}$and$1.9 \times 10^{-4} \mathrm{cm^2 s^{-1}}$ for four different strains of *E. coli* swimming in vitro. Wu et al. [279] determine RMC values for three different strains of *E. coli* ranging between $2 \times 10^{-8} \mathrm{cm^2 s^{-1}}$ and $4.6 \times 10^{-6} \mathrm{cm^2 s^{-1}}$ for cells swimming in a suspension medium. Using this data a diffusion coefficient of $D_A = 2 \times 10^{-5} \mathrm{cm^2 s^{-1}} = 7.2 \times 10^{-6} \mathrm{m^2 h^{-1}}$, so bacterial "diffusion" occurs at an order of magnitude slower than antibiotic diffusion.

7.2 Results

The modified settling model was simulated over 50000 hours (approximately 5.8 years) to give an approximation of a tank a few years into its working life. Figure 7.4 shows the concentration of solids at the end of the simulation. Layers 1, 2, 3 and 4 have TSS concentrations of around 77 $\mathrm{gm^{-3}}$, there is then a steep increase at layer 5 which has a TSS concentration of 17610 $\mathrm{gm^{-3}}$, increasing to 29730 $\mathrm{gm^{-3}}$

Parameter	Description	Typical Value	Reference
r	Specific growth rate of *E. coli*	0.5 h^{-1}	[38]
β_s	Bacteriostatic-resistance gene transfer term	10^{-17} $m^3CFU^{-1}h^{-1}$	[38, 39, 123]
β_l	Bacteriolytic-resistance gene transfer term	10^{-17} $m^3CFU^{-1}h^{-1}$	[38, 39, 123]
β_u	MDR gene transfer term	10^{-17} $m^3CFU^{-1}h^{-1}$	[38, 39, 123]
S_{in}	Concentration of susceptible bacteria in inflow	3.6×10^9 $CFU^{-1}m^{-3}$	[38, 204, 218]
R_{sin}	Concentration of bacteriostatic-resistant bacteria in inflow	1.2×10^9 $CFU^{-1}m^{-3}$	[38, 204, 218]
R_{lin}	Concentration of bacteriolytic-resistant bacteria in inflow	1.2×10^9 $CFU^{-1}m^{-3}$	[38, 204, 218]
R_{uin}	Concentration of multidrug-resistant bacteria in inflow	0 $CFU^{-1}m^{-3}$	[38, 204, 218]
α_s	Bacteriostatic-resistance fitness cost as a fraction of r	0.1	[38, 50]
α_l	Bacteriolytic-resistance fitness cost as a fraction of r	0.1	[38, 50]
α_u	MDR fitness cost as a fraction of r	0.1	[38, 50]
$A_{s_{in}}$	Influent concentration of bacteriostatic antibiotic	2.79 mg $m^{-3}h^{-1}$	[38]
$A_{l_{in}}$	Influent concentration of bacteriolytic antibiotic	2.79 mg $m^{-3}h^{-1}$	[38]
E_{max}	Maximum effect of antibiotics on bacterial growth	2	[38, 39]
H	Hill coeficient in E_{max} model	2	[38, 39]
MIC_R	MIC for bacteriostatic-resistant bacteria	2000 mg m^{-3}	[38]
MIC_S	MIC for bacteriostatic-sensitive bacteria	8 mg m^{-3}	[38]
MIC_l	MIC for bacteriolytic-sensitive bacteria	4 mg m^{-3}	[38]
μ	Carrying capacity of liquid slurry	10^{13} CFU m^{-3}	[38]
γ_s	Decay rate of bacteriostatic antibiotics	0.0029 h^{-1}	[38]
γ_l	Decay rate of bacteriolytic antibiotics	0.0029 h^{-1}	[38]
δ_S	Natural death rate of susceptible bacteria	0.001 h^{-1}	[187]
δ_R	Natural death rate of resistant bacteria	0.001 h^{-1}	[187]
δ_l	Antibiotic driven death rate of bacteriolytic-susceptible bacteria	0.01 h^{-1}	[213]
D_A	Antibiotic diffusion coefficient	3.6×10^{-5} m^2 h^{-1}	[273]
D_B	Bacteria diffusion coefficient	7.2×10^{-6} m^2 h^{-1}	
K_{ds}	Bacteriostatic antibiotic partition coefficient	8.317×10^{-5} m^3 g^{-1}	
K_{dl}	Bacteriolytic antibiotic partition coefficient	8.63×10^{-6} m^3 g^{-1}	

Table 7.3: Typical parameter values used for the antibiotics and bacterial equations in the settling model (equations 7.21 to 7.23 and equations 7.28 to 7.30).

at layer 10. This is potentially due to slower settling in high concentration zones leading to the development of a thick sludge at the bottom of the tank. This is similar to the observed collected solids at the bottom of the Sutton Bonington Slurry Tank when the tank is emptied [36]. The concentration of X over time is shown in Figure 7.5.

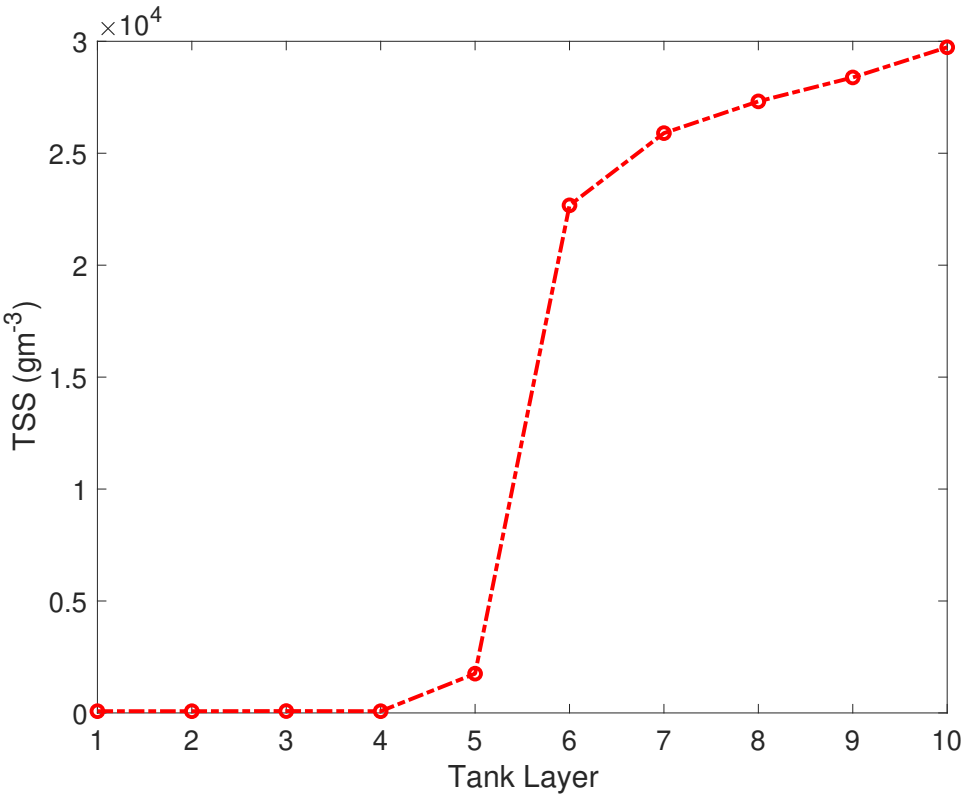


Figure 7.4: Concentration of total suspended solids (TSS) after 50000 hours with initial conditions $X_i(0) = 0$ for all i (equations 7.6 to 7.8).

This means that, in the 10th layer of the tank where the total solids concentration is approximately 30000 gm^{-3}, the available fraction of bacteriolytic antibiotic is given by

$$f_{al10} = \frac{A_{l10}^f}{A_{l10}} = \frac{1}{1 + K_{dl}X_{10}} \approx 0.79, \tag{7.37}$$

and similarly the available fraction of bacteriostatic antibiotic in the 10th layer is $f_{as10} = 0.29$. Figures 7.6a and 7.6b show the available fractions across each layer after 50000 hours. In layers 1 to 4 there is very little sorption of both A_l and A_s, in the deeper layers A_s is much more readily sorbed than A_l, as expected due to the partition coefficients. The available concentrations over time are shown in Figure 7.7.

Figure 7.8a shows the total concentration of A_s and A_l in each layer of the tank at the end of the simulation. As both A_s and A_l have the same parametrisation,

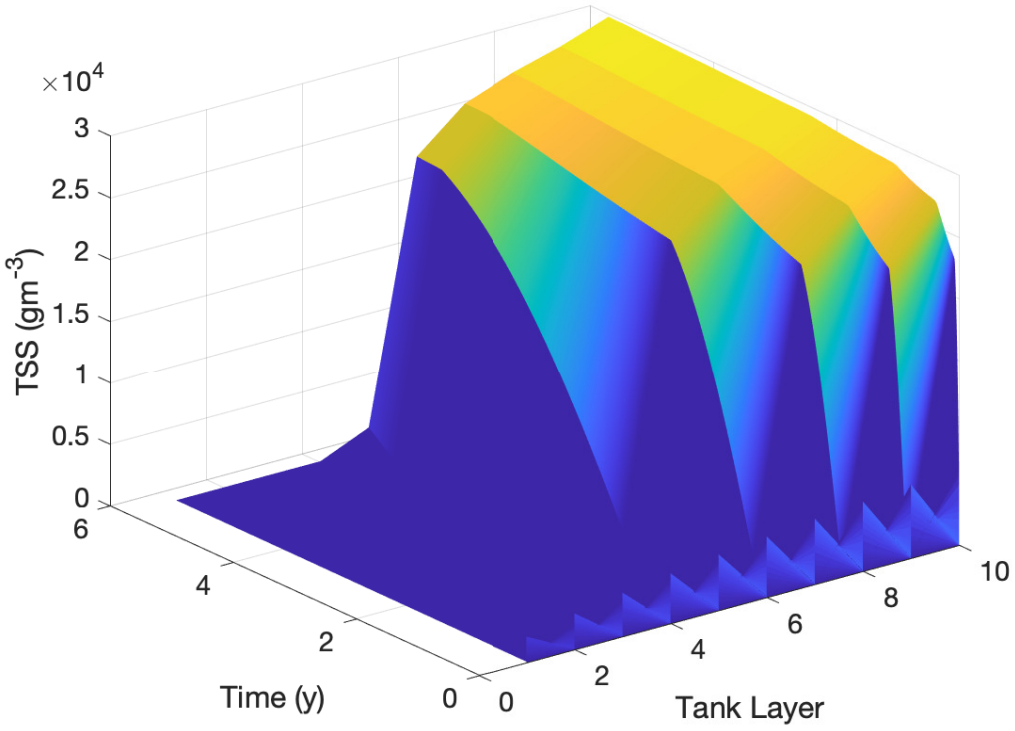
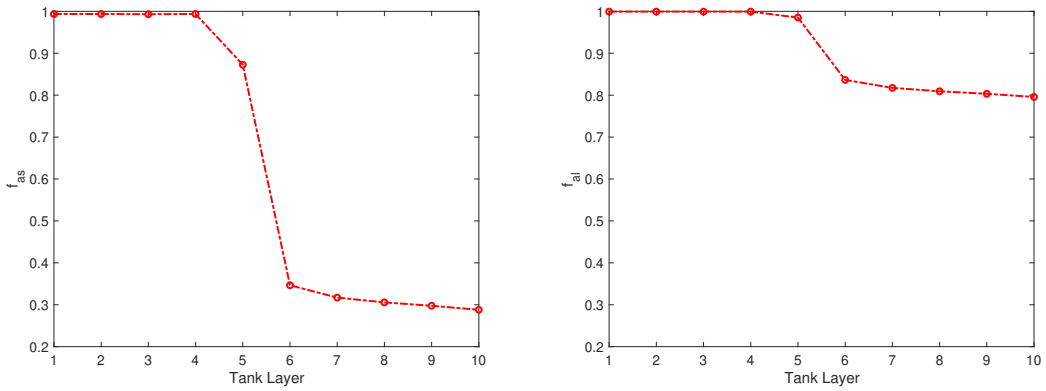


Figure 7.5: Concentration of total suspended solids (TSS) in each layer of the tank over time (equations 7.6 to 7.8). Here, colour indicates concentration.



(a) Available fraction of A_s.

(b) Available fraction of A_l.

Figure 7.6: Available fractions of A_s (f_{as}) and A_l (f_{al}) in each layer of the tank after 50000 hours (equations 7.21 to 7.23).

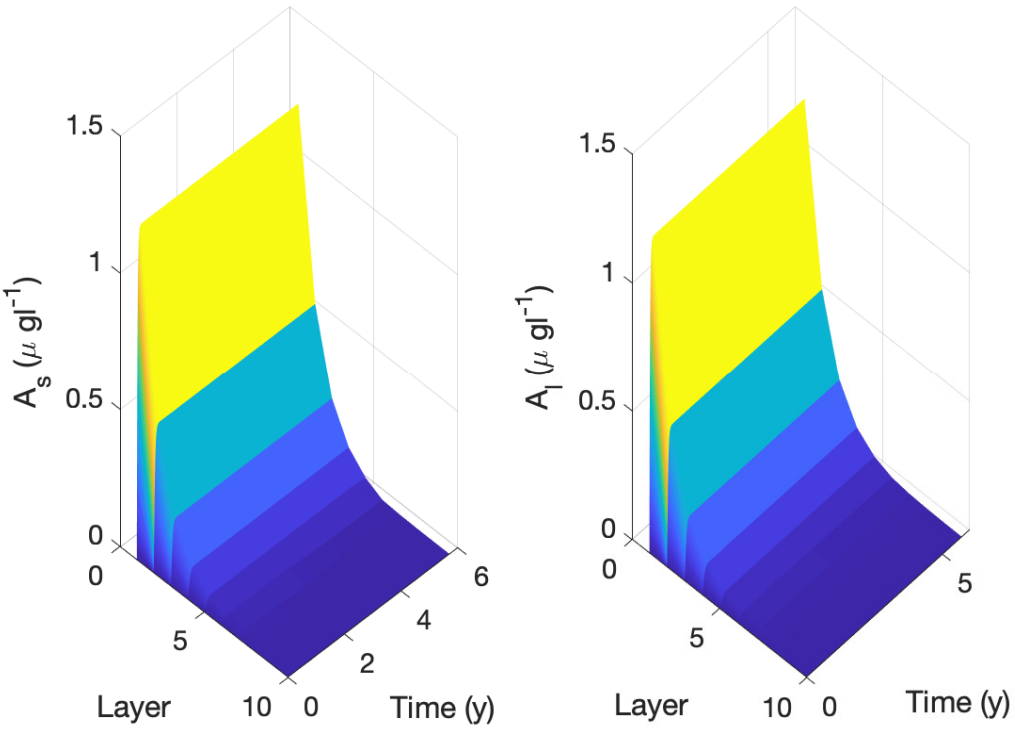


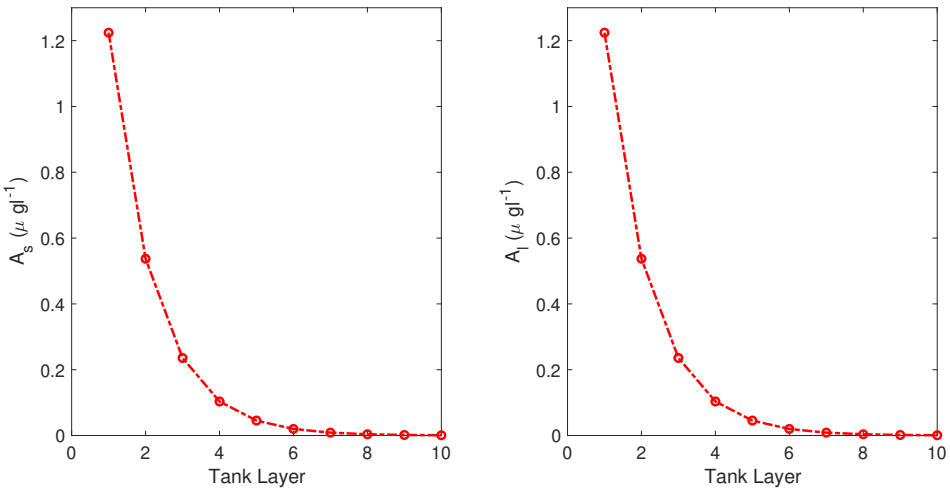
Figure 7.7: Available concentration of antibiotics in each layer of the tank over time (equations 7.21 to 7.23. Here, colour indicates concentration. Available fraction is calculated using equations 7.26 and 7.27.

they are at the same concentrations at each layer of the tank, decreasing from around 1.6 μg l^{-1} to nearly 0 μg l^{-1}. Figure 7.8b shows the available concentration of A_s and A_l in each layer of the tank and Figure 7.9 shows the difference in concentrations when omitting and including antibiotic. As in the first layers of the tank there is almost no sorbing of antibiotics (see Figure 7.6), and as both A_s and A_l are largely removed as they travel down the tank, the difference between available and total A_s ranges between 0.001 and 0.014 μg l^{-1} and the difference between available and total A_l ranges between 0 and 3.5×10^{-3} μg l^{-1}. From Figure 7.9, it can be seen that in general, there is a bigger difference for A_s (which is to be expected as A_s sorbs more strongly to the solids) and that in both cases, layer 6 shows the largest effect. This is due to the ratio between antibiotic concentration and solids concentration.

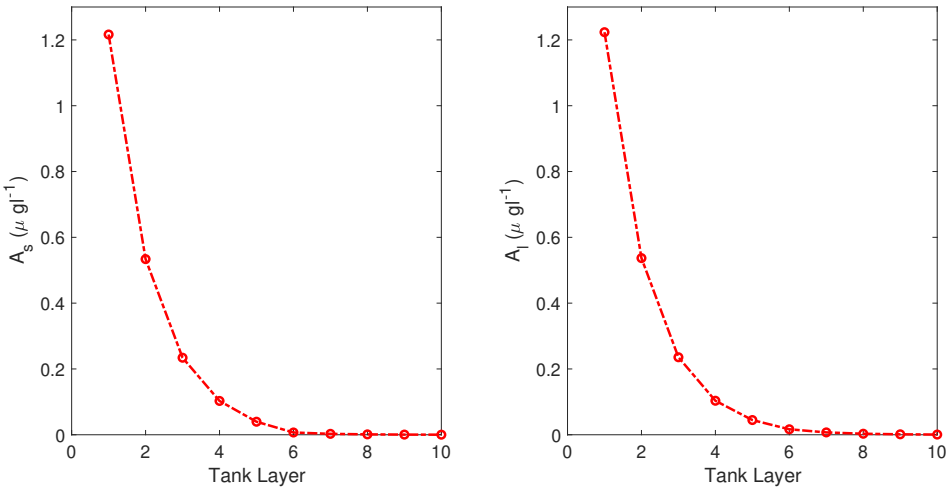
Figure 7.10 shows the concentration of bacteria over time in the presence of solids, and Figures 7.11a and 7.11b show the eventual proportions of the bacterial strains, S, R_s, R_l and R_u in each layer of the tank, in the case where sorption is included in the model and the case where sorption is ignored, respectively. In both cases the models predict that R_u makes up the majority of the bacteria at each layer of the tank, and that the proportion of R_u increases down the layers

of the tank. The results are very similar, to the point where the figures appear identical in many cases. Figure 7.12 shows the difference between bacterial phenotype concentrations when sorption is omitted and included. When sorption is omitted there are slightly higher proportions of all strains except multidrug resistant bacteria (R_u), as the reduction in antibiotic concentration reduces the selective pressure on the bacteria. However, the differences are, as mentioned before, very small. This is likely because the layers in which most sorption occurred already contained the least antibiotic, resulting in very little change between the total concentration of antibiotic and the available concentration. It appears that, under this parameterisation, sorption has little effect on the development of AMR in the tank.

As sorption in the tank can remove as much as 70% of bacteriostatic antibiotics and 30% of bacteriolytic antibiotics, see Figure 7.6, the model was also simulated with the antibiotic parameters inferred using MLE and data from the Sutton Bonington slurry tank in Chapter 6. These parameters suggest a higher inflow rate and slower degradation of bacteriostatic antibiotics than the parameters from the literature, meaning sorption will likely have more effect on the antibiotic and bacterial concentrations.



(a) Total concentration of A_s and A_l in each layer of the tank after 50000 hours with initial conditions $A_{si}(0) = A_{li}(0) = 0$ for all i (equations 7.21 to 7.23), simulated with parameter values as in Table 7.3.



(b) Available concentration of A_s and A_l in each layer of the tank after 50000 hours with initial conditions $A_{si}(0) = A_{li}(0) = 0$ for all i (equations 7.21 to 7.23), simulated with parameter values as in Table 7.3. Available fraction is calculated using equations 7.26 and 7.27.

Figure 7.8: Total and available antibiotic concentrations in each layer of the tank after 50000 hours.

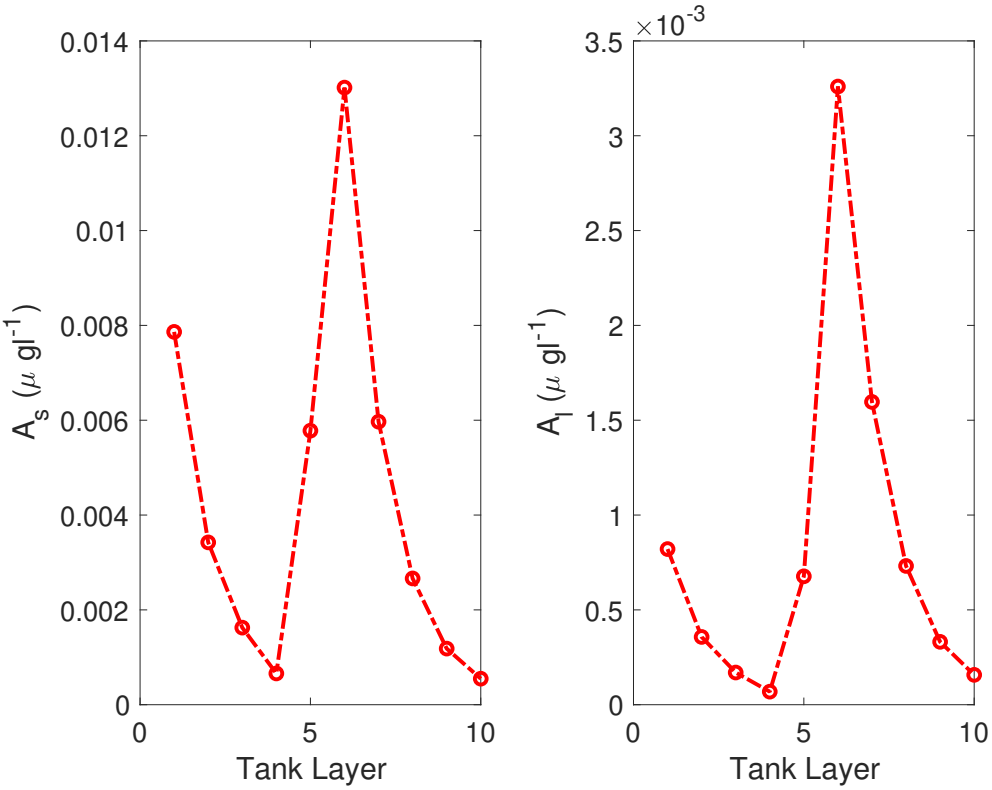


Figure 7.9: The difference in antibiotic concentration when sorption is omitted and included (see Figures 7.8a and 7.8b). The left panel shows the difference in bacteriostatic antibiotic concentration, A_s, and the right panel shows the difference in bacteriolytic antibiotic concentration, A_s.

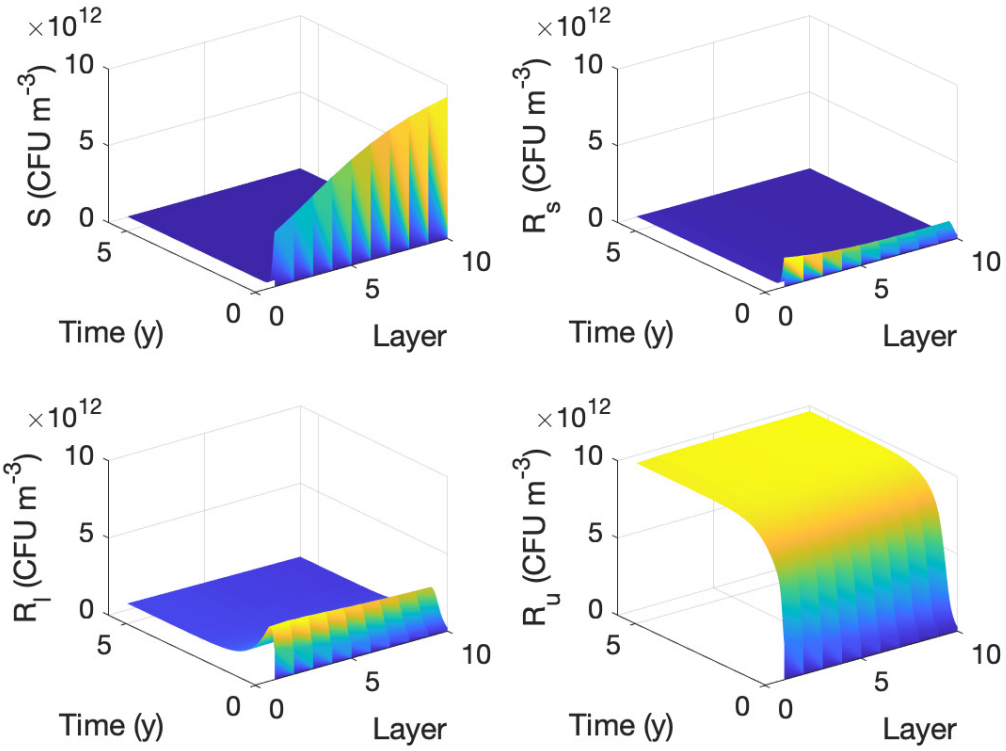
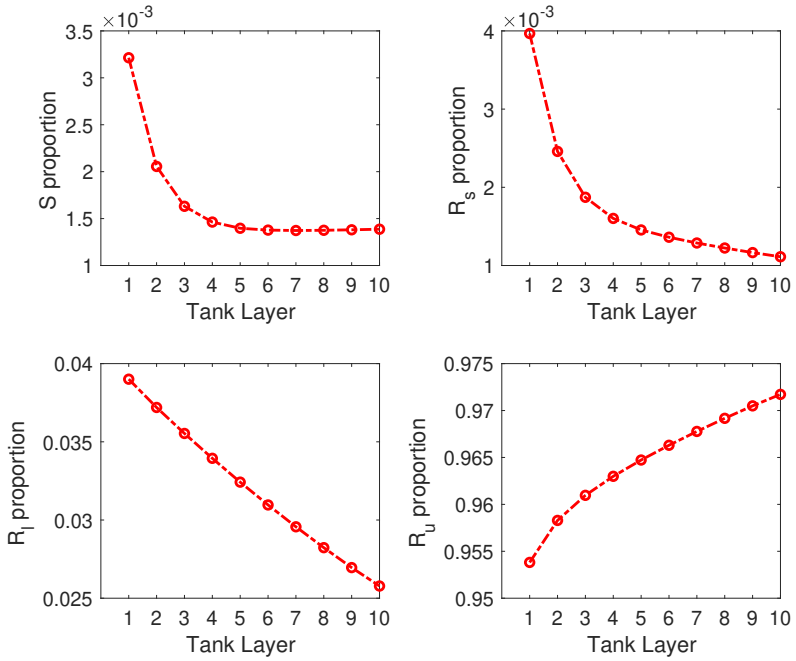
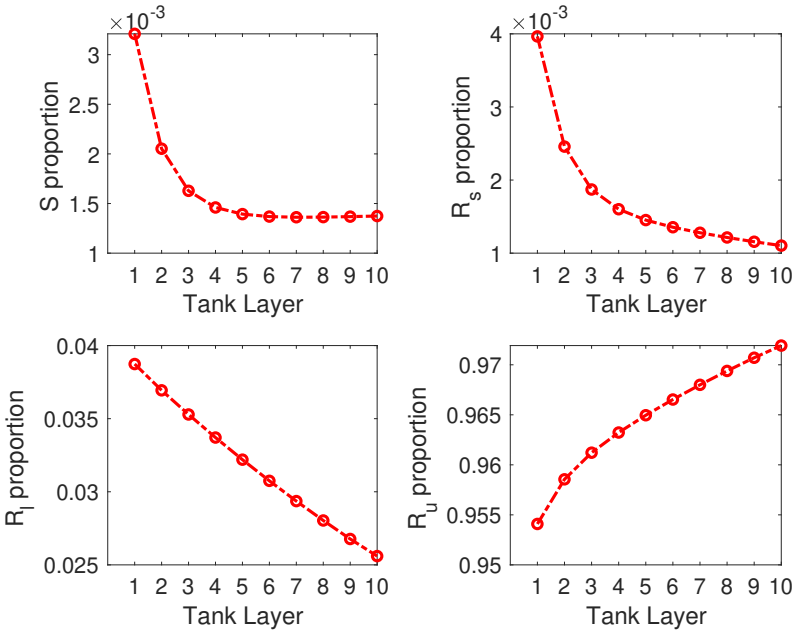


Figure 7.10: Concentration of bacteria in each layer of the tank over time (equations 7.28 to 7.30), simulated with parameter values as in 7.3. Here, colour indicates concentration.



(a) Proportions of S, R_s, R_l and R_u in each layer of the tank after 50000 hours with initial conditions $S_i(0) = R_{si}(0) = R_{li}(0) = R_{ui}(0) = 0$ (equations 7.28 to 7.30), simulated with parameter values as in 7.3. Here antibiotic sorption is included.



(b) Proportions of S, R_s, R_l and R_u in each layer of the tank after 50000 hours with initial conditions $S_i(0) = R_{si}(0) = R_{li}(0) = R_{ui}(0) = 0$ (equations 7.28 to 7.30), simulated with parameter values as in 7.3. Here antibiotic sorption is ignored.

Figure 7.11: A comparison of bacterial concentrations when sorption is omitted and included.

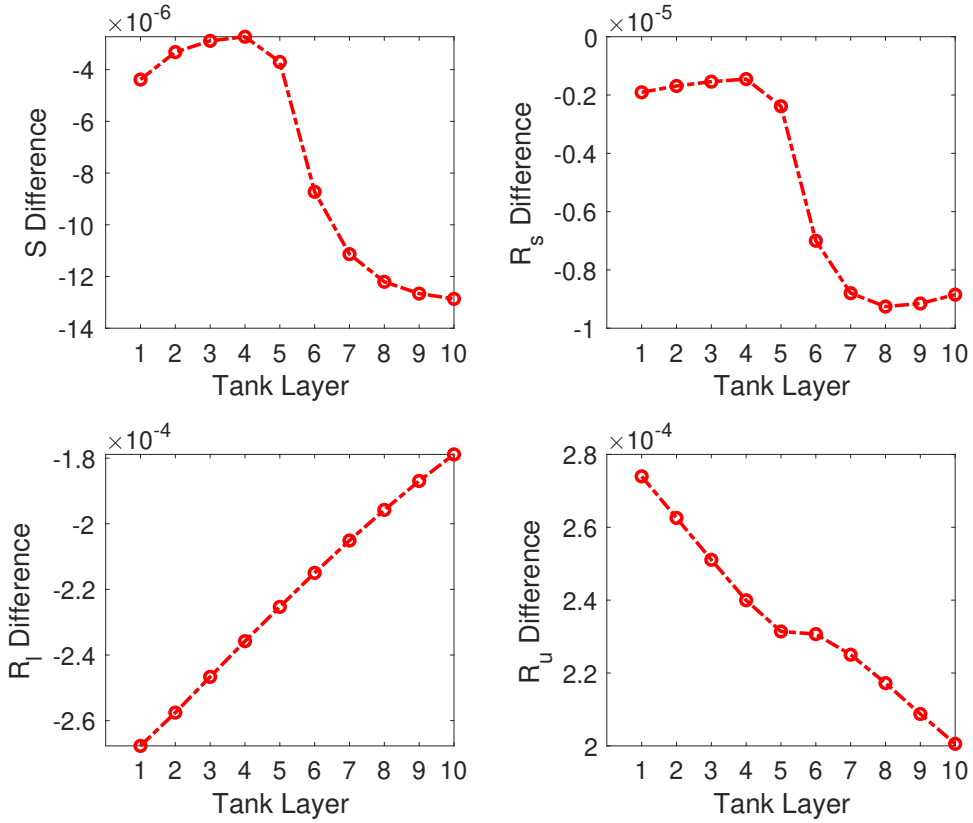


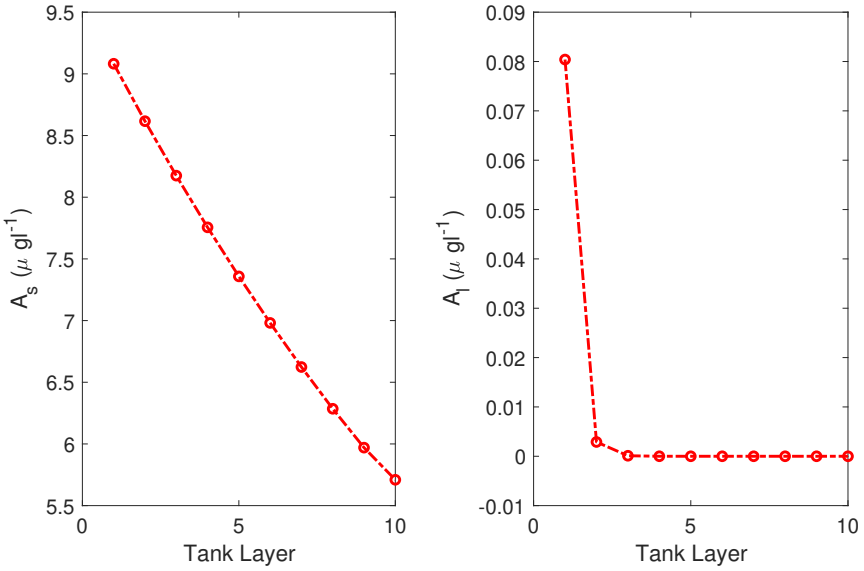
Figure 7.12: The difference in bacterial phenotype proportion when sorption is omitted and included (see Figures 7.11b and 7.11a). Here the differences in susceptible (S), bacteriostatic resistant (R_s), bacteriolytic resistant (R_l) and multidrug resistant (R_u) proportions are shown.

7.2.1 Using antibiotic parameters inferred from data

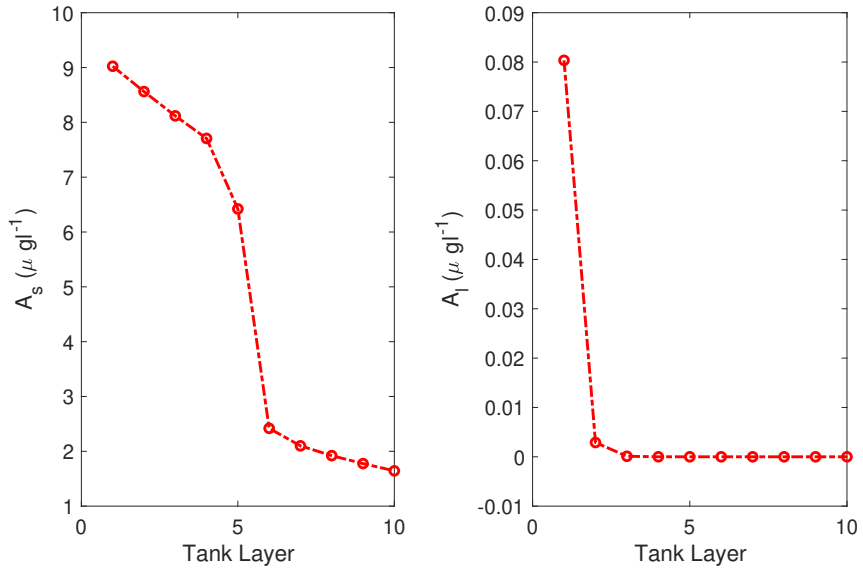
The antibiotic and bacterial models were also simulated using the antibiotic parameters inferred in Chapter 6. These parameters were inferred by comparing the equations for antibiotic concentration of the model described in Chapter 5 to data collected by Baena Nogueras et al. [37] at the University of Nottingham Sutton Bonington farm. The likelihood maximising values of the antibiotic degradation rates γ_s and γ_l were 1.115×10^{-4} and 6.494×10^{-2}, respectively. The inferred antibiotic influent rates were. $\theta_s = 5.868 \times 10^3 \mu\text{gh}^{-1}$ and $\theta_l = 1.367 \times 10^3 \mu\text{gh}^{-1}$, dividing these by the inflow rate of 613 lh^{-1} gives $A_{s_{in}} = 9.5726 \mu\text{gl}^{-1}$ $A_{l_{in}} = 2.2300 \mu\text{gl}^{-1}$. As in chapter 6, the MIC values were altered to reflect the antibiotics found by Baena Nogueras et al. [37], so that $MIC_l = 8$, $MIC_s = 125$ and MIC_R=64000.

Figure 7.13a shows the total concentration of A_s and A_l in each layer, simulated using the inferred antibiotic parameters. In contrast to Figure 7.8a, here the concentration of A_s is above $5.5 \mu\text{gl}^{-1}$ for all layers of the tank and the concentration of A_s is practically $0 \mu\text{gl}^{-1}$ in all layers except 1 and 2. The available concentration of antibiotic is shown in Figure 7.13b, in this case the effect of sorption can be clearly seen on the concentration of A_s.

Figures 7.14a and 7.14b show the proportions of the four strains of bacteria in each layer of the tank in the case where sorption is included in the model and the case where sorption is ignored, respectively. Here, the sorption of antibiotic has had an effect on the distributions of the different bacteria, especially in the case of S, which makes up around 4% more of layer 10 than in the no-sorption simulation.

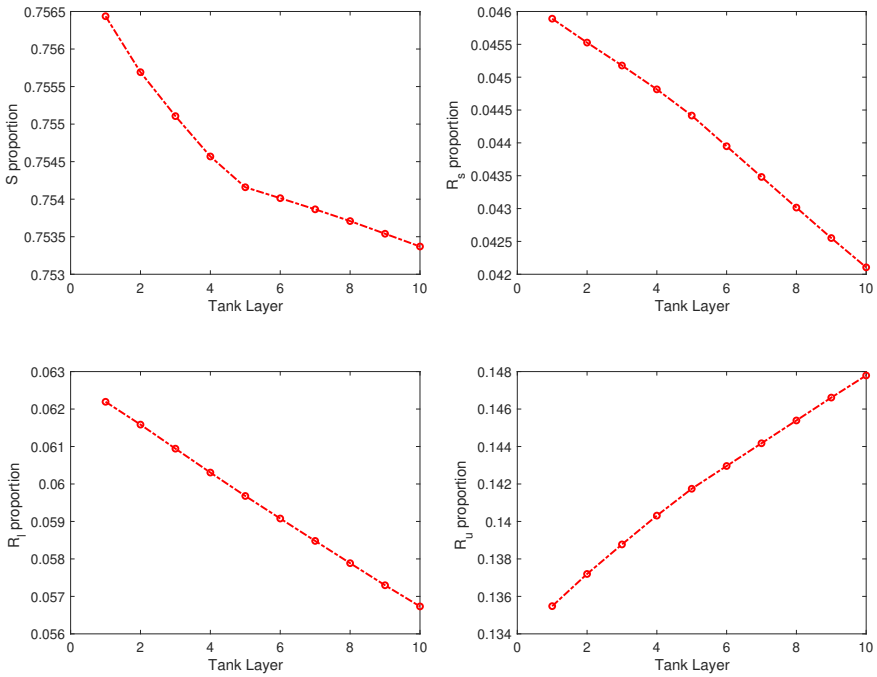


(a) The total concentration of A_s and A_l in each layer of the tank after 50000 hours with initial conditions $A_{si}(0) = A_{li}(0) = 0$ for all i (equations 7.21 to 7.23), simulated with parameter values as in 7.3 and the inferred antibiotic parameters from chapter 6.

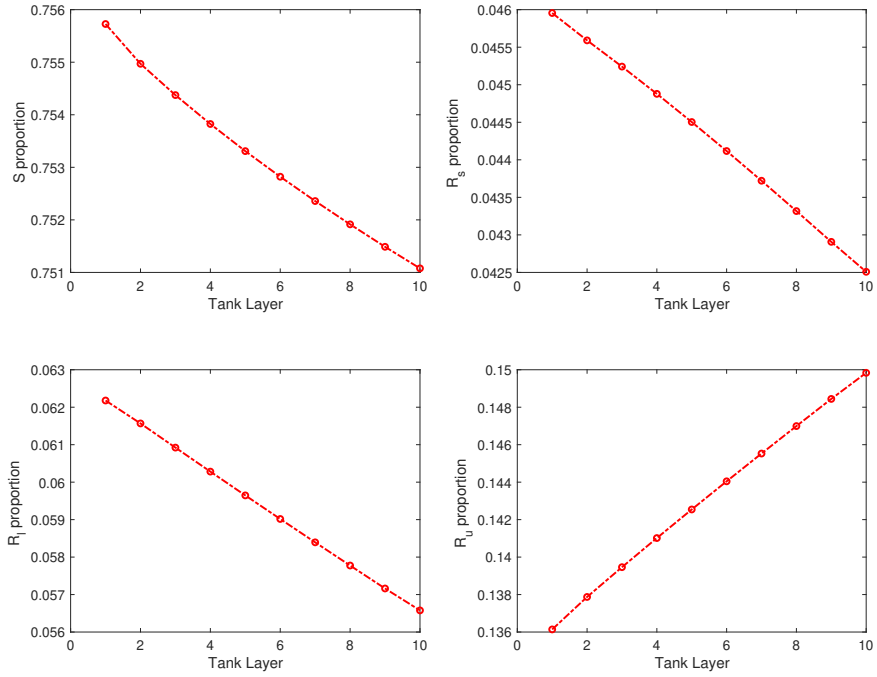


(b) The available concentration of A_s and A_l in each layer of the tank after 50000 hours with initial conditions $A_{si}(0) = A_{li}(0) = 0$ for all i (equations 7.21 to 7.23), simulated with parameter values as in 7.3 and the inferred antibiotic parameters from chapter 6.

Figure 7.13: A comparison of the total and available antibiotic concentrations when using parameters inferred in Chapter 6. Available fraction is calculated using equations 7.26 and 7.27.



(a) Proportions of S, R_s, R_l and R_u in each layer of the tank after 50000 hours with initial conditions $S_i(0) = R_{si}(0) = R_{li}(0) = R_{ui}(0) = 0$ (equations 7.28 to 7.30), simulated with parameter values as in 7.3 inferred antibiotic parameters from chapter 6. Here antibiotic sorption is included.



(b) Proportions of S, R_s, R_l and R_u in each layer of the tank after 50000 hours with initial conditions $S_i(0) = R_{si}(0) = R_{li}(0) = R_{ui}(0) = 0$ (equations 7.28 to 7.30), simulated with parameter values as in 7.3 inferred antibiotic parameters from chapter 6. Here antibiotic sorption is omitted.

Figure 7.14: A comparison of bacterial concentrations when sorption is omitted and included (using parameters inferred in Chapter 6).

7.2.2 Sensitivity Analysis

Sensitivity analysis was performed to determine which of the settling parameters most affected the suspended solids, bacterial and antibiotic distributions within the tank. As in Chapter 5 a one at a time sensitivity analysis was performed. In this case the outputs of interest were the mean concentration of solids in the tank, the proportion of multi-drug resistant bacteria and the average concentration of antibiotics throughout the tank. The sensitivity measure, S_x, is given by

$$S_x = \frac{\Delta P_{Sx}/P_{Sx}}{\Delta x/x}, \tag{7.38}$$

where P_{Sx} is the output of interest after a standard-parameter value simulation, x is the parameter being changed and Δx and ΔP_{Sx} represent the change in the parameter value and the resulting change in the model output, respectively [38, 225]. The parameters that were allowed to vary and their ranges are shown in table 7.4. As in chapter 5 the model was run for 20 years, to simulate the minimum expected lifespan of a slurry tank [223]. It should be noted that some parameter values within these ranges caused the simulation to become unstable (particularly as the influent rate, Q_{in}, varied) and so these points were omitted from the analysis.

Parameter	Range	Reference
Q_{in}	$2.942 - 44.13$ m^{3}d^{-1}	Herd sizes from SWWAS study
f_{ns}	$1 \times 10^{-3} - 1 \times 10^{-2}$	[40, 255]
r_p	$1 \times 10^{-3} - 1 \times 10^{-2}$ m^{3}g^{-1}	[40, 255]
r_h	$1 \times 10^{-4} - 1 \times 10^{-3}$ m^{3}g^{-1}	[40, 255]
X_{in}	$15000 - 50000$ gm^{-3}	[36]
v_0	$340 - 800$ md^{-1}	[40, 255]
v_0'	$100 - 400$ h^{-1}	[40, 255]
K_{ds}	$6.31 \times 10^{-5} - 9.55 \times 10^{-5}$ h^{-1}	[74]
K_{dl}	$6.73 \times 10^{-10} - 9.21 \times 10^{-6}$ h^{-1}	[272]

Table 7.4: The parameters considered for sensitivity testing the solids concentration model described by equations 7.6 to 7.8, and the ranges used.

Total suspended solids concentration

As sensitivity analysis generally requires a single output of interest, mean solids concentration is used as a proxy for the changing distribution of solids throughout the tank. When determining the sensitivity of solids concentration to the settling parameters in Table 7.4, the output of interest is the mean solids concentration

and is given by

$$P_X = \frac{1}{10}\sum_{i=1}^{10} X_i(\tau), \tag{7.39}$$

where τ is the end point of the simulation, in this case τ =20 years. Figure 7.15 shows the sensitivity of the solids concentration to the settling parameters. The solids concentration is most sensitive to the concentration of solids in the inflow, X_{in} (as would have been expected), the hindered settling velocity parameter, r_h. There is also some sensitivity to the slurry inflow rate Q_{in} and the maximum settling velocity, v_0.

Figure 7.16 shows how the mean concentration changes as the parameter varies. It appears that the value of r_h has a very clear effect on the distribution, as r_h increases the mean solids concentrations goes from less than $1{\times}10^4$ to $3{\times}10^4$ (the influent concentration) over a small parameter range. As the influent rate increases the mean concentration also tends to the influent concentration. As v_0 increases, the mean concentration decreases smoothly.

Figure 7.17 shows the concentration of solids after 20 years, when $r_h = 5 \times 10^{-4}$. Compared to Figure 7.4 (the same quantity calculated when $r_h = 4.6 \times 10^{-4}$), the distribution of solids increases much more smoothly throughout the tank. Given this level of sensitivity, data collection and subsequent model fitting to determine the settling parameters in dairy slurry would be important to accurately describe the distribution of solids throughout the tank. This kind of analysis could be performed using settling column experiments [40].

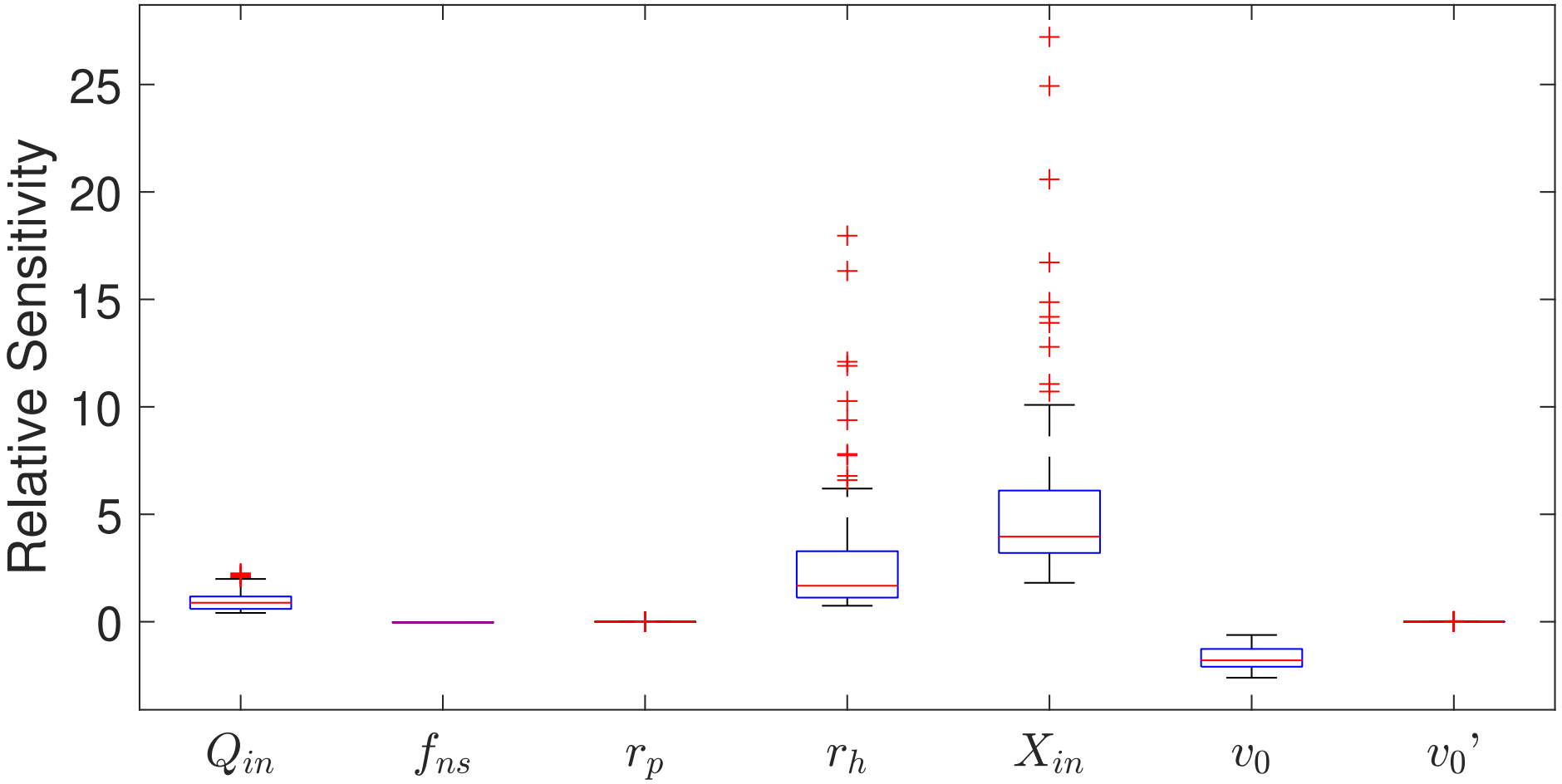


Figure 7.15: Sensitivity analysis of the mean suspended solids concentration model described by equations 7.6 to 7.8, in relation to the settling parameters listed in Table 7.4.

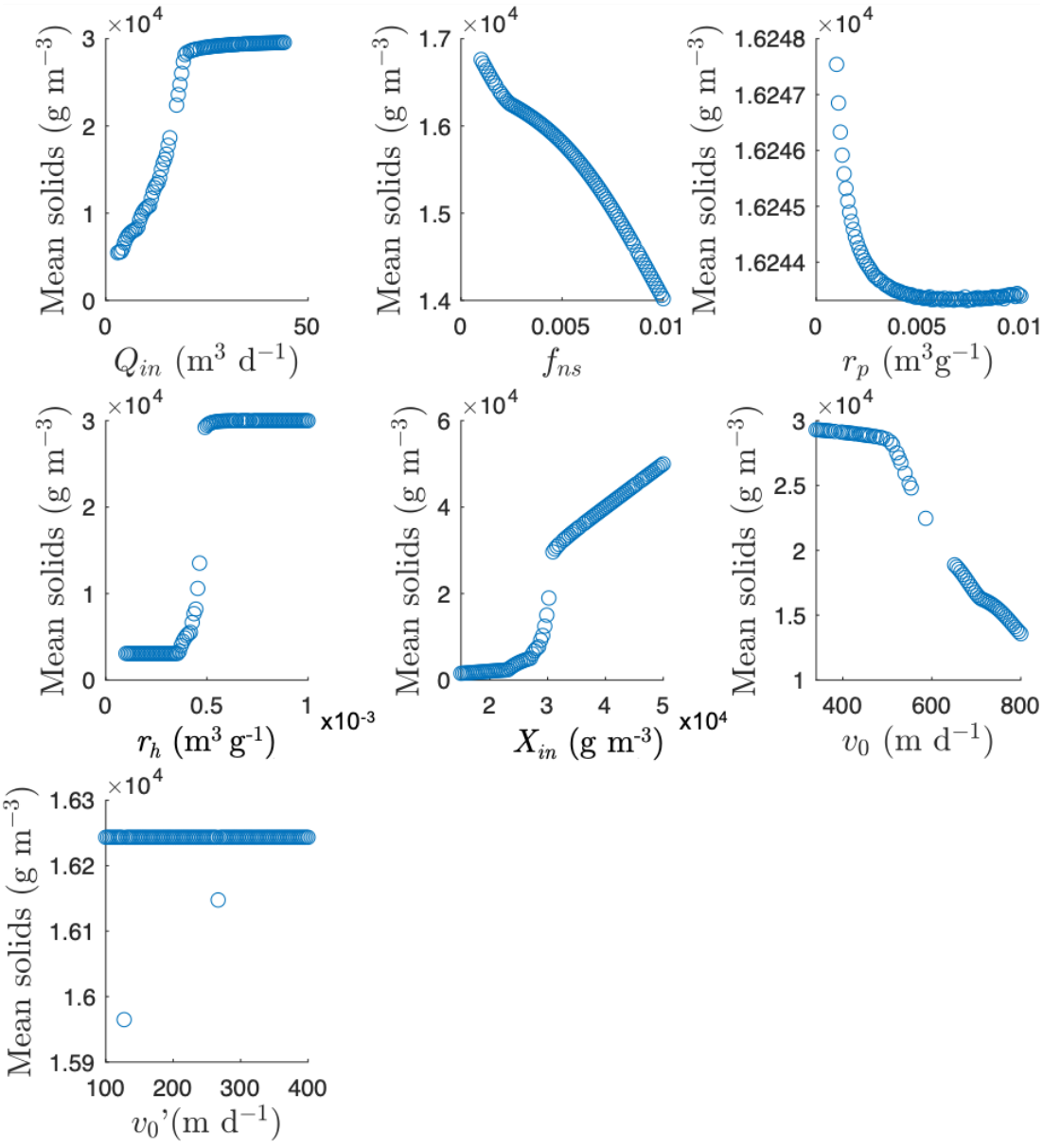


Figure 7.16: Mean suspended solids concentration in the model described by equations 7.6 to 7.8, after 20 years as the parameters in Table 7.4 vary.

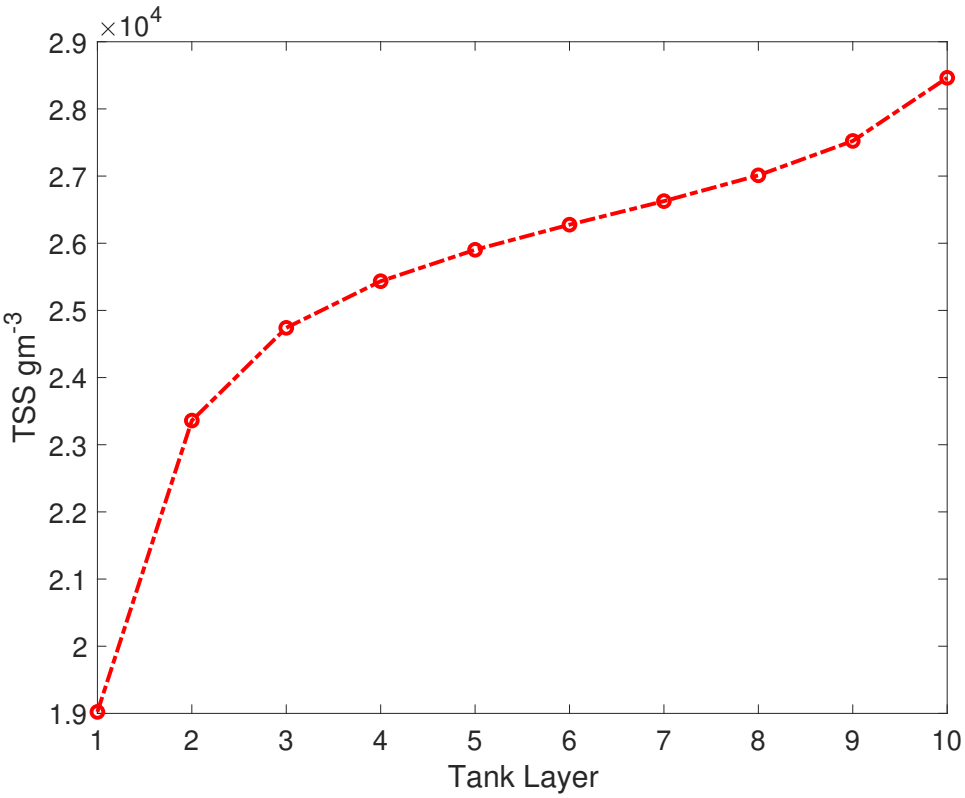


Figure 7.17: The distribution of total suspended solids (TSS) after 20 years when $r_h = 5 \times 10^{-4}$, in the model described by equations 7.6 to 7.8

Antibiotic concentration

Here the output of interest is the average total antibiotic concentration across all layers of the tank and is given by $P_A = \frac{1}{10}\sum_{i=1}^{10}(A_{si}^f(\tau) + A_{li}^f(\tau))$

Figure 7.18 shows the sensitivity of the average free antibiotic concentration to the settling parameters. Similarly to the solids concentration, the free antibiotic concentration is most sensitive to the inflow rate, X_{in}, the hindered settling velocity parameter, r_h. There is also some sensitivity to the slurry inflow rate Q_{in} and the maximum settling velocity, v_0. This was to be expected, as the solids concentration determines the concentration of available antibiotic. Figure 7.19 shows the average free concentrations after 20 years. In the cases of r_h, X_{in} and v_0, the antibiotic concentration decreases as the solids concentration increases (and vice versa). In general as Q_{in} increases so does the antibiotic concentration (as a greater total quantity of antibiotics is entering the tank per hour), except between $Q_{in} \approx 20 - 25$ m^{3}d^{-1}. This is around the point at which the solids concentration comes close to the influent concentration, and sorption removes antibiotics in greater quantities, this reaches a local minimum and then the antibiotic concentration begins to increase as before. As the partition coefficients K_{ds} and K_{dl} increase, the available concentration decreases, as would be expected. Fig-

ure 7.20 shows the concentrations of antibiotic at 20 years across the tank when $r_h = 0.5 \times 10^{-3}$. The bacteriostatic concentration is greatly decreased due to the greater concentration of solids in each layer under this parameterisation.

Multidrug-resistant proportion

Here the output of interest is the multidrug resistant proportion across all layers of the tank and the sensitivity parameter, P_{R_u}, is is given by

$$P_{R_u} = \frac{\sum_{i=1}^{10} R_{ui}(\tau)}{10 \sum_{i=1}^{10} N_i(\tau)}, \tag{7.40}$$

where $N_i(\tau) = S_i(\tau) + R_{si}(\tau) + R_{li}(\tau) + R_{ui}(\tau)$ and τ is 20 years, as before. Figure 7.21 shows the sensitivity of the multidrug-resistance to the settling parameters. As in the case of the solids and antibiotic concentrations, the system is most sensitive to r_h, X_{in} and Q_{in}. However, the effects are much less drastic than in the suspended solids and antibiotic cases. Using typical parameter values, $P_{Sx} \approx 0.96$, and the multidrug-resistant proportion never goes below 0.85 as the parameters vary, this can be seen in Figure 7.22. This analysis appears to indicate that the settling parameters have a relatively large effect on antibiotic concentration, but that doesn't translate to a large change in the bacterial population. In Chapter 5 it was shown that the bacterial population is sensitive to the antibiotic parameters and particularly bacteriolytic antibiotic, as the bacteriolytic antibiotic is less readily sorbed to the solids, this could explain the relative insensitivity of the multidrug-resistance to the settling parameters. Alternatively, it may be that, though the average antibiotic concentration is affected by settling, there is still a high enough antibiotic concentration in the first few layers of the tank to generate the necessary selective pressure for multidrug-resistance to emerge.

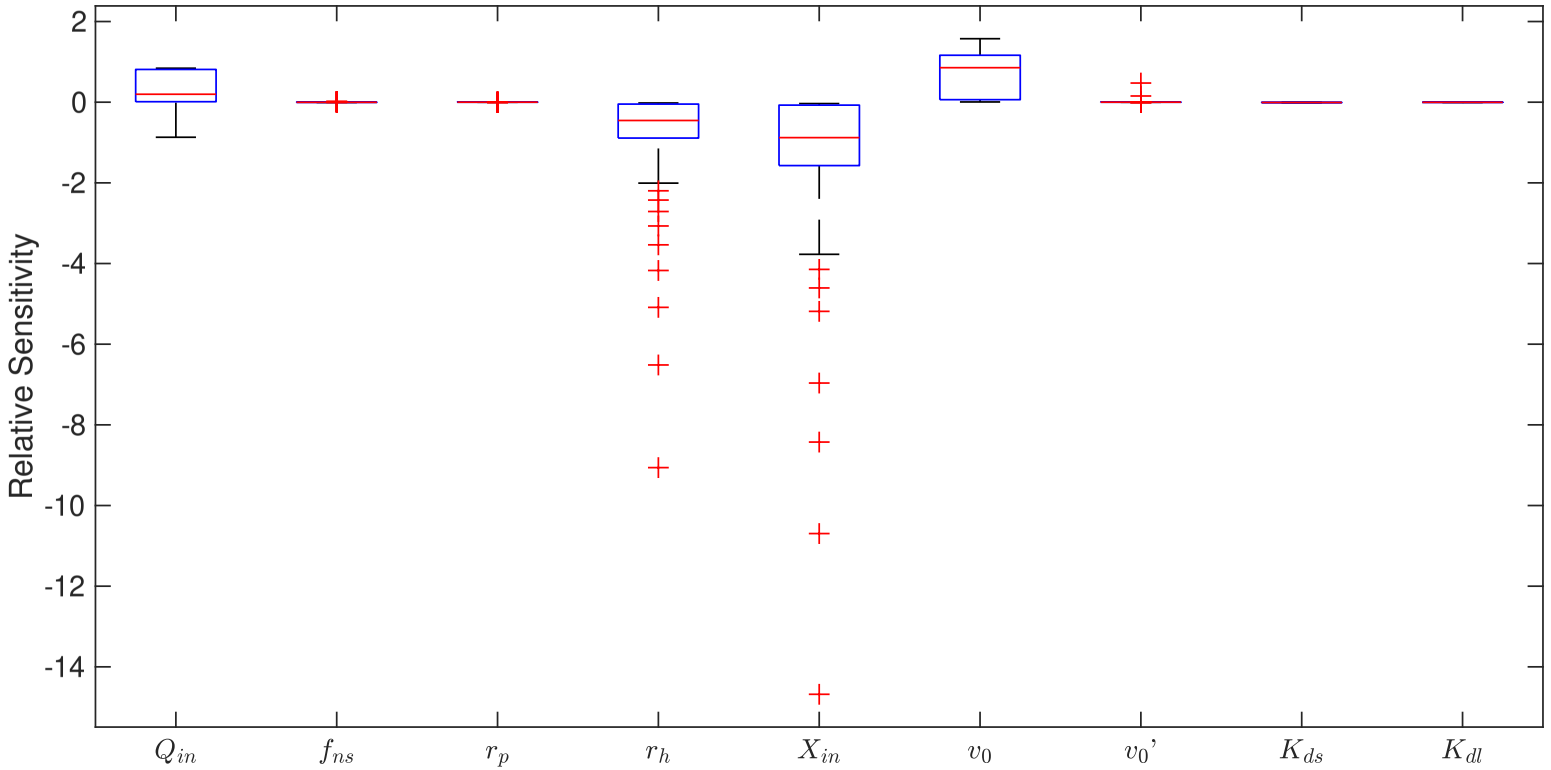


Figure 7.18: Sensitivity of average total antibiotic concentration in the model described by equations 7.21 to 7.23, in relation to the settling parameters listed in Table 7.4

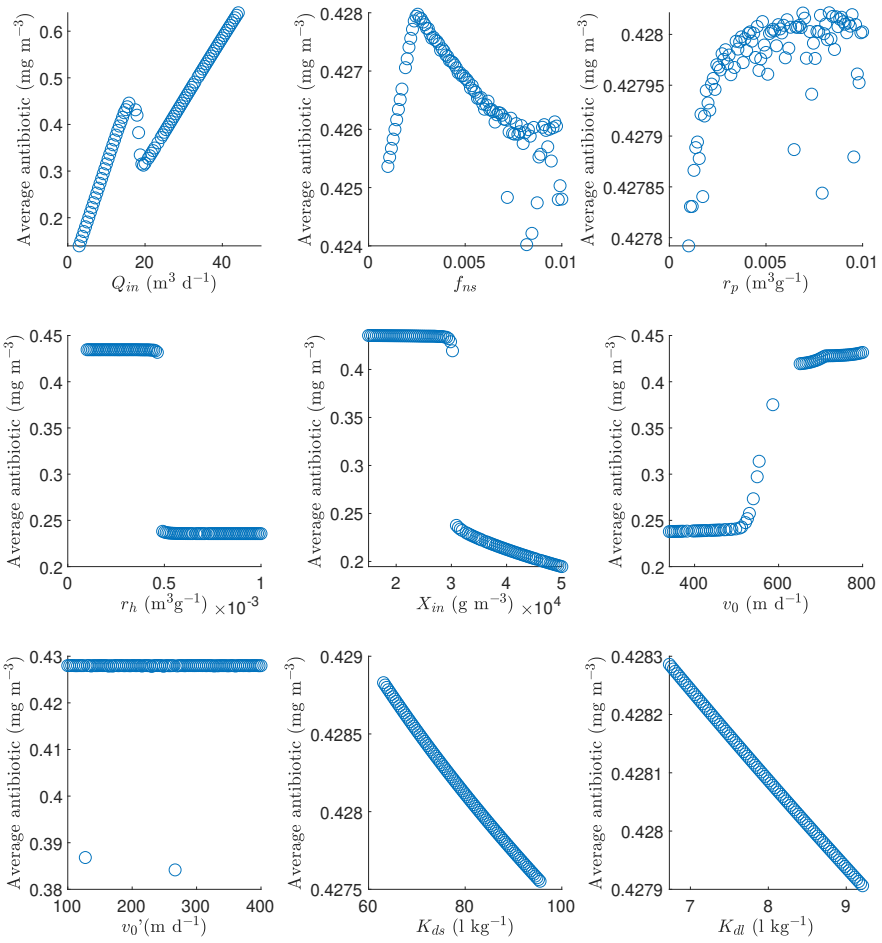


Figure 7.19: Average total concentration of available antibiotics in the model described by equations 7.21 to 7.23 after 20 years as the parameters in Table 7.4 vary.

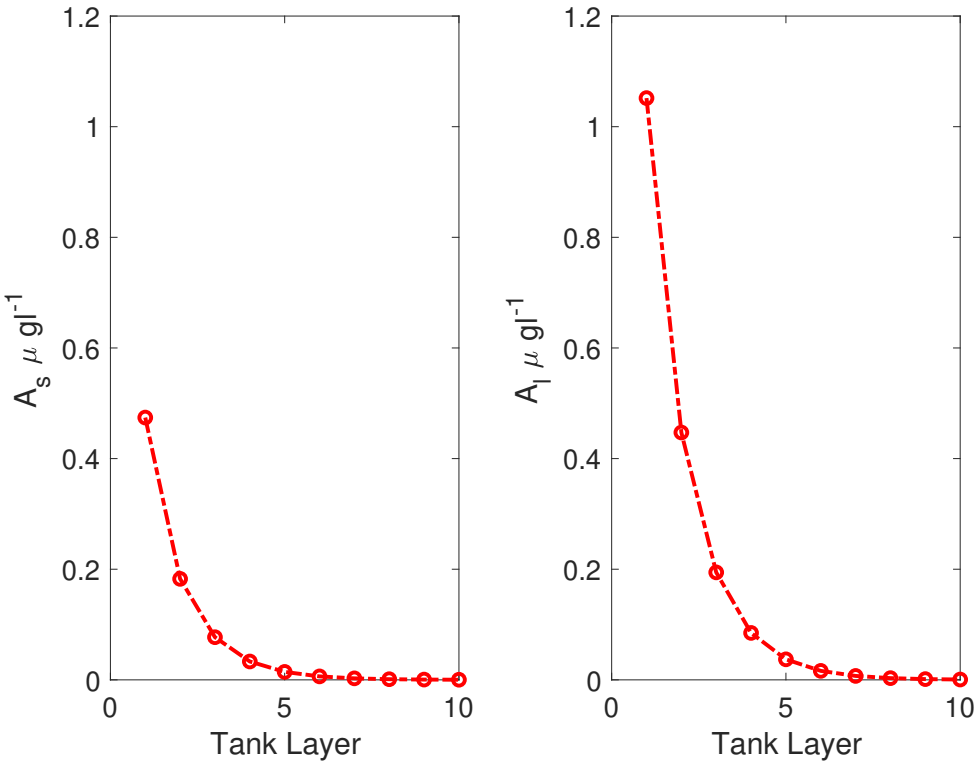


Figure 7.20: Concentrations of A_s and A_l in the model described by equations 7.21 to 7.23 at 20 years across the tank when $r_h = 0.5 \times 10^{-3}$

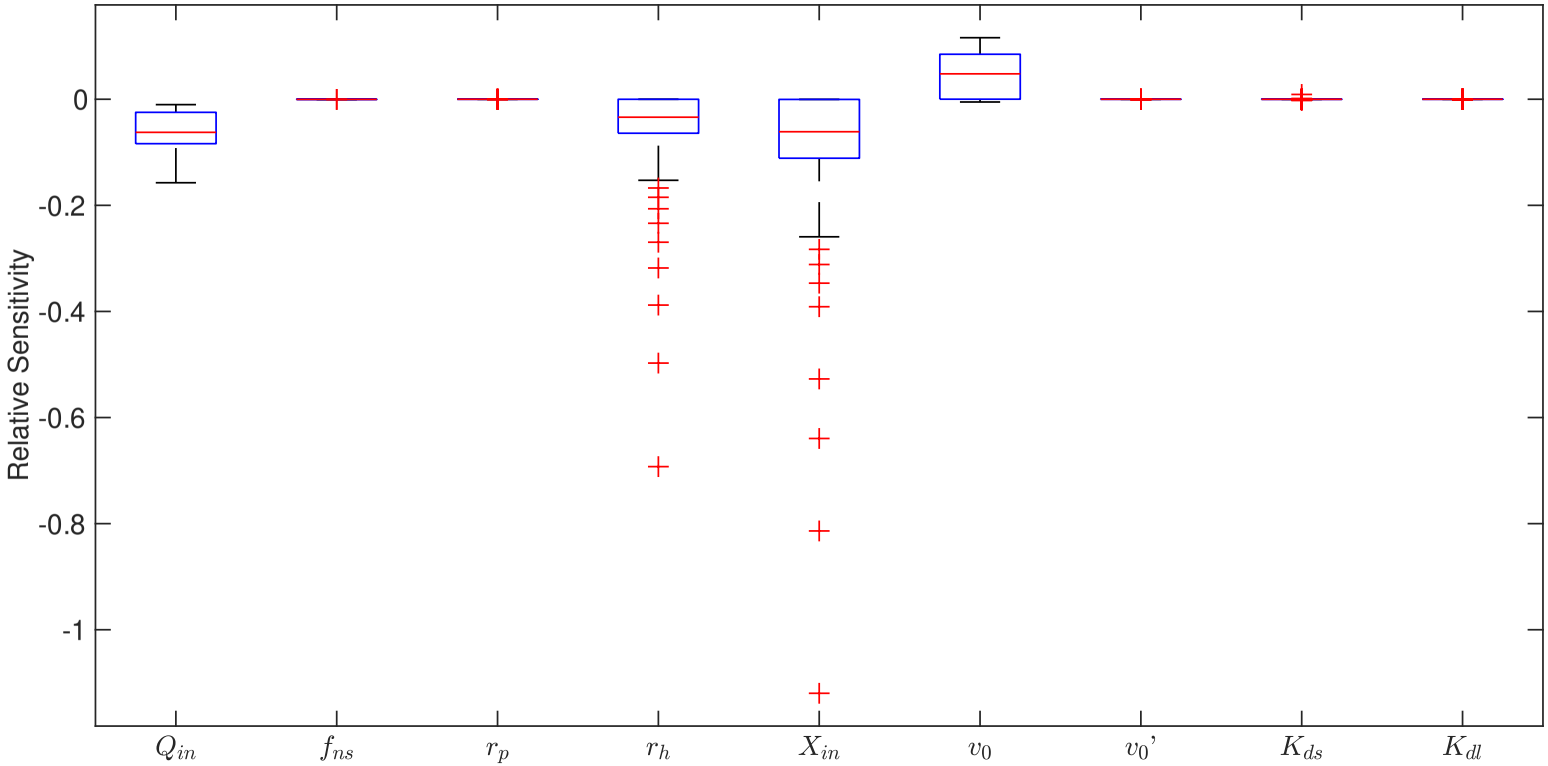


Figure 7.21: Sensitivity of multidrug-resistant proportion in the model described by equations 7.28 to 7.30, in relation to the settling parameters listed in Table 7.4

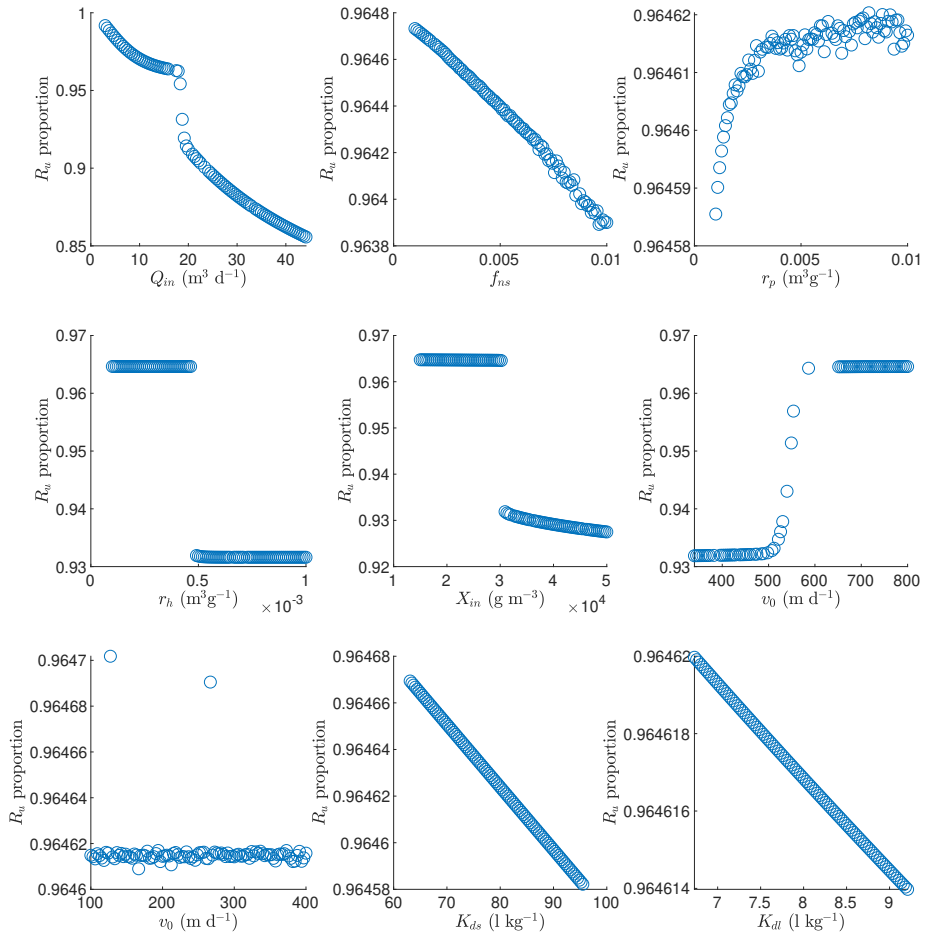


Figure 7.22: Multidrug-resistant proportion in the model described by equations 7.28 to 7.30, after 20 years as the parameters in Table 7.4 vary.

7.3 Summary

The inclusion of sorption dynamics in the model had little to no effect on the antibiotic concentration throughout the tank and subsequently little to no effect on the distribution of bacterial strains throughout the tank, when using parameter values from the literature. This is due to the highest concentrations of TSS occurring in the layers of the tank which have the lowest concentration of antibiotics. However, when using the antibiotic parameters inferred in Chapter 6 sorption made a clear difference to the concentration of A_s and a difference to the eventual proportions of the bacterial strains in the tank. However, the change was still relatively small, for example it didn't have any effect on the dominant strain within the tank using this particular model.

The model indicated that some antibiotic removal occurred through the layers of the tank, in both the case where parameters from Chapter 5 were used and in the case where inferred parameters from Chapter 6 were used. This corresponds with the results from Li et al. [280] who found that antibiotic removal occurred in both the primary and secondary clarifiers at waste-water treatment plants. It has also been noted by Van Epps and Lee [200] that there is evidence that antibiotic removal in slurry occurs due to sorption dynamics.

One of the difficulties with the model as presented, is that many of the specific parameters for settling in the slurry tank are unknown, and estimates have been chosen from the literature. For example, it is known that oxytetracycline sorbs strongly to solids but also that sorption is highly dependent on the make up of the sorbate [74, 266]. This is shown in evidenced in the discrepancies between Loke et al. [74] and Ngigi et al.'s [266] reported K_d of oxytetracycline in swine manure (8.317×10^{-5} m^3 g^{-1} and 1.337×10^{-3} m^3 g^{-1}, respectively). Likely then, the sorption of oxytetracycline to dairy wastewater slurry may differ significantly from swine manure or soil.

There are some problems with the Takács model [40]. It has been shown that, despite being a benchmark for wastewater modelling, the model solutions do not converge as the number of layers increases [256]. The problem is likely due to the use of the Stenstrom flux constraint, see equation 7.17, as Jeppsson and Diehl [254] show that, by using the Vesilind equation for settling velocity (see equation 7.5) combined with a different equation for the flux, consistent results can be generated. This indicates that the problem appears to be with the flux choice, rather than the governing continuity equation. As part of future work it may be worth testing different flux models and comparing to experiments to determine the best fit for modelling the slurry tank.

One major assumption made in the model setup is that filling and emptying

are instantaneous and constant. This assumption was made to maintain a constant slurry volume in the tank and simplify the simulations. However, this is very unrealistic. Much more likely (as discussed in chapter 5) is that the tank fills constantly but emptying occurs following a seasonal emptying schedule. The effect of this is that there would be no emptying-driven downward flow in the tank and the movement of bacteria, antibiotics and solids would be driven only by diffusion and settling for long periods of time. This would likely slow the movement of substances through the tank compared to the system modelled here. As part of future work it would be useful to remedy this. This could be done by employing a different settling model, allowing the number of layers to change over time or by allowing the volume of the layers to change during model simulation.

The inclusion of settling has introduced heterogeneity in the vertical direction within the tank, but this is typically the smallest dimension. Though the tank is 3m deep, it is approximately 36 metres across, so it might be expected that spatial variation across the tank could also be important. This concept is examined in the following chapter, which investigates partial differential equation models of the persistence and spread of AMR in the slurry tank.

Chapter 8

An advection-diffusion-reaction model of AMR in the slurry tank

In this chapter the development of two partial differential equation (PDE) models of AMR is described. The first model is a single-antibiotic model, based on the model developed by Baker et al. [38] and the second is a two-antibiotic model based on the model discussed in chapter 5. The single antibiotic model was included as a simple first case to test the PDE formulation. Both models are based on the advection-diffusion-reaction (ADR) equations and are simulated in both 1 and 2 dimensions. The governing equations are discussed and the reaction terms for the single-antibiotic and two-antibiotic models are given. A finite difference scheme for one-dimensional simulations is introduced and a finite element formulation is developed for the 2D case. Both models are simulated and the results are discussed in comparison to each other and to the models from previous chapters of this thesis.

The slurry tank model presented in the previous chapter incorporated settling and sorption dynamics whilst working under the assumption that slurry was horizontally homogenous but vertically inhomogenous: in essence assuming that slurry is deposited in a well-mixed layer at the top of the tank. However, in the case of the tank at Sutton Bonington (and in general for slurry stores), the vertical dimension is the shortest, and there is likely also horizontal inhomogeneity due to the location of the inlet and outlet. The Sutton Bonington tank has a radius of approximately 18 metres, therefore the surface area of a horizontal slice through the z axis has an area of 1000m^2. The model introduced in this chapter was developed to investigate the flow of slurry along the x and y axes.

The features, events and processes that are included and omitted in the model presented in this chapter are shown in Table 8.1.

Features

Included	Omitted
Tank	
Diameter Material (non-reactive)	Height (spatially homogenous in the z dimension) Volume (assumed constant)
Influent	
Bovine manure and faeces Bacteria (*E. coli* as sentinel organism) Antibiotics	Suspended and settling solids (focus on fluid flow) Heavy metals (simplicity) Other biocides (simplicity) Rain water (assumed that tank is covered) Parlour washings (simplicity)
Effluent	

Events

Included	Omitted
Filling (constant)	
Emptying (constant)	
	Mixing (substances are distributed by fluid flow)
	Cleaning (rare based on results from chapter 3)

Processes

Included	Omitted
Bacteriolytic antibiotics and bacteria	
Bacteriostatic antibiotics and bacteria	
Horizontal gene transfer	
	Sorption (simplicity)
	Solid settling (simplicity)
Antibiotic degradation	
Bacterial growth and death	
	Temperature effects (evidence that temperature does not affect *E. coli* in slurry [188])
	Seasonality (emptying and filling are constant)
Fluid flow (driven by tank inlet and outlet)	

Table 8.1: A summary of the features, processes and events which are included and omitted in the model presented in this chapter.

8.1 Methods

In this chapter it is assumed that the primary forces which determine the movement of antibiotics and bacteria in the slurry are advection (slurry flow) and diffusion (brownian motion and cell motility) and that these are occurring alongside the antibiotic and bacterial dynamics discussed in chapter 5. Therefore, an ADR framework was chosen for the antibiotic and bacterial dynamics. The ADR equations describe the distribution of a substance which is subject to transport by fluid flow, diffusion within the fluid and the effects of reactions with other agents in the fluid and is derived using conservation of mass [196]. It is used in various biological models [196,197] and in models of reactive transport [72]. ADR equations have been used to model bacterial swimming and chemotaxis [281] and bacterial concentrations in soils [282, 283].

8.1.1 1 Dimensional Governing Equations

In this section a finite difference scheme is established for the governing equations in one dimension. In this scenario slurry flows through the tank from inlet to outlet, modelled in 1 dimension. Due to the shape of the tank and the direction of the flow (see Figure 7.1), the cross-sectional area through which the slurry moves changes. Therefore, to establish the governing equations, the one dimensional ADR equation for transport through a volume with changing cross sectional area was derived. Figure 8.1 shows an example volume element, with changing cross-sectional area, $a(x)$, over the length scale Δx, where Δx is small. Let $X(x,t)$ be the concentration of some substance moving through the volume. Given that Δx is small and assuming that there is little variation in $a(x)$ over Δx, then $a(x)\Delta x X$ is the leading order amount of X in the volume element. Then, equating the rate of change of X in the volume with the flux in and out of the volume, and the reaction term, F_X, gives

$$\frac{\partial}{\partial t}(a(x)\Delta x X) + a(x)J(x) - a(x+\Delta x)J(x+\Delta x) - a(x)\Delta x F_X = 0. \tag{8.1}$$

Here, $J(x)$ is the flux per unit area and is given by a combination of the advective and diffusive fluxes:

$$J(x) = u(x)X - D_X\frac{\partial X}{\partial x}, \tag{8.2}$$

where $u(x)$ is the velocity and D_X is the diffusion coefficient of X. Dividing 8.1 through by Δx and letting $\Delta x \to 0$ gives

$$\frac{\partial X}{\partial t} = D_X\frac{\partial^2 X}{\partial x^2} - \left(u(x) - \frac{D_X}{a(x)}\frac{da}{dx}\right)\frac{\partial X}{\partial x} + F_X. \tag{8.3}$$

Equation 8.3 is then the governing ADR equation for this 1 dimensional model. The reaction terms for the one and two antibiotic models are given in sections 8.1.4 and 8.1.5, respectively.

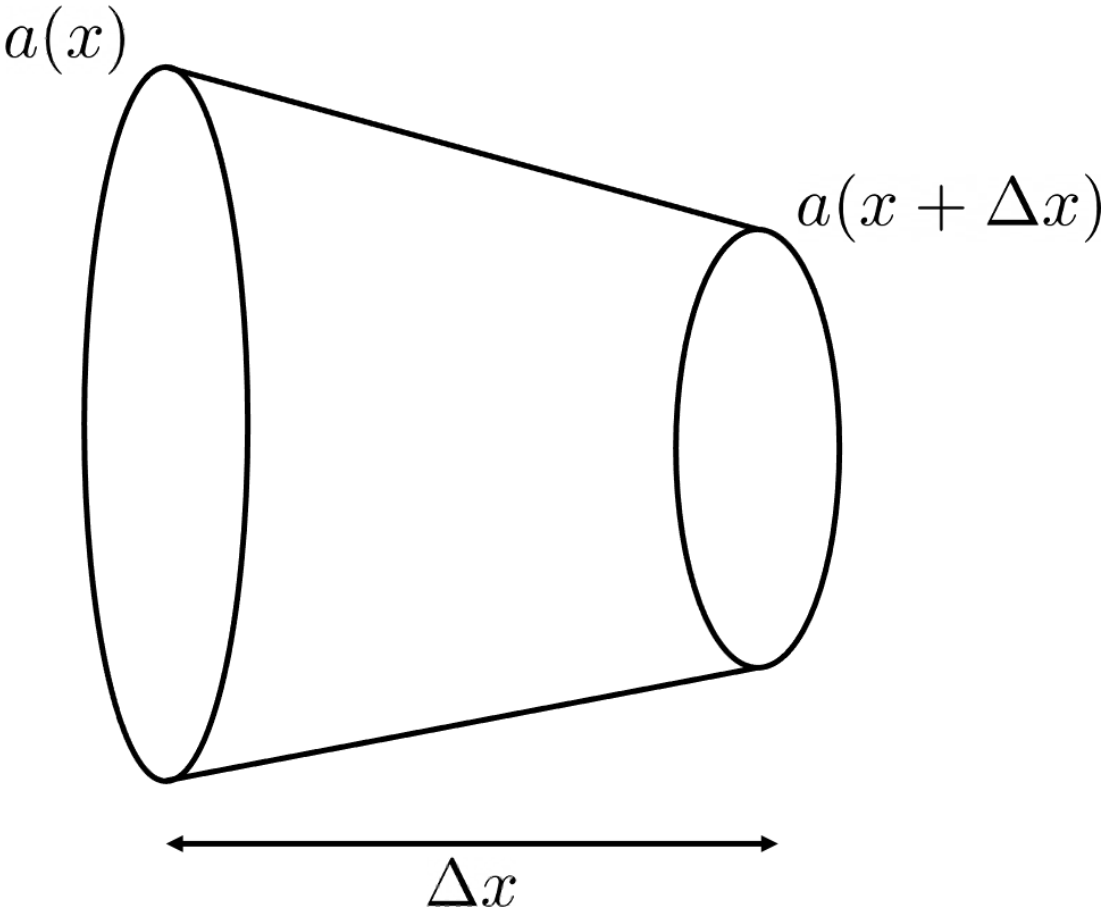


Figure 8.1: An volume element with changing cross-sectional area, used as an example to derive equation 8.1.

To simulate flow in the slurry tank, equation 8.3 can be discretised using a finite difference approximation with time step Δt and spatial step Δx and applying a first order upwind scheme (assuming that the sign of $u(x)$ is fixed) [72, 284] this can be written as

$$\frac{X_{t+1}^n - X_t^n}{\Delta t} = D_X \frac{X_t^{n+1} - 2X_t^n + X_t^{n-1}}{\Delta x^2} - \left(u^n - \frac{D_X}{a^n}\frac{a^n - a^{n-1}}{\Delta x}\right)\frac{X_t^n - X_t^{n-1}}{\Delta x} + F_{X_t^n} \tag{8.4}$$

rearranging then gives

$$\begin{aligned} X_{t+1}^n = X_t^n - \left(u^n - \frac{D_X}{a^n}\frac{a^n - a^{n-1}}{\Delta x}\right)\frac{\Delta t}{\Delta x}(X_t^n - X_t^{n-1}) + \\ D_X \frac{\Delta t}{\Delta x^2}(X_t^{n+1} - 2X_t^n + X_t^{n-1}) + \Delta t F_{X_t^n}. \end{aligned} \tag{8.5}$$

At the pipe inlet, a specified flux, or third type [72, 285], boundary condition

is imposed:

$$-u_{in}X + D_X\frac{\partial X}{\partial x} = -q_X \tag{8.6}$$

where u_{in} is the fluid velocity at the entrance to the the tank and q_X is the flux of X per unit area into the tank. This condition balances the advective and diffusive fluxes across the boundary. At the tank outlet, a Neumann boundary condition [286] is imposed:

$$\frac{\partial X}{\partial x} = 0. \tag{8.7}$$

The Neumann condition here dictates that concentrations do not change over the outlet boundary. This is determined by the assumption that there will be little change in the concentration of X in the outlet and can then be derived from continuity conditions. Across the boundary, $D_X\partial X/dx - u(x)X$ must be continuous. The velocity across the boundary is continuous by definition and, as it is assumed that $\partial X/dx = 0$ after the substance leaves the tank, $\partial X/dx = 0$ at the outlet of the tank.

At the boundaries ($n = 1$ at $x = 0$ at and $n = N$ at $x = 35.7$), equation 8.5 includes two values which don't exist in the basic discretisation, X_t^0 and X_t^{N+1}. To account for this, these are included as ghost nodes, the values of which are determined by the boundary conditions. The flux boundary condition in equation 8.6 is discretised and rearranged to give

$$X_t^0 = X_t^1 - \frac{\Delta x}{D_X}(u_{in}X_t^1 - q_X). \tag{8.8}$$

Similarly, equation 8.7 is discretised rearranged to give

$$X_t^N = X_t^{N+1}. \tag{8.9}$$

The flux per unit area of antibiotic and bacteria over the boundary is calculated by multiplying the inflow concentration by the influent velocity. Taking the single-antibiotic model as an example, in the case of antibiotic concentration, A, $q_A = u_{in}A_{in}$, where A_{in} is the concentration of A in the influent, similarly $q_S = u_{in}\rho_S\nu$ and $q_R = u_{in}(1-\rho_S)\nu$, where ν is the influent concentration of bacteria, and ρ_S is the proportion of susceptible bacteria in the influent.

The fluid velocity, $u(x)$ is determined using a continuity equation. In this model the inflow and outflow to the tank are considered to be at opposite ends of the tank, meaning the flow path length is given by the tank diameter. Thus, the cross section through which the slurry passes changes as slurry moves along the tank. If x axis passes through the centre of the tank, such that the lefthand-most point of the tank is situated at $x = 0$, the secant length at point x_a, perpendicular

to the x axis, is given by $s_a = 2\sqrt{r^2 - (x_a - r)^2}$, where r is the radius of the tank. The area that fluid passes through at x_a is given by $hs_a\text{m}^2$, where h is the height of the tank. The continuity equation for steady flow states

$$\rho u(x_1)a(x_1) = \rho u(x_2)a(x_2), \tag{8.10}$$

where ρ is the density of the fluid, u is the fluid velocity, a is the area that the fluid is passing across and x_1 and x_2 are locations on the x axis. Therefore, given an influent velocity u_{in} and the area of the influent pipe a_{in}, the velocity at any point x_a in the slurry tank is given by

$$u(x_a) = u_{in}\frac{a_{in}}{hs_a}. \tag{8.11}$$

Everywhere except the outlet and inlet, $a(x) = 2\sqrt{r^2 - (x - r)^2}$, therefore

$$\frac{da}{dx} = -\frac{2h(x - r)}{\sqrt{x(2r - x)}}. \tag{8.12}$$

Where, as before h is the height of the tank and r is the radius. At the inlet and outlet a finite difference approximation is used. Using the same discretisation as in equation 8.5, let a_1 be the cross-sectional area of the inlet and a_n be the cross-sectional area of the outlet, then

$$\frac{da_1}{dx} = \frac{a^1 - a^0}{\Delta x} \tag{8.13}$$

$$\frac{da_n}{dx} = \frac{a^n - a^{n-1}}{\Delta x}. \tag{8.14}$$

Assuming that the inlet has a constant cross-sectional area, $a_0 = a_1$ and $da_1/dx = 0$. These can then be substituted into equation 8.5.

8.1.2 2 Dimensional Governing Equations

The 2D model presented here considers a tank with the inlet and outlet at the same z coordinate on either side of the tank, z_f, though this may not be a realistic placement for the inlet and outlet. A slice is then taken through the tank at $z = z_f$, flow and distribution of antibiotics and bacteria are then modelled in this slice of the tank. Figure 8.2 shows the geometry of the model. As in [38] we assume a constant inflow and for simplicity we assume that the outflow is also constant. This assumption simplifies the governing equations as the volume of slurry throughout the tank remains constant.

The general ADR equation (when the diffusion coefficient is constant, cross-

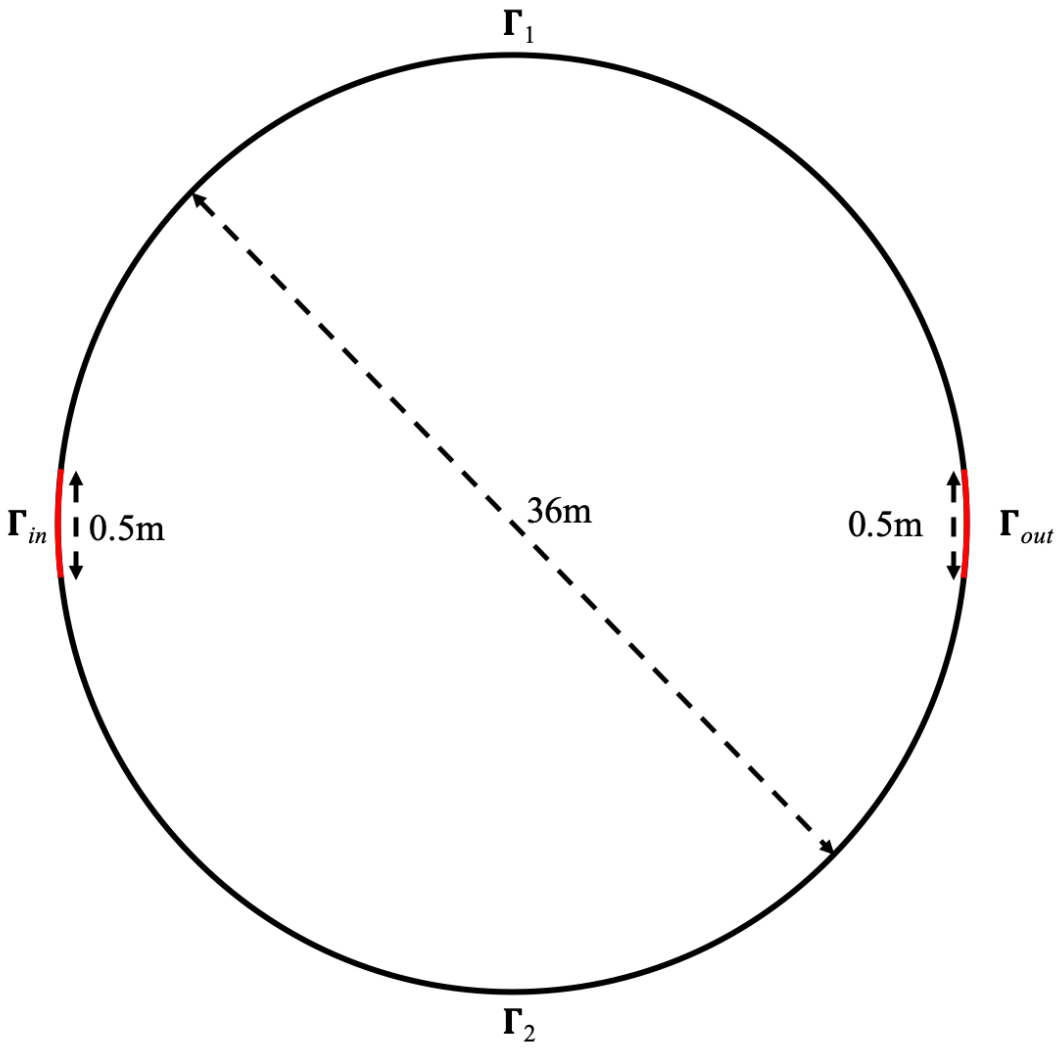


Figure 8.2: A 2D approximation of the SB farm slurry tank (not to scale). Γ_1 and Γ_2 are the walls of the tank and Γ_{in} and Γ_{out} are the inflow and outflow, respectively.

sectional area is constant and the flow is incompressible) is given by:

$$\frac{\partial X}{\partial t} = D_X \nabla^2 X - \mathbf{u} \cdot \nabla X + F_X, \tag{8.15}$$

where X is the concentration of some substance of interest, D_X is the diffusion coefficient of X, $\mathbf{u}$ is the velocity field and F_X is the reaction terms.

On the walls of the tank and at the outflow there are homogeneous Neumann boundary conditions, so that $\partial A/\partial n = \partial R/\partial n = \partial S/\partial n = 0$ on Γ_1, Γ_2, Γ_3, Γ_4 and Γ_{out} (the boundaries of the tank, as defined in Figure 8.2), as in [287]. At the inflow, a flux condition is imposed, as in the 1D case [72, 285]. Therefore the boundary conditions are

$$\left.\frac{\partial A}{\partial n}\right|_{\Gamma_1,\Gamma_2,\Gamma_{out}} = 0 \tag{8.16}$$

$$\left.\frac{\partial R}{\partial n}\right|_{\Gamma_1,\Gamma_2,\Gamma_{out}} = \left.\frac{\partial S}{\partial n}\right|_{\Gamma_1,\Gamma_2,\Gamma_{out}} = 0 \tag{8.17}$$

$$-Au_{in} - D_A\left.\frac{\partial A}{\partial n}\right|_{\Gamma_{in}} = -q_A \tag{8.18}$$

$$-Ru_{in} - D_R\left.\frac{\partial R}{\partial n}\right|_{\Gamma_{in}} = -q_R \tag{8.19}$$

$$-Su_{in} - D_S\left.\frac{\partial S}{\partial n}\right|_{\Gamma_{in}} = -q_S. \tag{8.20}$$

The flux of a substance X crossing over the boundary is given by the concentration of X in the influent multiplied by the velocity profile in the influent. For example, in the single-antibiotic model, the quantity of antibiotic, A, entering the tank per hour is 3.422mg [38], then the flux per unit area, $q_A = 3.422u_{in}(y)$, where $u_{in}(y)$ is the velocity profile over boundary between the inlet and the tank.

8.1.3 Finite Element Formulation of the ADR Problem

To solve the governing equations using finite element methods the system needs to be converted into a variational problem. Once again, the movement and evolution of a substance X within the slurry tank is modelled using the ADR equation (with incompressible flow):

$$\frac{\partial X}{\partial t} = D_X\nabla^2 X - \mathbf{u}\cdot\nabla X + F_X. \tag{8.21}$$

Following [287], a time grid is introduced with time step Δt. Then, using standard finite element practice and the backwards Euler method, so that $\partial X/\partial t$ is approximated by $\Delta t^{-1}(X^{n+1} - X^n)$, equation 8.21 was multiplied by a test function, v_1, and integrated to give

$$\int_\Omega \Delta t^{-1}(X^{n+1} - X^n)v_1 + \mathbf{u}\cdot\nabla X^{n+1}v_1 - D_X\nabla^2 X^{n+1}v_1 - F_X^{n+1}v_1 dx = 0. \tag{8.22}$$

Integrating the ∇^2 term of Equation 8.22 by parts gives

$$\int_\Omega D_X\nabla^2 X v_1 dx = \int_{\partial\Omega} D_X\frac{\partial X}{\partial n}v_1 ds - \int_\Omega D_X\nabla X\cdot\nabla v dx. \tag{8.23}$$

On the walls of the tank $\partial X/\partial n = 0$ (see equation 8.16) and on the inflow $D_X\partial X/\partial n = q_X - Xu_{in}$ (see equation 8.18). Using this, equation 8.23 can be rewritten as

$$\int_\Omega D_X\nabla^2 X v_1 dx = \int_{\Gamma_{in}} q_X - Xu_{in}v_1 ds - \int_\Omega D_X\nabla X\cdot\nabla v dx. \tag{8.24}$$

Substituting this into equation 8.22 gives

$$\int_{\Omega} \Delta t^{-1}(X^{n+1} - X^n)v_1 + \mathbf{u} \cdot \nabla X^{n+1} v_1 + D_X \nabla X^{n+1} \cdot \nabla v_1 - F_{X^{n+1}} v_1 dx - \int_{\Gamma_{in}} (q_X - X^{n+1} u_{in}) v_1 ds = 0. \tag{8.25}$$

This is the weak form of the 2D ADR problem posed in this chapter and is solved over a mesh of the slurry tank to simulate the model.

Flow in the 2D model

As in figure 8.2, slurry flows into the tank via a 0.5m diameter inlet. In the inlet it is assumed that flow is well developed and is modelled using the standard flow profile for flow between two stationary parallel plates. To determine whether the flow regime is turbulent or laminar the Reynold's number (Re) was calculated:

$$Re = \frac{\rho \bar{u}_{in} L}{\mu}, \tag{8.26}$$

where $\bar{u}_{in}$ is the average inflow velocity, ρ is the density of the slurry, L is the characteristic length and μ is the dynamic viscosity. Baker et al. [38] prescribe an inflow rate of 0.613m^3 h^{-1}, which translates to an average inflow velocity of 1.226m h^{-1} via the 0.5m diameter inlet. For simplicity the slurry is considered to be a Newtonian fluid. In reality the slurry is likely non-Newtonian, with viscosity which varies with shear stress, as recorded in [182]. At low rates of shear-stress Mashad et al. [182] recorded an apparent viscosity of 0.97 Pa s at a temperature of 30°C, which we assume will be approximately accurate for the simulation. The slurry density is assumed to be $\rho = 1000$kg m^{-3} [182]. Substituting these values into the Reynolds number gives $Re \approx 0.18$, so the flow is laminar in the inlet ($Re \approx 2000$ would indicate a turbulent flow [288]). As the diameter at the widest point of the tank is 35.7m, and the inlet is the narrowest area through which the slurry flows, the Reynolds number remains low enough throughout the tank that the flow is laminar.

At the inflow, Γ_{in}, it is assumed that the slurry is entering the tank from a 0.5m diameter inlet and is flowing under a laminar flow regime. The slurry is assumed to emerge into the tank with the same velocity profile with which it flows through the inlet, which is modelled as flow between two plates (as a slice has been taken through the system). The general velocity profile for flow between

two plates, where the centre line of the inlet is along $y = 0$, is given by

$$\mathbf{u_{in}} = (u_{in}, v_{in}) = \left(\frac{1}{2\mu} \frac{\partial p}{\partial x} (y^2 - r^2), 0 \right), \tag{8.27}$$

where $\partial p/\partial x$ is the pressure gradient (a constant), μ is the fluid viscosity and $2r$ is the distance between the plates. As both the pressure gradient and the viscosity are constant, let

$$U = -\frac{1}{2\mu} \frac{\partial p}{\partial x} \tag{8.28}$$

so that

$$u_{in} = U(r^2 - y^2). \tag{8.29}$$

The value of U can then be determined using the fluid flow rate. The flow rate of slurry in the inlet is $Q = 0.613\text{m}^3\text{ h}^{-1}$. The flow rate can also be calculated from the velocity by integrating over the area through which the fluid is flowing (a):

$$Q = \int_{a_{in}} \mathbf{u_{in}} \cdot \mathbf{n} \; da = \int_{-0.25}^{0.25} u_{in} \; dy = U \int_{-0.25}^{0.25} r^2 - y^2 \; dy = \frac{U}{48}, \tag{8.30}$$

where $\mathbf{n}$ is the inward facing normal, and using $\mathbf{u_{in}} \cdot \mathbf{n} = u_{in}$ and $da_{in} = (1)dy$ Using this result gives

$$Q = 0.613 = \frac{U}{48} \implies U = 48 \times 0.613 = 29.424, \tag{8.31}$$

so $u_{in} = 29.424(r^2 - y^2)$. On the walls of the tank (Γ_1,and Γ_2) there is a no slip boundary condition. The flow field can then be modelled using the Navier-Stokes equations. The Navier-Stokes equations for incompressible flow in 2 dimensions are given by

$$\frac{\partial u}{\partial t} + u\frac{\partial u}{\partial x} + v\frac{\partial u}{\partial y} - \nu \left(\frac{\partial^2 u}{\partial x^2} + \frac{\partial^2 u}{\partial x^2} \right) + \frac{1}{\rho}\frac{\partial p}{\partial x} = 0 \tag{8.32}$$

$$\frac{\partial v}{\partial t} + u\frac{\partial v}{\partial x} + v\frac{\partial v}{\partial y} - \nu \left(\frac{\partial^2 v}{\partial x^2} + \frac{\partial^2 v}{\partial x^2} \right) + \frac{1}{\rho}\frac{\partial p}{\partial x} = 0 \tag{8.33}$$

$$\frac{\partial u}{\partial x} + \frac{\partial v}{\partial y} = 0 \tag{8.34}$$

where $\mathbf{u} = (u, v)$ is the velocity and $\nu = \mu/\rho$ is the kinematic viscosity. The system has boundary conditions:

$$\mathbf{u}\Big|_{\Gamma_1, \Gamma_2} = (0, 0) \tag{8.35}$$

$$\mathbf{u}\,|_{\Gamma_{in}} = u_{in} = 29.424(0.0625 - y^2) \tag{8.36}$$

$$p\,|_{\Gamma_{out}} = 0 \tag{8.37}$$

The initial conditions were $\mathbf{u} = (0, 0)$ everywhere.

The Navier-Stokes equations were solved using a splitting method in FEniCS, following the scheme set out in [287]. This method requires the user to establish the variational formulation and solve the equations over a three step process, a sample script for this is provided in [287]. As the initial conditions were considered to be 0 everywhere, a time dependent solution was calculated. However, later simulations use the flow profile at a well developed point (assuming no time dependency). The flow regime is shown in Figure 8.3.

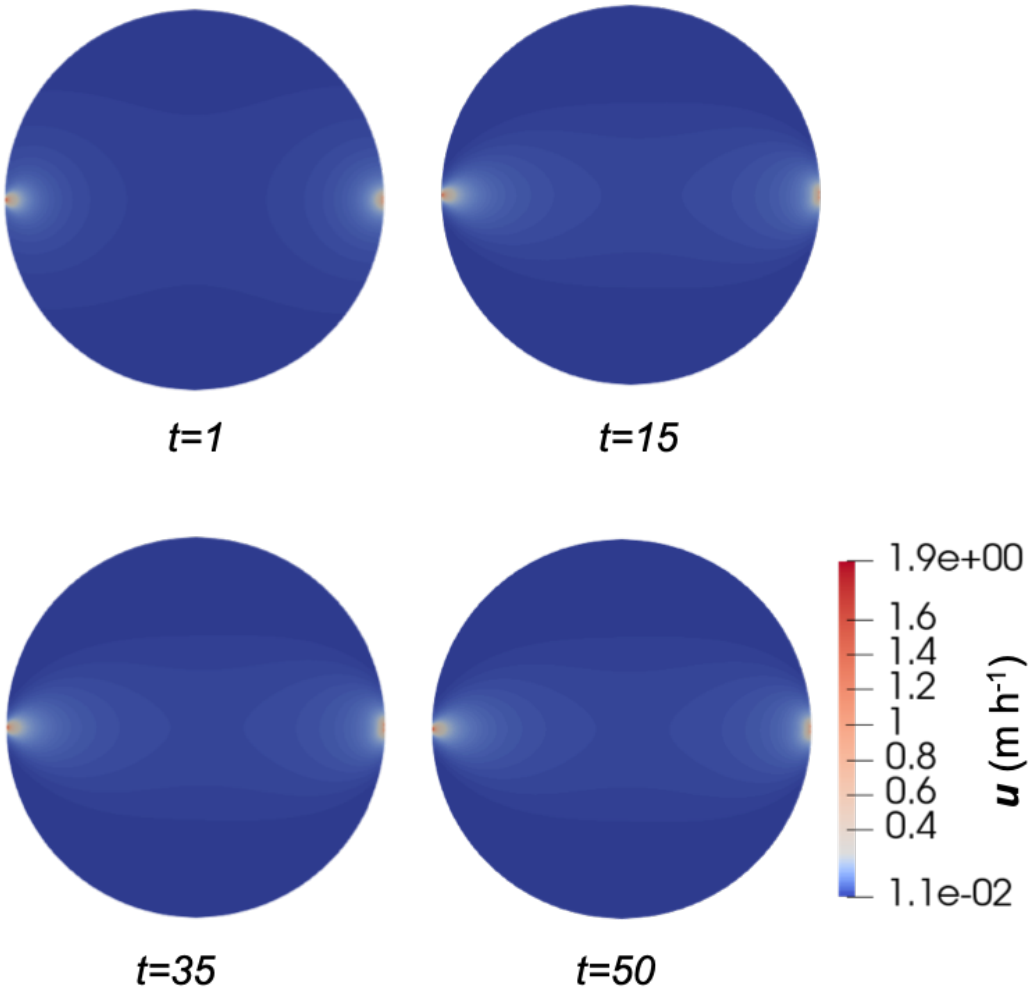


Figure 8.3: The velocity field, $\mathbf{u}$ in the tank at $t = 1$, $t = 15$, $t = 35$ and $t = 50$, generated by solving equations 8.32 to 8.34 with boundary conditions shown in equations 8.35 to 8.37.

8.1.4 Single-antibiotic model

In the single-antibiotic model the interactions between bacteria and a single antibiotic are considered, the reaction terms of the model are drawn largely from Baker et al. [38]. As in [38], there is a single antibiotic and bacteria are either susceptible or resistant to the antibiotic. The population dynamics are controlled by bacterial growth, horizontal gene transfer and natural cell death as discussed in Baker et al. [38], Volkova et al. [39] and Ayscue et al. [187]. Unlike the model proposed by Baker et al. [38], which models slurry as well mixed, the distribution of antibiotics and bacteria throughout the tank is governed by an ADR regime (the slurry is likely not well mixed, as discussed in chapter 7). The reaction terms for antibiotic, resistant and susceptible bacteria are given by:

$$F_A = -\gamma A \tag{8.38}$$

$$F_R = r(1-\alpha)\left(1-\frac{R+S}{\varphi}\right)E_R R + \frac{\beta SR}{S+R} - \delta_R R, \tag{8.39}$$

$$F_S = r\left(1-\frac{R+S}{\varphi}\right)E_S S - \frac{\beta SR}{S+R} - \delta_S S, \tag{8.40}$$

where A is the concentration of antibiotic, R is the concentration of resistant bacteria, S is the concentration of susceptible bacteria, γ is the degradation rate of antibiotic, r is the bacterial growth rate, α is the relative cost of antibiotic resistance, ψ is the carrying capacity of liquid slurry, β is the rate of horizontal gene transfer, and δ_R and δ_S are the natural death rates of resistant and susceptible bacteria, respectively. E_R and E_S are given by

$$E_R = 1 - \frac{E_{max}A^H}{MIC_R^H + A^H} \tag{8.41}$$

$$E_S = 1 - \frac{E_{max}A^H}{MIC_S^H + A^H}, \tag{8.42}$$

where E_{max} is the maximum effect of antibiotics on bacterial growth, H is the hill coefficient, MIC_R is the minimum inhibitory concentration of resistant bacteria and, similarly, MIC_S is the minimum inhibitory concentration of susceptible bacteria. Parameter values for this model are shown in table 8.2. The boundary conditions of the system are dependent on the geometry used for the simulation and were discussed for the 1 and 2D cases in previous sections.

8.1.5 Two-antibiotic model

The two-antibiotic model draws on the dynamics from the ODE model discussed in Chapter 5. It considers the growth of a population of *E. coli* in the presence of

Parameter	Description	Typical Value	Reference
r	Specific growth rate of *E. coli*	0.5 h^{-1}	[38]
β	Horizontal gene transfer rate	10^{-17} $m^3 CFU^{-1} h^{-1}$	[38, 39, 123]
u_{in}	Slurry inflow velocity	3.121 m h^{-1}	[38]
α	Relative fitness cost of resistance as a fraction of r	0.1	[38]
E_{max}	Maximum effect of antibiotics on bacterial growth	2	[38, 39]
H	Hill coeficient in E_{max} model	2	[38, 39]
MIC_R	MIC for bacteriostatic-resistant bacteria	2000 mg m^{-3}	[38]
MIC_S	MIC for bacteriostatic-sensitive bacteria	8 mg m^{-3}	[38]
φ	Carrying capacity of liquid slurry	10^{13} CFU m^{-3}	[38]
γ	Decay rate of antibiotics	0.0029 h^{-1}	[38]
δ_S	Natural death rate of susceptible bacteria	0.001 h^{-1}	[187]
δ_R	Natural death rate of resistant bacteria	0.001 h^{-1}	[187]
D_A	Antibiotic diffusion coefficient	3.6×10^{-5} m^2 h^{-1}	[273]
D_B	Bacterial diffusion coefficient	7.2×10^{-6} m^2 h^{-1}	
μ	Dynamic viscosity of slurry	3492kg $m^{-3} h^{-1}$	[182]
ρ	Density of slurry	1000 kg m^{-3}	

Table 8.2: Parameter values used to simulate the single-antibiotic advection diffusion model in 1D.

two types of antibiotic, bacteriostatic (A_s) and bacteriolytic (A_l), the *E. coli* can then be susceptible to both kinds of antibiotic (S), resistant to bacteriostatic antibiotics (R_s), resistant to bacteriostatic antibiotics (R_l) or resistant to both (R_u). Bacteriostatic and bacteriolytic antibiotics degrade at rates γ_s and γ_l respectively. The growth of all four strains of antibiotic follows the modified logistic growth model discussed in Chapter 5. The transfer of genetic material which confers bacteriostatic, bacteriolytic and multi-drug resistance occurs at rates β_s, β_l and β_u, respectively. Susceptible *E. coli* die at rate δ_S and all three resistant strains die at rate δ_R. Susceptible and bacteriostatic resistant bacteria can also die due to the activity of bacteriolytic antibiotic, which is modelled using Michaelis-menten kinetics. The reaction terms are given by

$$F_{A_s} = -\gamma_s A \tag{8.43}$$

$$F_{A_l} = -\gamma_l A \tag{8.44}$$

$$F_S = r\left(1 - \frac{N}{\varphi}\right) E_S S - S(\beta_s R_s + \beta_l R_l + \beta_u R_u) - \delta_S S - \delta_l S \frac{A_l}{MIC_l + A_l}, \tag{8.45}$$

$$F_{R_s} = r(1-\alpha_s)\left(1-\frac{N}{\varphi}\right)E_R R_s + R_s(\beta_s R_s - \beta_l R_l - \beta_u R_u) - \delta_R R_s - \delta_l R_s \frac{A_l}{MIC_l + A_l}, \tag{8.46}$$

$$F_{R_l} = r(1-\alpha_l)\left(1-\frac{N}{\varphi}\right)E_s R_l + R_l(-\beta_s R_s + \beta_l S - \beta_u R_u) - \delta_R R_l \tag{8.47}$$

and

$$F_{R_u} = r(1-\alpha_u)\left(1-\frac{N}{\varphi}\right)E_R R_u + R_s R_l(\beta_s + \beta_l) + \beta_u R_u(S + R_s + R_l) - \delta_R R_U. \tag{8.48}$$

Once again, the boundary conditions depend on the geometry of the system. Parameter values and definitions are shown in Table 8.3. In both the single and two-antibiotic models it is assumed that at $t = 0$ there are no antibiotics or bacteria in the tank.

As many of the parameters used in both the single-antibiotic and two-antibiotic models are the same as in previous chapters, there will be little discussion of model parameterisation here. Having established the governing equations for the two models, it is then possible to simulate them in one and two dimensions.

8.2 Results and Discussion

8.2.1 One dimensional modelling

The inflow pipe is initially assumed to have a diameter of 0.5m, meaning it has an area of approximately 0.196m^2. As before the inflow rate of slurry is initially assumed to be 0.613m^3 h^{-1}, which leads to an influent velocity of 3.122m h^{-1}. The velocity profile throughout the entire tank can then be calculated, the velocity profile is shown in Figure 8.4, in general, the velocity away from the outlet and inlet is approximately 0.01 m h^{-1}.

Though the finite-difference method is already stabilised using an upwinding discretisation, when running the model, it was found that the given values of D_A and D_B, combined with the the velocity profile shown in 8.4 led to numerical instabilities that stopped the model from converging. Two methods were used to stabilise the simulations: artificially increasing the cross-sectional area of the inflow pipe, reducing the influent velocity, and artificially increasing D_A and D_B, reducing the Péclet number and stabilising the simulations. Here these changes are referred to as "artificial" as they are known not to represent the true system and are made only to improve the stability of the numerical simulations. The increases to the cross-sectional area of the inlet and to the diffusion coefficients

Parameter	Description	Typical Value	Reference
r	Specific growth rate of *E. coli*	0.5 h^{-1}	[38]
β_s	Bacteriostatic-resistance gene transfer term	10^{-17} $m^3CFU^{-1}h^{-1}$	[38, 39, 123]
β_l	Bacteriolytic-resistance gene transfer term	10^{-17} $m^3CFU^{-1}h^{-1}$	[38, 39, 123]
β_u	MDR gene transfer term	10^{-17} $m^3CFU^{-1}h^{-1}$	[38, 39, 123]
λ	Rate of slurry inflow to tank	$613lh^{-1}$	[38]
ν	Concentration of bacteria in slurry inflow	6×10^{10} CFU m^{-3}	[38, 218]
ρ_s	Proportion of bacteriostatic-resistant bacteria in inflow	0.2	[204]
ρ_l	Proportion of bacteriolytic-resistant bacteria in inflow	0.2	[204]
ρ_u	Proportion of multidrug-resistant bacteria in inflow	0.0	[204]
α_s	Bacteriostatic-resistance fitness cost as a fraction of r	0.1	[38, 50]
α_l	Bacteriolytic-resistance fitness cost as a fraction of r	0.1	[38, 50]
α_u	MDR fitness cost as a fraction of r	0.1	[38, 50]
θ_s	Rate of bacteriostatic antibiotic inflow	1.711 mg h^{-1}	[38]
θ_l	Rate of bacteriolytic antibiotic inflow	1.711 mg h^{-1}	[38]
E_{max}	Maximum effect of antibiotics on bacterial growth	2	[38, 39]
H	Hill coeficient in E_{max} model	2	[38, 39]
MIC_R	MIC for bacteriostatic-resistant bacteria	2000 mg m^{-3}	[38]
MIC_S	MIC for bacteriostatic-sensitive bacteria	8 mg l^{-3}	[38]
MIC_l	MIC for bacteriolytic-sensitive bacteria	8 mg l^{-3}	[38]
μ	Carrying capacity of liquid slurry	10^{13} CFU m^{-3}	[38]
γ_s	Decay rate of bacteriostatic antibiotics	0.0029 h^{-1}	[38]
γ_l	Decay rate of bacteriolytic antibiotics	0.0029 h^{-1}	[38]
δ_S	Natural death rate of susceptible bacteria	0.001 h^{-1}	[187]
δ_R	Natural death rate of resistant bacteria	0.001 h^{-1}	[187]
δ_l	Antibiotic driven death rate of bacteriolytic-susceptible bacteria	0.01 h^{-1}	[213]
D_A	Antibiotic diffusion coefficient	3.6×10^{-5} m^2 h^{-1}	[273]
D_B	Bacterial diffusion coefficient	7.2×10^{-6} m^2 h^{-1}	
μ	Dynamic viscosity of slurry	$3492kg\ m^{-3}h^{-1}$	[182]
ρ	Density of slurry	1000 kg m^{-3}	

Table 8.3: Typical parameter values used for initial simulations of the two-antibiotic model.

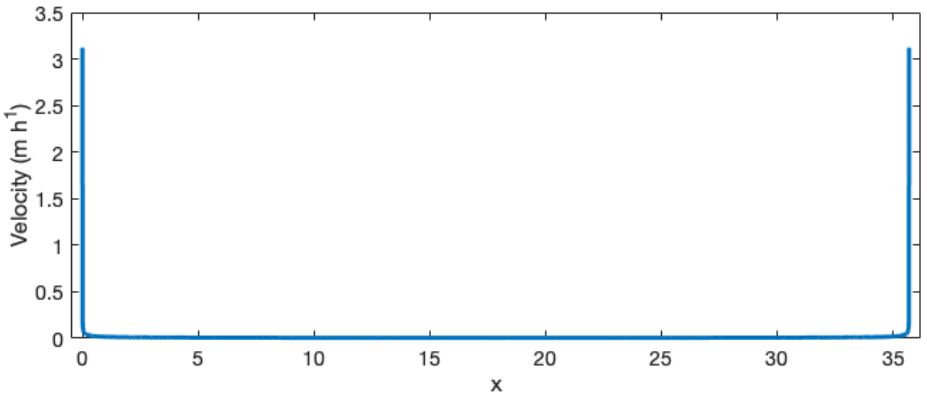


Figure 8.4: The velocity profile in the tank with a circular inflow pipe with a 0.5m diameter, calculated using equation 8.11.

were likely very unrealistic, but were performed to indicate how the model might be simulated. A binary search was performed to determine the lowest integer-value inlet area that led to numerical convergence whilst retaining the original values of D_A and D_B for varying Δt and Δx (the temporal and spatial step sizes, respectively). The results of these tests can be seen in Table 8.4. It appears that there is little interaction between inlet area size, spatial discretisation and simulation stability, but as Δt decreased, so did the inlet area required for model convergence. For the following simulations, the chosen values for temporal and spatial discretisation and inlet area were $\Delta t = 0.001$, $\Delta x = 0.5$ and $a_{in} = 6$, respectively. These values were chosen as there is a tradeoff to be made between inlet area size and the efficiency of running the simulations, especially over long timescales. This leads to the velocity profile shown in Figure 8.5.

		Δt			
		0.1	0.01	0.001	0.0001
Δx	0.5	51	17	6	2
	0.25	51	17	6	2
	0.125	51	17	6	2
	0.0625	51	17	6	2

Table 8.4: The minimum inlet area, a_{in} that led to convergence for varying values of the temporal and spatial step sizes, δt and δx, respectively.

On the other hand, to retain the original value of $a_{in} = 0.5$, the lowest values of D_A and D_B that led to convergence were $D_A = 3.6 \times 10^{-2}$ and $D_B = 7.2 \times 10^{-3}$. Both the increase in a_{in} and the increase in diffusion coefficients serve to decrease the Péclet number and hence improve the stability of the simulations.

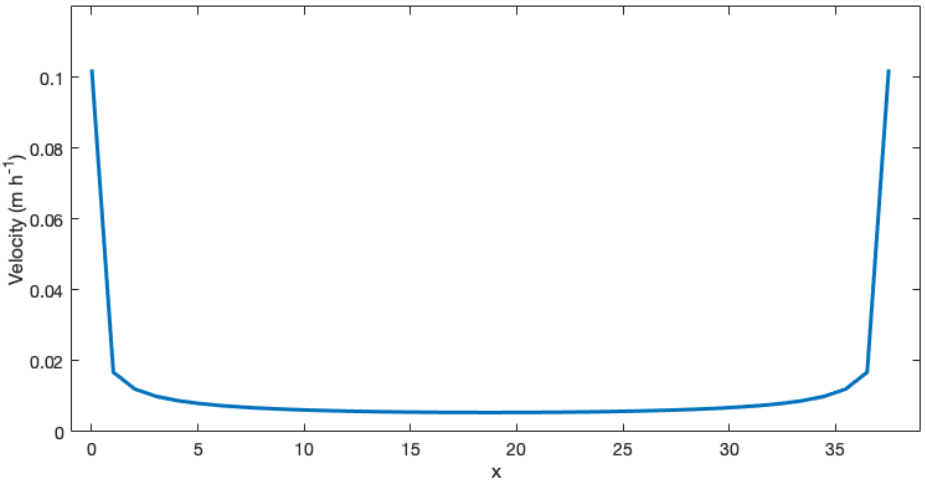


Figure 8.5: The velocity profile in the tank with a circular inflow pipe with a 3m diameter, calculated using equation 8.11.

Single-antibiotic model

Figure 8.6 shows the concentrations of S and R, simulated with increased diffusion. A front of susceptible bacteria moves through the tank over the first 250 hours. As the population of resistant bacteria at the inflow slowly grows, driven by selective pressure from the antibiotic concentration at the inlet, this growing population then begins to spread throughout the entire tank, and by $t = 5000$h, resistant bacteria make up the largest proportion of the population at every point along the tanks length. Given the tank volume and slurry velocity at the centre of the tank, the expected residence time for a non-reactive substance would be approximately 5000h, given how quickly the front of susceptible bacteria moves through the tank, this indicates that bacterial growth has more effect on the spread of bacteria than advection or diffusion.

Figure 8.7 shows the distribution of A in the tank over time with increased diffusion. The concentration peaks at the influent boundary, then the concentration grows slowly through the tank over time. By $t = 8000$h, the antibiotic concentration is around zero along the latter half of the tank.

Figures 8.8 and 8.9 show the bacterial and antibiotic concentration over time with decreased influent velocity, respectively. The results are similar to the increased diffusion case, though in general the bacterial fronts move more slowly through the tank, and the antibiotic makes it less far along the tank before being fully removed. Both the slowing of the bacterial fronts and the reduced distance travelled by the antibiotic are likely due to the lower diffusion in these simulations.

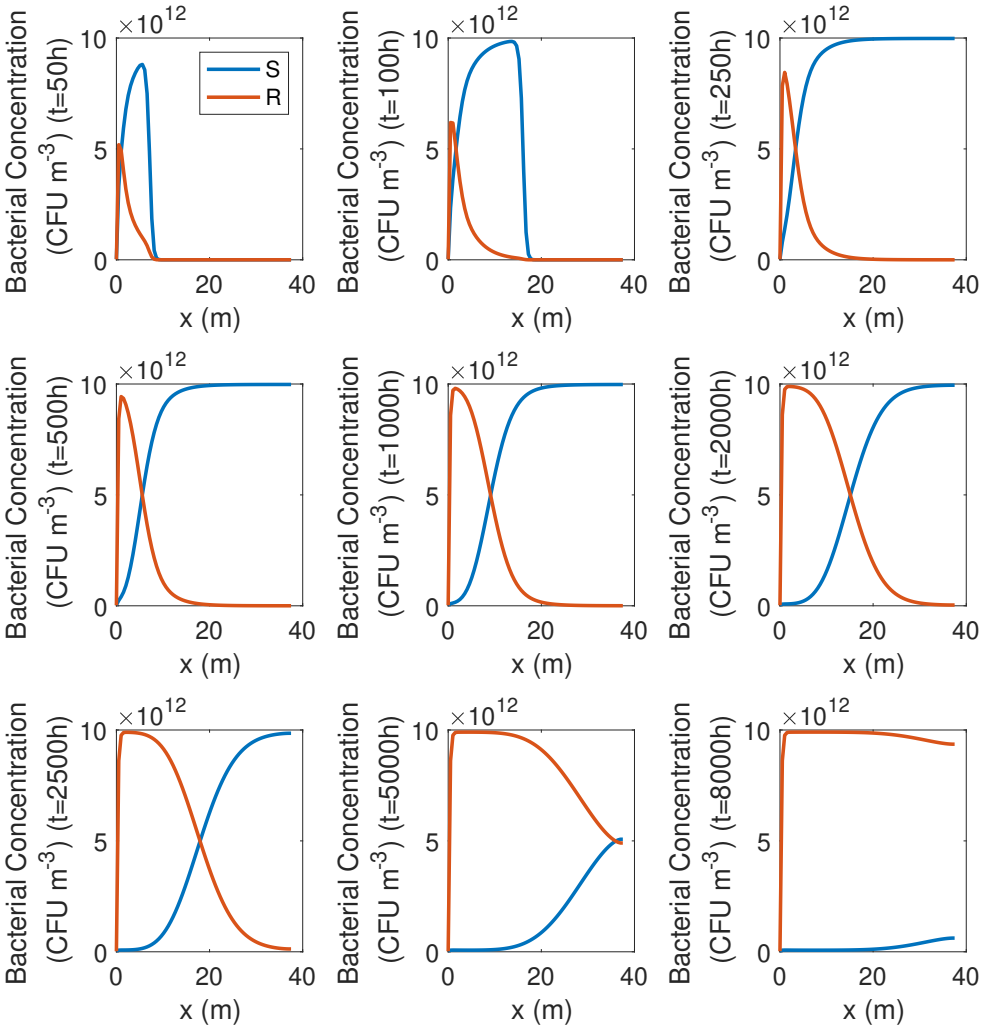


Figure 8.6: The concentrations of susceptible and resistant bacteria (S in blue and R in red) over time in the one dimensional, single-antibiotic model, where the diffusion coefficients, D_A and D_B, have been artificially increased to $D_A = 3.6 \times 10^{-2}$ and $D_B = 7.2 \times 10^{-3}$, to increase the stability of the simulation.

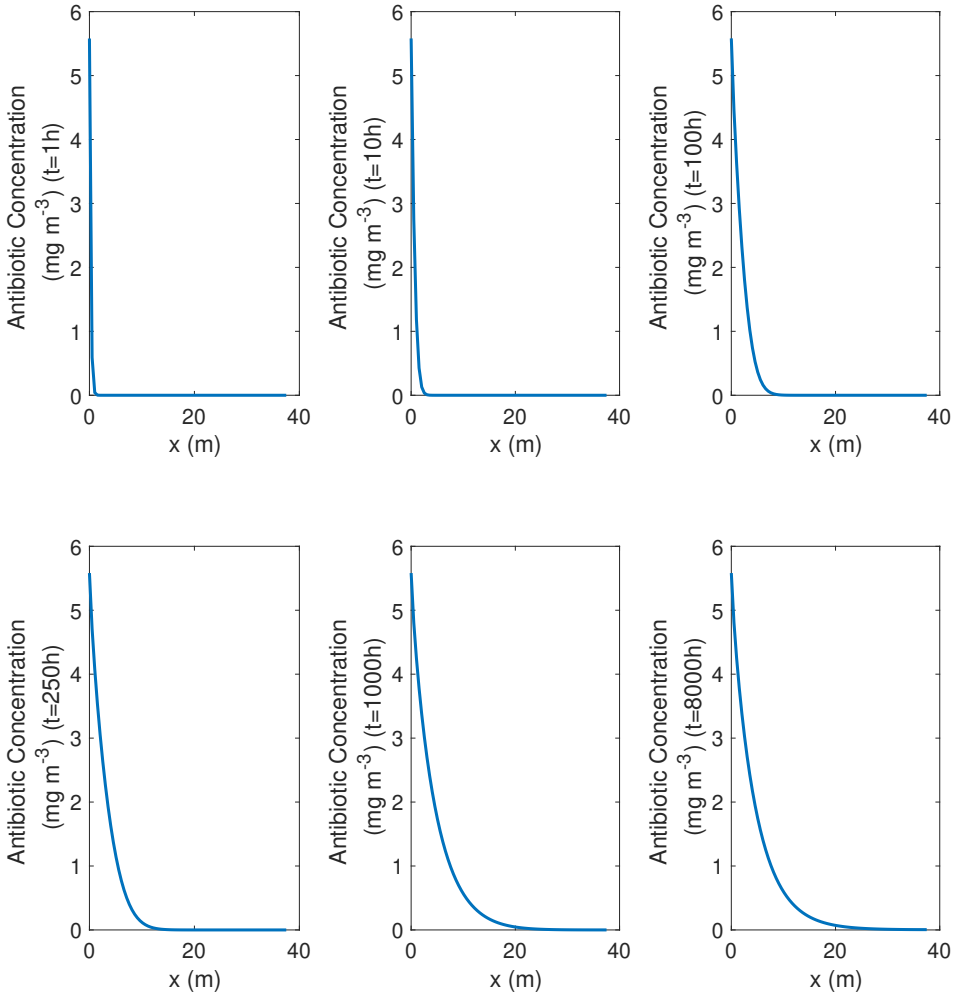


Figure 8.7: The concentration of antibiotic (A) over time in the one dimensional, single-antibiotic model, where the diffusion coefficients, D_A and D_B, have been artificially increased to $D_A = 3.6 \times 10^{-2}$ and $D_B = 7.2 \times 10^{-3}$, to increase the stability of the simulation.

Two-antibiotic model

In the case of the two antibiotic model, due to the parameter choices, the total antibiotic concentration ($A_s + A_l$) is the same as the concentration of A in the one antibiotic model, with $A_s = A_l = A/2$. Therefore, Figures 8.7 and 8.9 can be used as references for the antibiotics in the two-antibiotic model, in the increased diffusion and decreased velocity cases, respectively.

In terms of bacterial concentration, the increased diffusion and decreased influent velocity cases once gain yield similar results after 8000 hours (shown in Figures 8.10 and 8.11, respectively). However, in the case where a_{in} has been increased, there is larger population of R_s throughout the simulation. This may

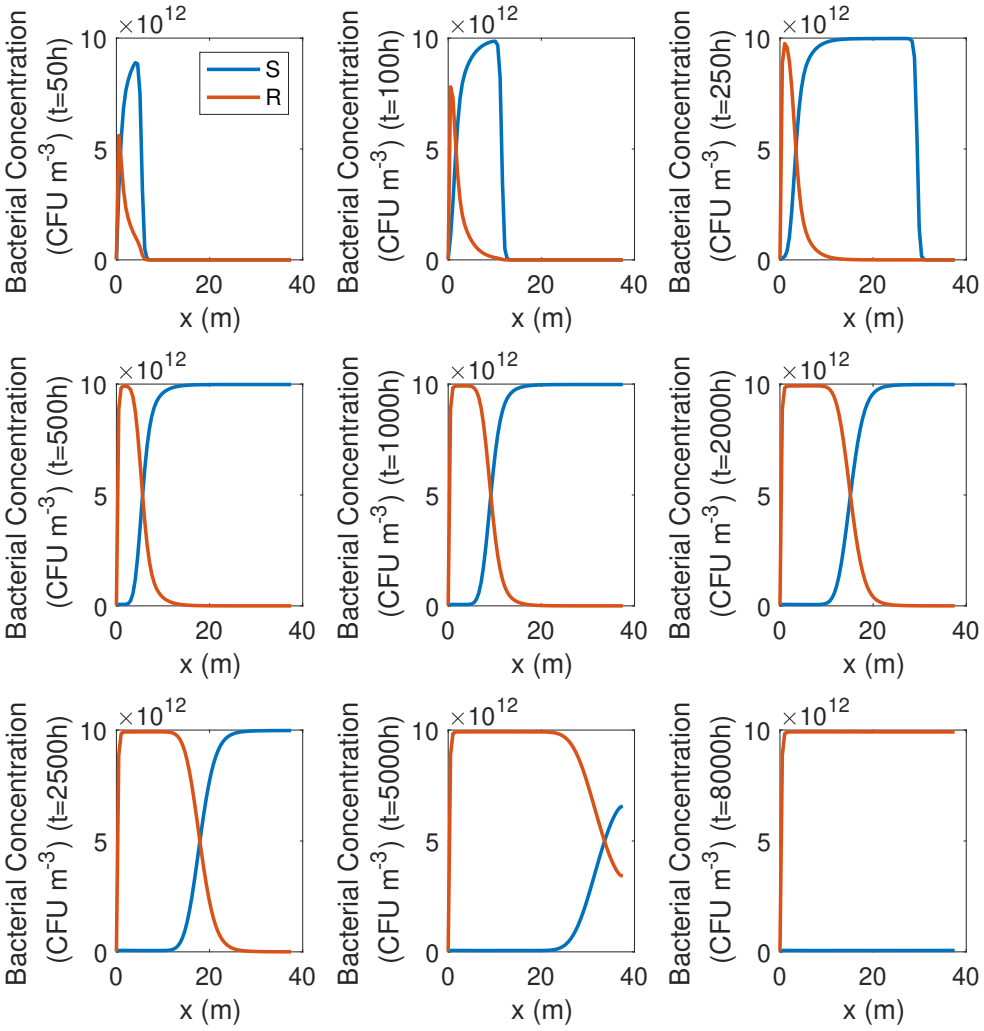


Figure 8.8: The concentrations of susceptible and resistant bacteria (S and R) over time in the one dimensional, single-antibiotic model, where the area of the inflow pipe has been artificially increased to 6m^2, to increase the stability of the simulation.

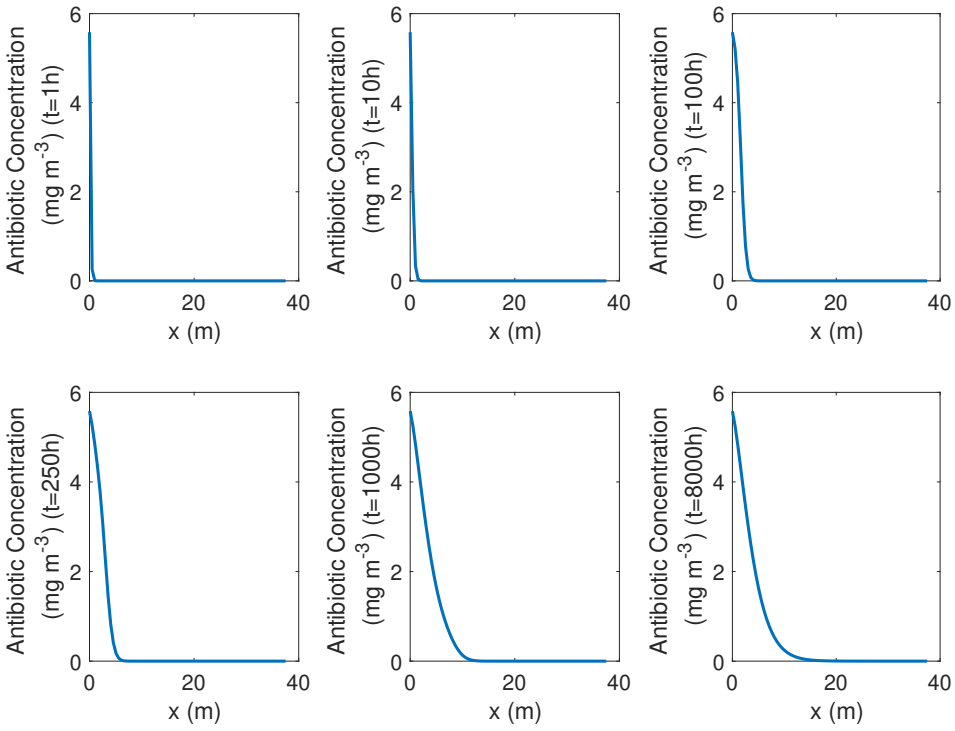


Figure 8.9: The concentration of antibiotic (A) over time in the one dimensional, single-antibiotic model, where the area of the inflow pipe has been artificially increased to 6m^2, to increase the stability of the simulation.

be due to the difference in antibiotic distribution, as in the increased a_{in} case, the antibiotic moves more slowly through the tank, so that away from the inlet, R_s bacteria are less likely to be inhibited. Once again, in the increased diffusion case the fronts of bacteria move more quickly and at $t = 8000$h, there is a greater concentration of R_s, R_l and S than in the decreased influent velocity case. Multidrug bacteria dominating the tank occurs faster than in the ODE model from Chapter 5, this may be due to the increased concentration of antibiotic at the inlet (compared to the average concentration in the ODE model), which increases environmental pressure for AMR to develop. Once multidrug resistance develops it then moves quickly through the tank, aided by the flow regime.

8.2.2 Two dimensional modelling

Single-antibiotic model

The governing equations were solved using FEniCS [287]. FEniCS is an open source program used for solving PDEs, which interfaces with Python. FEniCS solves PDEs in their variational formulation (in the case of this thesis, the weak formulation). Various mesh sizes and values of Δt were tested. The best result

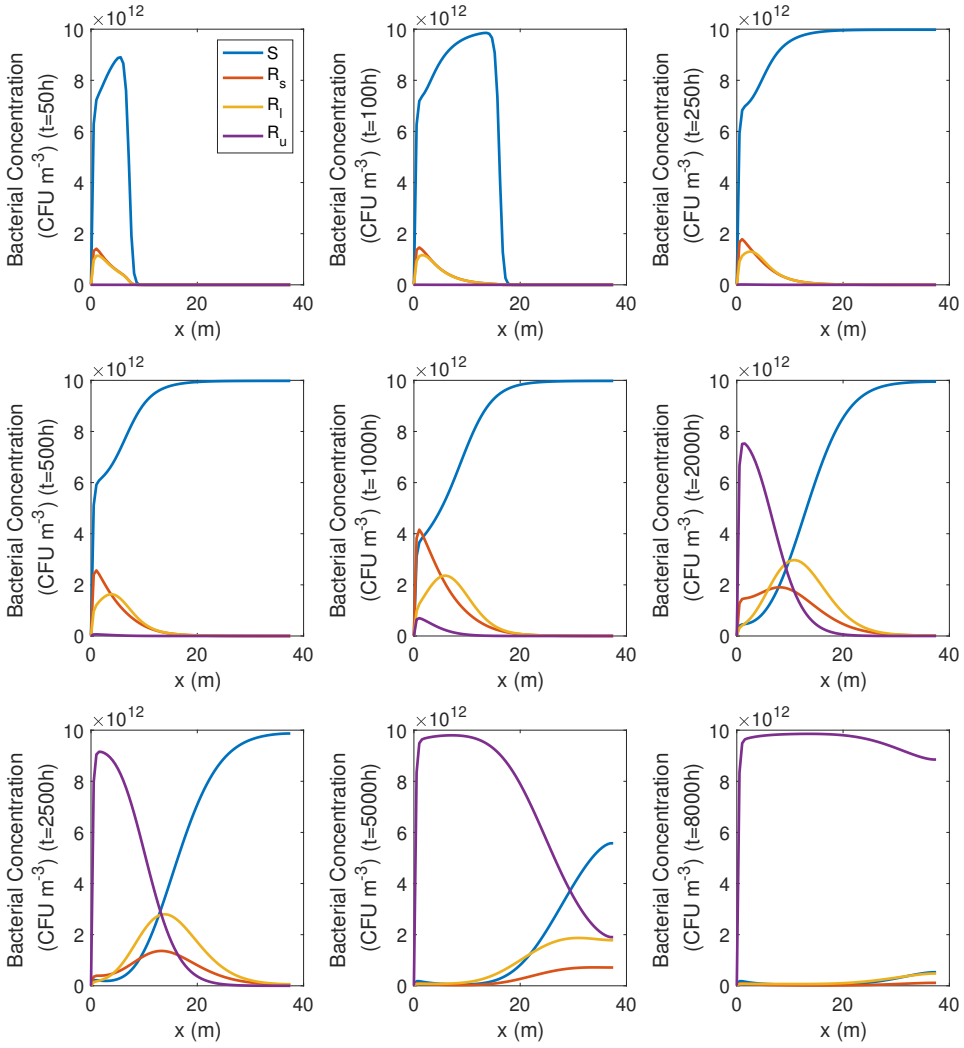


Figure 8.10: The concentrations of susceptible, bacteriostatic-resistant, bacteriolytic-resistant and multidrug-resistant bacteria (S, R_s, R_l and R_u, respectively) over time in the one dimensional, two-antibiotic model, where the diffusion coefficients, D_A and D_B, have been artificially increased to $D_A = 3.6 \times 10^{-2}$ and $D_B = 7.2 \times 10^{-3}$, to increase the stability of the simulation.

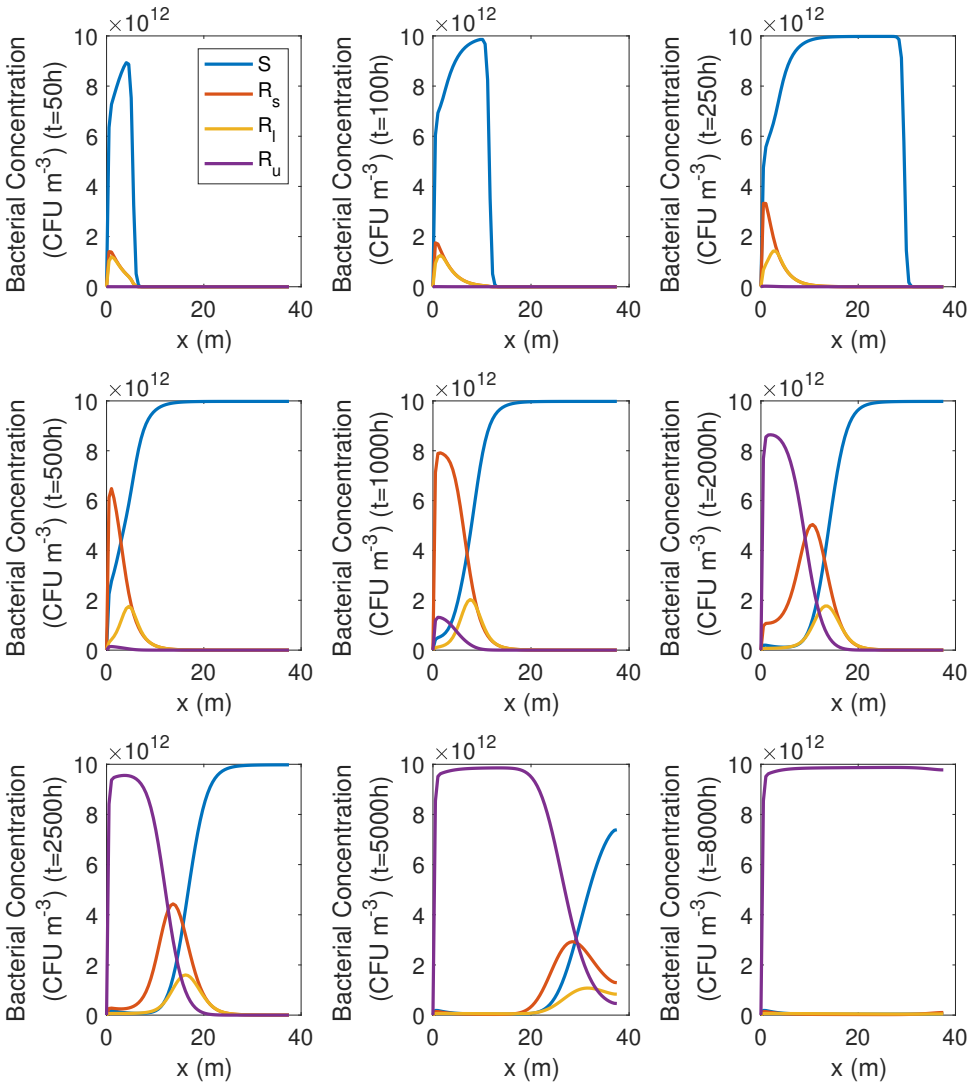


Figure 8.11: The concentrations of susceptible, bacteriostatic-resistant, bacteriolytic-resistant and multidrug-resistant bacteria (S, R_s, R_l and R_u, respectively) over time in the one dimensional, two-antibiotic model, where the area of the inflow pipe has been artificially increased to 6m^2, to increase the stability of the simulation.

(or the result that converged over the longest timescale) led to the system failing to converge at $t = 23$h, and was achieved with a mesh of approximately 512 cells across the diameter of the tank. Finer meshes than this were incredibly time intensive or would lead to memory faults in FEniCS. The results are shown in Figure 8.12. It should be noted that the results up until system fails to converge should not be considered accurate as, throughout the simulations, large numerical oscillations occurred. These oscillations are visible in Figure 8.13. Such oscillations are common when simulating high Péclet number flows and at prescribed concentration boundaries or fronts [72, 289]. These oscillations arise from numerical errors during computation. In this model, there is a discontinuity at the inlet as bacteria and antibiotics enter the tank which may be contributing to these numerical errors. The Péclet number is given by

$$P_e = LU/D \tag{8.49}$$

where L is a characteristic length, U is a characteristic velocity and D is the diffusion coefficient. At the inflow of the tank, where the characteristic length is 0.5m and the characteristic velocity is 1.226m h^{-1}, the Péclet numbers for antibiotics and bacteria are $P_{eA} \sim 16666$ and $P_{eR} \sim 83333$, respectively. This means that in both cases the system is advection driven.

In order to reduce these numerical oscillations and in an attempt to generate a solution which converges, two stabilisation techniques were implemented: a Streamline Upwind Petrov Galerkin (SUPG) scheme, and artificially increased diffusion. The SUPG scheme is explained below, and the increased diffusion approach is similar to that used in the one dimensional simulations discussed earlier in this chapter. In the case of the model described here, increasing diffusion (either along the streamlines as in SUPG or over the entire space) acts to smooth the discontinuity at the inlet as antibiotics and bacteria enter the tank.

Streamline Upwind Petrov Galerkin Stabilisation

As initial simulations led to large numerical oscillations, an SUPG. The SUPG scheme involves adding a weighted term to the equations as a kind of artificial diffusion [290] along the streamlines of the flow field and is often used in high Péclet number simulations of advection and diffusion. The additional terms are given by

$$\begin{aligned} r_A = \int_\Omega (\Delta t^{-1}(A^{n+1} - A^n)v_1 + \mathbf{u} \cdot \nabla A^{n+1} v_1 + D_A \nabla X^{n+1} \cdot \nabla v_1 - \\ F_{A^{n+1}} v_1) \tau (\mathbf{u} \cdot \nabla v_1) dx \end{aligned} \tag{8.50}$$

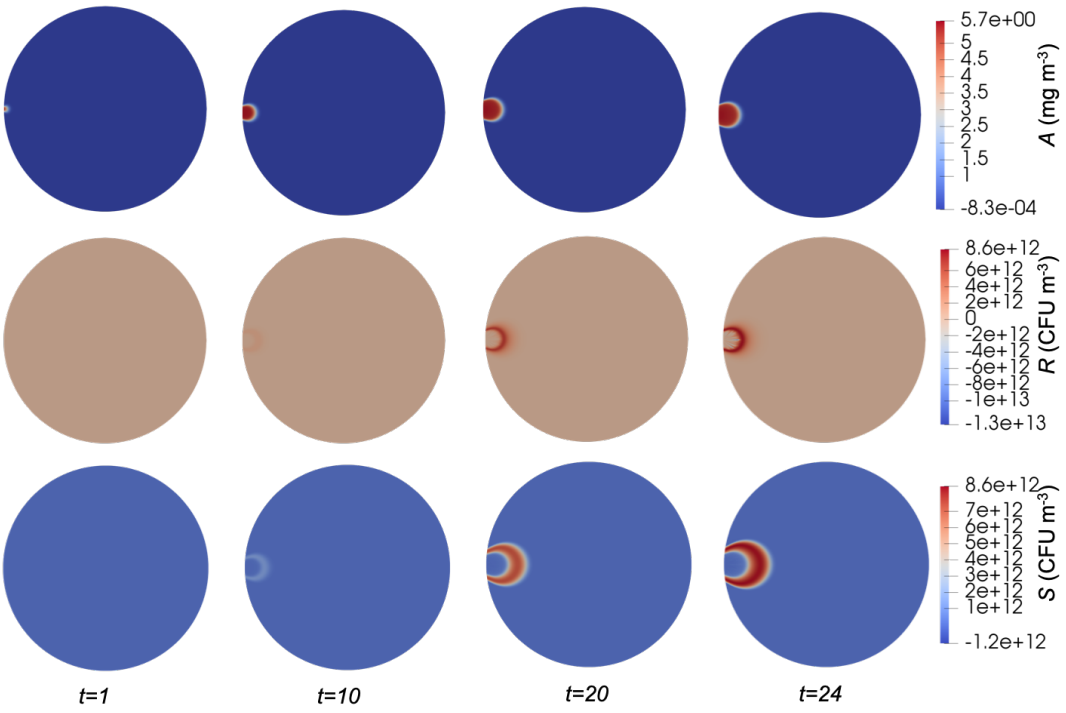


Figure 8.12: The concentrations of antibiotic and of susceptible and resistant bacteria (A, S and R) over time in the two dimensional, single-antibiotic model. The model failed to converge at $t = 24$h.

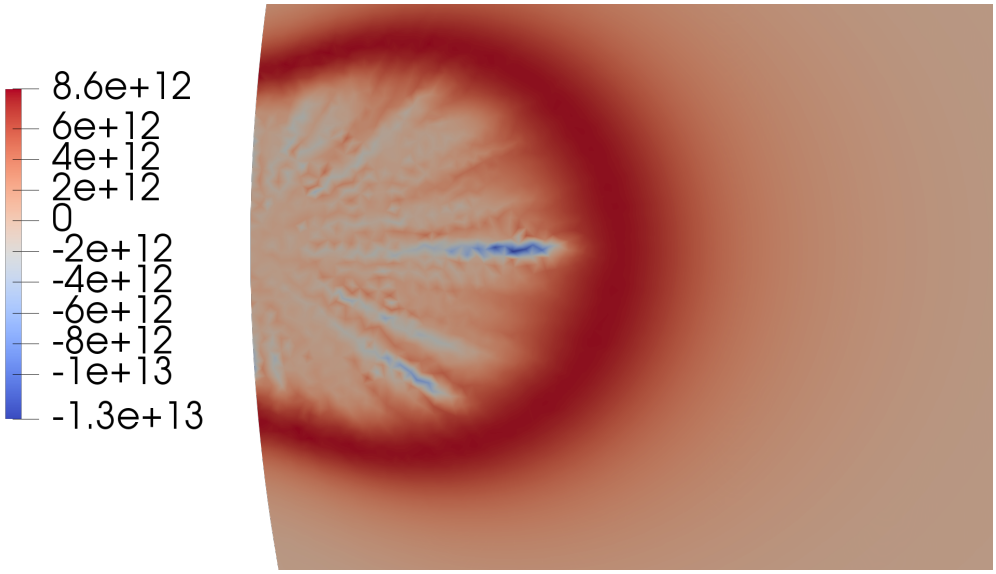


Figure 8.13: A close up of the concentration of resistant bacteria at the inflow of the tank in the two dimensional, single-antibiotic model, showing large numerical oscillations.

$$r_R = \int_\Omega \Delta(t^{-1}(R^{n+1} - R^n)v_2 + \mathbf{u} \cdot \nabla R^{n+1} v_2 + D_R \nabla R^{n+1} \cdot \nabla v_3 - F_{R^{n+1}} v_2)\tau(\mathbf{u} \cdot \nabla v_2)dx \tag{8.51}$$

$$r_S = \int_\Omega \Delta(t^{-1}(S^{n+1} - S^n)v_3 + \mathbf{u} \cdot \nabla S^{n+1} v_3 + D_S \nabla S^{n+1} \cdot \nabla v_1 - F_{S^{n+1}} v_3)\tau(\mathbf{u} \cdot \nabla v_3)dx \tag{8.52}$$

where τ_A and τ_B are the SUPG weighting functions. These weight functions are user defined [291]. Various weighting functions were tested, but the results presented in this chapter were generated using the following values:

$$\tau_A = \frac{h^2}{4(2D_A + \|\mathbf{u}\|h)} \tag{8.53}$$

and

$$\tau_R = \frac{h^2}{4(2D_R + \|\mathbf{u}\|h)}, \tag{8.54}$$

where h is the diameter of a cell within the mesh.

The SUPG scheme does improve overall stability of the solution (the system fails to converge at $t = 29$h rather than $t = 23$h in the non-stabilised case), but there are still large numerical oscillations within the system. The results are the simulation are shown in Figure 8.14 and as before, the numerical oscillations are visible in Figure 8.15.

Artificial diffusion

In order to both determine whether the instabilities in the simulation were caused by the high Péclet number or by some other factor, the diffusion coefficients for antibiotics, D_A and D_B, were artificially increased. The diffusion coefficients were both simultaneously increased by an order of magnitude (maintaining the 10 to 1 ratio of D_A to D_B), then the model was run from $t = 0$ to $t = 2500$ h (chosen due to time restrictions) and the results were recorded. This was repeated four times, so that on the last model run $D_A = 3.6 \times 10^{-1}$ and $D_B = 3.6 \times 10^{-2}$.

The effects of increasing the diffusion (without SUPG stabilising) are as follows:

- Increased one order of magnitude ($D_A = 3.6 \times 10^{-4},\ D_B = 3.6 \times 10^{-5}$): Simulations fail to converge at $t = 32$ hours.

- Increased two orders of magnitude ($D_A = 3.6 \times 10^{-3},\ D_B = 3.6 \times 10^{-4}$): Simulation runs to at least $t = 2500$ hours, with large spurious oscillations (same order of magnitude as bacterial concentration), including greater concentrations of R and S than allowed by the model. R makes up a

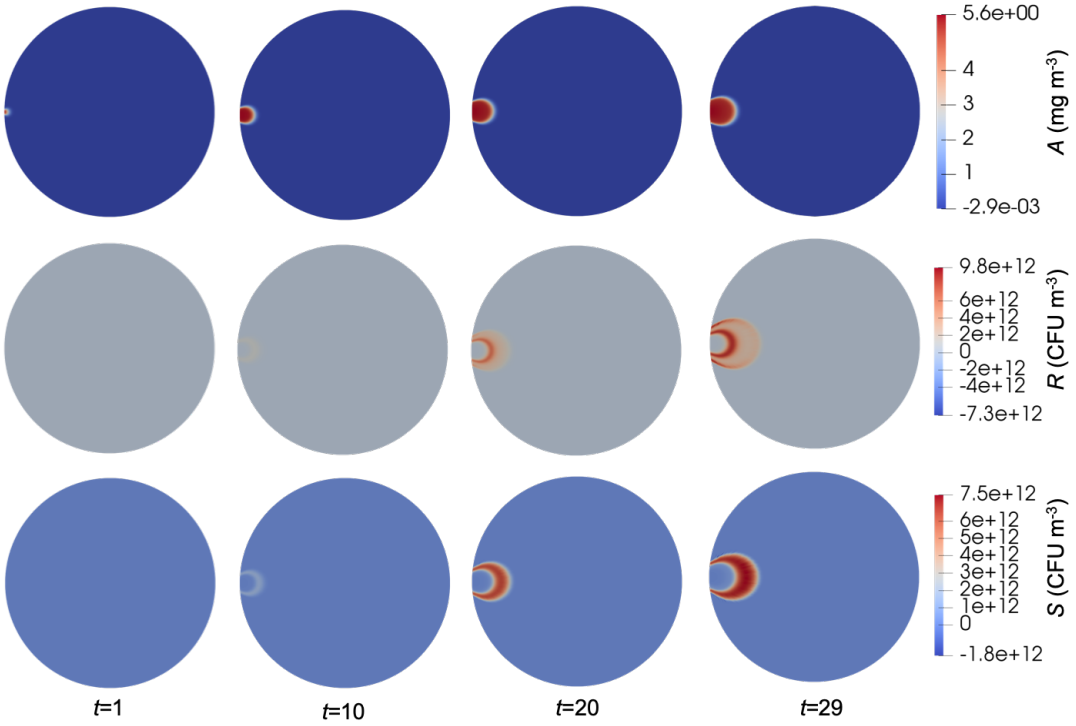


Figure 8.14: The concentrations of antibiotic and of susceptible and resistant bacteria (A, S and R) over time in the two dimensional, single-antibiotic model, stabilised using a Streamlined Upwind Galerkin Method. The model failed to converge at $t = 29$h.

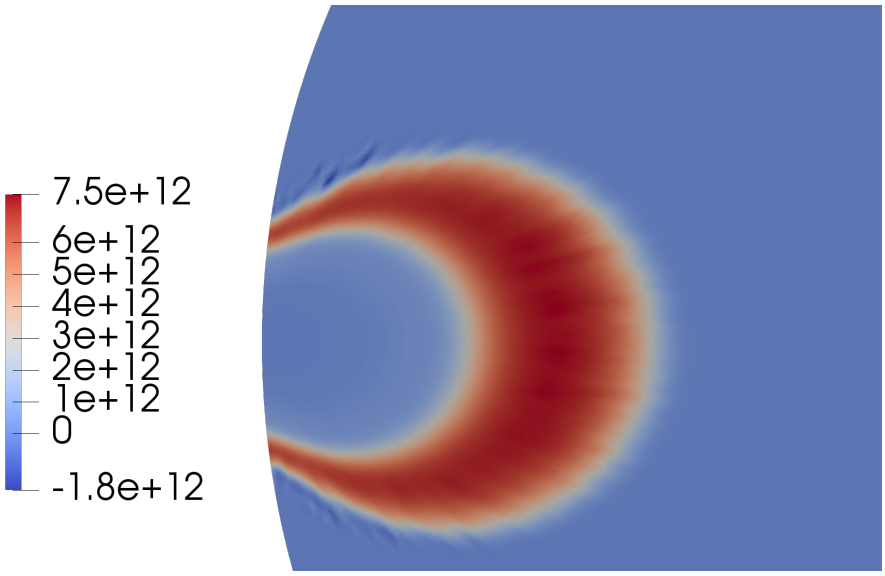


Figure 8.15: A close up of the concentration of susceptible bacteria at the inflow of the tank, in the two dimensional, single-antibiotic model, stabilised using a Streamlined Upwind Galerkin Method, showing large numerical oscillations.

large proportion of the tank, though there are pockets where susceptible populations still exist.

- Increased three orders of magnitude ($D_A = 3.6 \times 10^{-2},\ D_B = 3.6 \times 10^{-3}$):

Simulation runs to at least t=2500 hours, with small spurious oscillations (ten orders of magnitude smaller than bacterial concentration).

- Increased four orders of magnitude ($D_A = 3.6 \times 10^{-1}$, $D_B = 3.6 \times 10^{-2}$): Simulation runs to at least t=2500 hours, with no spurious oscillations, R dominates the tank by the end of the simulation.

Figure 8.16 shows the model simulated with $D_A = 0.36$ and $D_B = 0.072$. There are no spurious oscillations and the simulation converges at all time points. Similar to the simulations in one-dimension, susceptible bacteria initially dominate the tank before a spreading wave of resistant bacteria moves through the tank, the top and bottom right areas (above the outflow) are the last locations to change from mostly susceptible bacteria to mostly resistant.

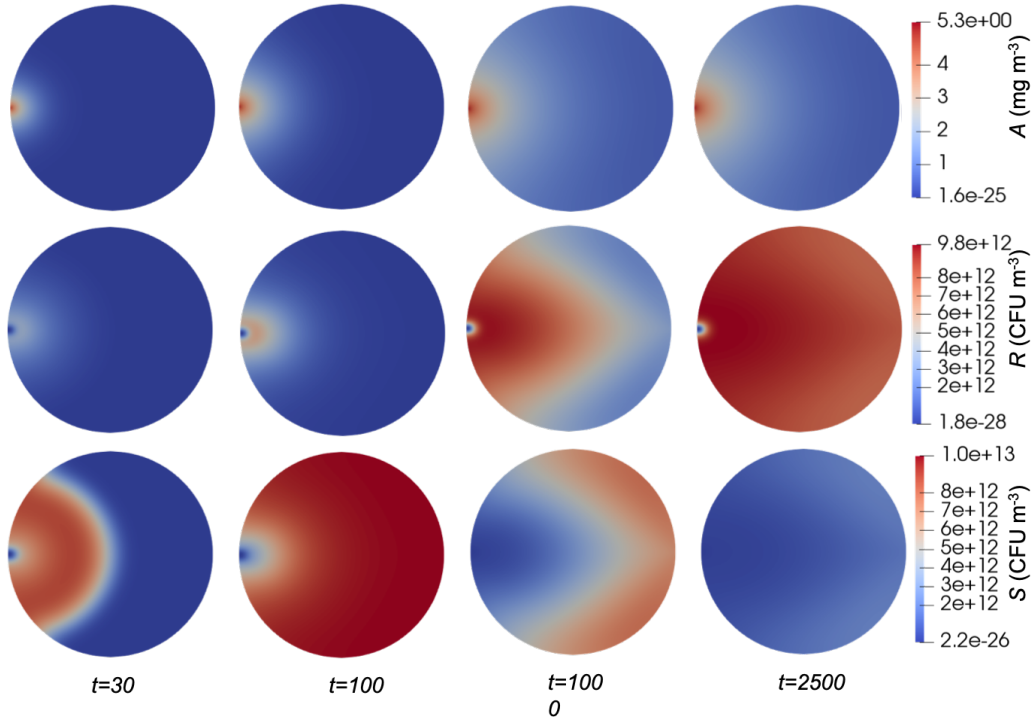


Figure 8.16: The concentrations of antibiotic and of susceptible and resistant bacteria (A, S and R) over time in the two dimensional, single-antibiotic model, where the diffusion coefficients, D_A and D_B, have been artificially increased to $D_A = 3.6 \times 10^{-1}$ and $D_B = 3.6 \times 10^{-2}$, to increase the stability of the simulation.

The 2D simulation produces qualitatively similar results to the 1D simulation with the same diffusion coefficients, shown in 8.17. In the 1D system the early development of resistant bacteria is faster, but the eventual takeover of the tank by resistant bacteria occurs more slowly. Though it was not possible to run the 2D model with realistic diffusion coefficients, this indicates that the 1D simulation

could potentially be used to estimate the behaviour of the 2D system at lower values of the diffusion coefficients.

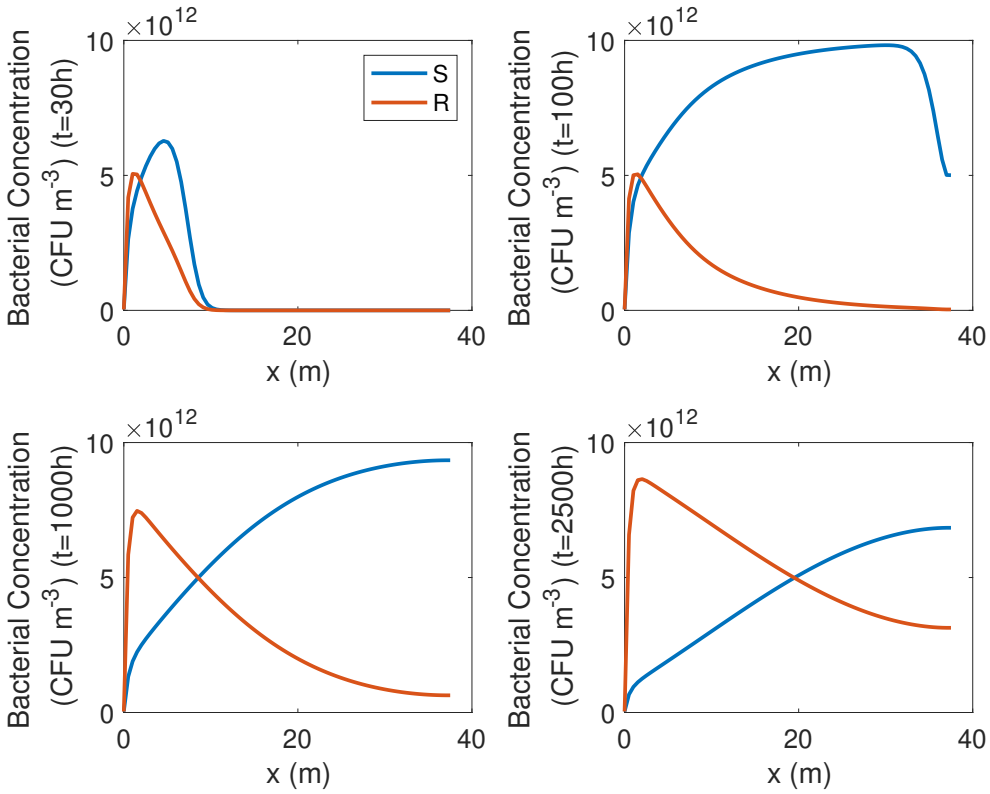


Figure 8.17: The concentrations of antibiotic and of susceptible and resistant bacteria (A, S and R) over time in the one dimensional, single-antibiotic model, where the diffusion coefficients, D_A and D_B, have been artificially increased to $D_A = 3.6 \times 10^{-1}$ and $D_B = 3.6 \times 10^{-2}$, to increase the stability of the simulation.

Two-antibiotic model

As in the single-antibiotic model, the simulations do not converge in the case where $D_A = 3.6 \times 10^{-5}$ and $D_B = 3.6 \times 10^{-6}$, both with and without SUPG stabilisation. Increasing the diffusion coefficients to $D_A = 3.6 \times 10^{-1}$, $D_B = 3.6 \times 10^{-2}$ allows the simulation to run without diverging, but still leads to large numerical oscillations. This is likely due to the reduction in mesh density, as a lower mesh density also led to more instability in the single-antibiotic case. A simulation with artificially increased diffusion is shown in Figure 8.18. As before, the velocity field at $t = 50$h was used. Similar to the 1D model, susceptible bacteria dominate the tank at first, then bacteriolytic-resistant bacteria, which eventually begin to give way to multidrug-resistant bacteria. A 1D simulation was done with the same diffusion coefficients for comparison, shown in Figure 8.19. The dynamics are similar, but multi-drug resistant bacteria are more prevalent

at $t = 8000$h in the 1D case than in the 2D case. Once again indicating that the 1D case may reasonably approximate the overall dynamics of the system.

8.2.3 Discussion

Simulations in both one and two dimensions were prone to non-convergence. Furthermore, simulations required significant computational time, especially in the 2D case, which also exhibited numerical oscillations. In both the 1D and 2D cases measures were taken to reduce these instabilities, including introducing artificial diffusion, altering the mesh size, upwinding, and the SUPG methods. Instabilities and numerical oscillations are a well known problem when simulating high Péclet number advection-diffusion models [72], especially in cases of highly variable concentration fields, as is true of this model. As expected, a high density spatial mesh and the addition of artificial diffusion led to increased stability. However this additional diffusion increases the speed at which both antibiotics and microbes move through the tank. The modelling predicts qualitatively similar results to the ODE model presented in Chapter 5 and in the model developed by Baker et al. [38]. An interesting aspect of both the PDE model and the settling model is that, under the given parameter conditions, they predict that antibiotics are removed from the slurry by the time it reaches the effluent. However, antibiotics have been found in slurry storage effluent [200]. This discrepancy could be due to a difference in the retention time within the tank, the omission of mixing in this model, or differences in the degradation rate of the antibiotics.

A number of assumptions about the physical characteristics of the slurry tank environment were made in order to simplify the model equations. These included an equal inflow and outflow of slurry, so that the volume of slurry in the tank was constant; no mixing in the tank other than by fluid flow, which simplified the velocity field; the assumption that the slurry is a newtonian fluid, once again simplifying the fluid flow dynamics; finally, no settling dynamics were considered within the model, so that the density and viscosity of slurry remain constant throughout the tank. It is very unlikely that inflow and outflow of slurry in the tank is constant, as the tank fills throughout the day whereas it is emptied either when slurry is to be used for muck spreading or when the tank is approaching capacity. The model presented here could simulate time dependent filling and emptying, by implementing flow boundary conditions that vary with time. However, in order to model non-equal influent and effluent rates would require considering more complicated fluid dynamics, such as free surface equations. The free-surface equations could be avoided by incorporating a floating lid (a feature in some slurry tanks), so that the top layer of fluid can be modelled as flat.

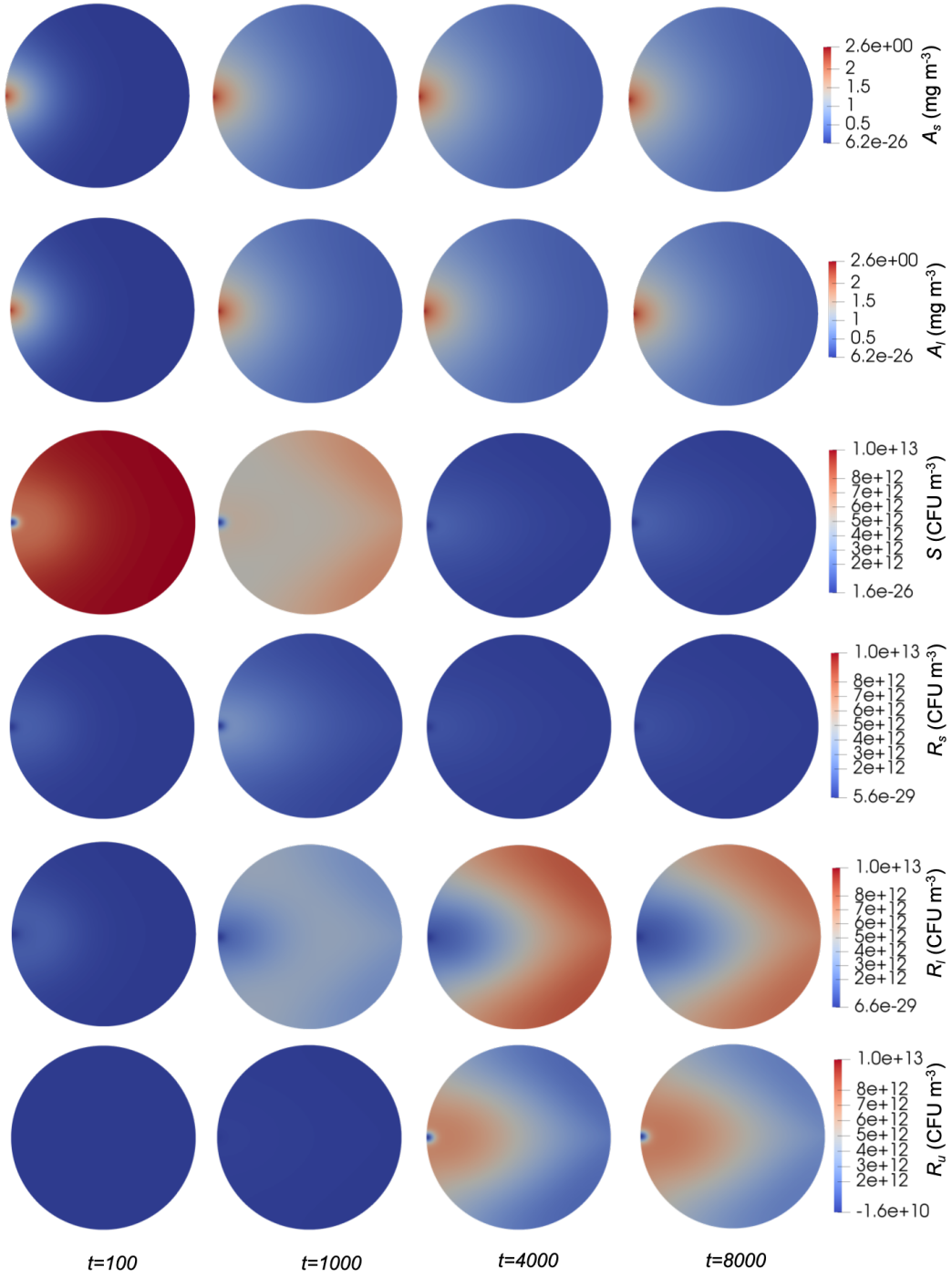


Figure 8.18: The concentrations of the bacteriostatic and bacteriolytic antibiotic and susceptible, bacteriostatic-resistant, bacteriolytic-resistant and multidrug-resistant bacteria (A_s, A_l, S, R_s, R_l and R_u, respectively) over time in the two dimensional, single-antibiotic model, where the diffusion coefficients, D_A and D_B, have been artificially increased to $D_A = 3.6 \times 10^{-1}$ and $D_B = 3.6 \times 10^{-2}$, to increase the stability of the simulation.

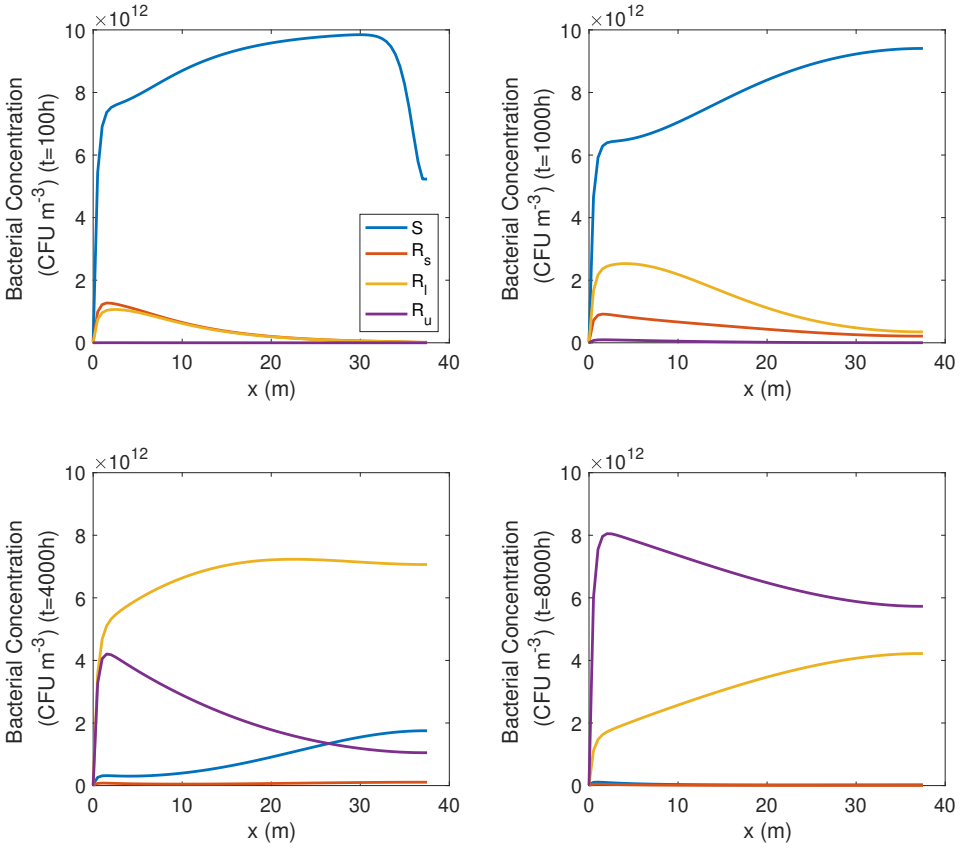


Figure 8.19: The concentrations of the bacteriostatic and bacteriolytic antibiotic and susceptible, bacteriostatic-resistant, bacteriolytic-resistant and multidrug-resistant bacteria (A_s, A_l, S, R_s, R_l and R_u, respectively) over time in the two dimensional, single-antibiotic model, where the diffusion coefficients, D_A and D_B, have been artificially increased to $D_A = 3.6 \times 10^{-1}$ and $D_B = 3.6 \times 10^{-2}$, to increase the stability of the simulation.

The mixer attached to the tank at Sutton Bonington is mounted on the side of the slurry tank. To model this, the best approach would likely be a 3D model, which would require even more computing power than the 2D model, but would be able to account for dynamics such as the rotor mixer. The most complete model would also incorporate settling dynamics.

To attain results in both the one- and two-dimensional cases diffusion had to be increased to achieve simulation stability, which brings the results of both systems into question. Furthermore, the assumption of continuous filling and emptying, which is unrealistic for the slurry tank, will also be affecting the results. Both the 1D and 2D models were relatively time-intensive to run, furthermore the stability of the 1D model was highly sensitive to parameter values within the range suggested by the literature and from the inference performed in previous chapters, meaning that it would not converge. This made sensitivity analysis or

further parameter estimation unfeasible at the time of writing.

8.3 Summary

In this chapter an ADR framework for modelling AMR in the slurry environment is presented. Two models are discussed, a single-antibiotic model, with reaction dynamics based on the Baker et al. model [38], and a two-antibiotic model, with reaction dynamics based on the model detailed in Chapter 5. These models were then simulated in one and two dimensions, using a finite difference scheme and a finite element scheme, respectively. The fluid velocity dynamics were calculated using the continuity equations in the 1D case and the Navier-Stokes equations in the 2D case.

In both the 1D and 2D cases there were problems with numerical stability, likely due to the high Péclet number and the front of bacteria and antibiotics at the inlet of the tank. Various stabilisation methods were used to attempt to solve eliminate these instabilities, including upwinding (in the 1D case), changes to the timestepping regime and the mesh discretisation, increasing the overall rate of diffusion of both antibiotics and bacteria, decreasing the velocity at the inlet (in the 1D case) and using an SUPG scheme (in the 2D case). Increasing diffusion led to solutions that converged in both systems, but increased the speed at which bacteria and antibiotics moved through the tank. Likely in an unrealistic way. For future work, alternative stabilisation methods could be implemented. One possibility might be to introduce a finer spatial mesh at the influent whilst retaining a coarser mesh throughout the rest of the tank [72]. This might reduce the numerical instability caused by the front of antibiotics and bacteria, whilst reducing the computing power required compared to a uniformly fine mesh over the entire space. Another option in the 2D case could be to use discontinuity capturing [289], which is known to reduce oscillations in situations where streamline diffusion is not sufficient for stability.

Despite problems with model stability, it was possible to generate some simulations of the problem. The model predictions are similar to those from previous chapters. Using parameter values from the literature, it is predicted that resistant bacteria dominate the tank, specifically multi-drug resistant bacteria in the two-antibiotic case. Simulations show that bacterial growth contributes more to the spread of AMR through the tank than advection or diffusion. However, given the assumptions made in this chapter and the problems with model stability, no conclusions should be drawn from the results. It is possible that the PDE model could adapted to different geometries and media where continuous flow is a more reasonable assumption. In fact, the framework of this model might be better

suited to a different problem, such as the flow of hospital waste through sewer pipes, where dynamics such as settling, open air storage and mixing are likely to be less prevalent.

Chapter 9

Conclusion

The aim of this thesis was to develop and test new models of agricultural antimicrobial resistance (AMR), specifically focussed on dairy farm slurry storage. To do this, and following the objectives set out in the introduction of this thesis, a literature review was performed, data was collected from farms and slurry tanks across Great Britain as part of the Should We Worry About Slurry (SWWAS) project and from this information a conceptual model of the AMR in the slurry tank was developed. Following this, an ordinary differential equation (ODE) model was developed based on the models in [38,39], this model then contributed to the development of two more models which included solid settling and fluid flow dynamics. These models were then used to identify possible AMR risk factors and hopefully illuminate new areas of research and data collection. The key risk factors investigated via modelling were the use of bacteriolytic and bacteriostatic antibiotics and the effects of the slurry storage regime. The SWWAS project also investigated heavy metal concentration, antibiotic residue concentration and a number of farm practice factors. The models were also used to assess the effects of varying model assumptions on the feasibility of modelling and improvements to knowledge gained by the model. In some places increased mathematical complexity led to interesting insights to the problem, whereas in others, increased complexity made simulating the problem much more difficult, and made it difficult to derive new knowledge. This may have been due to the choices of which model elements to make more complex, or may be that earlier, simpler models, had reached a good balance between complexity and informativeness.

Through field research and the development of new mathematical models, the persistence and spread of AMR in the dairy slurry tank has been investigated. The SWWAS project documented the presence of extended spectrum β-lactamase producing (ESBL), colistin resistant and carbapenem resistant *E. coli* across the country, alongside a survey of farm processes and heavy metal content in dairy slurry. ESBL *E. coli* was detected in the slurry tanks of 60% of the 15 farms

surveyed and three cefotaxime resistance genes, not previously detected in agriculture, were found. No carbapenem or colistin resistant *E. coli* were detected, which is promising, as carbapenem and colistin are considered last resort antibiotics [19, 20]. Antibiotic residue analysis indicated that the antibiotic at highest concentrations in slurry tanks is oxytetracycline. Cefoperazone was the most commonly detected antibiotic, but after conversations with the School of Pharmacy at the University of Nottingham, it appears that its detection may have been in error and could have been another molecule with a similar structure. Eight known co-selective heavy metals were also detected. Correlation analysis was performed to determine whether farm practices, antibiotic concentration or metal concentration correlated with the detection of ESBL *E. coli*. Weak correlations were found between ESBL detection and reported use of neomycin and kanamycin, herd size, disposal of waste milk into the slurry store and 10 of the heavy metals analysed. However, none of the correlations were statistically significant (either before or after a Bonferroni correction).

Using knowledge from SWWAS and the literature, a conceptual model of AMR in a working slurry tank was outlined. A new model of AMR in the slurry tank was then developed, encompassing farm process factors and bacterial sensitivity to both bacteriostatic and bacteriolytic antibiotics. The outputs of this model were then compared to data from a working dairy farm. Maximum likelihood estimation and Bayesian inference were used to infer model parameters. This model was then extended to incorporate greater complexity from two different sources: firstly solids-settling dynamics were incorporated into the model, and separately a PDE model was developed to investigate the effects of fluid flow on the development of AMR.

The first mathematical model developed, an ODE model, incorporated bacterial growth in the presence of bacteriostatic and bacteriolytic antibiotics. This model differed from previous models (and introduced more complexity), by including the two kinds of antibiotics and the filling and emptying regime of the tank. Analysis of this model led to the novel finding that the development of multidrug resistance may be more sensitive to the parameters associated with bacteriolytic antibiotic than those associated with bacteriostatic antibiotics. The results also indicated that increasing the intervals between emptying the tank and increasing the permanently stored fraction of slurry within the tank could both delay the development of multidrug-resistance. Steady state analysis of the model indicates that as the stored volume of slurry increased, the stable steady state transitions from multidrug resistant bacteria dominating the tank, to susceptible bacteria. This result implies that higher volume slurry storage solutions like slurry pits may be less risky in terms of environmental AMR than smaller

stores like slurry tanks.

Outputs from the ODE model were analysed alongside data from the University of Nottingham Sutton Bonington Campus dairy farm. Inference techniques were used to establish possible antibiotic and bacterial parameters for the model. One of the most interesting discoveries in this chapter, was that the functional carrying capacity of the slurry appears to be of a similar order of magnitude to the influent concentration of bacteria predicted from the literature. If the influent concentration is accurate this implies that the *E. coli* populations are not thriving in the slurry tank, as was assumed in previous models [38]. However, this doesn't speak to the prevalence of AMR amongst that reduced population. The data also shows that bacteriostatic antibiotics are more prevalent in the tank than bacteriolytic antibiotics, likely due to slower degradation in slurry. The rate of horizontal gene transfer (HGT) was also inferred from the data, the inferred values are higher than expected from the literature, though this may be due to the specific medium of dairy slurry.

The core of the ODE model was then incorporated into two new models: one which incorporated solid settling dynamics and antibiotic sorption in the tank, and another which modelled fluid flow in the tank alongside bacterial and antibiotic reaction mechanics. These models assume that the distribution of antibiotics and bacteria is spatially heterogenous and is determined by the antibiotic and bacterial properties alongside fluid flow and diffusion. Both of these models showed that antibiotic is likely being removed from the tank before it reaches the outflow. If this is the case, it would mean that slurry being spread onto croplands was not increasing the selective pressure in the soil environment. Antibiotic removal or persistence in the slurry tank could be measured by analysing antibiotic concentrations at the influent and effluent of slurry stores over time. Furthermore, both predict that, under standard parameter conditions, multidrug-resistant bacteria dominate the tank within the timescales of interest, which is in line with the steady state analysis performed on the original ODE model. The increased complexity of these two models does increase understanding of the problem, but, especially in the case of the PDE model, the extra time required to run the models proved prohibitive to more in depth analysis. Without the appropriate data to compare the settling model to, and given that the PDE model could not be simulated without incorporating unrealistic changes to parameter values, it is hard to draw conclusions from either model. It is similarly difficult to determine whether the increased complexity of the models adds value compared to the simpler ODE model. Hence designing a high resolution model is not a high priority until more data can be collected.

Though the models described throughout this thesis include more dynam-

ics and processes than their predecessors, they still omit a number of processes known to affect the development and persistence of AMR (see Chapter 4). As possible avenues of future research, these models could be extended to include the effects of metal co-resistance [64], stochastic rates of HGT [121], cross-species transmission of resistance genes [13] and individual antibiotics, rather than treating them as generic mass of bacteriolytic and bacteriostatic antibiotics. Based on the existing data from the EVAL-FARMS project [36], and the work of Munck et al. [189], which posits that multidrug resistance emerges based on co-resistance or co-sensitivity, a model which incorporates individual antibiotics and resistances should be a priority, given the collection of appropriate data.

In basic terms, the modelling and research in this thesis indicates that there are resistant bacteria in dairy slurry (see chapter 3), that longer slurry storage times could reduce the rate at which AMR develops (see chapter 5), that antibiotics which kill bacteria contribute more to the development of multidrug resistance than antibiotics that inhibit bacterial reproduction (see chapter 5), that the fitness cost of AMR plays a large role in the development of AMR (see chapter 5), that some antibiotics are being removed from the tank before they reach the effluent (see chapters 7 and 8), and that using parameter inference, it was possible to estimate key antibiotic and bacterial parameters (see chapter 6).

One of the advantages of the models presented here is that they can be easily adapted to other systems where AMR might arise due to the use of antibiotics. This includes things like wastewater treatment plants, pharmaceutical manufacturing wastewater and hospital sewerage and waste systems [31]. The models could also be adapted to model the persistence and spread of AMR in other bacteria. Though this would require re-parameterising and including effects of other factors such as temperature, which affect other bacteria more than *E. coli* in dairy manure [188]. Both options present an interesting opportunities for future work. Models are best utilised for risk analysis and policy change in the presence of data and at present there is little data from dairy slurry stores that can be used to better validate the modelling approach. It is recommended that data be collected from slurry stores detailing the presence of antibiotics and bacteria and identifying the the bacterial resistances at the store influent, effluent and in the main body of the store. Ideally a time series of data would be collected, to fully identify how these change over time. Knowledge of emptying frequency and antibiotic prescription quantity could also contribute to better modelling approaches. Furthermore, a scaled-down slurry tank experiment, where influent concentrations of antibiotics and bacteria were known and controlled, would allow accurate estimation of antibiotic degradation rates in slurry and could be used to analyse the effects of bacterial dynamics such as HGT and heavy metal co-resistance on

the prevalence and proliferation of AMR. Once such data is collected it may be possible to use modelling to provide concrete policy recommendations to help mitigate the spread of environmental AMR by the dairy industry.

Appendix A

Should We Worry About Slurry Supporting Documents

A.1 Slurry Questionnaire

Slurry Questionnaire

Milking herd size:

No. youngstock on farm:

Which system most closely describes your farm?

Descriptor	System 1	System 2	System 3	System 4	System 5
Calving pattern[1]	Spring	Block / AYR	Block / AYR	AYR	AYR
Grazing days	> 274 days	183-274 days	91-182 days	0-90 days	Housed
Feeding approach	Grazed grass with limited supplementary concentrates. Silage and/or fodder crops fed during shortfalls in grazed forage	Grazed grass with more use of conserved forage and supplementary concentrates	Grazed grass with partial mixed ration and supplementary concentrates	Limited use of grazed grass. Total mixed ration, or partial mixed ration with supplementary concentrates	No use of grazed grass. Total mixed ration or partial mixed ration with higher use of supplementary concentrates

For systems 1-4, please indicate what proportion of time your milking herd is housed or on hard standing (i.e. where slurry is being collected) per month e.g. if the cows are at grass 24 hours a day put 0; if they are housed overnight only put 0.5; if they are fully housed put 1:

	Jan	Feb	Mar	Apr	May	Jun	Jul	Aug	Sep	Oct	Nov	Dec
Days Housed												
Proportion of milking herd housed by day												
Nights Housed												
Proportion of milking herd housed at night												

What are your cows being fed when housed?

What bedding is used?

Is slurry being collected from youngstock? If so, from which age range?

SLURRY TANK

Solid separation method (if any):

Volume and dimensions:

Covered/Open?

Feeding rate / frequency:

Mixing method and frequency (if any):

Any additives (i.e. slurry bugs)?

What is added, how often & volume:

Emptying frequency:

Liquid to solid ratio:

End point of liquids & solids:

Post slurry tank treatment (if any):

Cleaning method (if any):

ANTIMICROBIAL USE

What cleaning products are regularly used on farm that will end up in the slurry tank?

Which chemical(s) is used in footbaths?

Concentration:

Approximate daily footbath volume:

Which antibiotics are routinely used on farm for:

Mastitis treatment?

Lameness treatment?

Calf health issues?

Dry cow therapy?

Any other antibiotics used over the past 12 months?

Which antibiotics have been used historically?

Antibiotic	**Date usage stopped**

Where are antibiotics disposed?

What is the destination of waste milk?

A.2 SWWAS Pharmacy report

Title: Quantification Antibiotics in Dairy waste

Samples povided by: Emma Gregson

Type of analysis: LC-MS/MS study. Experiment to determine the levels of a panel of antibiotics in dairy waste

Sample preparation time: 4 days

MS time: 2 session

Analyst: Catharine Ortori, Centre for Analytical Bioscience, School of Pharmacy, University of Nottingham

Sample analysed 25/1/19

Analysis method: The LC-ESI-MS/MS method was based on that described by Rosa María Baena-Nogueras , Thomas Dodsworth , Catherine Ortori , Hytham Ahmed, David, A. Barrett , Rachel L. Gomes (manuscript in preparation, please refer to it for detail)

Equipment: The HPLC system used was a modular Shimadzu VP series with pumps, autosampler and column oven. The HPLC column used was a Phenomenex Gemin C18, 150 x 2.1, 3µ particle size, held at 40^{o}C.

A 4000 Qtrap triple quadrupole mass spectrometer (Sciex, UK) equipped with an electro spray ionisation (ESI) interface, used in multiple reaction monitoring and linear ion trap modes, was used to quantify the antibiotics and confirm their identity.

Sample extraction: Samples were thawed and vortexed. 5ml or 5g sample was either dispensed or weighed into a buffer containing 0.025M EDTA with 0.025M ammonium acetate in water (pH5) and 25 % acetonitrile. The solids were dispersed vigorously for 15min, centrifuged and diluted to 100ml with water. Solid phase extraction, using 5ml Agilent SAX

followed by Oasis HLB, was used to clean to sample and concentrate the antibiotics. The samples were dried and reconstituted in 1ml 25% acetonitrile in water.

Standards and Quality Control samples

Standards: A panel of antibiotic standards was prepared, diluted to create a calibration line at appropriate concentrations and extracted using the protocol; this was performed in parallel, with courtesy Helena Gomes, School of Engineering.

Quality Control Samples: One sample was prepared 4 times to check for variability due to extraction.

Quantification

Quantification of the antibiotics was performed using extracted calibration standards. Quantification was performed using Analyst 1.6. Identification of each compound in the samples was confirmed by LC retention times of each standard, where available, and precursor/product triggered enhanced product ion spectra. These product ion spectra are used to confirm identity by comparison with the Metlin database.

Results Where detected the measured concentrations of antibiotics in each sample are presented in Table 1 as expressed in ng/ml.

Quantification Antibiotics in Dairy waste

Table 1 Concentrations of antbiotics (ng/ml)

Sample Name	AMP	AMX	CFT	CLOX	CLOX	CLX	CPR	CPZ*	CQM	CXM	ENR*
Location 01	No Peak	No Peak	No Peak	No Peak	No Peak	No Peak	Trace	3.78	No Peak	No Peak	No Peak
Location 02	No Peak	No Peak	No Peak	No Peak	No Peak	No Peak	No Peak	2.02	No Peak	No Peak	No Peak
Location 03	No Peak	No Peak	No Peak	No Peak	No Peak	No Peak	No Peak	5.23	No Peak	No Peak	No Peak
Location 05	No Peak	No Peak	No Peak	No Peak	No Peak	No Peak	No Peak	2.54	No Peak	No Peak	No Peak
Location 06	No Peak	No Peak	No Peak	No Peak	No Peak	No Peak	No Peak	2.91	No Peak	No Peak	No Peak
Location 09	No Peak	No Peak	No Peak	No Peak	No Peak	No Peak	No Peak	9.53	No Peak	No Peak	No Peak
Location 10	No Peak	No Peak	No Peak	No Peak	No Peak	No Peak	No Peak	9.11	No Peak	No Peak	No Peak
Location 15	No Peak	No Peak	No Peak	No Peak	No Peak	No Peak	No Peak	7.69	No Peak	No Peak	No Peak
Location 16pre	No Peak	No Peak	No Peak	No Peak	No Peak	No Peak	No Peak	8.69	No Peak	No Peak	No Peak
Location 16post	No Peak	No Peak	No Peak	No Peak	No Peak	No Peak	No Peak	8.93	No Peak	No Peak	No Peak
Location 18	No Peak	No Peak	No Peak	No Peak	No Peak	No Peak	No Peak	2.62	No Peak	No Peak	No Peak
Location 19	No Peak	No Peak	No Peak	No Peak	No Peak	No Peak	No Peak	4.38	No Peak	No Peak	No Peak
Location 21_1	No Peak	No Peak	No Peak	No Peak	No Peak	No Peak	No Peak	6.85	No Peak	No Peak	No Peak
Location 23	No Peak	No Peak	No Peak	No Peak	No Peak	No Peak	No Peak	6.06	No Peak	No Peak	No Peak
Location 24	No Peak	No Peak	No Peak	No Peak	No Peak	No Peak	Trace	No Peak	No Peak	No Peak	No Peak

- *ID confirmed by location only and so putative

Table 1 (cont) Concentrations of antbiotics (ng/ml)

Sample Name	FLO	LCM**	NOV**	OTC**	PEN	SDX	SDZ*	SMX	TMP	TYL**
Location 01	No Peak	0.204	No Peak	No Peak	No Peak	No Peak	No Peak	No Peak	No Peak	No Peak
Location 02	No Peak	No Peak	0.261	No Peak	No Peak	No Peak	0.929	No Peak	No Peak	No Peak
Location 03	No Peak	0.22	0.336	3.89	No Peak	No Peak	No Peak	No Peak	No Peak	No Peak
Location 05	No Peak	1.63	No Peak	No Peak	No Peak	No Peak	No Peak	No Peak	No Peak	No Peak
Location 06	No Peak	0.201	No Peak	5.72	No Peak	No Peak	No Peak	No Peak	No Peak	No Peak
Location 09	No Peak	4.47	0.428	6.86	No Peak	No Peak	1.17	No Peak	No Peak	No Peak
Location 10	No Peak	No Peak	0.14	4.91	No Peak	No Peak	No Peak	No Peak	No Peak	No Peak
Location 15	No Peak	No Peak	No Peak	11.8	No Peak	No Peak	No Peak	No Peak	No Peak	No Peak
Location 16pre	No Peak	No Peak	No Peak	38.4	5.04	No Peak	2.05	No Peak	No Peak	0.664
Location 16post	No Peak	No Peak	No Peak	14.9	No Peak	No Peak	1.35	No Peak	No Peak	2.42
Location 18	No Peak	0.3	No Peak	3.85	**3.53**	No Peak	No Peak	No Peak	No Peak	No Peak
Location 19	No Peak	No Peak	No Peak	No Peak	**1.45**	No Peak	No Peak	No Peak	No Peak	No Peak
Location 21	No Peak	4.33	1.28	10.4	**No Peak**	No Peak	No Peak	No Peak	No Peak	No Peak
Location 23	No Peak	0.237	No Peak	No Peak	4.11	No Peak	No Peak	No Peak	No Peak	No Peak
Location 24	No Peak	0.344	1.84	No Peak	18.3	No Peak	No Peak	No Peak	No Peak	No Peak

*ID confirmed by location only and so putative.

** Confirmed by Enhanced Product ion spectra

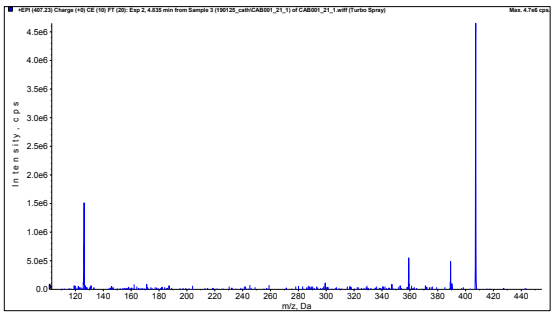
Limits of quantification are also provided in Table 2.

Antibiotic	Family	Abbrevia-tion	LOQ
Amoxicillin	Penicillin	AMX	0.2
Ampicillin	Penicillin	AMP	2
Cephalexin	Cephalosporin	CLX	0.4
Cephalotin	Cephalosporin	CLT	Monitored not quantified
Cephapirin	Cephalosporin	CPR	Monitored not quantified
Cephoperazone	Cephalosporin	CPZ	2
Cephquinome	Cephalosporin	CQM	2
Cephtiofur	Cephalosporin	CFT	0.4
Cloxacillin	Penicillin	CLOX	0.2
Enrofloxacin	Quinolone	ENR	Monitored not quantified
Florfenicol	Amphenicol	FLO	Monitored not quantified
Lincomycin	Lincosamides	LCM	0.02
Novobiocin	Quinolone	NOV	0.02
Oxytetracycline	Tetracycline	OTC	2
Penicillin-G	Penicillin	PEN	2
Sulfadiazine	Sulphonamide	SDZ	0.2
Sulfadoxine	Sulphonamide	SDX	Monitored not quantified
Trimethoprim		TMP	0.02
Tylosin	Macrolide	TYL	0.4

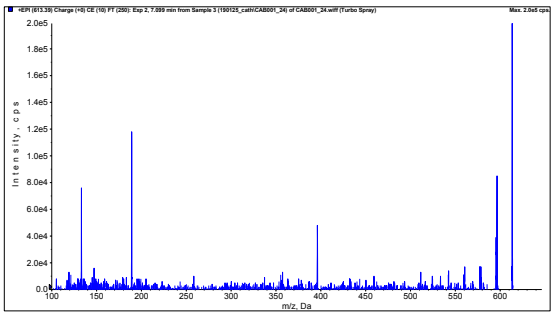
Compound Identification. The antibiotics were confirmed by comparing the retention time with that of the standard and generating enhanced product ion spectra for comparison with that of the database held by Metlin (Scripps, online). See overleaf.

Quantification Antibiotics in Dairy waste

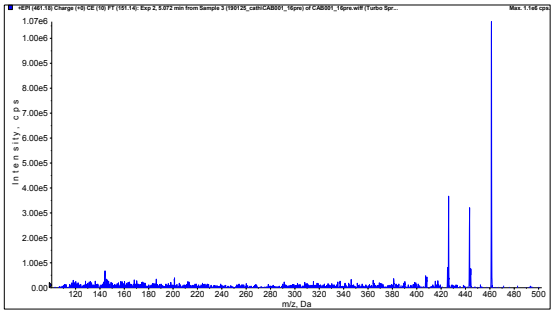
Lincomycin as found at Location 21



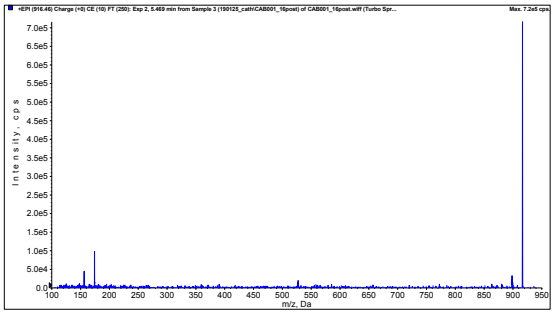
Novobiocin as found at Location 24



Oxytetracycline as found at Location 16Pre



Tylosin as found at Location 16Post



Reproducibility, recovery and matrix effects.

Reproducibility is estimated from the coefficient of variance from a repeat extraction of Sample 21. The CVs for lincomycin, novobiocin and oxytetracyclin are 7, 10 and 14% which are within the 15% acceptable limit. It was not necessary to estimate recovery as it was accounted by use of the extracted calibration line. No attempt was made to calculate any matrix effects.

Conclusion.

A few of the antibiotics in the current panel were detected above the limit of detection. Of those that were positive identities have been provided.

A.3 SWWAS APHA report

Should we worry about slurry?

Bridging the Gaps- Systems-level approaches to antimicrobial resistance

APHA report August 2017

Summary

The aim of the project was to investigate the presence of ESBL, carbapenem and colistin resistant *E. coli* in slurry from 15 dairy farms in the UK. The majority of farms were visited twice over a 6 month period, and one sample from the slurry tank was collected at each visit (n=30 samples collected in total). An aliquot of each slurry sample was used for isolation and confirmation tests for ESBL, carbapenem and colistin resistant *E. coli*. Of all the slurry samples tested, 50 % contained *E. coli* and 26.7% contained ESBL *E. coli.* None of the samples tested were positive for carbapenem or colistin resistant *E. coli.*

Methods:

Bacterial isolation:

Samples of slurry were received in the lab between 3/5/2017 and 25/7/2017. Isolation of bacteria from the slurry samples was based on published EU methods. This method was outlined in EU Decision 2013/652/EU and protocols from the EU Reference Laboratory (www.crl-ar.eu). Briefly, 1g of slurry was added to 9 ml of BPW. This bacterial suspension was then plated immediately onto MacConkey agar (McC) to determine the extent of *E. coli* prevalence before enrichment. The bacterial suspensions were then incubated for 18 – 22 hours at 37°C to enrich the bacterial populations. An aliquot (100µl) of enriched broths from each sample was then plated onto the following agar media: MacConkey agar containing 1 mg cefotaxime /L (McC-CTX), and CHROMagar ESBL (CA-ESBL) were used to detect AmpC/ESBL phenotype *E. coli,* and chromID CARBA and chromID OXA-48 for detection of carbapenem resistant *E. coli*. Bacterial growth on plates was recorded semi quantitatively. Oxidase / indole testing from blood agar was used to determine *E. coli* species identity from positive growth.

Results:

The results of growth of *E. coli* only from slurry samples on the six agar media are shown in Table 1. Of the 30 slurry samples received, 36.7 % (n=11) were positive for *E. coli* growth from McConkey agar alone (using

non-enriched BPW media suspensions). The proportion of samples that were positive for ESBL *E. coli* growth after enrichment was: 16.7% (n=5) from McC-CTX and 26.7% (n=8) from CA-ESBL. The ESBL gene responsible for the resistance phenotype was identified in 7 of those samples (i.e 23% of all slurry samples tested). There was no evidence for carbapenem resistant or colistin resistant *E. coli* in these slurry samples. Of the 8 slurry samples that were positive for ESBL *E. coli*, 7 isolates were successfully identified for ESBL gene type by PCR gene amplification and sequencing. These results are also shown in Table 1 for the respective slurry samples. The CTX-M gene types detected in slurry samples were CTX-M-15 (n=2, awaiting confirmation), CTX-M-14 (n=2), CTX-M-65 (n=1), CTX-M-36 (n=1), and CTX-M-8 (n=1). There were 4 samples (1 (visit 2), 2 (visit 2), 9 and 19 (visit2)) that were negative for *E .coli* on MacConkey agar at the pre-enrichment stage, but produced growth on ESBL agars after enrichment in BPW, suggesting that the numbers of *E. coli* in these slurry samples was below the level of detection (n=100 cfu/g faeces) for this method at the pre-enrichment stage. If these 4 samples are included in the calculations for the proportion of slurry samples positive for *E. coli* at the pre-enriched or at the post enriched stage then the overall percentage of positive slurry samples increases to 50%.

Conclusions

Of the 30 slurry samples tested, up to 50% contained *E. coli* and up to 26.7% contained ESBL *E. coli* with up to 5 different types of identifiable CTX-M genes. This is a slightly higher level of diversity in CTX-M gene type than that reported from a longitudinal farm study in which only three CTX-M types (CTX-M-1, -14 and -15) were detected (Horton et al., 2016). If confirmed then slurry pits could therefore be a source of farm land contamination by ESBL *E. coli*.

Table 1 *E. coli* growth from slurry samples

Sample ID	Growth of E. coli on agar media					
	McC (pre-enrichment)	ESBL Resistance (post enrichment)		Carbapenem resistance (post enrichment)		Colistin res. (post enrichment)
		McC-CTX	CA-ESBL	OXA-48	CARBA	McC-Col
1	+	-	-	-	-	-
1 (visit 2)	-	-	+ (CTM-15[a])	-	-	-
2	+	+	-	-	-	-
2 (visit 2)	-	-	+ (CTM-15[a])	-	-	-
3	-	-	-	-	-	-
3 (visit 2)	-	-	-	-	-	-
5	+	-	-	-	-	-
5 (visit 2)	+	-	+ (CTM-14)	-	-	-
6	-	-	-	-	-	-
6 (visit 2)	-	-	-	-	-	-
9	-	-	+ (CTM-14)	-	-	-
9 (visit 2)	-	-	-	-	-	-
10	-	-	-	-	-	-
14	+	-	-	-	-	-
15	+	+	-	-	-	-
15 (visit 2)	-	-	-	-	-	-
16-pre	+	+	-	-	-	-
16-pre (visit 2)	-	-	-	-	-	-
16-bio	+	+	-	-	-	-
16-bio (visit 2)	-	-	-	-	-	-
18	-	-	-	-	-	-
18 (visit 2)	-	-	-	-	-	-
19	+	+ (CTXM-65)	+ (CTXM-65)	-	-	-
19 (visit 2)	-	-	+ (CTXM-36)	-	-	-
21	-	-	-	-	-	-
21 (visit 2)	-	-	-	-	-	-
23	+	-	+ (no seq.)	-	-	-
23 (visit 2)	-	-	-	-	-	-
24	+	-	+ (CTXM-8)	-	-	-
24 (visit 2)	-	-	-	-	-	-
% Pos growth	36.7	16.7	26.7	0	0	0

[a] CTX-M 15 type needs to be confirmed, no seq. = gene sequence not able to be determined.

References

Horton, R.A., Duncan, D., Randall, L.P., Chappell, S., Brunton, L.A., Warner, R., Coldham, N.G., Teale, C.J., 2016. Longitudinal study of CTX-M ESBL-producing E. coli strains on a UK dairy farm. Res Vet Sci 109, 107-113.

Appendix B

Acronym Glossary

- AAU - Agricultural Antibiotic Usage
- AGP - Agricultural Growth Promoter
- AHDB - Agriculture and Horticulture Development Board
- AMR - Antimicrobial Resistance
- APHA - The Animal and Plant Health Agency
- ARG - Antimicrobial Resistance Gene
- BE - Before Enrichment
- ESBL - Extended-Spectrum β-Lactamase
- FDA - U.S. Food and Drug Administration
- FSA - Food Standards Agency
- GB - Great Britain
- HGT - Horizontal Gene Transfer
- ICP-AES - Inductively Coupled Plasma Atomic Emissions Spectroscopy
- MAPE - Mean Averaged Percentage Error
- MAU - Medical Antibiotic Usage
- MCC - Minimum Co-selective Concentrations
- MDR - Multidrug-resistant
- MIC - Minimum Inhibitory Concentration

- MLE - Maximum Likelihood Estimation
- MCMC - Markov Chain Monte Carlo
- NAS - Nucleic Acid Synthesis
- NVZ - Nitrate Vulnerable Zone
- ODE - Ordinary Differential Equation
- PC - Production Capacity
- PDE - Partial Differential Equation
- PE - Post Enrichment
- PSI - Protein Synthesis Inhibitor
- RUMA - Responsible Use of Medicines in Agriculture Alliance
- SWWAS - Should We Worry About Slurry?
- TRB -Tetracycline Resistant Bacteria
- TRG - Tetracycline Resistant Gene
- TSS - Total suspended solids

Bibliography

[1] "What is antimicrobial resistance?." `http://www.who.int/features/qa/75/en/`. Accessed: 7/11/2016.

[2] J. O'Neill, "Review on antimicrobial resistance, 2015. antimicrobials in agriculture and the environment: Reducing unnecessary use and waste, chaired by Jim O'Neill. December 2015," 2015.

[3] A. Lateef, "The microbiology of a pharmaceutical effluent and its public health implications," *World Journal of Microbiology and Biotechnology*, vol. 20, no. 2, pp. 167–171, 2004.

[4] O. Cardoso, J.-M. Porcher, and W. Sanchez, "Factory-discharged pharmaceuticals could be a relevant source of aquatic environment contamination: review of evidence and need for knowledge," *Chemosphere*, vol. 115, pp. 20–30, 2014.

[5] D. Li, M. Yang, J. Hu, J. Zhang, R. Liu, X. Gu, Y. Zhang, and Z. Wang, "Antibiotic-resistance profile in environmental bacteria isolated from penicillin production wastewater treatment plant and the receiving river," *Environmental microbiology*, vol. 11, no. 6, pp. 1506–1517, 2009.

[6] D. Li, T. Yu, Y. Zhang, M. Yang, Z. Li, M. Liu, and R. Qi, "Antibiotic resistance characteristics of environmental bacteria from an oxytetracycline production wastewater treatment plant and the receiving river," *Appl. Environ. Microbiol.*, vol. 76, no. 11, pp. 3444–3451, 2010.

[7] K. Kümmerer, "Resistance in the environment," *Journal of Antimicrobial Chemotherapy*, vol. 54, no. 2, pp. 311–320, 2004.

[8] T. U. Berendonk, C. M. Manaia, C. Merlin, D. Fatta-Kassinos, E. Cytryn, F. Walsh, H. Bürgmann, H. Sørum, M. Norström, M.-N. Pons, *et al.*, "Tackling antibiotic resistance: the environmental framework," *Nature Reviews Microbiology*, vol. 13, no. 5, p. 310, 2015.

[9] S. Thanner, D. Drissner, and F. Walsh, "Antimicrobial resistance in agriculture," *MBio*, vol. 7, no. 2, pp. e02227–15, 2016.

[10] T. F. Schäberle and I. M. Hack, "Overcoming the current deadlock in antibiotic research," *Trends in microbiology*, vol. 22, no. 4, pp. 165–167, 2014.

[11] T. B. Nielsen, E. P. Brass, D. N. Gilbert, J. G. Bartlett, and B. Spellberg, "Sustainable discovery and development of antibiotics—is a nonprofit approach the future?," *The New England journal of medicine*, vol. 381, no. 6, p. 503, 2019.

[12] L. L. Ling, T. Schneider, A. J. Peoples, A. L. Spoering, I. Engels, B. P. Conlon, A. Mueller, T. F. Schäberle, D. E. Hughes, S. Epstein, *et al.*, "A new antibiotic kills pathogens without detectable resistance," *Nature*, vol. 517, no. 7535, pp. 455–459, 2015.

[13] J. E. Davies, "Origins, acquisition and dissemination of antibiotic resistance determinants," *Ciba Foundation Symposium 207 - Antibiotic Resistance: Origins, Evolution, Selection and Spread Novartis Foundation Symposia*, pp. 15–35, 2007.

[14] R. Wise, T. Hart, O. Cars, M. Streulens, R. Helmuth, P. Huovinen, and M. Sprenger, "Antimicrobial resistance is a major threat to public health," *British Medical Journal*, vol. 317, no. 7159, pp. 609–611, 1998.

[15] "Department of health amr systems map." `https://www.gov.uk/government/uploads/system/uploads/attachment_data/file/387746/Microbial_Maps.pdf`. Accessed: 27/06/2017.

[16] W. Witte, "Medical consequences of antibiotic use in agriculture," *Science*, vol. 279, no. 5353, pp. 996–997, 1998.

[17] D. L. Smith, A. D. Harris, J. A. Johnson, E. K. Silbergeld, and J. G. Morris, "Animal antibiotic use has an early but important impact on the emergence of antibiotic resistance in human commensal bacteria," *Proceedings of the National Academy of Sciences*, vol. 99, no. 9, pp. 6434–6439, 2002.

[18] H. Aubry-Damon, K. Grenet, P. Sall-Ndiaye, D. Che, E. Cordeiro, M.-E. Bougnoux, E. Rigaud, Y. Le Strat, V. Lemanissier, L. Armand-Lefèvre, *et al.*, "Antimicrobial resistance in commensal flora of pig farmers," *Emerging Infectious Diseases*, vol. 10, no. 5, p. 873, 2004.

[19] R. L. Nation and J. Li, "Colistin in the 21st century," *Current opinion in infectious diseases*, vol. 22, no. 6, p. 535, 2009.

[20] A. S. Chaudhary, "A review of global initiatives to fight antibiotic resistance and recent antibiotics' discovery," *Acta Pharmaceutica Sinica B*, vol. 6, no. 6, pp. 552–556, 2016.

[21] Y.-Y. Liu, Y. Wang, T. R. Walsh, L.-X. Yi, R. Zhang, J. Spencer, Y. Doi, G. Tian, B. Dong, X. Huang, *et al.*, "Emergence of plasmid-mediated colistin resistance mechanism MCR-1 in animals and human beings in china: a microbiological and molecular biological study," *The Lancet infectious diseases*, vol. 16, no. 2, pp. 161–168, 2016.

[22] J. E. Hillerton and E. A. Berry, "The management and treatment of environmental streptococcal mastitis.," *The Veterinary Clinics of North America. Food Animal Practice*, vol. 19, no. 1, pp. 157–169, 2003.

[23] D. I. Massé, N. M. C. Saady, and Y. Gilbert, "Potential of biological processes to eliminate antibiotics in livestock manure: an overview," *Animals*, vol. 4, no. 2, pp. 146–163, 2014.

[24] S. MacDiarmid, "Antibacterial drugs used against mastitis in cattle by the systemic route," *New Zealand Veterinary Journal*, vol. 26, no. 12, pp. 290–295, 1978.

[25] R. Erskine, P. Bartlett, P. Crawshaw, and D. Gombas, "Efficacy of intramuscular oxytetracycline as a dry cow treatment for Staphylococcus aureus mastitis," *Journal of dairy science*, vol. 77, no. 11, pp. 3347–3353, 1994.

[26] S. Pyörälä, "Treatment of mastitis during lactation," *Irish Veterinary Journal*, vol. 62, no. 4, p. S40, 2009.

[27] F. Wichmann, N. Udikovic-Kolic, S. Andrew, and J. Handelsman, "Diverse antibiotic resistance genes in dairy cow manure," *MBio*, vol. 5, no. 2, pp. e01017–13, 2014.

[28] O. Williams, I. Clark, R. L. Gomes, T. Perehinec, J. L. Hobman, D. J. Stekel, R. Hyde, C. Dodds, and E. Lester, "Removal of copper from cattle footbath wastewater with layered double hydroxide adsorbents as a route to antimicrobial resistance mitigation on dairy farms," *Science of the Total Environment*, vol. 655, pp. 1139–1149, 2019.

[29] AHDB Dairy, "Cost effective slurry storage stategies, AHDB dairy." `https://dairy.ahdb.org.uk/resources-library/technical-information/health-welfare/cost-effective-slurry-storage-strategies/#.XKXrsetKhTY`, 2019. Accessed: 04/04/2019.

[30] J. Cornelisse, D. Peterse, and E. R. Toussaint, "Formalin foot baths in the prevention of interdigital dermatitis in cattle," *Tijdschrift voor diergeneeskunde*, vol. 107, no. 22, pp. 835–840, 1982.

[31] A. C. Singer, H. Shaw, V. Rhodes, and A. Hart, "Review of antimicrobial resistance in the environment and its relevance to environmental regulators," *Frontiers in microbiology*, vol. 7, p. 1728, 2016.

[32] L.-J. Zhou, G.-G. Ying, S. Liu, R.-Q. Zhang, H.-J. Lai, Z.-F. Chen, and C.-G. Pan, "Excretion masses and environmental occurrence of antibiotics in typical swine and dairy cattle farms in china," *Science of the Total Environment*, vol. 444, pp. 183–195, 2013.

[33] L. Chambers, Y. Yang, H. Littier, P. Ray, T. Zhang, A. Pruden, M. Strickland, and K. Knowlton, "Metagenomic analysis of antibiotic resistance genes in dairy cow feces following therapeutic administration of third generation cephalosporin," *PloS one*, vol. 10, no. 8, p. e0133764, 2015.

[34] M.-L. Ackers, B. E. Mahon, E. Leahy, B. Goode, T. Damrow, P. S. Hayes, W. F. Bibb, D. H. Rice, T. J. Barrett, L. Hutwagner, *et al.*, "An outbreak of escherichia coli o157: H7 infections associated with leaf lettuce consumption," *Journal of infectious diseases*, vol. 177, no. 6, pp. 1588–1593, 1998.

[35] M. Maeusli, B. Lee, S. Miller, Z. Reyna, P. Lu, J. Yan, A. Ulhaq, N. Skandalis, B. Spellberg, and B. Luna, "Horizontal gene transfer of antibiotic resistance from acinetobacter baylyi to escherichia coli on lettuce and subsequent antibiotic resistance transmission to the gut microbiome," *Msphere*, vol. 5, no. 3, 2020.

[36] EVAL-FARMS, "Evaluating the threat of antimicrobial resistance in agricultural manures and slurries," 2021. Data obtained from ongoing grant.

[37] R. M. Baena Nogueras, T. Dodsworth, C. Ortori, H. Ahmed, D. A. Barrett, and R. L. Gomes, "Analysis of veterinary antibiotics to inform on their persistence and fate as a route to antimicrobial resistance in the dairy farm environment.," *Journal of Hazardous Materials*, In review.

[38] M. Baker, J. L. Hobman, C. E. R. Dodd, S. J. Ramsden, and D. J. Stekel, "Mathematical modelling of antimicrobial resistance in agricultural waste highlights importance of gene transfer rate," *FEMS Microbiology Ecology*, vol. 92, no. 4, 2016.

[39] V. V. Volkova, C. Lanzas, Z. Lu, and Y. T. Gröhn, "Mathematical model of plasmid-mediated resistance to ceftiofur in commensal enteric Escherichia coli of cattle," *PLoS One*, vol. 7, no. 5, p. e36738, 2012.

[40] I. Takács, G. G. Patry, and D. Nolasco, "A dynamic model of the clarification-thickening process," *Water research*, vol. 25, no. 10, pp. 1263–1271, 1991.

[41] F. C. Tenover, "Mechanisms of antimicrobial resistance in bacteria," *American journal of infection control*, vol. 34, no. 5, pp. S3–S10, 2006.

[42] H. Ochman, J. G. Lawrence, and E. A. Groisman, "Lateral gene transfer and the nature of bacterial innovation," *Nature*, vol. 405, no. 6784, pp. 299–304, 2000.

[43] C. M. Thomas and K. M. Nielsen, "Mechanisms of, and barriers to, horizontal gene transfer between bacteria," *Nature reviews microbiology*, vol. 3, no. 9, pp. 711–721, 2005.

[44] S. M. Soucy, J. Huang, and J. P. Gogarten, "Horizontal gene transfer: building the web of life," *Nature Reviews Genetics*, vol. 16, no. 8, pp. 472–482, 2015.

[45] J. P. Gogarten and J. P. Townsend, "Horizontal gene transfer, genome innovation and evolution," *Nature Reviews Microbiology*, vol. 3, no. 9, pp. 679–687, 2005.

[46] J. S. Bradley and J. B. Sauberan, "292 antimicrobial agents," *Principles and Practice of Pediatric Infectious Disease*, pp. 1453–1484, 2012.

[47] J. Clardy, M. A. Fischbach, and C. R. Currie, "The natural history of antibiotics," *Current biology*, vol. 19, no. 11, pp. R437–R441, 2009.

[48] J. Davies and D. Davies, "Origins and evolution of antibiotic resistance," *Microbiology and molecular biology reviews*, vol. 74, no. 3, pp. 417–433, 2010.

[49] C. Walsh, "Molecular mechanisms that confer antibacterial drug resistance," *Nature*, vol. 406, no. 6797, pp. 775–781, 2000.

[50] A. H. Melnyk, A. Wong, and R. Kassen, "The fitness costs of antibiotic resistance mutations," *Evolutionary applications*, vol. 8, no. 3, pp. 273–283, 2015.

[51] D. I. Andersson and B. R. Levin, "The biological cost of antibiotic resistance," *Current opinion in microbiology*, vol. 2, no. 5, pp. 489–493, 1999.

[52] D. I. Andersson and D. Hughes, "Antibiotic resistance and its cost: is it possible to reverse resistance?," *Nature Reviews Microbiology*, 2010.

[53] M. Subbiah, E. M. Top, D. H. Shah, and D. R. Call, "Selection pressure required for long-term persistence of bla cmy-2-positive inca/c plasmids," *Applied and Environmental Microbiology*, vol. 77, no. 13, pp. 4486–4493, 2011.

[54] P. L. Conlin, J. R. Chandler, and B. Kerr, "Games of life and death: antibiotic resistance and production through the lens of evolutionary game theory," *Current Opinion in Microbiology*, vol. 21, pp. 35–44, 2014.

[55] S. B. Baloda, L. Christensen, and S. Trajcevska, "Persistence of a salmonella entericaserovar typhimurium dt12 clone in a piggery and in agricultural soil amended with salmonella-contaminated slurry," *Applied and environmental microbiology*, vol. 67, no. 6, pp. 2859–2862, 2001.

[56] J. C. Chee-Sanford, R. I. Mackie, S. Koike, I. G. Krapac, Y.-F. Lin, A. C. Yannarell, S. Maxwell, and R. I. Aminov, "Fate and transport of antibiotic residues and antibiotic resistance genes following land application of manure waste," *Journal of environmental quality*, vol. 38, no. 3, pp. 1086–1108, 2009.

[57] E. Saussereau and L. Debarbieux, "Bacteriophages in the experimental treatment of pseudomonas aeruginosa infections in mice," in *Advances in virus research*, vol. 83, pp. 123–141, Elsevier, 2012.

[58] P. M. Bennett, "Genome plasticity: insertion sequence elements, transposons and integrons, and dna rearrangement," *Genomics, Proteomics, and Clinical Bacteriology: Methods and Reviews*, pp. 71–113, 2004.

[59] A. Fraise, "Biocide abuse and antimicrobial resistance—a cause for concern?," *Journal of antimicrobial chemotherapy*, vol. 49, no. 1, pp. 11–12, 2002.

[60] P. F. Mc Dermott, R. D. Walker, and D. G. White, "Antimicrobials: modes of action and mechanisms of resistance," *International journal of toxicology*, vol. 22, no. 2, pp. 135–143, 2003.

[61] F. Silva, O. Lourenço, J. A. Queiroz, and F. C. Domingues, "Bacteriostatic versus bactericidal activity of ciprofloxacin in Escherichia coli assessed

by flow cytometry using a novel far-red dye," *The Journal of antibiotics*, vol. 64, no. 4, pp. 321–325, 2011.

[62] L. A. Dever, "Mechanisms of bacterial resistance to antibiotics," *Archives of Internal Medicine*, vol. 151, p. 886, Jan 1991.

[63] A. H. Delcour, "Outer membrane permeability and antibiotic resistance," *Biochimica et Biophysica Acta (BBA)-Proteins and Proteomics*, vol. 1794, no. 5, pp. 808–816, 2009.

[64] C. Baker-Austin, M. S. Wright, R. Stepanauskas, and J. Mcarthur, "Co-selection of antibiotic and metal resistance," *Trends in Microbiology*, vol. 14, no. 4, pp. 176–182, 2006.

[65] C. Pal, J. Bengtsson-Palme, E. Kristiansson, and D. J. Larsson, "Co-occurrence of resistance genes to antibiotics, biocides and metals reveals novel insights into their co-selection potential," *BMC genomics*, vol. 16, no. 1, p. 964, 2015.

[66] B. Levin, M. Lipsitch, V. Perrot, S. Schrag, R. Antia, L. Simonsen, N. Moore Walker, and F. Stewart, "The population genetics of antibiotic resistance," *Clinical infectious diseases*, vol. 24, no. Supplement_1, pp. S9–S16, 1997.

[67] B. Levin, "Models for the spread of resistant pathogens.," *The Netherlands journal of medicine*, vol. 60, no. 7 Suppl, pp. 58–64, 2002.

[68] L. Brown, J. M. Wolf, R. Prados-Rosales, and A. Casadevall, "Through the wall: extracellular vesicles in gram-positive bacteria, mycobacteria and fungi," *Nature Reviews Microbiology*, vol. 13, pp. 620–630, Jan 2015.

[69] H. F. Hemond and E. J. Fechner, *Chemical fate and transport in the environment*. Elsevier, 2014.

[70] S. M. Mitchell, J. L. Ullman, A. L. Teel, and R. J. Watts, "Hydrolysis of amphenicol and macrolide antibiotics: Chloramphenicol, florfenicol, spiramycin, and tylosin," *Chemosphere*, vol. 134, pp. 504 – 511, 2015.

[71] A. Berge, E. Atwill, and W. Sischo, "Animal and farm influences on the dynamics of antibiotic resistance in faecal Escherichia coli in young dairy calves," *Preventive Veterinary Medicine*, vol. 69, no. 1–2, pp. 25 – 38, 2005.

[72] K. Spitz, J. Moreno, *et al.*, *A practical guide to groundwater and solute transport modeling*. John Wiley and sons, 1996.

[73] Z. Qiang and C. Adams, "Potentiometric determination of acid dissociation constants (pk a) for human and veterinary antibiotics," *Water research*, vol. 38, no. 12, pp. 2874–2890, 2004.

[74] M.-L. Loke, J. Tjørnelund, and B. Halling-Sørensen, "Determination of the distribution coefficient (logkd) of oxytetracycline, tylosin a, olaquindox and metronidazole in manure," *Chemosphere*, vol. 48, no. 3, pp. 351–361, 2002.

[75] J. Sangster, "Octanol-water partition coefficients of simple organic compounds," *Journal of Physical and Chemical Reference Data*, vol. 18, no. 3, pp. 1111–1229, 1989.

[76] E. Jenne, *Adsorption of metals by geomedia: variables, mechanisms, and model applications*. Elsevier, 1998.

[77] Z. Xu, J.-g. Cai, and B.-c. Pan, "Mathematically modeling fixed-bed adsorption in aqueous systems," *Journal of Zhejiang University SCIENCE A*, vol. 14, no. 3, pp. 155–176, 2013.

[78] N. Ayawei, A. N. Ebelegi, and D. Wankasi, "Modelling and interpretation of adsorption isotherms," *Journal of Chemistry*, vol. 2017, 2017.

[79] M. D. LeVan and T. Vermeulen, "Binary langmuir and freundlich isotherms for ideal adsorbed solutions," *The Journal of Physical Chemistry*, vol. 85, no. 22, pp. 3247–3250, 1981.

[80] Y. Liu, "Some consideration on the langmuir isotherm equation," *Colloids and Surfaces A: Physicochemical and Engineering Aspects*, vol. 274, no. 1-3, pp. 34–36, 2006.

[81] M. N. Carvalho, C. A. de Abreu, M. Benachour, D. C. Sales, O. S. Baraúna, and M. A. da Motta Sobrinho, "Applying combined langmuir–freundlich model to the multi-component adsorption of btex and phenol on smectite clay," *Adsorption Science & Technology*, vol. 30, no. 8-9, pp. 691–699, 2012.

[82] B. Meibohm and H. Derendorf, "Basic concepts of pharmacokinetic/pharmacodynamic (pk/pd) modelling," *International journal of clinical pharmacology and therapeutics*, vol. 35, no. 10, pp. 401–413, 1997.

[83] A. P. Singh, Y. G. Shin, and D. K. Shah, "Application of pharmacokinetic-pharmacodynamic modeling and simulation for antibody-drug conjugate development," *Pharmaceutical research*, vol. 32, no. 11, pp. 3508–3525, 2015.

[84] C. Csajka and D. Verotta, "Pharmacokinetic–pharmacodynamic modelling: history and perspectives," *Journal of pharmacokinetics and pharmacodynamics*, vol. 33, no. 3, pp. 227–279, 2006.

[85] H. Zou, P. Banerjee, S. S. Y. Leung, and X. Yan, "Application of pharmacokinetic-pharmacodynamic modeling in drug delivery: Development and challenges," *Frontiers in Pharmacology*, vol. 11, 2020.

[86] N. Ting, *Dose finding in drug development*. Springer Science & Business Media, 2006.

[87] E. I. Nielsen and L. E. Friberg, "Pharmacokinetic-pharmacodynamic modeling of antibacterial drugs," *Pharmacological reviews*, vol. 65, no. 3, pp. 1053–1090, 2013.

[88] R. Dunlop, S. Mcewen, A. Meek, R. Clarke, W. Black, and R. Friendship, "Associations among antimicrobial drug treatments and antimicrobial resistance of fecal Escherichia coli of swine on 34 farrow-to-finish farms in ontario, canada," *Preventive Veterinary Medicine*, vol. 34, no. 4, pp. 283–305, 1998.

[89] T. F. Landers, B. Cohen, T. E. Wittum, and E. L. Larson, "A review of antibiotic use in food animals: perspective, policy, and potential," *Public health reports*, vol. 127, no. 1, pp. 4–22, 2012.

[90] J. I. R. Castanon, "History of the use of antibiotic as growth promoters in european poultry feeds," *Poultry Science*, vol. 86, pp. 2466–2471, Jan 2007.

[91] D. F. Maron, T. J. Smith, and K. E. Nachman, "Restrictions on antimicrobial use in food animal production: an international regulatory and economic survey," *Globalization and health*, vol. 9, no. 1, p. 48, 2013.

[92] H. Hao, G. Cheng, Z. Iqbal, X. Ai, H. I. Hussain, L. Huang, M. Dai, Y. Wang, Z. Liu, Z. Yuan, and et al., "Benefits and risks of antimicrobial use in food-producing animals," *Frontiers in Microbiology*, vol. 5, Dec 2014.

[93] B.-A. Tenhagen, G. Köster, J. Wallmann, and W. Heuwieser, "Prevalence of mastitis pathogens and their resistance against antimicrobial agents in dairy cows in Brandenburg, Germany," *Journal of Dairy Science*, vol. 89, no. 7, pp. 2542–2551, 2006.

[94] F. Nicholson, S. Smith, B. Alloway, C. Carlton-Smith, and B. Chambers, "Quantifying heavy metal inputs to agricultural soils in england and wales," *Water and Environment Journal*, vol. 20, no. 2, pp. 87–95, 2006.

[95] A. E. van den Bogaard, L. B. Jensen, and E. E. Stobberingh, "Vancomycin-resistant enterococci in turkeys and farmers," *New England Journal of Medicine*, vol. 337, no. 21, pp. 1558–1559, 1997.

[96] A. Van den Bogaard, R. Willems, N. London, J. Top, and E. Stobberingh, "Antibiotic resistance of faecal enterococci in poultry, poultry farmers and poultry slaughterers," *Journal of Antimicrobial Chemotherapy*, vol. 49, no. 3, pp. 497–505, 2002.

[97] K. L. Tang, N. P. Caffrey, D. B. Nóbrega, S. C. Cork, P. E. Ronksley, H. W. Barkema, A. J. Polachek, H. Ganshorn, N. Sharma, J. D. Kellner, *et al.*, "Restricting the use of antibiotics in food-producing animals and its associations with antibiotic resistance in food-producing animals and human beings: a systematic review and meta-analysis," *The Lancet Planetary Health*, vol. 1, no. 8, pp. e316–e327, 2017.

[98] P. Joosten, D. Ceccarelli, E. Odent, S. Sarrazin, H. Graveland, L. Van Gompel, A. Battisti, A. Caprioli, A. Franco, J. A. Wagenaar, *et al.*, "Antimicrobial usage and resistance in companion animals: a cross-sectional study in three European countries," *Antibiotics*, vol. 9, no. 2, p. 87, 2020.

[99] R. D. Booton, A. Meeyai, N. Alhusein, H. Buller, E. Feil, H. Lambert, S. Mongkolsuk, E. Pitchforth, K. K. Reyher, W. Sakcamduang, *et al.*, "One health drivers of antibacterial resistance: Quantifying the relative impacts of human, animal and environmental use and transmission," *One Health*, vol. 12, p. 100220, 2021.

[100] E. Uberoi, "UK dairy industry statistics," 2020.

[101] "Storing silage, slurry and agricultural fuel oil." `https://www.gov.uk/guidance/storing-silage-slurry-and-agricultural-fuel-oil#slurry`. Accessed: 31/05/2017.

[102] "Managing slurry on farms." `http://www.hse.gov.uk/pubns/ais9.pdf`. Accessed: 31/05/2017.

[103] F. A. Nicholson, S. J. Groves, and B. J. Chambers, "Pathogen survival during livestock manure storage and following land application," *Bioresource technology*, vol. 96, no. 2, pp. 135–143, 2005.

[104] Post Report 588, "Reducing UK antibiotic use in animals," 2018.

[105] Farming Monthly, "EU bans prophylactic use of antibiotics in farming." Available at `https://www.`

farmingmonthly.co.uk/livestock/animal-health/11179-eu-bans-prophylactic-use-of-antibiotics-in-farming/, 2018. Accessed: 2017/06/27.

[106] "Great Britain, Department of Agriculture, Environment and Rural Affairs, Nitrates Action Programme 2015-2018 and Phosphorus Regulations." Available at https://www.daera-ni.gov.uk/publications/2015-2018-nitrates-action-programme-and-phosphorus-regulations-and-associ Accessed: 2019-04-04.

[107] B. M. Swift, M. Bennett, K. Waller, C. Dodd, A. Murray, R. L. Gomes, B. Humphreys, J. L. Hobman, M. A. Jones, S. E. Whitlock, *et al.*, "Anthropogenic environmental drivers of antimicrobial resistance in wildlife," *Science of the Total Environment*, vol. 649, pp. 12–20, 2019.

[108] Food Standards Agency, "Managing farm manures for food safety." https://www.food.gov.uk/sites/default/files/media/document/manuresguidance%20%281%29.pdf, 2009. Accessed: 2019/10/08.

[109] RUMA, "Targets task force report 2017." https://www.ruma.org.uk/wp-content/uploads/2017/10/RUMA-Targets-Task-Force-Report-2017-FINAL.pdff, 2017. Accessed: 2019/10/23.

[110] RUMA, "Targets task force: One year on." https://www.ruma.org.uk/wp-content/uploads/2018/11/RUMA-TTF-1-year-on-Full-Report-FINAL.pdf, 2018. Accessed: 2019/10/23.

[111] C. Cogliani, H. Goossens, and C. Greko, "Restricting antimicrobial use in food animals: lessons from europe," *Microbe*, vol. 6, no. 6, p. 274, 2011.

[112] F. M. Aarestrup, A. M. Seyfarth, H.-D. Emborg, K. Pedersen, R. S. Hendriksen, and F. Bager, "Effect of abolishment of the use of antimicrobial agents for growth promotion on occurrence of antimicrobial resistance in fecal enterococci from food animals in Denmark," *Antimicrobial Agents and chemotherapy*, vol. 45, no. 7, pp. 2054–2059, 2001.

[113] V. Homem and L. Santos, "Degradation and removal methods of antibiotics from aqueous matrices–a review," *Journal of environmental management*, vol. 92, no. 10, pp. 2304–2347, 2011.

[114] L. Rosso, J. Lobry, S. Bajard, and J. Flandrois, "Convenient model to describe the combined effects of temperature and pH on microbial growth.," *Applied and environmental microbiology*, vol. 61, no. 2, pp. 610–616, 1995.

[115] J. Chen, F. C. Michel, S. Sreevatsan, M. Morrison, and Z. Yu, "Occurrence and persistence of erythromycin resistance genes (erm) and tetracycline resistance genes (tet) in waste treatment systems on swine farms," *Microbial Ecology*, vol. 60, pp. 479–486, Jun 2010.

[116] Y. M. Awad, S.-C. Kim, S. A. M. A. El-Azeem, K.-H. Kim, K.-R. Kim, K. Kim, C. Jeon, S. S. Lee, and Y. S. Ok, "Veterinary antibiotics contamination in water, sediment, and soil near a swine manure composting facility," *Environmental Earth Sciences*, vol. 71, no. 3, pp. 1433–1440, 2013.

[117] Q. Sui, J. Zhang, J. Tong, M. Chen, and Y. Wei, "Seasonal variation and removal efficiency of antibiotic resistance genes during wastewater treatment of swine farms," *Environmental Science and Pollution Research*, pp. 1–10, 2015.

[118] A. Göbel, A. Thomsen, C. S. Mcardell, A. Joss, and W. Giger, "Occurrence and sorption behavior of sulfonamides, macrolides, and trimethoprim in activated sludge treatment," *Environmental Science & Technology*, vol. 39, no. 11, pp. 3981–3989, 2005.

[119] H. Dolliver, S. Gupta, and S. Noll, "Antibiotic degradation during manure composting," *Journal of Environment Quality*, vol. 37, no. 3, p. 1245, 2008.

[120] B. van Bunnik and M. Woolhouse, "Modelling the impact of curtailing antibiotic usage in food animals on antibiotic resistance in humans," *Royal Society open science*, vol. 4, no. 4, p. 161067, 2017.

[121] Q. J. Leclerc, J. A. Lindsay, and G. M. Knight, "Mathematical modelling to study the horizontal transfer of antimicrobial resistance genes in bacteria: current state of the field and recommendations," *Journal of the Royal Society Interface*, vol. 16, no. 157, p. 20190260, 2019.

[122] D. A. Barber, G. Y. Miller, and P. E. McNAMARA, "Models of antimicrobial resistance and foodborne illness: examining assumptions and practical applications," *Journal of food protection*, vol. 66, no. 4, pp. 700–709, 2003.

[123] X. Zhong, J. E. Kro, E. M. Top, S. M. Krone, *et al.*, "Accounting for mating pair formation in plasmid population dynamics," *Journal of theoretical biology*, vol. 262, no. 4, pp. 711–719, 2010.

[124] D. Roux, O. Danilchanka, T. Guillard, V. Cattoir, H. Aschard, Y. Fu, F. Angoulvant, J. Messika, J.-D. Ricard, J. J. Mekalanos, *et al.*, "Fitness cost of antibiotic susceptibility during bacterial infection," *Science translational medicine*, vol. 7, no. 297, pp. 297ra114–297ra114, 2015.

[125] V. V. Volkova, Z. Lu, C. Lanzas, H. M. Scott, and Y. T. Gröhn, "Modelling dynamics of plasmid-gene mediated antimicrobial resistance in enteric bacteria using stochastic differential equations," *Scientific Reports*, vol. 3, p. 2463, 2013.

[126] V. V. Volkova, Z. Lu, C. Lanzas, and Y. Grohn, "Evaluating targets for control of plasmid-mediated antimicrobial resistance in enteric commensals of beef cattle: a modelling approach," *Epidemiology & Infection*, vol. 141, no. 11, pp. 2294–2312, 2013.

[127] V. V. Volkova, Z. Lu, T. Besser, and Y. T. Gröhn, "Modeling the infection dynamics of bacteriophages in enteric Escherichia coli: estimating the contribution of transduction to antimicrobial gene spread," *Applied and environmental microbiology*, vol. 80, no. 14, pp. 4350–4362, 2014.

[128] I. H. Spicknall, B. Foxman, C. F. Marrs, and J. N. Eisenberg, "A modeling framework for the evolution and spread of antibiotic resistance: literature review and model categorization," *American journal of epidemiology*, vol. 178, no. 4, pp. 508–520, 2013.

[129] S. Kim, H. Park, and K. Chandran, "Propensity of activated sludge to amplify or attenuate tetracycline resistance genes and tetracycline resistant bacteria: A mathematical modeling approach," *Chemosphere*, vol. 78, no. 9, pp. 1071–1077, 2010.

[130] R. Seviour and P. H. Nielsen, *Microbial ecology of activated sludge*. IWA publishing, 2010.

[131] G. C. Amos, E. Gozzard, C. E. Carter, A. Mead, M. J. Bowes, P. M. Hawkey, L. Zhang, A. C. Singer, W. H. Gaze, E. M. H. Wellington, and et al., "Validated predictive modelling of the environmental resistome," *The ISME Journal*, vol. 9, no. 6, pp. 1467–1476, 2015.

[132] M. Gillings, Y. Boucher, M. Labbate, A. Holmes, S. Krishnan, M. Holley, and H. W. Stokes, "The evolution of class 1 integrons and the rise of antibiotic resistance," *Journal of bacteriology*, vol. 190, no. 14, pp. 5095–5100, 2008.

[133] M. R. Gillings, "Lateral gene transfer, bacterial genome evolution, and the anthropocene," *Annals of the New York Academy of Sciences*, vol. 1389, no. 1, pp. 20–36, 2017.

[134] A. C. Birkegård, T. Halasa, N. Toft, A. Folkesson, and K. Græsbøll, "Send more data: a systematic review of mathematical models of antimicrobial resistance," *Antimicrobial Resistance & Infection Control*, vol. 7, no. 1, p. 117, 2018.

[135] J.-M. López-Lozano, D. L. Monnet, A. Yagüe, A. Burgos, N. Gonzalo, P. Campillos, and M. Saez, "Modelling and forecasting antimicrobial resistance and its dynamic relationship to antimicrobial use: a time series analysis," *International journal of antimicrobial agents*, vol. 14, no. 1, pp. 21–31, 2000.

[136] D. Monnet, J.-M. López-Lozano, P. Campillos, A. Burgos, A. Yagüe, and N. Gonzalo, "Making sense of antimicrobial use and resistance surveillance data: application of arima and transfer function models," *Clinical Microbiology and Infection*, vol. 7, pp. 29–36, 2001.

[137] D. L. Monnet, F. M. MacKenzie, J. M. López-Lozano, A. Beyaert, M. Camacho, R. Wilson, D. Stuart, and I. M. Gould, "Antimicrobial drug use and methicillin-resistant Staphylococcus aureus, aberdeen, 1996–2000," *Emerging infectious diseases*, vol. 10, no. 8, p. 1432, 2004.

[138] M. A. Aldeyab, D. L. Monnet, J. M. Lopez-Lozano, C. M. Hughes, M. G. Scott, M. P. Kearney, F. A. Magee, and J. C. Mcelnay, "Modelling the impact of antibiotic use and infection control practices on the incidence of hospital-acquired methicillin-resistant Staphylococcus aureus: a time-series analysis," *Journal of Antimicrobial Chemotherapy*, vol. 62, no. 3, pp. 593–600, 2008.

[139] P. A. Roberts, R. M. Huebinger, E. Keen, A.-M. Krachler, and S. Jabbari, "Mathematical model predicts anti-adhesion–antibiotic–debridement combination therapies can clear an antibiotic resistant infection," *PLoS computational biology*, vol. 15, no. 7, p. e1007211, 2019.

[140] L. Ternent, R. J. Dyson, A.-M. Krachler, and S. Jabbari, "Bacterial fitness shapes the population dynamics of antibiotic-resistant and-susceptible bacteria in a model of combined antibiotic and anti-virulence treatment," *Journal of theoretical biology*, vol. 372, pp. 1–11, 2015.

[141] G. Lambert, S. Vyawahare, and R. H. Austin, "Bacteria and game theory: the rise and fall of cooperation in spatially heterogeneous environments," *Interface Focus*, vol. 4, no. 4, pp. 20140029–20140029, 2014.

[142] E. Gullberg, S. Cao, O. G. Berg, C. Ilbäck, L. Sandegren, D. Hughes, and D. I. Andersson, "Selection of resistant bacteria at very low antibiotic concentrations," *PLoS Pathogens*, vol. 7, no. 7, 2011.

[143] K. Velten, *Mathematical modeling and simulation: introduction for scientists and engineers*. John Wiley & Sons, 2009.

[144] G. M. Knight, N. G. Davies, C. Colijn, F. Coll, T. Donker, D. R. Gifford, R. E. Glover, M. Jit, E. Klemm, S. Lehtinen, *et al.*, "Mathematical modelling for antibiotic resistance control policy: do we know enough?," *BMC infectious diseases*, vol. 19, no. 1, p. 1011, 2019.

[145] C. Seiler and T. U. Berendonk, "Heavy metal driven co-selection of antibiotic resistance in soil and water bodies impacted by agriculture and aquaculture," *Frontiers in microbiology*, vol. 3, 2012.

[146] V. Srinivasan, H. Nam, L. Nguyen, B. Tamilselvam, S. Murinda, and S. Oliver, "Prevalence of antimicrobial resistance genes in Listeria monocytogenes isolated from dairy farms," *Foodbourne Pathogens & Disease*, vol. 2, no. 3, pp. 201–211, 2005.

[147] J. Shere, K. Bartlett, and C. Kaspar, "Longitudinal study of Escherichia coli O157: H7 dissemination on four dairy farms in wisconsin," *Applied and Environmental Microbiology*, vol. 64, no. 4, pp. 1390–1399, 1998.

[148] A. Schmid, S. Hörmansdorfer, U. Messelhäusser, A. Käsbohrer, C. Sauter-Louis, and R. Mansfeld, "Prevalence of extended-spectrum β-lactamase-producing Escherichia coli on Bavarian dairy and beef cattle farms," *Applied and environmental microbiology*, vol. 79, no. 9, pp. 3027–3032, 2013.

[149] J. Hordijk, E. A. Fischer, T. van Werven, S. Sietsma, L. Van Gompel, A. J. Timmerman, M. P. Spaninks, D. J. Heederik, M. Nielen, J. A. Wagenaar, *et al.*, "Dynamics of faecal shedding of ESBL-or AmpC-producing Escherichia coli on dairy farms," *Journal of Antimicrobial Chemotherapy*, vol. 74, no. 6, pp. 1531–1538, 2019.

[150] M. Gonggrijp, I. Santman-Berends, A. Heuvelink, G. Buter, G. Van Schaik, J. Hage, and T. Lam, "Prevalence and risk factors for extended-spectrum β-lactamase-and AmpC-producing Escherichia coli in dairy farms," *Journal of dairy science*, vol. 99, no. 11, pp. 9001–9013, 2016.

[151] I. Santman-Berends, M. Gonggrijp, J. Hage, A. Heuvelink, A. Velthuis, T. Lam, and G. van Schaik, "Prevalence and risk factors for extended-spectrum β-lactamase or ampc-producing Escherichia coli in organic dairy herds in the netherlands," *Journal of dairy science*, vol. 100, no. 1, pp. 562–571, 2017.

[152] L. Brunton, D. Duncan, N. Coldham, L. Snow, and J. Jones, "A survey of antimicrobial usage on dairy farms and waste milk feeding practices in England and Wales," *Veterinary Record*, vol. 171, no. 12, pp. 296–296, 2012.

[153] D. A. Tadesse, S. Zhao, E. Tong, S. Ayers, A. Singh, M. J. Bartholomew, and P. F. McDermott, "Antimicrobial drug resistance in Escherichia coli from humans and food animals, united states, 1950–2002," *Emerging infectious diseases*, vol. 18, no. 5, p. 741, 2012.

[154] "Highest priority critically important antimicrobials." `https://www.who.int/foodsafety/cia/en/`. Accessed: 31/3/2021.

[155] R. Davies and A. Wales, "Antimicrobial resistance on farms: a review including biosecurity and the potential role of disinfectants in resistance selection," *Comprehensive Reviews in Food Science and Food Safety*, vol. 18, no. 3, pp. 753–774, 2019.

[156] G. Rossolini, M. D'andrea, and C. Mugnaioli, "The spread of ctx-m-type extended-spectrum β-lactamases," *Clinical Microbiology and Infection*, vol. 14, pp. 33–41, 2008.

[157] Scientific Advisory Group on Antimicrobials of the Committee for Medicinal Products for Veterinary Use *et al.*, "Reflection paper on the use of third and fourth generation cephalosporins in food producing animals in the european union: development of resistance and impact on human and animal health," *Journal of veterinary pharmacology and therapeutics*, vol. 32, no. 6, pp. 515–533, 2009.

[158] H. C. Neu, "Aztreonam activity, pharmacology, and clinical uses," *The American journal of medicine*, vol. 88, no. 3, pp. S2–S6, 1990.

[159] R. Cantón and T. M. Coque, "The ctx-m β-lactamase pandemic," *Current opinion in microbiology*, vol. 9, no. 5, pp. 466–475, 2006.

[160] "Sewage sludge in agriculture: code of practice for England, Wales and Northern Ireland." `https://www.gov.uk/government/publications/sewage-sludge-in-agriculture-code-of-practice/`

sewage-sludge-in-agriculture-code-of-practice-for-england-wales-and-north
producers-test-the-soil. Accessed: 21/12/2020.

[161] M. M. Mukaka, "A guide to appropriate use of correlation coefficient in medical research," *Malawi medical journal*, vol. 24, no. 3, pp. 69–71, 2012.

[162] T. K. Kim, "T test as a parametric statistic," *Korean journal of anesthesiology*, vol. 68, no. 6, p. 540, 2015.

[163] M. J. Day, K. L. Hopkins, D. W. Wareham, M. A. Toleman, N. Elviss, L. Randall, C. Teale, P. Cleary, C. Wiuff, M. Doumith, *et al.*, "Extended-spectrum β-lactamase-producing Escherichia coli in human-derived and foodchain-derived samples from England, Wales, and Scotland: an epidemiological surveillance and typing study," *The Lancet Infectious Diseases*, vol. 19, no. 12, pp. 1325–1335, 2019.

[164] E. Liebana, M. Batchelor, K. Hopkins, F. Clifton-Hadley, C. Teale, A. Foster, L. Barker, E. Threlfall, and R. Davies, "Longitudinal farm study of extended-spectrum β-lactamase-mediated resistance," *Journal of clinical microbiology*, vol. 44, no. 5, pp. 1630–1634, 2006.

[165] E. Watson, S. Jeckel, L. Snow, R. Stubbs, C. Teale, H. Wearing, R. Horton, M. Toszeghy, O. Tearne, J. Ellis-Iversen, *et al.*, "Epidemiology of extended spectrum beta-lactamase E. coli (ctx-m-15) on a commercial dairy farm," *Veterinary microbiology*, vol. 154, no. 3, pp. 339–346, 2012.

[166] R. Horton, D. Duncan, L. Randall, S. Chappell, L. Brunton, R. Warner, N. Coldham, and C. Teale, "Longitudinal study of CTX-M ESBL-producing E. coli strains on a UK dairy farm," *Research in veterinary science*, vol. 109, pp. 107–113, 2016.

[167] A. C. Cormier, G. Chalmers, T. A. McAllister, S. Cook, R. Zaheer, H. M. Scott, C. Booker, R. Read, and P. Boerlin, "Extended-spectrum-cephalosporin resistance genes in Escherichia coli from beef cattle," *Antimicrobial agents and chemotherapy*, vol. 60, no. 2, pp. 1162–1163, 2016.

[168] H. Heuer, H. Schmitt, and K. Smalla, "Antibiotic resistance gene spread due to manure application on agricultural fields," *Current opinion in microbiology*, vol. 14, no. 3, pp. 236–243, 2011.

[169] EFSA Panel on Biological Hazards (BIOHAZ), A. Ricci, A. Allende, D. Bolton, M. Chemaly, R. Davies, P. S. Fernández Escámez, R. Girones,

K. Koutsoumanis, R. Lindqvist, *et al.*, "Risk for the development of antimicrobial resistance (AMR) due to feeding of calves with milk containing residues of antibiotics," *EFSA Journal*, vol. 15, no. 1, p. e04665, 2017.

[170] "RUMA position on feeding waste milk to calves." `https://www.ruma.org.uk/ruma-position-on-feeding-waste-milk-to-calves/`. Accessed: 21/12/2020.

[171] "Progiene digicur advance." `https://www.tfmsuperstore.co.uk/products/progiene-digicur-advance-footbath-5ltr-sheep-cattl/`. Accessed: 21/12/2020.

[172] "EUCAST database." `https://mic.eucast.org/Eucast2/`. Accessed: 17/04/2020.

[173] J. Bengtsson-Palme and D. J. Larsson, "Concentrations of antibiotics predicted to select for resistant bacteria: Proposed limits for environmental regulation," *Environment International*, vol. 86, pp. 140–149, 2016.

[174] A. Pohl, A. Lübke-Becker, and W. Heuwieser, "Minimum inhibitory concentrations of frequently used antibiotics against Escherichia coli and Trueperella pyogenes isolated from uteri of postpartum dairy cows," *Journal of dairy science*, vol. 101, no. 2, pp. 1355–1364, 2018.

[175] G. S. Bisacchi and J. I. Manchester, "A new-class antibacterial almost. Lessons in drug discovery and development: A critical analysis of more than 50 years of effort toward ATPase inhibitors of DNA gyrase and topoisomerase IV," *ACS infectious diseases*, vol. 1, no. 1, pp. 4–41, 2015.

[176] M. Liu and S. Douthwaite, "Resistance to the macrolide antibiotic tylosin is conferred by single methylations at 23S rRNA nucleotides G748 and A2058 acting in synergy," *Proceedings of the National Academy of Sciences*, vol. 99, no. 23, pp. 14658–14663, 2002.

[177] S. Garneau-Tsodikova and K. J. Labby, "Mechanisms of resistance to aminoglycoside antibiotics: overview and perspectives," *Medchemcomm*, vol. 7, no. 1, pp. 11–27, 2016.

[178] J. D. Palmeira and H. M. N. Ferreira, "Extended-spectrum beta-lactamase (ESBL)-producing Enterobacteriaceae in cattle production–a threat around the world," *Heliyon*, vol. 6, no. 1, p. e03206, 2020.

[179] H. Kang, "The prevention and handling of the missing data," *Korean journal of anesthesiology*, vol. 64, no. 5, p. 402, 2013.

[180] S. J. Winham, C. L. Colby, R. R. Freimuth, X. Wang, M. De Andrade, M. Huebner, and J. M. Biernacka, "SNP interaction detection with random forests in high-dimensional genetic data," *BMC bioinformatics*, vol. 13, no. 1, p. 164, 2012.

[181] M. Kyselková, J. Jirout, N. Vrchotová, H. Schmitt, and D. Elhottová, "Spread of tetracycline resistance genes at a conventional dairy farm," *Frontiers in microbiology*, vol. 6, p. 536, 2015.

[182] H. M. El-Mashad, W. K. Van Loon, G. Zeeman, and G. P. Bot, "Rheological properties of dairy cattle manure," *Bioresource Technology*, vol. 96, no. 5, pp. 531–535, 2005.

[183] Department of Health, "Nitrate vulnerable zones guidance." `https://www.gov.uk/government/collections/nitrate-vulnerable-zones#nvz-designations-2017-to-2020`, 2017. Accessed: 2019/10/08.

[184] European Community, "Survey of wastes spread on land - final report." `http://ec.europa.eu/environment/waste/studies/compost/landspreading.pdf`, 2001.

[185] Department for Environment, Food and Rural Affairs , "Using nitrogen fertilisers in nitrate vulnerable zones." Available at `https://www.gov.uk/guidance/using-nitrogen-fertilisers-in-nitrate-vulnerable-zones`, 2018. Accessed: 2019/04/04.

[186] A. H. Van Hoek, D. Mevius, B. Guerra, P. Mullany, A. P. Roberts, and H. J. Aarts, "Acquired antibiotic resistance genes: an overview," *Frontiers in microbiology*, vol. 2, p. 203, 2011.

[187] P. Ayscue, C. Lanzas, R. Ivanek, and Y. Gröhn, "Modeling on-farm Escherichia coli O157: H7 population dynamics," *Foodborne Pathogens and Disease*, vol. 6, no. 4, pp. 461–470, 2009.

[188] S. Biswas, P. K. Pandey, and T. B. Farver, "Assessing the impacts of temperature and storage on Escherichia coli, Salmonella, and L. monocytogenes decay in dairy manure," *Bioprocess and biosystems engineering*, vol. 39, no. 6, pp. 901–913, 2016.

[189] C. Munck, H. K. Gumpert, A. I. N. Wallin, H. H. Wang, and M. O. Sommer, "Prediction of resistance development against drug combinations by collateral responses to component drugs," *Science translational medicine*, vol. 6, no. 262, pp. 262ra156–262ra156, 2014.

[190] B. R. Levin, F. Baquero, P. P. Ankomah, and I. C. McCall, "Phagocytes, antibiotics, and self-limiting bacterial infections," *Trends in microbiology*, vol. 25, no. 11, pp. 878–892, 2017.

[191] F. Daschner, "Inhibition of cell wall synthesis by sulfonamides and trimethoprim," *Chemotherapy*, vol. 22, no. 1, pp. 12–18, 1976.

[192] N. Wald-Dickler, P. Holtom, and B. Spellberg, "Busting the myth of "static vs cidal": a systemic literature review," *Clinical Infectious Diseases*, vol. 66, no. 9, pp. 1470–1474, 2018.

[193] J.-M. Ghuysen and R. Hakenbeck, *Bacterial cell wall*. Elsevier, 1994.

[194] P. Bennett, "Plasmid encoded antibiotic resistance: acquisition and transfer of antibiotic resistance genes in bacteria," *British journal of pharmacology*, vol. 153, no. S1, pp. S347–S357, 2008.

[195] D. R. Ibrahim, C. E. Dodd, D. J. Stekel, S. J. Ramsden, and J. L. Hobman, "Multidrug resistant, extended spectrum β-lactamase (ESBL)-producing Escherichia coli isolated from a dairy farm," *FEMS microbiology ecology*, vol. 92, no. 4, 2016.

[196] J. D. Murray, "Mathematical biology: I. An introduction," 2002.

[197] L. Edelstein-Keshet, *Mathematical models in biology*. SIAM, 2005.

[198] T. Pecht, A. C. Aschenbrenner, T. Ulas, and A. Succurro, "Modeling population heterogeneity from microbial communities to immune response in cells," *Cellular and Molecular Life Sciences*, vol. 77, no. 3, pp. 415–432, 2020.

[199] C. Spalding, E. Keen, D. J. Smith, A.-M. Krachler, and S. Jabbari, "Mathematical modelling of the antibiotic-induced morphological transition of Pseudomonas aeruginosa," *PLoS Computational Biology*, vol. 14, no. 2, p. e1006012, 2018.

[200] A. Van Epps and L. Blaney, "Antibiotic residues in animal waste: occurrence and degradation in conventional agricultural waste management practices," *Current Pollution Reports*, vol. 2, no. 3, pp. 135–155, 2016.

[201] Y. Wu, M. Williams, L. Smith, D. Chen, and R. Kookana, "Dissipation of sulfamethoxazole and trimethoprim antibiotics from manure-amended soils," *Journal of Environmental Science and Health, Part B*, vol. 47, no. 4, pp. 240–249, 2012.

[202] R. E. Hornish and S. Katarski, "Cephalosporins in veterinary medicine-ceftiofur use in food animals," *Current topics in medicinal chemistry*, vol. 2, no. 7, pp. 717–731, 2002.

[203] M. Jiang, L. Wang, and R. Ji, "Biotic and abiotic degradation of four cephalosporin antibiotics in a lake surface water and sediment," *Chemosphere*, vol. 80, no. 11, pp. 1399–1405, 2010.

[204] A. A. Sawant, N. V. Hegde, B. A. Straley, S. C. Donaldson, B. C. Love, S. J. Knabel, and B. M. Jayarao, "Antimicrobial-resistant enteric bacteria from dairy cattle," *Applied and environmental microbiology*, vol. 73, no. 1, pp. 156–163, 2007.

[205] "Pathogens - the cause of mastitis." `https://dairy.ahdb.org.uk/technical-information/animal-health-welfare/mastitis/pathogens-the-cause-of-mastitis/#.XrvpMhNKiL5`. Accessed: 13/5/2020.

[206] A. Cutler, *Ecological dynamics in compost-amended soils and the resulting effects on Escherichia coli survival*. PhD thesis, University of Vermont, 2016.

[207] J. Kim, M. W. Shepherd, and X. Jiang, "Evaluating the effect of environmental factors on pathogen regrowth in compost extract," *Microbial ecology*, vol. 58, no. 3, pp. 498–508, 2009.

[208] D. Godwin and J. H. Slater, "The influence of the growth environment on the stability of a drug resistance plasmid in Escherichia coli K12," *Microbiology*, vol. 111, no. 1, pp. 201–210, 1979.

[209] B. R. Levin, F. M. Stewart, and V. A. Rice, "The kinetics of conjugative plasmid transmission: fit of a simple mass action model," *Plasmid*, vol. 2, no. 2, pp. 247–260, 1979.

[210] C. Curds, "Computer simulations of microbial population dynamics in the activated-sludge process," *Water Research*, vol. 5, no. 11, pp. 1049–1066, 1971.

[211] R. P. Novick, "Plasmid incompatibility.," *Microbiological reviews*, vol. 51, no. 4, p. 381, 1987.

[212] V. Economou and P. Gousia, "Agriculture and food animals as a source of antimicrobial-resistant bacteria," *Infection and Drug Resistance*, vol. 8, p. 49, 2015.

[213] L. Norcia, A. Silvia, and S. Hayashi, "Studies on time-kill kinetics of different classes of antibiotics against veterinary pathogenic bacteria including Pasteurella, Actinobacillm and Escherichia coli," *The Journal of antibiotics*, vol. 52, no. 1, pp. 52–60, 1999.

[214] X. Jiang, J. Morgan, and M. P. Doyle, "Fate of Escherichia coli O157: H7 in manure-amended soil," *Applied and environmental microbiology*, vol. 68, no. 5, pp. 2605–2609, 2002.

[215] P. McGee, D. Bolton, J. Sheridan, B. Earley, and N. Leonard, "The survival of Escherichia coli o157: H7 in slurry from cattle fed different diets," *Letters in Applied Microbiology*, vol. 32, no. 3, pp. 152–155, 2001.

[216] A. Maule, "Survival of verocytotoxigenic Escherichia coli O157 in soil, water and on surfaces," *Journal of Applied Microbiology*, vol. 88, no. S1, pp. 71S–78S, 2000.

[217] K. Palaniappan and R. A. Holley, "Use of natural antimicrobials to increase antibiotic susceptibility of drug resistant bacteria," *International journal of food microbiology*, vol. 140, no. 2-3, pp. 164–168, 2010.

[218] F. Reinthaler, J. Posch, G. Feierl, G. Wüst, D. Haas, G. Ruckenbauer, F. Mascher, and E. Marth, "Antibiotic resistance of E. coli in sewage and sludge," *Water research*, vol. 37, no. 8, pp. 1685–1690, 2003.

[219] T. E. Kearney, M. Larkin, and P. Levett, "The effect of slurry storage and anaerobic digestion on survival of pathogenic bacteria," *Journal of Applied Bacteriology*, vol. 74, no. 1, pp. 86–93, 1993.

[220] "MathWorks choose an ode solver." `https://uk.mathworks.com/help/matlab/math/choose-an-ode-solver.html`. Accessed: 29/3/2021.

[221] A. Handel, R. R. Regoes, and R. Antia, "The role of compensatory mutations in the emergence of drug resistance," *PLoS computational biology*, vol. 2, no. 10, p. e137, 2006.

[222] T.-F. C. Mah and G. A. O'Toole, "Mechanisms of biofilm resistance to antimicrobial agents," *Trends in microbiology*, vol. 9, no. 1, pp. 34–39, 2001.

[223] Department for Environment, Food and Rural Affairs, "Storing silage, slurry and agricultural fuel oil." `https://www.gov.uk/guidance/storing-silage-slurry-and-agricultural-fuel-oil`, 2018. Accessed: 2020/11/1.

[224] F. Pianosi, K. Beven, J. Freer, J. W. Hall, J. Rougier, D. B. Stephenson, and T. Wagener, "Sensitivity analysis of environmental models: A systematic review with practical workflow," *Environmental Modelling & Software*, vol. 79, pp. 214–232, 2016.

[225] A. Saltelli, M. Ratto, T. Andres, F. Campolongo, J. Cariboni, D. Gatelli, M. Saisana, and S. Tarantola, *Global sensitivity analysis: the primer*. John Wiley & Sons, 2008.

[226] T. Vogwill and R. C. MacLean, "The genetic basis of the fitness costs of antimicrobial resistance: a meta-analysis approach," *Evolutionary applications*, vol. 8, no. 3, pp. 284–295, 2015.

[227] L. Hofmann, B. Rieck, and F. Sadlo, "Visualization of 4D vector field topology," *Computer Graphics Forum*, vol. 37, no. 3, pp. 301–313, 2018.

[228] S. Hernando-Amado, F. Sanz-Garcia, P. Blanco, and J. L. Martinez, "Fitness costs associated with the acquisition of antibiotic resistance," *Essays in biochemistry*, vol. 61, no. 1, pp. 37–48, 2017.

[229] B. H. Ter Kuile, N. Kraupner, and S. Brul, "The risk of low concentrations of antibiotics in agriculture for resistance in human health care," *FEMS Microbiology Letters*, vol. 363, no. 19, 2016.

[230] V. J. Savage, I. Chopra, and A. J. O'Neill, "Staphylococcus aureus biofilms promote horizontal transfer of antibiotic resistance," *Antimicrobial agents and chemotherapy*, vol. 57, no. 4, pp. 1968–1970, 2013.

[231] J. L. Balcázar, J. Subirats, and C. M. Borrego, "The role of biofilms as environmental reservoirs of antibiotic resistance," *Frontiers in microbiology*, vol. 6, p. 1216, 2015.

[232] C. Pal, K. Asiani, S. Arya, C. Rensing, D. J. Stekel, D. J. Larsson, and J. L. Hobman, "Metal resistance and its association with antibiotic resistance," in *Advances in microbial physiology*, vol. 70, pp. 261–313, Elsevier, 2017.

[233] M. Vos, L. Sibleyras, L. K. Lo, E. Hesse, W. H. Gaze, and U. Klümper, "Zinc can counteract selection for ciprofloxacin resistance," *bioRxiv*, p. 780981, 2019.

[234] J. G. Lawrence and H. Ochman, "Reconciling the many faces of lateral gene transfer," *TRENDS in Microbiology*, vol. 10, no. 1, pp. 1–4, 2002.

[235] S. G. Mulamattathil, H. Esterhuysen, and P. Pretorius, "Antibiotic-resistant gram-negative bacteria in a virtually closed water reticulation system," *Journal of applied microbiology*, vol. 88, no. 6, pp. 930–937, 2000.

[236] "Novobiocin." `https://pubchem.ncbi.nlm.nih.gov/source/hsdb/7443`. Accessed: 28/12/2020.

[237] O. B. Samuelsen and Ø. Bergh, "Efficacy of orally administered florfenicol and oxolinic acid for the treatment of vibriosis in cod (Gadus morhua)," *Aquaculture*, vol. 235, no. 1-4, pp. 27–35, 2004.

[238] M. Varga, "Chapter 3 - therapeutics," in *Textbook of Rabbit Medicine (Second Edition)* (M. Varga, ed.), pp. 137 – 177, Butterworth-Heinemann, second edition ed., 2014.

[239] J. E. Maddison, A. D. J. Watson, and J. Elliott, "Chapter 8 - antibacterial drugs," in *Small Animal Clinical Pharmacology (Second Edition)* (J. E. Maddison, S. W. Page, and D. B. Church, eds.), pp. 148 – 185, Edinburgh: W.B. Saunders, second edition ed., 2008.

[240] M. Kester, K. D. Karpa, and K. E. Vrana, *Elsevier's Integrated Review Pharmacology E-Book: with STUDENT CONSULT Online Access*. Elsevier Health Sciences, 2011.

[241] D. H. Smith and B. D. Davis, "Mode of action of novobiocin in Escherichia coli," *Journal of bacteriology*, vol. 93, no. 1, pp. 71–79, 1967.

[242] J. J. Rahal and M. S. Simberkoff, "Bactericidal and bacteriostatic action of chloramphenicol against meningeal pathogens," *Antimicrobial agents and chemotherapy*, vol. 16, no. 1, pp. 13–18, 1979.

[243] S. Biswas, J.-M. Brunel, J.-C. Dubus, M. Reynaud-Gaubert, and J.-M. Rolain, "Colistin: an update on the antibiotic of the 21st century," *Expert review of anti-infective therapy*, vol. 10, no. 8, pp. 917–934, 2012.

[244] "Nitrofurantoin." `https://pubchem.ncbi.nlm.nih.gov/source/hsdb/3135#section=Toxicity-Summary`. Accessed: 28/12/2020.

[245] H. Kropp, L. Gerckens, J. G. Sundelof, and F. M. Kahan, "Antibacterial activity of imipenem: the first thienamycin antibiotic," *Reviews of infectious diseases*, vol. 7, no. Supplement_3, pp. S389–S410, 1985.

[246] H.-J. BUSSE, C. WÖSTMANN, and E. P. BARKER, "The bactericidal action of streptomycin: membrane permeabilization caused by the insertion

of mistranslated proteins into the cytoplasmic membrane of Escherichia coli and subsequent caging of the antibiotic inside the cells due to degradation of these proteins," *Microbiology*, vol. 138, no. 3, pp. 551–561, 1992.

[247] M. S. Dorfman, R. S. Wagner, T. Jamison, B. Bell, and D. W. Stroman, "The pharmacodynamic properties of azithromycin in a kinetics-of-kill model and implications for bacterial conjunctivitis treatment," *Advances in therapy*, vol. 25, no. 3, pp. 208–217, 2008.

[248] S. M. Lynch, *Introduction to applied Bayesian statistics and estimation for social scientists*. Springer Science & Business Media, 2007.

[249] I. J. Myung, "Tutorial on maximum likelihood estimation," *Journal of mathematical Psychology*, vol. 47, no. 1, pp. 90–100, 2003.

[250] D. Van Ravenzwaaij, P. Cassey, and S. D. Brown, "A simple introduction to Markov Chain Monte–Carlo sampling," *Psychonomic bulletin & review*, vol. 25, no. 1, pp. 143–154, 2018.

[251] S. Brooks, A. Gelman, G. Jones, and X.-L. Meng, *Handbook of Markov Chain Monte Carlo*. CRC press, 2011.

[252] C. Winckler and A. Grafe, "Use of veterinary drugs in intensive animal production," *Journal of soils and sediments*, vol. 1, no. 2, p. 66, 2001.

[253] "Permastore slurry tanks." `https://www.permastore.com/applications/slurry/`. Accessed: 9/4/2021.

[254] U. Jeppsson and S. Diehl, "An evaluation of a dynamic model of the secondary clarifier," *Water Science and technology*, vol. 34, no. 5-6, pp. 19–26, 1996.

[255] A. Abusam and K. Keesman, "Dynamic modeling of sludge compaction and consolidation processes in wastewater secondary settling tanks," *Water environment research*, vol. 81, no. 1, pp. 51–56, 2009.

[256] R. Bürger, S. Diehl, and I. Nopens, "A consistent modelling methodology for secondary settling tanks in wastewater treatment," *Water research*, vol. 45, no. 6, pp. 2247–2260, 2011.

[257] A. Wehrhan, R. Kasteel, J. Simunek, J. Groeneweg, and H. Vereecken, "Transport of sulfadiazine in soil columns—experiments and modelling approaches," *Journal of contaminant hydrology*, vol. 89, no. 1-2, pp. 107–135, 2007.

[258] P. Srinivasan, A. K. Sarmah, and M. Manley-Harris, "Sorption of selected veterinary antibiotics onto dairy farming soils of contrasting nature," *Science of the total environment*, vol. 472, pp. 695–703, 2014.

[259] F. Polesel, K. Lehnberg, W. Dott, S. Trapp, K. V. Thomas, and B. G. Plósz, "Factors influencing sorption of ciprofloxacin onto activated sludge: experimental assessment and modelling implications," *Chemosphere*, vol. 119, pp. 105–111, 2015.

[260] X.-R. Xu and X.-Y. Li, "Sorption and desorption of antibiotic tetracycline on marine sediments," *Chemosphere*, vol. 78, no. 4, pp. 430–436, 2010.

[261] H. L. Reddy and R. M. Ford, "Analysis of biodegradation and bacterial transport: Comparison of models with kinetic and equilibrium bacterial adsorption," *Journal of contaminant hydrology*, vol. 22, no. 3-4, pp. 271–287, 1996.

[262] U. Jeppsson, M.-N. Pons, I. Nopens, J. Alex, J. Copp, K. Gernaey, C. Rosén, J.-P. Steyer, and P. Vanrolleghem, "Benchmark simulation model no 2: general protocol and exploratory case studies," *Water Science and Technology*, vol. 56, no. 8, pp. 67–78, 2007.

[263] L. B. Verdickt, I. Y. Smets, and J. F. Van Impe, "On the number of grid layers required for accurate simulation of a convection-diffusion model for secondary settling tanks," *IFAC Proceedings Volumes*, vol. 37, no. 3, pp. 201–206, 2004.

[264] M. Stenstrom, *A dynamic model and computer compatible control strategies for wastewater treatment plants*. PhD thesis, Clemson University, 1976.

[265] A. C. Kolz, S. K. Ong, and T. Moorman, "Sorption of tylosin onto swine manure," *Chemosphere*, vol. 60, no. 2, pp. 284–289, 2005.

[266] A. Ngigi, Y. S. Ok, and S. Thiele-Bruhn, "Biochar-mediated sorption of antibiotics in pig manure," *Journal of hazardous materials*, vol. 364, pp. 663–670, 2019.

[267] J. Tolls, "Sorption of veterinary pharmaceuticals in soils: a review," *Environmental science & technology*, vol. 35, no. 17, pp. 3397–3406, 2001.

[268] A. B. Boxall, P. Blackwell, R. Cavallo, P. Kay, and J. Tolls, "The sorption and transport of a sulphonamide antibiotic in soil systems," *Toxicology letters*, vol. 131, no. 1-2, pp. 19–28, 2002.

[269] M. Carballa, G. Fink, F. Omil, J. M. Lema, and T. Ternes, "Determination of the solid–water distribution coefficient (Kd) for pharmaceuticals, estrogens and musk fragrances in digested sludge," *Water research*, vol. 42, no. 1-2, pp. 287–295, 2008.

[270] P. Sukul, M. Lamshöft, S. Zühlke, and M. Spiteller, "Sorption and desorption of sulfadiazine in soil and soil-manure systems," *Chemosphere*, vol. 73, no. 8, pp. 1344–1350, 2008.

[271] W. Gong, X. Liu, H. He, L. Wang, and G. Dai, "Quantitatively modeling soil–water distribution coefficients of three antibiotics using soil physicochemical properties," *Chemosphere*, vol. 89, no. 7, pp. 825–831, 2012.

[272] Y.-L. Zhang, S.-S. Lin, C.-M. Dai, L. Shi, and X.-F. Zhou, "Sorption–desorption and transport of trimethoprim and sulfonamide antibiotics in agricultural soil: effect of soil type, dissolved organic matter, and ph," *Environmental Science and Pollution Research*, vol. 21, no. 9, pp. 5827–5835, 2014.

[273] A. N. Soriano, K. G. Adamos, P. B. Bonifacio, A. P. Adornado, V. C. Bungay, and R. Vairavan, "Determination of diffusion coefficients of various livestock antibiotics in water at infinite dilution," in *EPJ Web of Conferences*, vol. 162, p. 01083, EDP Sciences, 2017.

[274] Z. Wang, M. Kim, and G. Rosen, "Validating models of bacterial chemotaxis by simulating the random motility coefficient," in *2008 8th IEEE International Conference on BioInformatics and BioEngineering*, pp. 1–5, IEEE, 2008.

[275] R. M. Ford, B. R. Phillips, J. A. Quinn, and D. A. Lauffenburger, "Measurement of bacterial random motility and chemotaxis coefficients: I. Stopped-flow diffusion chamber assay," *Biotechnology and bioengineering*, vol. 37, no. 7, pp. 647–660, 1991.

[276] R. M. Ford and D. A. Lauffenburger, "Measurement of bacterial random motility and chemotaxis coefficients: II. Application of single-cell-based mathematical model," *Biotechnology and bioengineering*, vol. 37, no. 7, pp. 661–672, 1991.

[277] X. Zhang, C. Zhao, N. Guo, and Q. Chen, "Numerical simulation of the spread of bacteria in water flow considering the process of reproductions," in *IOP Conference Series: Earth and Environmental Science*, vol. 146, p. 012040, IOP Publishing, 2018.

[278] B. R. Phillips, J. A. Quinn, and H. Goldfine, "Random motility of swimming bacteria: single cells compared to cell populations," *AIChE journal*, vol. 40, no. 2, pp. 334–348, 1994.

[279] M. Wu, J. W. Roberts, S. Kim, D. L. Koch, and M. P. DeLisa, "Collective bacterial dynamics revealed using a three-dimensional population-scale defocused particle tracking technique," *Appl. Environ. Microbiol.*, vol. 72, no. 7, pp. 4987–4994, 2006.

[280] J. Li, W. Cheng, L. Xu, Y. Jiao, S. A. Baig, and H. Chen, "Occurrence and removal of antibiotics and the corresponding resistance genes in wastewater treatment plants: effluents' influence to downstream water environment," *Environmental Science and Pollution Research*, vol. 23, no. 7, pp. 6826–6835, 2016.

[281] R. Dillon, L. Fauci, and D. Gaver III, "A microscale model of bacterial swimming, chemotaxis and substrate transport," *Journal of theoretical biology*, vol. 177, no. 4, pp. 325–340, 1995.

[282] R. W. Lewis, W. K. Pao, and X.-S. Yang, "Instability and reaction-diffusion transport of bacteria," *Communications in numerical methods in engineering*, vol. 20, no. 10, pp. 777–787, 2004.

[283] R. Lindqvist and G. Bengtsson, "Dispersal dynamics of groundwater bacteria," *Microbial ecology*, vol. 21, no. 1, pp. 49–72, 1991.

[284] D. Causon and C. Mingham, *Introductory finite difference methods for PDEs*. Bookboon, 2010.

[285] J. Koch and W. Nowak, "A method for implementing dirichlet and third-type boundary conditions in ptrw simulations," *Water Resources Research*, vol. 50, no. 2, pp. 1374–1395, 2014.

[286] S. Mazumder, *Numerical methods for partial differential equations: finite difference and finite volume methods*. Academic Press, 2015.

[287] H. P. Langtangen, A. Logg, and A. Tveito, *Solving PDEs in Python: The FEniCS Tutorial I*. Springer International Publishing, 2016.

[288] N. Rott, "Note on the history of the reynolds number," *Annual review of fluid mechanics*, vol. 22, no. 1, pp. 1–12, 1990.

[289] D. Kuzmin, "A guide to numerical methods for transport equations," 2010.

[290] D. Torlo, F. Ballarin, and G. Rozza, "Stabilized weighted reduced basis methods for parametrized advection dominated problems with random inputs," *SIAM/ASA Journal on Uncertainty Quantification*, vol. 6, no. 4, pp. 1475–1502, 2018.

[291] A. Sendur, "A comparative study on stabilized finite element methods for the convection-diffusion-reaction problems," *Journal of Applied Mathematics*, vol. 2018, 2018.